



Molecular Imaging of Prostate Cancer

A thesis submitted to University College London for the degree of Doctor of Philosophy

Athar Haroon | December 2021



Supervisors

Professor Jamshed Bomanji

Professor Mark Emberton

Declaration

I, Athar Haroon, confirm that the work presented in this thesis is my own. Where information has been derived from other sources, I confirm that this has been indicated in the thesis.

Abstract

Chapter 1 addresses the introduction to the thesis and provides epidemiology, etiology, metastatic spread, current diagnostics and clinical need of new biomarker for risk stratification of prostate cancer.

Chapter 2 provides a detailed analysis of the distribution pattern of the three most used choline tracers: ^{18}F -methylcholine, ^{11}C -choline, and ^{18}F -ethylcholine in metabolically and anatomically disease-free patients. The ranges of SUV_{max} , SUV_{mean} and standard deviations have been presented. Potential pitfalls in evaluation of “non-avid” but clinically significant presentation of different disease entities are also addressed. The chapter provides overview of the variations in choline uptake pattern which is vital for assessment of various organs when imaging is performed for evaluation of metastatic disease.

Chapter 3 presents the feasibility of assessing dynamic ^{18}F Ethyl Choline PET with a view to do kinetic modelling in clinical setting of biochemical relapse of Prostate Cancer. This critical piece of work underpins the quantification, tracer kinetics and demonstrates that cancerous tissue shows abnormal perfusion. From these observations I was able to conclude that ^{18}F Choline can act as a biomarker to assess angiogenesis in prostate cancer and introduces ^{18}F Choline as a biomarker for further work presented in chapter 4-8.

Chapter 4 addresses the detection of clinically significant and insignificant prostate cancer on ^{18}F -FECH PET/CT and I correlated findings with template guided prostate mapping biopsy (TPM). Sensitivity and Specificity data of ^{18}F -FECH PET/CT has been provided.

Chapter 5 addresses the accuracy of ^{18}F Choline PET/MR which is compared to reference standard (template guided prostate mapping biopsy). This work suggests that data obtained

from ^{18}F Choline PET/MR can allow detection of clinically significant and insignificant prostate cancer. I noted that multiple previous treatments can give false positive results and ^{18}F Choline PET/MR is the imaging investigation of choice post HIFU. Moreover, false negative results with ^{18}F Choline PET/MR can be due to very small volume (≤ 2 mm) disease.

Chapter 6 presents the differential diagnosis of abnormal tracer accumulation in the Prostate and periprostatic tissue.

Chapter 7 provides spectrum of skeletal findings on dual-phase ^{18}F -fluoroethylcholine (FECH) PET/CT performed during the work-up of patients referred for suspected prostate cancer relapse. I have provided quantification data and explained that SUV_{max} in isolation cannot be used to characterize these lesions as benign or malignant. Minimal overlap of benign and malignant lesions also exists.

Chapter 8 addresses the clinical utility of ^{18}F Choline in the setting of clinical trial in collaboration with Uro-oncology, Nuclear Medicine and Radiology departments. This critical work compares ^{18}F Choline PET-CT and Whole-Body MRI in assessment and decision-making process for salvage treatment of focal radio-recurrent prostate cancer. This chapters concludes that at present WB-MRI cannot be used alone as imaging modality for investigation of biochemical relapse of Prostate Cancer.

Chapter 9 is a summary of main findings and discussions from chapters in this thesis. It also highlights the potential applications and future perspectives of novel biomarkers for imaging of prostate cancer.

Appendices

Appendix 1 List of publications and abstracts

Appendix 2 summarises academic outputs such as prizes, publications as first author and as co-author, abstracts, book chapters, lectures on prostate cancer, papers, courses attended, and grants awarded.

Appendix 3 is the ethical approval letter for the FORECAST study.

Appendix 4 includes the clinical trial Performa for the ^{18}F Choline PET-CT and $\text{Tc}^{99\text{m}}$ Bone Scan .

Appendix 5 briefly describes the Radiopharmacy i.e., synthesis of ^{18}F Choline.

Appendix 6 includes the standard operating procedures (SOP) for the relevant ^{18}F Choline PET-CT and ^{18}F Choline PET-MR examination.

Impact Statement

Over the last 40 years, positron emission tomography (PET) has revolutionised the imaging of cancer. Extra benefits are brought by combining PET with anatomical modalities such as cross-sectional tomography (CT) or magnetic resonance imaging (MRI). A deep understanding of anatomy and function is provided by these equipments when specific radiolabelled biomarkers are used to evaluate disease processes. My thesis focused on the evaluation of one such biomarker “Choline”. Increased concentration of choline in tissues reflects cell membrane proliferation, thus we can image cancer using this biomarker.

Before abnormality is evaluated, defining normality is a challenge. I studied the physiological distribution of Choline and this work included largest analysis of the three variants of this biomarker. I was able to conclude that there is only marginal difference in the physiological distribution of these tracers. A feasibility study using dynamic ^{18}F Choline PET in prostate cancer patients helped demonstrate that abnormal perfusion associated with cancer cells can be imaged with ^{18}F Choline and this biomarker can be used to image angiogenesis.

The question whether ^{18}F Choline can detect clinically significant prostate cancer with an established validation technique was also addressed. I correlated the findings on ^{18}F Choline PET-CT and ^{18}F Choline PET-MR with template guided prostate biopsy. This was the first work of its kind and showed that ^{18}F Choline PET-CT/PET-MR can detect clinically significant cancer.

In my thesis I also evaluated the spectrum of skeletal findings detected during ^{18}F Choline PET imaging as part of staging work up for prostate cancer. I was able to demonstrate that ^{18}F Choline PET can detect skeletal lesions, however, quantification, using standardised uptake values (SUV) alone cannot be used to detect skeletal metastases.

Finally, the clinical utility of ^{18}F Choline in comparison to whole body MRI was evaluated in the setting of a prospective clinical trial. This collaborative work concluded that whole Body MRI cannot be used alone as imaging modality for investigation of prostate cancer.

So far through my work, I have generated 5 papers and 8 abstracts as first author or co-author. The work on skeletal findings of ^{18}F Choline featured as cover image of leading UK nuclear medicine journal.

I feel honoured to be awarded 1st student research prize by the British Nuclear Medicine Society at the 41st Annual meeting held at the Brighton Conference Centre (21st-24th April 2013).

Summary

Molecular imaging of cell membranes can be done in clinical setting. The physiological distribution of three versions of most used radiolabelled choline is similar with only minor statistical differences. Dynamic choline PET study is feasible and kinetic modelling data suggests that radiolabelled choline has potential to act as a biomarker to assess angiogenesis. Radiolabelled choline can detect clinically significant prostate cancer as validated by template guided biopsies. There are different causes of accumulation of radiolabelled choline in the prostate and reading physician should be aware of the differential diagnosis. The causes of accumulation of radiolabelled choline in the skeleton include both benign and malignant causes however SUVmax cannot be used alone to characterise these lesions. Comparing results of whole body MRI and Choline PET-CT in a prospective clinical trial suggests that WB-MRI cannot be used alone for investigation of biochemical relapse of prostate cancer.

Acknowledgements

I would like to thank Professor Jamshed Bomanji for giving me the opportunity to work at the Institute of Nuclear Medicine (INM), University College London Hospital NHS and accepting me as a PhD student. He has been hugely supportive throughout my time as Nuclear Medicine specialist registrar and then as Consultant at Barts Health NHS Trust. I am thankful for his guidance that helped me publish and present at local, regional, national, and international levels. Most importantly, he has always been there as a mentor, teacher, and supervisor.

I am grateful to Professor Mark Emberton for his support and sharing his vision to improve prostate cancer diagnosis by encouraging use of novel molecular imaging biomarkers using PET/CT and PET/MR. I would also like to thank Professor Hashim U Ahmed who has provided support with his valuable comments and managed to set up clinical trial between departments of Radiology, Nuclear Medicine and Uro-oncology and I was given the opportunity to participate in FORECAST clinical trial.

I want to thank Professor Brian Hutton for his support with the kinetic modelling of ¹⁸F Choline. Special thanks to Kjell Erlandsson for helping me with complex kinetic modelling analysis. I also want to thank the technologists at the Institute of Nuclear Medicine particularly Raymond Endozo and Rayjanah Allie who have always been there and went out of the way to help with technical aspect of PET/CT. I wish to thank John Dickson for taking time out of his busy routine and helping me set up the Choline protocol.

I would like to thank Professor Stefano Fanti and Mohsen Beheshti who provided his support with the initial chapters of this thesis related to physiological distribution of Choline. I would like to mention Ahmad Almuhaideb who worked as Nuclear Medicine Fellow from Saudi

Arabia and provided his input with initial stages of my thesis. I am grateful to Dr Alex Freeman Consultant histopathologist at UCLH who has always been supportive, exchanged ideas and provided input with histology data.

I would like to thank Abi Kanthabalan, Arash Latifoltojar and Taimur Shah for working over FORECAST Trial. I am grateful to Sola Adeleke and Simon Wan who worked extremely hard to organise the case report forms for the clinical trial. Dr Naeem Soomro from The Newcastle Upon Tyne Hospitals who provided very constructive feedback in drafting results and presenting those in an organised manner.

A big thank you to Shehla, my wife and my beautiful kids who have been anchor of support for me in the most difficult of times. Professor Ahmed Rafique Akhtar and my family friend Dr Abdul Jalil who have always been an inspiration.

I would like to dedicate this thesis to my father Major (Retd) Haroon Shahid and my mother Lt Col (Retd) Farkhanda Haroon for their help, support, love and prayers. They have been instrumental in providing me emotional support.

Table of Contents

DECLARATION	3
ABSTRACT	4
IMPACT STATEMENT	7
SUMMARY	8
ACKNOWLEDGEMENTS	9
LIST OF ABBREVIATIONS	14
CHAPTER 1: INTRODUCTION TO THESIS	16
EPIDEMIOLOGY	16
ETIOLOGY	16
METASTATIC SPREAD	16
CURRENT DIAGNOSTICS	17
CLINICAL NEED FOR NEW BIOMARKER AND DEFINING NORMALITY	19
SETTING UP MOLECULAR IMAGING TO STUDY MICRO-ENVIRONMENT	19
RISK STRATIFICATION AND ¹⁸ F CHOLINE PET-CT	20
RISK STRATIFICATION AND ¹⁸ F CHOLINE PET-MR	20
VARYING APPEARANCES OF THE PROSTATE GLAND	21
SPECTRUM OF METASTATIC DISEASE WITH PROSTATE CANCER	21
PET-CT AS “TRIAGE TEST” FOR BETTER SELECTION OF PATIENTS FOR FOCAL SALVAGE THERAPY	21
CHAPTER 2: PHYSIOLOGICAL DISTRIBUTION OF CHOLINE	25
AIM	25
INTRODUCTION	27
METHODS	27
¹¹ C-CHOLINE	28
¹⁸ F-METHYLCHOLINE	29
¹⁸ F-ETHYLCHOLINE	29
RESULTS	31
.....	38
DISCUSSION	39
CONCLUSION	49
CHAPTER 3: MOLECULAR IMAGING OF TUMOUR BLOOD VESSELS PROLIFERATION(ANGIOGENESIS) IN PROSTATE CANCER USING DYNAMIC ¹⁸F CHOLINE PET-CT	51
INTRODUCTION:	57
MATERIAL AND METHODS	61
DISCUSSION	81
CONCLUSION	84
REFERENCES	85
CHAPTER 4 : ¹⁸F-CHOLINE PET-CT FOR ASSESSMENT OF CLINICALLY SIGNIFICANT PROSTATE CANCER	87
ABSTRACT	88
INTRODUCTION	90
MATERIALS AND METHODS	91
RESULTS	99
CONCLUSION	113
REFERENCES	115
CHAPTER 5 : VALIDATING ¹⁸F CHOLINE PET/MR WITH TEMPLATE BIOPSY AS GOLD STANDARD	117
INTRODUCTION	120
MATERIALS AND METHODS	121
RESULTS	131
DISCUSSION	143
CONCLUSION:	155

REFERENCES	156
CHAPTER 6: MAPPING THE PHENOTYPIC APPEARANCES OF PROSTATE ON PET-CT AND PET-MR	158
ABSTRACT.....	160
INTRODUCTION	162
BIOMARKERS.....	163
DIFFERENTIAL DIAGNOSIS.....	164
CONCLUSION.....	184
REFERENCES	185
CHAPTER 7:COMPARISON OF BONE SCAN AND ¹⁸F CHOLINE PET-CT.....	188
ABSTRACT.....	189
INTRODUCTION	190
MATERIALS AND METHODS.....	191
RESULTS.....	193
DISCUSSION	201
REFERENCES	209
CHAPTER 8: ROLE OF ¹⁸F CHOLINE AS A NOVEL DIAGNOSTIC COMPLEX	210
INTRODUCTION	213
METHODS AND MATERIALS	215
RESULTS.....	221
CONCLUSION.....	235
REFERENCES	236
CHAPTER 9: SUMMARY OF CONCLUSIONS	239
APPENDICES	245
APPENDIX 1-PUBLICATIONS.....	245
APPENDIX 2 -ACADEMIC OUTPUT	248
A) PRIZES/AWARDS: BRITISH NUCLEAR MEDICINE SOCIETY ANNUAL MEETING-1 ST STUDENT RESEARCH PRIZE.....	248
B) PUBLICATIONS AS FIRST AUTHOR.....	249
1) <i>Multicentre study evaluating extra prostatic uptake of ¹¹C-Choline, ¹⁸F -Methyl Choline and ¹⁸F Ethyl Choline in male patients: Physiological distribution, statistical differences, imaging pearls and normal variants.</i>	249
2) <i>¹⁸F-FECH PET/CT to assess clinically significant disease in Prostate Cancer: Correlation with Maximum and Total Cancer Core Length Obtained via MRI-Guided Template Mapping Biopsies.....</i>	250
3) <i>Spectrum of metastatic and non-metastatic skeletal findings with dual-phase ¹⁸F FECH PET-CT in patients with biochemical relapse of prostate cancer.....</i>	251
C) LETTER TO EDITOR	253
D) PUBLICATIONS AS CO-AUTHOR	255
1) <i>Role of Focal salvage ablative therapy in localised radiorecurrent prostate cancer.....</i>	255
2) <i>The FORECAST study-Focal recurrent assessment and salvage treatment for radiorecurrent prostate cancer.....</i>	256
E) ABSTRACTS	257
F) BOOK CHAPTERS	267
<i>PET-Clinics</i>	267
<i>Management of Urological Cancer.....</i>	268
G) LECTURES ON PROSTATE CANCER (LOCAL , REGIONAL, NATIONAL, AND INTERNATIONAL)	269
H) TITLE COVER IMAGE.....	273
APPENDIX 3 -ETHICS APPROVAL LETTER	274
APPENDIX 4- CLINICAL TRIAL PERFORMA	281
FORECAST PET-CT REPORTING PERFORMA.....	281
FORECAST-BONE SCAN PERFORMA	288
APPENDIX 5-RADIOPHARMACY-SYNTHESIS OF ¹⁸F CHOLINE.....	292
APPENDIX 6 -STANDARD OPERATING PROCEDURES	296

18F CHOLINE PET CT	296
18F CHOLINE PET-MR SOP	300

List of Abbreviations

ADC	Apparent Diffusion Coefficient
ANOVA	Analysis of Variance
ADT	Androgen Deprivation Therapy
AUC	Area Under the Curve
BCR	Biochemical Relapse
BS	Bone Scan
CI	Confidence Interval
CT	Computed Tomography
DCE	Dynamic Contrast Enhanced
DICOM	Digital Imaging and Communications in Medicine
DWI	Diffusion Weighted Imaging
EBRT	External Beam Radiotherapy
FN	False Negative
FP	False Positive
IQR	Interquartile Range
IRAS	Integrated Research Approval System
mDixon	Multiecho Dixon
MDT	Multidisciplinary Team
mp	Multiparametric
MR	Magnetic resonance
MRI	Magnetic Resonance Imaging
PACS	Picture Archiving and Communication System
PCa	Prostate Cancer
PET	Positron Emission Tomography
PSA	Prostate Specific Antigen
PSMA	Prostate Specific Membrane Antigen
REC	Research Ethics Committee

ROC Receiver Operating Characteristic
ROI Region of Interest
SD Standard Deviation
SE Spin Echo
SI Signal Intensity
T2W T2-weighted
TE Time to Echo or Echo Time
TN True Negative
TNM Tumour, Nodes, Metastases
TP True Positive
TR Time to Repeat or Repetition Time
TSE Turbo Spin Echo
UCL University College London
UCLH University College London Hospital
WB-MRI Whole Body Magnetic Resonance Imaging

CHAPTER 1: Introduction to Thesis

Epidemiology

In men, prostate cancer is the most common cancer in the UK and there is an increase in incidence of prostate cancer over the past two decades. Prostate cancer is a major cause of cancer related-mortality with around 46,700 cases diagnosed in 2014 (1). It is estimated that between 2014-2035 there would be approximately 233 per 100,000 males with this disease (1). Following prostatectomy within 10 years, recurrence is documented in 20-50% of the cases and rates in excess of 50% have been reported following external beam radiation therapy (2).

Etiology

The etiology of prostate cancer development and mechanisms of prostate cancer progression remains to be further investigated. Possible underlying genetic mechanisms can be gene amplification, gene mutations and changes in expression of androgen receptor co-regulatory proteins (3). Several dietary factors have been consistently associated with risk in observational studies, including selenium and vitamin E, fat intake, red meat, fish, vitamin D, soy and phytoestrogens (4).

Metastatic Spread

The exact metastatic pathway in prostate cancer is not entirely understood. Several lines of evidence suggest the existence of a backward metastatic pathway through veins from the prostate to the spine. This is in addition to common hematogenous spread via the vena cava.

Lymph nodes, bone, lung, and liver are the most frequent sites of distant prostate cancer metastases. Metastases to the spine can be independent of lung metastases and also precede liver metastases in many prostate cancers (5). There is gradual decrease in spine involvement from lumbar to the cervical level.

The most commonly used staging system for Prostate Cancer is American Joint Committee on Cancer (AJCC) TNM (6).

Current Diagnostics

MRI has a key role in the primary diagnosis of prostate cancer. For patients with biochemical relapse, the most commonly used investigations are as follows:

- a) Computed Tomography (CT)
- b) Bone Scan (Technetium-99m)
- c) Positron emission tomography-computed tomography (PET-CT)

Computed Tomography (CT scan)

The main role for CT, is assessment of nodal and distant metastatic disease particularly in patients with radio recurrent prostate cancer. As CT provides anatomical information, lymph node metastases are detected based on size criteria (measured in short axis). The sensitivity of CT for detection of nodal metastases ranges from 20-60% (7). Soft tissue metastases to the lungs and liver can be detected using soft tissue window settings. Multiplanar reconstructions of CT data can provide images of musculoskeletal system for evaluation of bone metastases. In a meta-analysis of 24 studies, CT and MRI demonstrated poor

performance in the detection and exclusion of metastatic lymph nodes from prostate cancer (pooled sensitivity was 42% (25-56%) for CT and 39% (22-56%) for MRI (8)

Bone Scan

Isotope Bone Scan is the most commonly performed test for evaluation of bone metastases. Tc^{99m} is attached to either methylene diphosphonate (MDP) or hydroxy diphosphonate (HDP). The patient is imaged with a gamma camera following injection of radiotracer. Bone Scan has low specificity as there are several non-malignant conditions which are tracer avid e.g., inflammatory, traumatic and degenerative disease processes (9). Sensitivity can be limited for PSA values of <20 ng/ml (10) and probability of bone scan positivity may reach $<10\%$ detection if PSA is <10 ng/ml (7).

Positron Emission Tomography-Computed Tomography (PET-CT)

PET has emerged as a promising imaging tool and is gradually making its way into the pathway for prostate cancer management. The combination of CT with PET (PET-CT) provides a powerful imaging modality which delivers both functional and anatomical information. There are several cellular features which can be imaged with PET such as increased proliferation, receptor expression and metabolic activity (11). Using PET, radiolabelled tracers can provide more insight into management of prostate cancer. At the time I started my research, ^{18}F FDG was one of the earliest tracers used in PET imaging and its role was limited due to poor sensitivity, poor resolution of prostate cancer and excreted activity in the urinary bladder, making assessment difficult.

Clinical need for new biomarker and defining normality

Choline is an integral part of the cell membrane and there is increase in cell proliferation in cancer cells as the phospholipid demand increases. High concentration of Choline can be imaged by positron emission tomography (PET) using radiolabelled choline (^{18}F or ^{11}C). There is an increasing need to have more sensitive image of the whole body for early staging of cancer. In this context, it is essential that normal distribution of biomarkers is available which can be cross referenced during research and clinical work up. There is limited literature describing normal distribution of radiolabelled choline in the body (12). These reports provide limited evaluation of a small number of organs in the body, thus, there is clinical need to perform detailed analysis of all variants of Choline.

Setting up molecular imaging to study micro-environment

To make early diagnosis of cancer it is essential that imaging tests with novel biomarkers can provide information about cellular microenvironment. Angiogenesis is a process of new blood vessel formation observed in physiological as well as pathological states e.g., tissue repair after injury and metastatic spread of cancer respectively (13). Molecular imaging techniques can help assess the damage to blood vessels by providing information about the kinetics of tracer perfusion in the cancerous tissue. There is thus a need to have feasibility data for these tracers. To address this, a PET-CT protocol which is easy to implement on different vendor PET-CT cameras and which provides reproducible qualitative and quantitative data is needed.

Risk Stratification and ¹⁸F Choline PET-CT

Pathology within the prostate gland represents a spectrum of disease in terms of risk. Validation of findings on PET-CT with a reference standard such as biopsy is important to provide true picture of presence or absence of disease. Although, there are plenty of reports correlating findings of PET-CT with ultrasound guided biopsies, there is no report in the literature where findings on Choline PET-CT are correlated with a validated, more accurate standard such as template mapping biopsy (14). Since, the clinicians are using more advanced risk classification systems, there is a need to align the results of Choline PET-CT with uniform method of risk classification system. It is important to explore whether Choline PET-CT can detect clinically significant, insignificant disease and delineate the causes of false positive or false negative results.

Risk stratification and ¹⁸F Choline PET-MR

Integration of PET with MRI as simultaneous PET/MR has added advantage of providing complementary biological and anatomical information. This technique can broaden the horizon of molecular imaging, however, the need for validating this methodology with reference tests such as biopsy remains. There is no report in literature where Choline PET/MR results are compared with Template mapping biopsies.

Varying appearances of the Prostate gland

Biological heterogeneity in prostate cancer presents as a diagnostic challenge and there can be varying appearances of prostate at different stages. Knowledge of spectrum of findings with different biomarkers is also crucial. As there exists a wide differential for abnormal tracer accumulation in prostate gland it is important to have awareness of range of prostatic and periprostatic pathologies.

Spectrum of metastatic disease with Prostate Cancer

In the past decade, tremendous work has been done in elucidating the potential role of PET biomarkers in supplementing MRI for the detection of metastatic disease in morphologically normal lymph nodes, the bone marrow, and the skeleton. While ^{18}F -fluorodeoxyglucose (FDG) is the most common PET/CT tracer worldwide, the results in cases of prostate cancer are less than ideal (15). Consequently, other tracers have been investigated for this purpose, and choline emerged as one of the most common non-FDG PET biomarkers for evaluation of prostate cancer (16). The need to evaluate the spectrum of skeletal findings on ^{18}F -FECH PET/CT in patients undergoing investigation for biochemical relapse of prostate cancer remains.

PET-CT as “Triage Test” for better selection of patients for focal salvage therapy

Finally, it is very important to diagnose intra and extra prostatic disease accurately. Anatomical and functional imaging test should be able to help clinicians decide best treatment for prostate cancer patients. If the recurrent disease is localised, then salvage treatment may be considered an option. There is a drive to introduce new minimally invasive and focal treatments such as high frequency focussed ultrasound (HIFU). Before these treatments are offered it is important to know which imaging test i.e., Bone Scan, Whole Body MRI or ^{18}F Choline is more accurate for detection of radio recurrent prostate cancer.

This thesis will attempt to fill the gaps in knowledge outlined above.

REFERENCES

1. Comprehensive Cancer Information - National Cancer Institute [Internet]. 1980 [cited 2021 Jun 30]. Available from: <https://www.cancer.gov/>
2. Chism DB, Hanlon AL, Horwitz EM, Feigenberg SJ, Pollack A. A comparison of the single and double factor high-risk models for risk assignment of prostate cancer treated with 3D conformal radiotherapy. *Int J Radiat Oncol Biol Phys*. 2004 Jun 1;59(2):380–5.
3. Howard N, Clementino M, Kim D, Wang L, Verma A, Shi X, et al. New developments in mechanisms of prostate cancer progression. *Semin Cancer Biol*. 2019 Aug;57:111–6.
4. Wilson KM, Mucci LA. Diet and Lifestyle in Prostate Cancer. *Adv Exp Med Biol*. 2019;1210:1–27.
5. Bubendorf L, Schöpfer A, Wagner U, Sauter G, Moch H, Willi N, et al. Metastatic patterns of prostate cancer: an autopsy study of 1,589 patients. *Hum Pathol*. 2000 May;31(5):578–83.
6. Edge SB, Compton CC. The American Joint Committee on Cancer: the 7th Edition of the AJCC Cancer Staging Manual and the Future of TNM. *Ann Surg Oncol*. 2010 Jun 1;17(6):1471–4.
7. Kane CJ, Amling CL, Johnstone PAS, Pak N, Lance RS, Thrasher JB, et al. Limited value of bone scintigraphy and computed tomography in assessing biochemical failure after radical prostatectomy. *Urology*. 2003 Mar;61(3):607–11.
8. Hövels AM, Heesakkers R a. M, Adang EM, Jager GJ, Strum S, Hoogeveen YL, et al. The diagnostic accuracy of CT and MRI in the staging of pelvic lymph nodes in patients with prostate cancer: a meta-analysis. *Clin Radiol*. 2008 Apr;63(4):387–95.
9. Padhani AR, Makris A, Gall P, Collins DJ, Tunariu N, de Bono JS. Therapy monitoring of skeletal metastases with whole-body diffusion MRI. *J Magn Reson Imaging*. 2014 May;39(5):1049–78.
10. Tanaka N, Fujimoto K, Shinkai T, Nakai Y, Kuwada M, Anai S, et al. Bone scan can be spared in asymptomatic prostate cancer patients with PSA of ≤ 20 ng/ml and Gleason score of ≤ 6 at the initial stage of diagnosis. *Jpn J Clin Oncol*. 2011 Oct;41(10):1209–13.
11. Rayn KN, Elnabawi YA, Sheth N. Clinical implications of PET/CT in prostate cancer management. *Transl Androl Urol*. 2018 Oct;7(5):844–54.
12. Schillaci O, Calabria F, Tavolozza M, Ciccio C, Carlani M, Caracciolo CR, et al. 18F-choline PET/CT physiological distribution and pitfalls in image interpretation: experience in 80 patients with prostate cancer. *Nuclear medicine communications*. 2010;31(1):39–45.

13. Folkman J. Angiogenesis in cancer, vascular, rheumatoid and other disease. *Nat Med.* 1995 Jan;1(1):27–31.
14. Ahmed HU, Hu Y, Carter T, Arumainayagam N, Lecornet E, Freeman A, et al. Characterizing clinically significant prostate cancer using template prostate mapping biopsy. *J Urol.* 2011 Aug;186(2):458–64.
15. Jadvar H. Prostate Cancer: PET with 18F-FDG, 18F- or 11C-Acetate, and 18F- or 11C-Choline. *J Nucl Med.* 2011 Jan 1;52(1):81–9.
16. Price DT, Coleman RE, Liao RP, Robertson CN, Polascik TJ, DeGrado TR. Comparison of [18 F]fluorocholine and [18 F]fluorodeoxyglucose for positron emission tomography of androgen dependent and androgen independent prostate cancer. *J Urol.* 2002 Jul;168(1):273–80.

CHAPTER 2: Physiological Distribution of Choline

Aim

To evaluate the visceral localization of the three most commonly used choline-based radiotracers (^{11}C -choline, ^{18}F -methylcholine, and ^{18}F -ethylcholine) with the aim of analysing uptake in metabolically and anatomically disease-free patients.

Methods

A total of 1250 standardized uptake values (SUV_{max} , SUV_{mean}) were analysed in 45 anatomical regions in 45 patients (15 patients with ^{11}C -choline, 15 with ^{18}F -methylcholine, and 15 with ^{18}F -ethylcholine). These patients were selected from a cohort of 3721 choline PET/CT studies performed at three teaching hospitals over a period of 10 years. They had no evidence of metabolically active primary disease, metastatic disease, or altered morphology on the CT component of the study or any evidence of disease elsewhere on other imaging modalities. The sites of primary disease (prostate and seminal vesicles) were excluded from evaluation.

Results

No adverse effect was documented when using the three tracers. Visceral localization was same for all three tracers. Viscera with a statistical difference in intensity of uptake included the choroid plexus ($p=0.0001$), occipital lobe ($p=0.014$), parietal lobe ($p=0.008$), cerebellum ($p=0.003$), parotid ($p=0.005$), submandibular gland ($p=0.001$), tonsils ($p=0.001$), thyroid

($p=0.0001$), lungs ($p=0.001$), aorta ($p=0.001$), pulmonary artery ($p=0.0001$), liver segments I ($p=0.005$), III ($p=0.005$), IVB ($p=0.03$), and V ($p=0.01$), spleen [hilum ($p=0.0009$), body ($p=0.0001$)], pancreas [head ($p=0.0001$), body ($p=0.01$), tail ($p=0.002$)], oesophagus ($p=0.001$), stomach ($p=0.0001$), duodenum ($p=0.0002$), large intestine ($p=0.008$), and rectum ($p=0.0001$). Elsewhere no statistical difference was observed. Excreted activity was noted in the kidneys and bladder.

Conclusion

This study demonstrates that the visceral localization of ^{11}C -choline, ^{18}F -methylcholine, and ^{18}F -ethylcholine in disease-free patients is similar. Depending on the tracer uptake pattern, the viscera can be divided into two distinct categories: those with a statistically significant difference in uptake and those with no difference in uptake. The study outlines the range of SUVs for various organs for the three tracers and identifies some of the potential pitfalls in evaluation of “non-avid” but clinically significant presentation of different disease entities.

Introduction

Choline is essential for the biosynthesis of phosphatidylcholine and other phospholipids which are an integral part of the cell membrane. There is increased cell proliferation in cancer cells and phospholipid demand increases. This high content can be imaged by positron emission tomography (PET) using choline labeled with ^{18}F or ^{11}C . The rate of radiolabelled choline uptake in tumours is an indicator of the tumour cell proliferation rate (in both hypoxia and normoxia), whereas with ^{18}F -fluorodeoxyglucose (FDG) tumour hypoxia is closely associated with tumour uptake, and radiolabelled choline might detect malignancies earlier than the ^{18}F -FDG (1). We aimed to evaluate the physiological distribution of the three most commonly used choline-based tracers, namely ^{11}C -choline, ^{18}F -methylcholine, and ^{18}F -ethylcholine. These tracers have variable biokinetics and absorption in the body, but to our knowledge this is the first study to evaluate differences in the physiological biodistribution of these tracers with the aim of analysing statistical differences in metabolically and anatomically disease-free patients.

Methods

As this was a retrospective study, institutional review board or ethical committee approval was not obtained. We retrospectively reviewed cases referred to our institutes for imaging with choline. As most centres rely on use of a single choline-based tracer, depending on availability of an onsite cyclotron and commercial availability, we recruited patients from three different centres:

- University Hospital Sant'Orsola Malpighi, Bologna, Italy, which uses ^{11}C -choline,
- St. Vincent's Hospital, Linz, Austria, which uses ^{18}F -methylcholine,

- University College London Hospital, London, UK, which uses ^{18}F -ethylcholine.

At each centre, the patient database of radiolabelled choline PET scans was reviewed. Inclusion criteria were adult male patients who had been referred for ^{11}C -choline, ^{18}F -methylcholine, or ^{18}F -ethylcholine based imaging for prostate cancer. Major inclusion criteria were no evidence of tracer-avid disease, no history of documented disease in the viscera being analysed, no history of secondary malignancy or documented metastatic disease on any imaging modality, and no history of organ transplantation.

^{11}C -choline

^{11}C -Choline was synthesized according to the solid-phase method in a modified commercial synthesis module (TRACER lab; GE Healthcare). $^{11}\text{CO}_2$ produced by a PET trace cyclotron (GE Healthcare) was converted into $^{11}\text{CH}_3\text{I}$ by the conventional LiAlH_4/HI reaction. $^{11}\text{CH}_3\text{I}$ was used for the N-methylation of dimethylaminoethanol (60 μL) placed directly on a solid-phase support (C18 SepPak Light; Waters). After a washing step with ethanol and water, ^{11}C -choline retained on a cation exchange resin (SepPak Accell Plus CM; Waters) was eluted with saline, sterilized by a 0.22- μm filter, and collected in a final volume of 8 mL. Radiochemical purity was evaluated by means of a high-performance liquid chromatography radio detector equipped with a reversed-phase column, and the concentration of organic solvents was measured by gas chromatography. Endotoxin content was measured by the conventional lysosomal acid lipase method (Cambrex Bioscience). The patients fasted for at least 6 h before the PET acquisition and received an intravenous injection of 370–555 MBq of ^{11}C -choline. Starting 5 min after injection (in accordance with the ^{11}C -choline kinetics results), emission data were acquired at 2–3 bed positions (the ADVANCE has an axial field of view of 15 cm) for 5 min at each position. The parameters of the multidetector helical CT

scan were 140 kV, 80 mA, 0.8 s per tube rotation, slice thickness of 5 mm, pitch of 6, and table speed of 22.5 mm/s. CT images were used for both attenuation correction of emission data and image fusion.

¹⁸F-Methylcholine

¹⁸F-FCH (fluoromethyl-dimethyl-2-hydroxyethyl-ammonium) was synthesized on-site (lasocholine), as described by Vassiliev et al. (2). Imaging was performed with an integrated PET/CT system (Discovery LS; GE Medical Systems, Milwaukee, Wis.) that consisted of a full-ring PET scanner with a 14.6-cm transverse field of view and an in-plane resolution of 4.8 mm full-width at half-maximum at the centre of the field of view and a four-section CT scanner. All PET images were acquired in the two-dimensional mode (4 min emission per bed position), reconstructed with a standard reconstruction ordered-subset expectation maximization iterative algorithm (two iterative steps), and reformatted into transverse, coronal, and sagittal views. As a routine protocol, imaging started 1 min after intravenous injection of FCH (4.07 MBq per kilogram of body weight), with acquisition of dynamic PET images at one constant bed position of the pelvic region (covering the pelvic floor and urinary bladder) for 8 min (1 min per frame) to overcome the effect of urinary activity in the bladder. Six- or seven-bed position whole-body images were acquired with an acquisition time of 4 min per bed position from the thigh to the base of the skull 10 min after injection. The number of images acquired depended on the size of the patient. Unenhanced CT was performed for localization and attenuation correction (140 kV, 0.5 s per rotation, 5.0-mm reconstructed section thickness, 0.5-mm overlap) with a low-beam current modulation (80–120 mA) (3). The reformatted transverse, coronal, and sagittal views were used for interpretation.

¹⁸F-Ethylcholine

¹⁸F-FECH was provided by Erigal (Erigal Limited, Downs Road, Sutton, Surrey, UK), synthesized as described by Hara et al. (4). All quality control parameters were fulfilled during

the commercial preparation. Patients were injected with 300-370 MBq of ^{18}F -FECH [effective dose 12.95 mSv]. Whole-body PET/CT images were acquired 60 min after tracer injection. The CT acquisition parameters included: scout 120 kVp, 10 mA; CT 140 kVp, 80 mA, 0.8 s, pitch 1.75; CT slices 5 mm (70-cm FOV PET AC), 2.5 mm (50-cm FOV Std), 2.5 mm (50-cm FOV Lung). PET acquisition parameters were 3D attenuation-corrected and non-attenuation-corrected images, 20 subsets with iterative reconstructions. CT images were used to produce attenuation correction values for PET emission reconstruction and fused PET/CT presentation.

At all three centres, patients were asked to empty their bladder before the start of the scan to minimize the effect of excreted activity in the adjacent tissues.

PET/CT Reading

The evaluation of studies was performed in stages:

From the database only those cases were selected which were negative for any tracer-avid extra prostatic disease on the original scan report. In these subjects the case notes were reviewed. Only those patients were selected who did not have any evidence of disease progression or metastases over a prolonged follow-up period (range 1.5-5 years) following the original study. In the first instance a radiologist (A.H.) reviewed the CT component of the PET/CT studies (all tracers) to exclude altered morphology, normal anatomical variants which may affect the SUV, and evidence of metastatic disease based on radiological appearances.

The final review of the PET/CT studies was performed by A.H. and L.Z. utilizing a Xeleris workstation (GE Healthcare) which allows simultaneous scrolling through the corresponding PET, CT, fused, and MIP (maximum intensity projection) images. At this stage 45 anatomical regions were selected after mutual agreement. Semiquantitative analysis of tracer uptake was performed using the SUV_{max} (maximum standardized uptake value) and SUV_{mean} .

Regions of interest (ROIs) were drawn over three consecutive slices on the PET images centered around the maximum voxel value, and SUV_{max} and SUV_{mean} in the selected ROIs were recorded. The ROIs were always placed well within the limits of the activity distribution to minimize the partial volume effect.

Statistical analysis

SUV_{max} and SUV_{mean} were calculated using a 1 cm^3 volume of interest. The values thus obtained were plotted against the ROIs; range and standard deviations were further calculated. ANOVA was performed between ^{11}C -choline, ^{18}F -methylcholine and ^{18}F -ethylcholine to ascertain whether there was any statistical difference between the three tracers. In the event of a significant difference ($p < 0.05$), further analysis between the groups was performed to identify which groups had a statistically significant difference.

Results

The age range of the selected subjects was 40-85 years (median 55 years). No adverse effect was documented secondary to tracer injection in any of these patients. The conventional MIP images showed physiological uptake of radiolabelled choline at the following sites: choroid plexus, pituitary gland, salivary glands, tonsils, liver, spleen, pancreas, bone marrow, lungs, and gastrointestinal tract (Fig. 1). The anatomical regions evaluated are listed in Tables 1 and 2.

TABLE 1: SUV_{max} with ¹¹C-choline, ¹⁸F-methylcholine, and ¹⁸F-ethylcholine. The standard deviation and p value (calculated with ANOVA test) are listed. If there was a significant difference (p<0.05), further analysis between groups was performed to identify which groups had a statistically significant difference. This is displayed in the last column, “Significance between tracers,” and highlighted.

Region	¹¹ C-choline (C)		¹⁸ F-ethylcholine (E)		¹⁸ F-methylcholine (M)		p value	Significance between tracers
	Mean	SD	Mean	SD	Mean	SD	ANOVA	
Choroid plexus	0.938	0.165	0.46	0.21	0.94	0.23	0.0001	E<C/M
Frontal lobe	0.27	0.24	0.17	0.13	0.22	0.05	0.34	
Occipital lobe	0.27	0.21	0.14	0.08	0.28	0.05	0.014	E<C/M
Parietal lobe	0.22	0.12	0.11	0.06	0.23	0.02	0.008	E<C/M
Temporal lobe	0.28	0.12	0.2	0.09	0.33	0.12	0.04	
Cerebellum	0.29	0.11	0.17	0.07	0.26	0.08	0.003	E<C/M
Pituitary	2.04	0.59	1.85	0.52	2.26	0.71	0.44	
Lacrimal gland	1.89	0.56	1.99	0.7	2	0.61	0.95	
Eye	0.72	0.51	0.52	0.3	0.83	0.15	0.22	
Parotid	5.25	1.63	4.8	1.05	6.59	1.69	0.005	M>C/E
Submandibular gland	6.61	1.94	5.03	0.74	6.97	1.36	0.001	E<C/M
Tonsils	2.19	0.86	2.25	0.57	3.47	1.04	0.001	M>C/E
Submental	1.98	0.97	2.17	0.49	3.2	0.26	0.21	
Thyroid	2.35	0.66	1.37	0.42	2.7	0.74	0.0001	E<C/M
Right upper lobe	0.73	0.27	0.58	0.15	0.89	0.4	0.02	E<M
Left upper lobe	0.73	0.24	0.52	0.11	0.89	0.44	0.005	E<C/M
Right middle lobe	0.66	0.28	0.5	0.18	0.73	0.42	0.12	
Right lower lobe	0.86	0.34	0.58	0.21	1.12	0.54	0.001	E<C/M
Left lower lobe	0.92	0.39	0.7	0.18	1.05	0.52	0.06	
Aorta	0.74	0.28	0.58	0.22	0.92	0.2	0.001	E<C/M

Pulmonary artery	0.59	0.28	0.53	0.22	0.9	0.16	0.0001	M>C/E
Right hilum	1.45	0.58	1.01	0.29	1.65	0.45	0.01	E<C/M
Left hilum	1.01	0.46	0.84	0.34	1.76	0.55	0.0001	M>C/E
Liver I	7.07	2.16	7.81	1.45	9.39	1.57	0.005	M>C/E
Liver II	7.88	2.67	8.96	1.76	9.45	1.32	0.12	
Liver III	8.14	2.07	9.33	1.15	10.49	1.89	0.005	M>C
Liver IVA	8.84	3.1	9.7	1.78	10.7	1.98	0.07	
Liver IVB	8.32	2.5	9.45	1.24	10.44	1.4	0.03	M>C
Liver V	7.8	2.01	9.97	1.46	9.13	1.63	0.01	M>C
Liver VI	8.26	2.22	9.98	1.2	8.99	2.55	0.14	
Liver VII	8.69	2.53	9.53	1.44	9.3	2.11	0.57	
Liver VIII	8.44	2.98	9.6	0.75	9.97	1.81	0.16	
Spleen, hilum	3.01	1.2	2.08	0.75	3.79	0.96	0.0009	E<M
Spleen, body	4.84	1.39	2.76	0.63	5.14	1.02	0.0001	E<C/M
Pancr. head	10.44	3.37	6.86	1.91	11.16	2.27	0.0001	E<C/M
Pancr. body	9.18	2.77	6.77	1.67	9.35	2.15	0.01	E<C/M
Pancr. tail	8.94	2.34	6.6	1.88	9.18	1.9	0.002	E<C/M
Oesophagus	1.01	0.38	0.95	0.36	1.49	0.46	0.001	M>C/E
Stomach	6.66	1.74	3.96	1.54	6.93	1.99	0.0001	E<C/M
Duodenum	3.89	1.78	3.56	1.18	5.87	1.41	0.0002	M>C/E
Small intestine	3.85	1.74	3.57	0.6	4.66	1.06	0.057	-
Large intestine	3.97	3.08	1.5	0.66	2.91	1.15	0.008	E<C/M
Sigmoid	2.06	0.61	1.62	0.86	2.65	0.76	0.002	M>C/E
Rectum	1.58	0.4	1.42	0.59	2.52	0.49	0.0001	M>C/E
Kidney	12.67	4.9	8.23	1.27	19	2.99	0.0001	All:E<C<M
Bladder	12.49	14.86	23.15	14.97	38.86	18.73	0.0005	M>C/E

TABLE 2: SUV_{mean} with ¹¹C-choline, ¹⁸F-methylcholine, and ¹⁸F-ethylcholine. The standard deviation and p value (calculated with ANOVA test) are listed. If there was a significant difference (p<0.05), further analysis between groups was performed to identify which groups had a statistically significant difference. This is displayed in the last column, “Significance between tracers,” and has been highlighted.

Region	¹¹ C-choline (C)		¹⁸ F-ethylcholine (E)		¹⁸ F-methylcholine (M)		p value	Significance between tracers
	Mean	SD	Mean	SD	Mean	SD	ANOVA	
Choroid plexus	0.47	0.17	0.35	0.16	0.45	0.06	0.23	
Frontal lobe	0.14	0.09	0.13	0.09	0.15	0.03	0.90	
Occipital lobe	0.15	0.11	0.12	0.06	0.2	0.07	0.23	
Parietal lobe	0.12	0.05	0.1	0.05	0.13	0.01	0.39	
Temporal lobe	0.18	0.09	0.16	0.07	0.24	0.09	0.21	
Cerebellum	0.18	0.08	0.14	0.05	0.15	0.01	0.22	
Pituitary	1.15	0.44	1.42	0.38	1.14	0.33	0.18	
Lacrimal gland	1.21	0.4	1.61	0.55	1.3	0.31	0.23	
Eye	0.45	0.32	0.37	0.13	0.49	0.03	0.46	
Parotid	4.26	1.2	4.46	0.99	5.13	1.52	0.17	
Submandibular gland	5.06	1.35	4.5	0.73	5.08	1.03	0.25	
Tonsils	1.59	0.76	1.88	0.47	2.37	0.74	0.04	C<M
Submental	1.45	0.63	1.88	0.39	2.23	0.06	0.15	
Thyroid	1.75	0.34	1.21	0.35	1.87	0.51	0.001	E<C/M
Right upper lobe	0.58	0.16	0.53	0.15	0.6	0.26	0.60	
Left upper lobe	0.63	0.31	0.49	0.1	0.67	0.31	0.14	
Right middle lobe	0.51	0.12	0.45	0.15	0.56	0.29	0.33	

Right lower lobe	0.71	0.29	0.54	0.19	0.83	0.46	0.06	
Left lower lobe	0.76	0.37	0.67	0.18	0.76	0.44	0.73	
Aorta	0.59	0.21	0.55	0.2	0.66	0.13	0.26	
Pulmonary artery	0.46	0.23	0.48	0.18	0.62	0.13	0.04	M>C/E
Right hilum	1.12	0.44	0.92	0.23	1.15	0.25	0.17	
Left hilum	0.78	0.33	0.75	0.28	1.23	0.35	0.0003	M>C/E
Liver I	5.9	1.93	7.2	1.47	7.5	1.21	0.02	C<M
Liver II	6.46	2.33	8.33	1.5	7.1	1.4	0.04	E>C/M
Liver III	6.5	1.76	8.89	1.13	8.15	1.43	0.0007	C<E/M
Liver IVA	7.46	2.57	9.3	1.93	8.32	1.46	0.12	
Liver IVB	7.39	2.16	9.08	1.23	8.16	1.77	0.12	
Liver V	6.7	1.51	9.69	1.45	7.24	1.39	0.0001	E>C/M
Liver VI	7.2	1.68	9.58	1.37	7.61	1.39	0.001	E>C/M
Liver VII	7.53	2.16	9.24	1.56	7.73	1.93	0.06	
Liver VIII	7.22	2.8	9.38	0.77	8.26	1.67	0.03	C<E
Spleen, hilum	2.23	0.85	1.85	0.46	2.46	0.57	0.09	
Spleen, body	4.09	0.85	2.68	0.59	4.23	0.9	0.0001	E<C/M
Pancr. head	8.63	2.63	6.21	1.67	8.57	1.85	0.004	E<C/M
Pancr. body	7.38	2.44	6.3	1.5	6.79	1.68	0.38	
Pancr. tail	7.28	2.35	6.01	1.82	6.8	1.5	0.21	
Oesophagus	0.78	0.31	0.86	0.34	1.08	0.33	0.04	C<M
Stomach	5.5	1.65	3.67	1.4	5.17	1.68	0.01	E<C/M
Duodenum	2.81	1.26	3.32	1.23	4.07	0.87	0.01	C<E/M
Small intestine	2.98	1.13	3.36	0.57	3.29	0.83	0.46	
Large intestine	3.26	2.73	1.37	0.6	1.82	0.64	0.01	C<E
Sigmoid	1.6	0.52	1.44	0.81	1.67	0.47	0.59	
Rectum	1.22	0.34	1.3	0.53	1.68	0.35	0.009	M>C/E
Kidney	9.99	2.68	7.94	1.33	15.09	2.77	0.0001	All: E<C<M
Bladder	10.11	12.75	21.07	12.93	28.62	12.74	0.001	C<E/M

On “subjective assessment,” the pattern of tracer distribution was similar, and the readers were unable to differentiate between the three tracers. Visceral localization was almost the same for all three choline-based tracers.

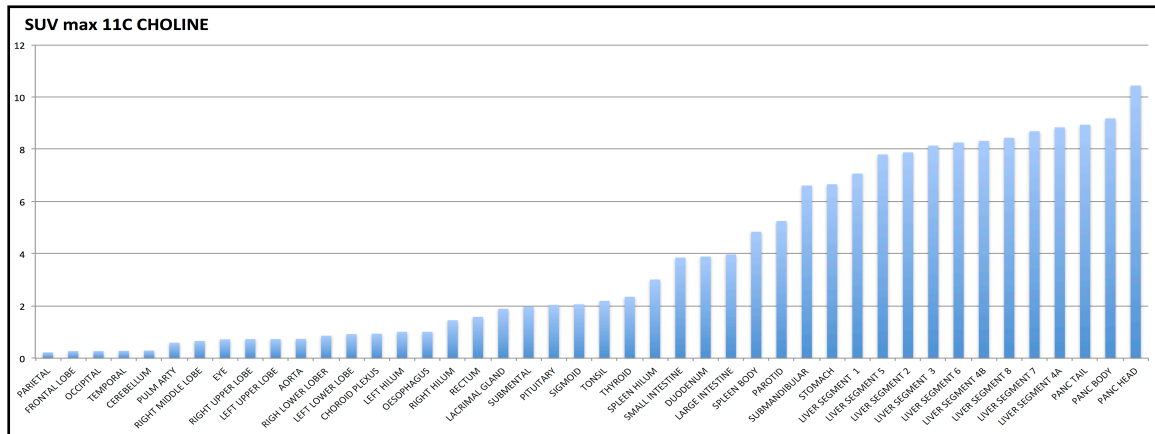
On “objective” assessment and based on detailed statistical analysis of tracer uptake, two distinct categories were obtained:

- (a) Viscera with no statistically significant difference in uptake between the choline-based tracers
- (b) Viscera with a statistically significant difference in uptake between the choline-based tracers

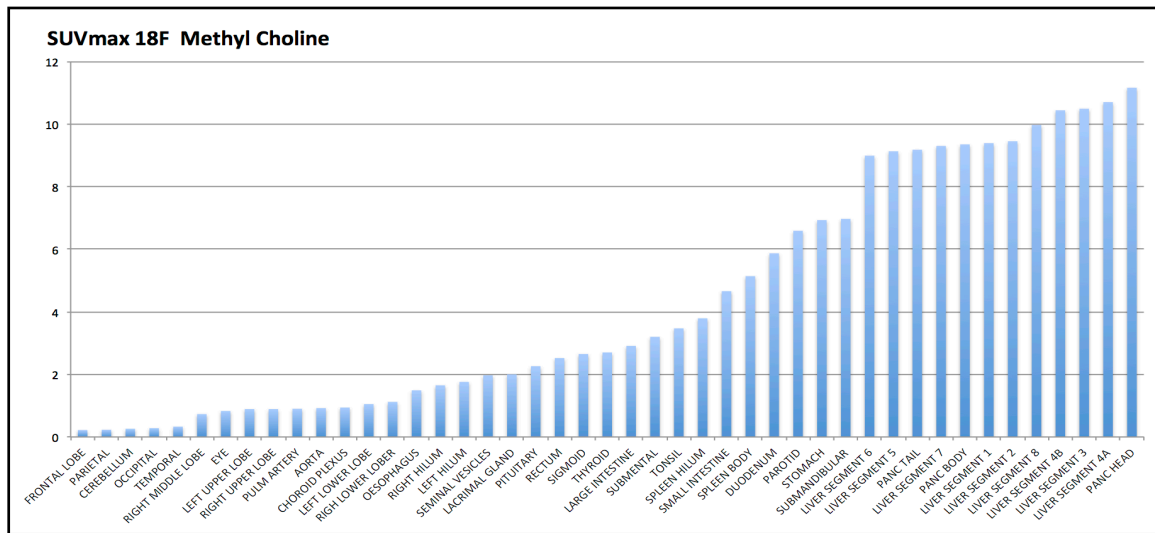
Viscera with no statistical difference between uptake of ^{11}C -choline, ^{18}F -methylcholine, and ^{18}F -ethylcholine included the frontal lobe, temporal lobe, pituitary gland, lacrimal glands, eyes, submental nodes, right middle lobe of the lung, right lower lobe, left lower lobe, liver segments VI, VII, and VIII, and small intestine, The p values for SUV_{max} and SUV_{mean} are shown in Tables 1 and 2.

Viscera with a statistical difference in intensity of uptake included the choroid plexus ($p=0.0001$), occipital lobe ($p=0.014$), parietal lobe ($p=0.008$), cerebellum ($p=0.003$), parotid ($p=0.005$), submandibular gland ($p=0.001$), tonsils ($p=0.001$), thyroid ($p=0.0001$), right upper lobe ($p=0.02$), left upper lobe ($p=0.005$), right lower lobe ($p=0.001$), aorta ($p=0.001$), pulmonary artery ($p=0.0001$), right hilum ($p=0.01$), left hilum ($p=0.0001$), liver segments I ($p=0.005$), III ($p=0.005$), IVB ($p=0.03$), and V ($p=0.01$), spleen [hilum ($p=0.0009$), body ($p=0.0001$)], pancreas [head ($p=0.0001$), body ($p=0.01$), tail ($p=0.002$)], oesophagus ($p=0.001$), stomach ($p=0.0001$), duodenum ($p=0.0002$), large intestine ($p=0.008$), and rectum ($p=0.0001$). Excreted activity was noted in the kidneys and bladder. The findings are listed in detail in Tables 1 and 2.

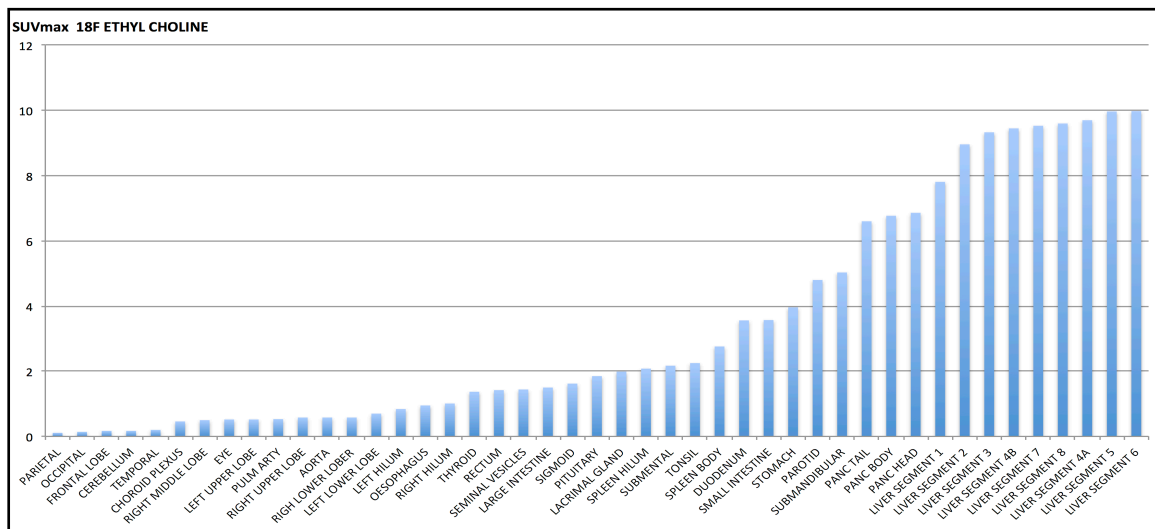
FIGURE 1a-f. SUV_{max} (a-c) and SUV_{mean} (d-f) values for the three tracers



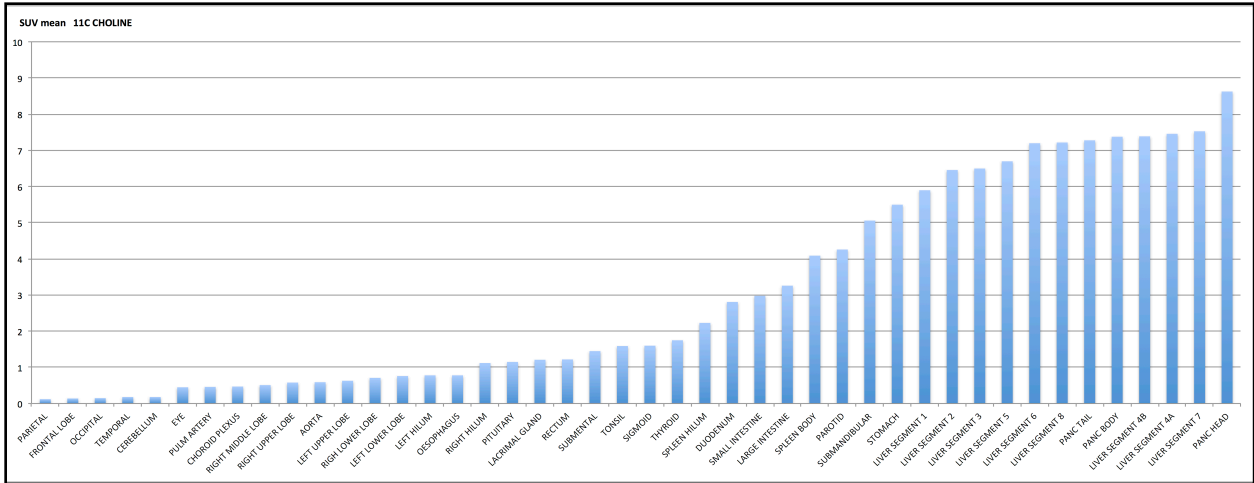
1a



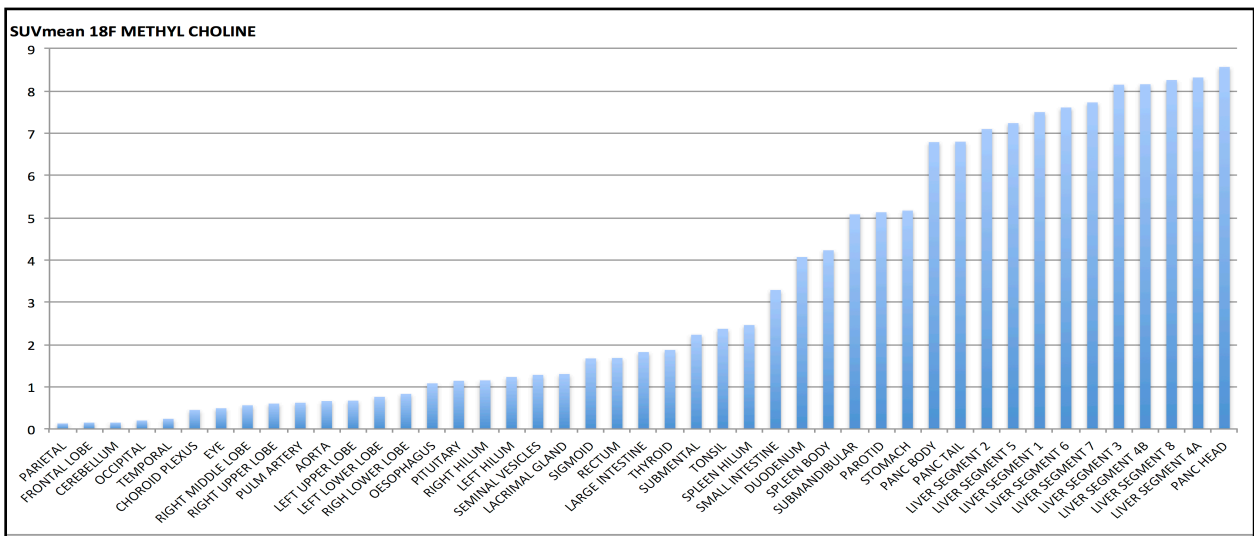
1b



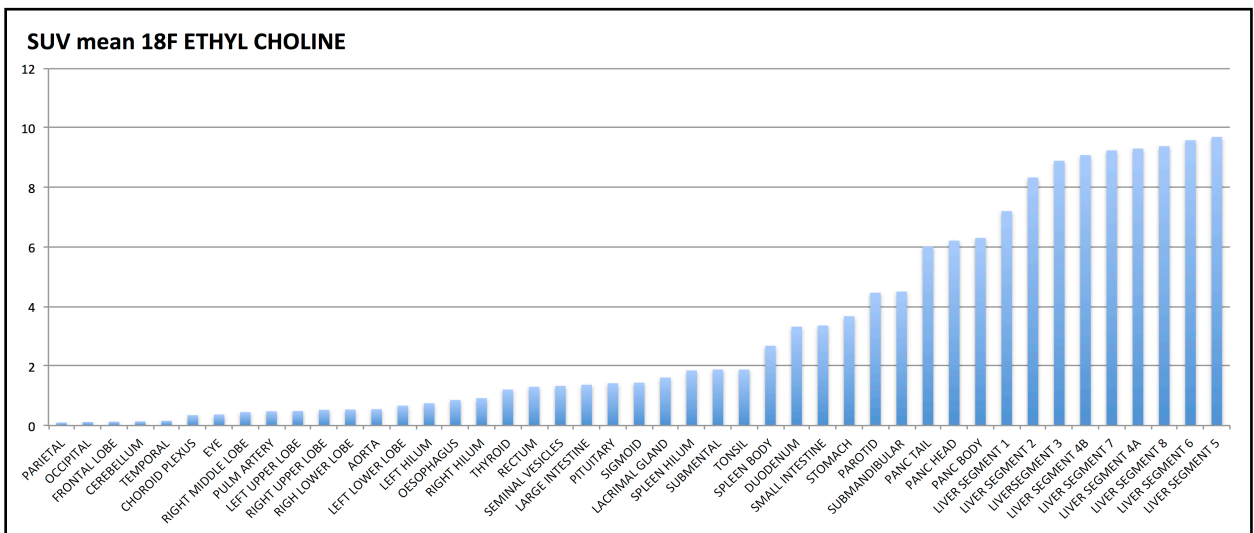
1c



1d



1e



1f

Discussion

This work is the first study to compare and quantify the statistical differences in the uptake pattern of the three most used radiolabelled choline-based PET tracers, i.e., ^{11}C -choline, ^{18}F -methylcholine, and ^{18}F -ethylcholine.

The pituitary gland was avid for all three tracers, with no significant difference in the uptake pattern between them (p value for SUV_{max} 0.44, p value for SUV_{mean} 0.18). Further confirmation was sought with the help of PET/MRI utilizing ^{18}F -ethylcholine, which yielded anatomical and functional information about the pituitary gland (Figs. 2,3). Our findings in respect of pituitary gland uptake differ from the work of colleagues (5) who have not listed the pituitary gland as a choline-tracer-avid structure. Moreover, a previous study by Schillaci et al. (6) describing the physiological uptake of choline found only one case in which the pituitary gland was tracer avid on choline PET. The reason for the latter results is unclear; however, it can be speculated that it relates to the PET/CT field of view, as most centres image from the skull base to the mid-thigh level and it is very easy to miss a structure located at the edge of the field of view.



FIGURE 2: ¹⁸F-ethylcholine PET (MIP) image showing uptake in the pituitary, salivary glands, liver, spleen, kidneys, pancreas, and bowel. There is excreted activity in the urinary bladder.

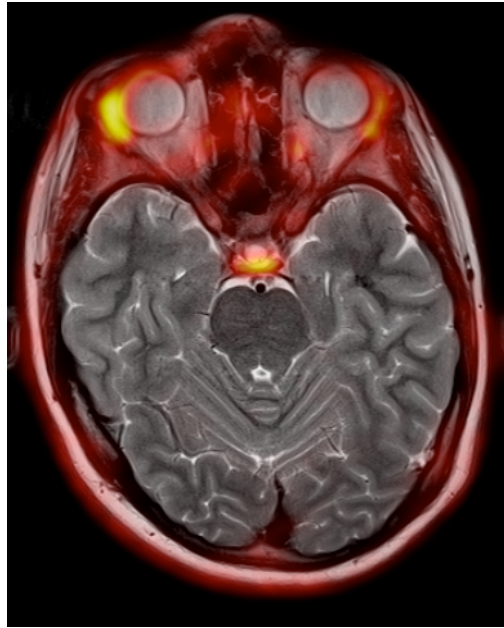


FIGURE 3: Simultaneous 18F-ethylcholine PET/MR scan at the level of the pituitary gland: axial T2-weighted image demonstrating physiological uptake in the pituitary gland

The choroid plexus demonstrated mild to moderate bilateral symmetrical uptake . No activity was noted in the spinal cord, essentially confirming that activity is not present in the cerebrospinal fluid.

Brain uptake of choline is low compared to that in the extracerebral tissues. There are two kinds of energy-dependent transport system for choline incorporation in the cell membrane (7):

a) Phosphoryl choline synthesis: This is present in all mammalian cells.

b) Acetyl choline synthesis: This is present in the synaptosomes (cholinergic nerve endings), and the transport of choline is coupled to acetyl choline synthesis.

The fact that phosphoryl choline synthesis is increased in tumours, forms the basis for the clinical application of choline-based tracers in brain cancer imaging. However, we would

highlight that in some non-malignant (clinically significant) pathologies of the brain parenchyma, choline-based tracers may not demonstrate increased uptake although the blood-brain barrier is broken. An example is cerebral infarction (Fig. 4), where the intensity of uptake (low-grade uptake not apparent on visual inspection) does not differ from that in normal brain parenchyma.

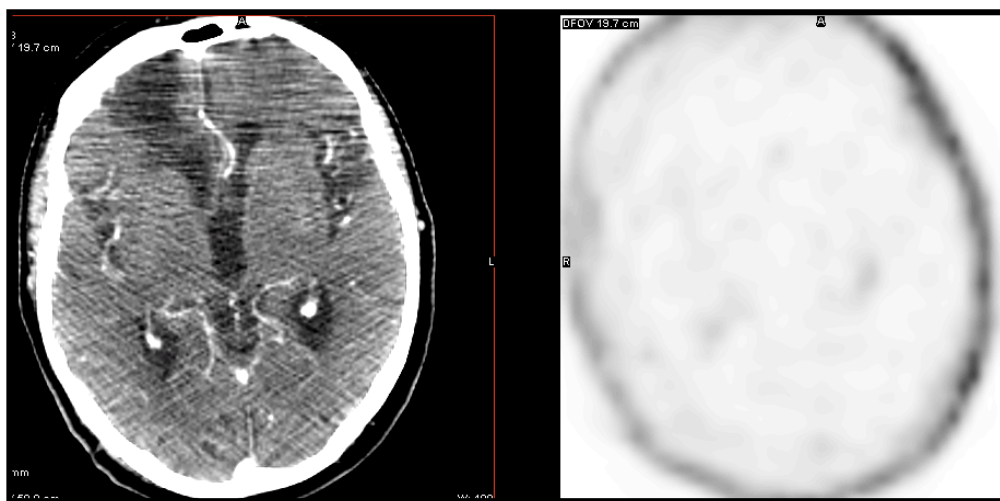


FIGURE 4: Contrast-enhanced CT and PET with ^{18}F -methylcholine in a patient with right-sided frontal lobe encephalomalacia as a sequela of a previous infarct. Physiological lack of avidity in the brain parenchyma makes it challenging to exclude such anatomical abnormalities. This is evident in the CT image and very difficult to appreciate on the PET only image.

The thyroid is an important structure which shows mildly increased tracer uptake on ^{18}F -methylcholine PET. However, it is not clear whether this increase is related to an inflammatory process (autoimmune thyroiditis, etc.) or simply reflects a physiological pattern. Asymmetrical focal uptake in the thyroid gland should be correlated with CT to assess gland asymmetry and evaluated further with ultrasound to exclude an underlying neoplastic process (Fig. 5).



FIGURE 5: Axial ^{18}F Ethyl Choline PET/CT image of the thyroid showing asymmetrical uptake in the left lobe of the thyroid gland. Fine-needle aspiration cytology showed a hyperplastic nodule (Thy2). Subtle low-density uptake in the right lobe was due to a colloid cyst.

Salivary glands are avid for choline-based tracers. No statistical difference in submandibular gland uptake was observed between ^{18}F -methylcholine and ^{11}C -choline, while lower uptake was seen for ^{18}F -ethylcholine. The difference in the SUV_{max} values ranged between 5 and 7 for the three tracers, but the presence of dental metalwork poses a challenge when attempting to exclude underlying malignancy as metalwork can cause beam hardening and may also affect the SUV. This problem can be partly addressed by utilizing a beam-hardening algorithm (appropriately adjusting the window level settings to decrease the

intensity of metal beam artefact at the metal soft tissue interface). Such areas are best evaluated on multiplanar reconstructions.

In lungs, the role of choline has been evaluated for malignancies like adenocarcinoma and bronchoalveolar cell cancer (8, 9, 10). Lung parenchyma is non-avid for all three tracers, with the exception that curvilinear uptake was noted along the thoracic wall, predominantly at the lung bases and at the periphery. This may represent a dependent change as patients were scanned in the supine position. The surface tension of lung parenchyma is maintained by surfactant secreted by type II alveolar cells. Increased concentration of surfactant is seen in the alveoli in cases of pulmonary edema. If there is diffuse increased uptake in the lungs (Fig. 6), without any underlying focal abnormality of lung tissue, this may indirectly represent a sequela of pulmonary venous imbalance (in most cases secondary to cardiomegaly and heart failure).

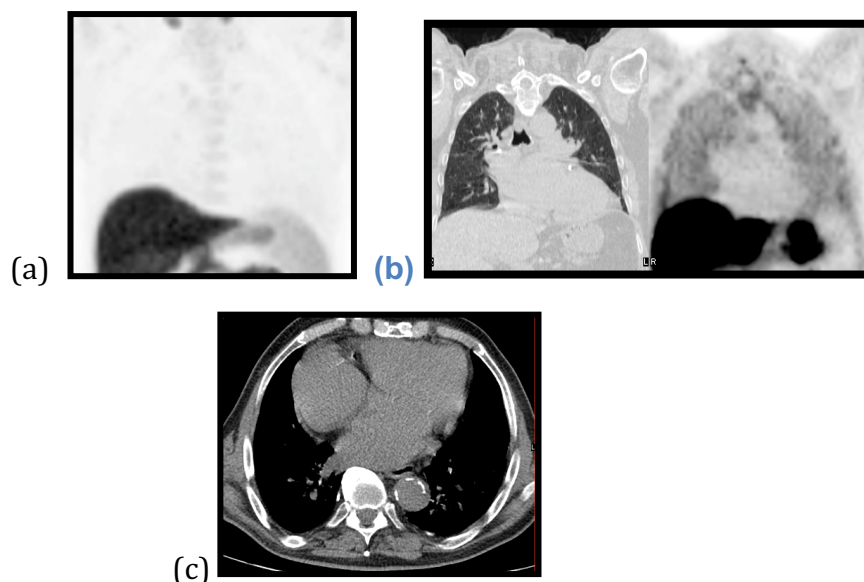


Figure 6: Physiological uptake pattern with 18F Ethyl Choline is shown in Figure 6 (a). Fig 6 (b) relates to diffuse increased uptake with 18F Ethyl Choline in the lungs in a patient with

cardiomegaly (c) and enlarged pulmonary arteries causing pulmonary venous imbalance which may have been an indirect sequela of cardiomyopathy.

Diffuse increased uptake of choline was seen in the liver with all three tracers. The SUV_{max} values for ^{18}F -methylcholine were noted to be highest, followed by those for ^{11}C -choline and ^{18}F -ethylcholine. A statistically significant difference in values was observed between ^{18}F -methylcholine and ^{11}C -choline, the difference being greatest for liver segment III (SUV_{max} $p=0.005$).

There was a statistically significant difference in the uptake by the splenic body compared with the splenic hilum [SUV_{mean} : $p=0.0001$ (body) vs $p=0.09$ (hilum); SUV_{max} : $p=0.0001$ (body) vs $p=0.0009$ (hilum)], with least uptake seen with ^{18}F -ethylcholine.

A heterogeneous pattern of uptake was seen within the pancreas when comparing the pancreatic head, body, and tail (Fig. 1), with the pancreatic head being the most avid of all the soft tissue structures (excluding excretory activity in the kidneys/bladder). There was no statistically significant difference between the uptake of ^{18}F -methylcholine and ^{11}C -choline in the pancreatic head. Least uptake was seen with ^{18}F -ethylcholine; this difference was statistically significant, and the pancreatic uptake of this tracer was less than that in the liver.

The gastrointestinal tract also demonstrated a heterogeneous pattern of uptake. An interesting observation was the lack of an absolute anatomical cut-off regarding definition of an avid and a non-avid region in the transverse colon. It was noted that the distal small bowel, cecum, and proximal/mid transverse colon were less avid for all three choline-based tracers. The zone of avid/non-avid transition appeared to vary between the mid transverse colon and the splenic flexure. Beyond the splenic flexure, the descending colon, sigmoid colon, and rectum were again noted to be avid. The mid/distal part of the small bowel, the cecum, the

ascending colon, and the mid part of the transverse colon were non-avid. The zone of transition of metabolic activity varied slightly between the three tracers, but there was clearly a transition from non-avid bowel to heterogeneously avid bowel at the mid transverse colon level overlapping with the arterial course of the middle colic artery. Physiological colon uptake of ^{11}C has been demonstrated to be lower than uptake in the small intestine (rapid turnover of the epithelial cells could be a contributory factor), whereas physiological colon uptake of FDG is higher than in the small intestine (1). The role of choline PET in the detection of colon cancer has been described previously (1, 11). We would like to highlight that focal moderate to intense uptake in the region of non-avid territory (i.e., mid small bowel to mid transverse colon) should be investigated for possible malignant lesions (Fig. 7).

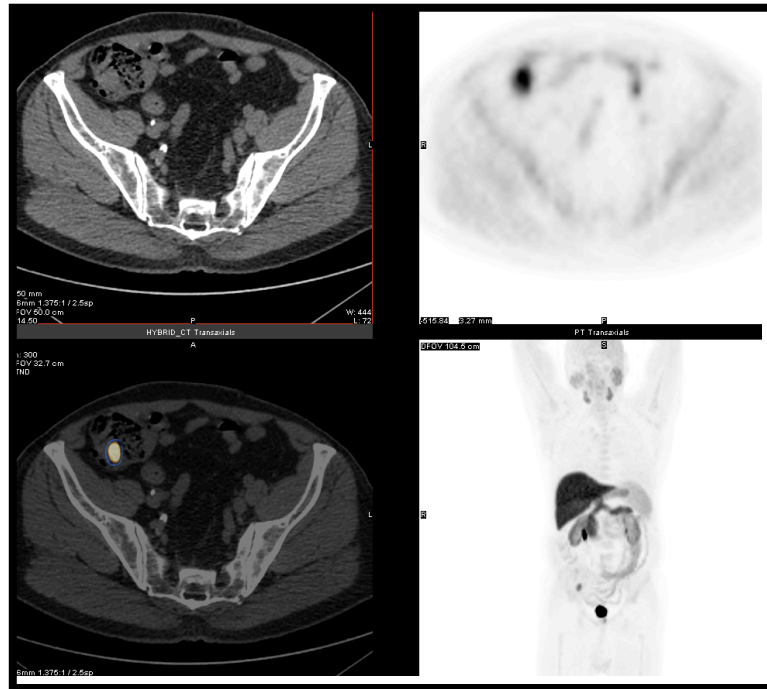


Fig 7: As choline activity is lacking in the distal part of the small bowel (unlike with ^{18}F FDG, where uptake in the ileo-caecal region is normal variant), any evidence of choline kinase activity should be considered cautiously in this region. Note that in this case there is focal uptake with ^{18}F Ethyl Choline in the caecum which was confirmed with biopsy to be tubule-villous adenoma.

Limitations of the study

One potential criticism of this study is that we evaluated those patients who had a previous history of prostate malignancy. It would be ethically difficult to justify radiation exposure of healthy volunteers simply to evaluate normal biodistribution. We therefore relied on evaluation of retrospective data, but we attempted to optimize selection of patients as far as possible, in that the available anatomical and functional studies were negative for any evidence of tracer-avid or structural disease. Theoretically, there is a possibility that these patients had micro metastases which were undetectable by imaging modalities; however, we did not find any evidence of malignant disease in the clinical and/or imaging follow-up studies.

Most of the patients were referred for possible disease relapse following an original diagnosis of prostate cancer and the study was restricted to male subjects. We could not recruit female patients as not all three institutes were performing choline PET as part of the routine clinical care for gynaecological malignancies. The cases were recruited from three different institutes (University College London Hospital, London, UK; Department of Nuclear Medicine, University Hospital Sant' Orsola Malpighi, Bologna, Italy; and St. Vincent's Hospital, Linz, Austria) since there was no single centre where evaluation of suspected prostate cancer relapse was being performed with all three tracers at the same time. In this respect, one restriction is the need for an onsite cyclotron for synthesis of ^{11}C -choline.

We excluded evaluation of the genitourinary structures at previous possible disease sites, e.g., prostate gland and seminal vesicles, to avoid the possibility of measuring SUVs in the region of a previous cancerous tissue.

Finally, the use of different acquisition and reconstruction protocols may also have been a source of bias in SUV measurement and data analysis.

Conclusion

This study comprised a detailed analysis of the distribution pattern of the three most used choline tracers: ^{18}F -methylcholine, ^{11}C -choline, and ^{18}F -ethylcholine. The ranges of SUV_{max} and SUV_{mean} and standard deviations have been presented. In addition, some potential pitfalls in evaluation of “non-avid” but clinically significant presentation of different disease entities have been identified. Although the visceral biodistribution is generally similar for the choline-based tracers, knowledge of the physiological distribution and specific variations in uptake patterns is vital for assessment of various organs when imaging is performed for evaluation of metastatic disease.

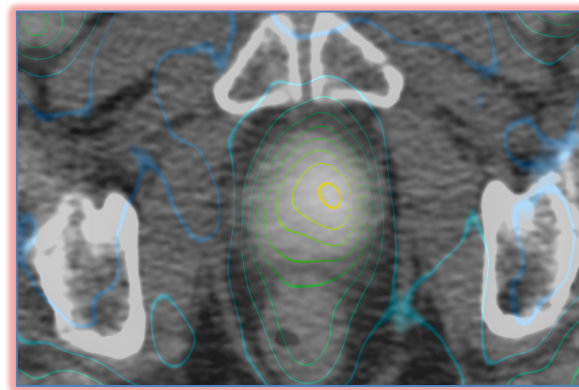
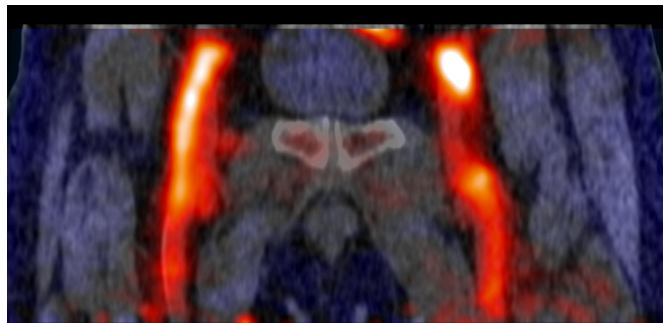
ACKNOWLEDGEMENT

There is no conflict of interest to declare, and no funding was received for this study. This work was undertaken at University College London Hospital, London, which receives a proportion of its funding from the UK’s Department of Health NIHR Biomedical Research Centres funding scheme.

References:

1. Terauchi T, Tateishi U, Maeda T, et al. A Case of Colon Cancer Detected by Carbon-11 Choline Positron Emission Tomography/Computed Tomography: An Initial Report. *Japanese Journal of Clinical Oncology*. 2007;37(10):797–800. doi:10.1093/jjco/hym102.
2. Vassiliev D, Krasikova R, Kutznetsova O, Federova O, Nader M. Simple HPLC method for the detection of N, N-dimethylaminoethanol in the preparation of [N-methyl-11C] choline. *Eur J Nucl Med Mol Imaging*. 2003;30:342P.
3. Beheshti M, Imamovic L, Broinger G, et al. 18F choline PET/CT in the preoperative staging of prostate cancer in patients with intermediate or high risk of extracapsular disease: a prospective study of 130 patients. *Radiology*. 2010;254(3):925–933. doi:10.1148/radiol.09090413.
4. DeGrado TR, Baldwin SW, Wang S, et al. Synthesis and evaluation of (18)F-labeled choline analogs as oncologic PET tracers. *J Nucl Med*. 2001;42(12):1805–1814.
5. DeGrado TR, Reiman RE, Price DT, Wang S, Coleman RE. Pharmacokinetics and radiation dosimetry of 18F-fluorocholine. *J Nucl Med*. 2002;43(1):92–96.
6. Schillaci O, Calabria F, Tavolozza M, et al. 18F-choline PET/CT physiological distribution and pitfalls in image interpretation: experience in 80 patients with prostate cancer. *Nucl Med Commun*. 2010;31(1):39–45.
7. Friedland RP, Mathis CA, Budinger TF, Moyer BR, Rosen M. Labeled Choline and Phosphorylcholine: Body Distribution and Brain Autoradiography: Concise Communication. *J Nucl Med*. 1983;24(9):812–815.
8. Wang T, Li J, Chen F, et al. Choline Transporters in Human Lung Adenocarcinoma: Expression and Functional Implications. *Acta Biochimica et Biophysica Sinica*. 2007;39(9):668–674. doi:10.1111/j.1745-7270.2007.00323.x.
9. Peng Z, Liu Q, Li M, Han M, Yao S, Liu Q. Comparison of 11C-Choline PET/CT and Enhanced CT in the Evaluation of Patients With Pulmonary Abnormalities and Locoregional Lymph Node Involvement in Lung Cancer. *Clinical Lung Cancer*. 2012;13(4):312–320. doi:10.1016/j.clcc.2011.09.005.
10. Balogova S, Huchet V, Kerrou K, et al. Detection of bronchioloalveolar cancer by means of PET/CT and 18F-fluorocholine, and comparison with 18F-fluorodeoxyglucose. *Nuclear Medicine Communications*. 2010;1. doi:10.1097/MNM.0b013e3283369654.
11. Calabria FF, Crusco S, Ciccio C, Schillaci O. A Case of Colon Cancer Incidentally Detected by 18F-Choline PET/CT. *Clin Nucl Med*. 2013. doi:10.1097/RLU.0b013e3182a43045.

CHAPTER 3: Molecular Imaging of Tumour Blood Vessels Proliferation(Angiogenesis) in Prostate Cancer Using Dynamic ¹⁸F Choline PET-CT



Overview:

In this chapter the feasibility of assessing dynamic ^{18}F Ethyl Choline PET is assessed with a view to do kinetic modelling in clinical setting of biochemical relapse of Prostate Cancer.

Research questions:

This is a proof of concept study with following research questions

1. Is it clinically feasible to perform dynamic Choline PET study?
2. Can we quantify uptake with standardised uptake value (SUV)?
3. Can we evaluate the tracer kinetics?
4. Can we demonstrate correlation between ^{18}F Choline kinetic variables with histological grade (Gleason Score) and biochemical parameter (Serum PSA)?
5. Can we conclude from above that ^{18}F Choline can act as a biomarker to assess angiogenesis in prostate cancer?

Rationale:

Cancer causes changes at molecular level with damage to blood vessels. Molecular imaging techniques with novel biomarkers can help assess this damage by assessing kinetics of tracer perfusing the cancerous tissue. This can indirectly provide a way to quantify perfusion i.e. angiogenesis with hybrid imaging. Development of such PET-CT protocol can have two advantages

- a) **Staging:** Detection of metastatic disease when dynamic protocol is combined with whole body PET-CT imaging.

b) **Surrogate Angiogenesis biomarker:** Therapeutic potential of anti-angiogenic drugs can be assessed at baseline and after treatment and we can quantify these parameters with imaging. Hence it can measure the effect of a specific treatment.

It would be useful to assess the feasibility and practicalities of development of such PET-CT imaging protocol because this can have potential clinical impact.

Aims:

1. To assess the clinical feasibility of performing dynamic Choline PET study.
2. To quantify uptake with standardised uptake value (SUV).
3. To evaluate tracer kinetics.
4. To demonstrate correlation between ^{18}F Choline kinetic variables with histological grade (Gleason Score) and biochemical parameter (serum PSA).
5. To prove the angiogenesis potential of ^{18}F Choline.

Author declaration

All of the work in this chapter was conceived, analysed and written by myself, under the supervision of Professor Jamshed Bomanji Consultant Nuclear Medicine and Clinical Head at the Institute of Nuclear Medicine, University College London Hospital. Part of the clinical data input was provided by Dr Ahmad Almuhaideb; overseas fellow from Saudi Arabia while he was completing his fellowship. Scan retrieval was facilitated by Raymond Endozo Lead PET-CT Technologist. John Dickson lead the physics aspect of Choline PET-CT services. Kjell Erlandsson UCL provided input for kinetic modelling.

Abbreviation Key:

PET: Positron Emission Tomography

MRI: Magnetic Resonance Imaging

CT: Crosssectional Tomography

mpMRI: multiparametric Magnetic Resonance Imaging

PI-RADS: Prostate Imaging Reporting and Data system

HIFU: High Frequency Focussed Ultrasound

MBq: Mega-becquerel

SOP: Standard Operating Procedure

ROC: Receiver Operator Characteristics

AUC: Area under the curve

CI: Confidence Interval

SUVmax: Maximum Standardised Uptake Value

PACS: Picture Archive Communication System

DWI: Diffusion Weighted Images

Introduction:

In UK there were around 47, 200 men diagnosed with Prostate cancer in 2015. In men it is the most common cancer in the UK and among adults the second most common cancer in the UK (1). The incidence of prostate cancer is increasing (2). For organ-confined disease the treatment options include surgery, interventional procedures or radiation therapy. If the disease is advanced the treatment options are hormonal therapy, palliative radiation therapy or chemotherapy. Thus it is crucial to detect the true extent of disease. If the imaging modalities fail to detect local and distant cancer with persistent rise in biomarkers then it should be assumed that patient has micro metastases undetectable by imaging modalities. The current methods for imaging and staging of Prostate cancer are imperfect (3). Transrectal ultrasound (TRUS), computed CT, magnetic resonance imaging and bone scans may not reveal the true extent of disease. It is a diagnostic challenge to differentiate recurrent disease and post treatment scar tissue on conventional imaging (2).

At cellular level one of the characteristic feature of carcinogenesis is enhanced cell proliferation and membrane synthesis with increased demand on phospholipids (4). Modulation of trans-membrane signalling relies on phospholipids and in other words the metabolic activity of Choline reflects both proliferation and signalling in transformed cells (2) (5) (6) .

Angiogenesis is a process of new blood vessel formation and it is a feature of physiological as well as pathological states such as development, tissue repair, ischemia response, tumour growth and metastatic tumour spread (7).

In prostate cancer the process is marked by destabilization of existing blood vessels with endothelial fenestration, opening inter-endothelial contacts and formation of trans-endothelial gaps. There is further detachment of endothelial cells with migration and proliferation of quiescent endothelial cells. It then involves abnormal leakiness of vessels and reflects chaotic arrangement of prostate cancer microvascular bed. On the other hand, blood vessel remodelling consists of structural stabilization of newly formed blood vessels (8).

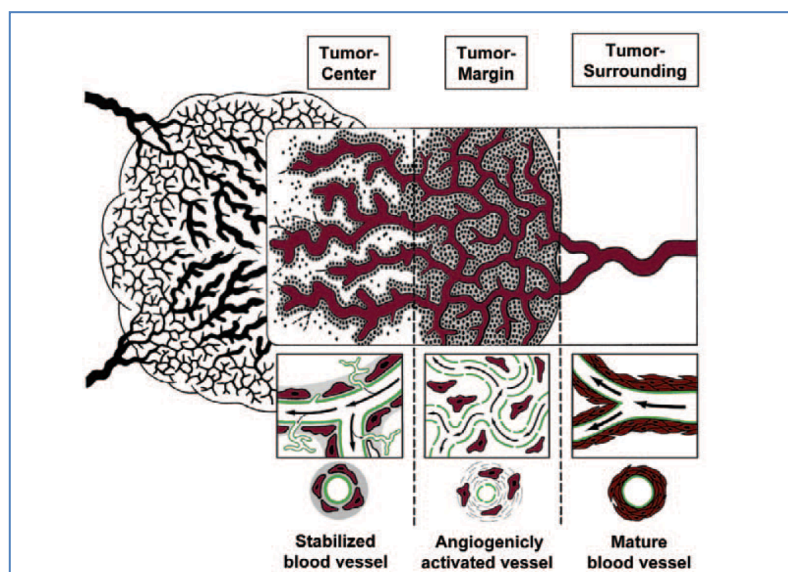


Fig: Blood vessel stabilization in the tumour centre and this is associated with necrosis of tumour tissue. The dense network of partly chaotically organised and immature blood vessels in the tumour margin show a tight relation to the tumour cell clusters. Remodelling is imaged with PET. **Reference:** Anticancer Research 29: 1823-1830 (2009)

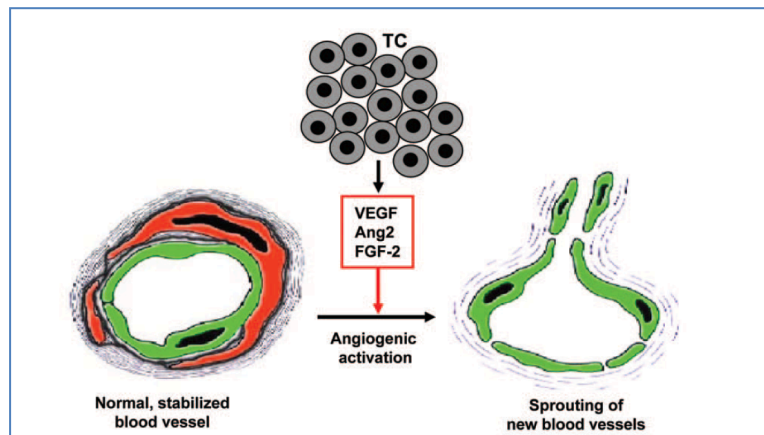


Fig: This figure illustrates stabilized capillary with closed endothelium (green), pericytes (red) tightly attached to the endothelium and a basement membrane (dark grey) which is clasping both cell types. Pro-angiogenic factors (VEGF, FGF-2) secreted by tumour cells (TC), the vessel wall is disintegrated. Detached endothelial cells (green) migrate and proliferate. Sprouting of new blood vessels from pre-existing blood vessels (angiogenesis) is the end product. **Reference:** Anticancer Research 29: 1823-1830 (2009)

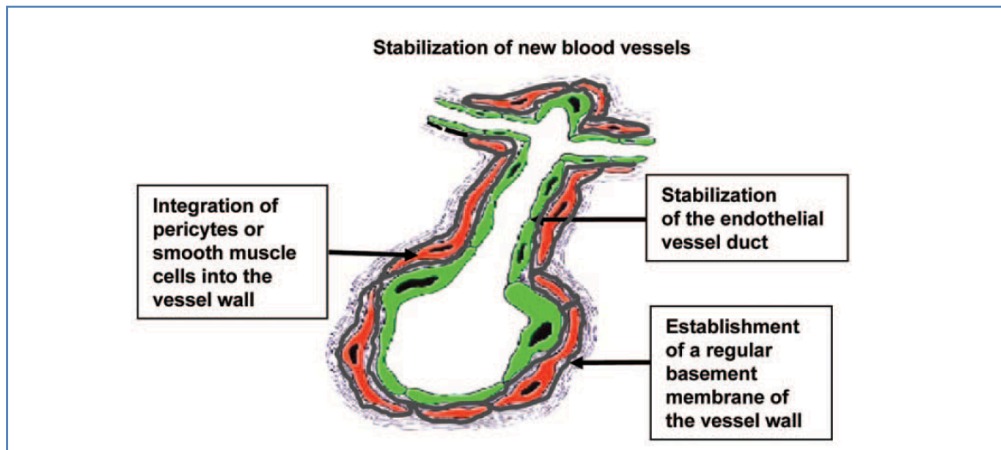


Fig: Restabilization of endothelial cell layer (green), re-integration of pericytes(red) into the vessel wall and re-establishment of basement membrane.

Reference: Anticancer Research 29: 1823-1830 (2009)

The main physiological driver of the process of angiogenesis is to perfuse and oxygenate the tissues hence this process can be evaluated by studying parameters like regional perfusion, function and metabolism (9). PET is the most sensitive and specific technique to assess by imaging the molecular pathways in vivo particularly in humans (10). Following internalization by injection, the tracer reaches the target. Position of radiolabelled molecules can be assessed spatiotemporally. Dynamic time activity curves can provide in-depth analysis of molecular micro-environment with reconstruction algorithms, images are constructed

tomographically with in-depth analysis of molecular micro-environment (using dynamic studies with the help of regional time activity curves) (9).

At University College London Hospital NHS Trust the setting up of ^{18}F Choline PET/CT project involved an initial feasibility work to assess the usefulness of ^{18}F Fluoro-Ethyl Choline PET/CT for prostate cancer. In our institute Choline positron emission tomography (PET/CT) is currently used as diagnostic tool in restaging prostate cancer patients in setting of biochemical relapse of prostate cancer. This work includes assessing the kinetics of uptake of ^{18}F Choline in prostate cancer. Quantification of uptake with standardised uptake value (SUV), the kinetic influx constant K_i from graphical analysis were assessed. We also performed correlation between Gleason Score and PSA.

Material and methods

Patients:

A total of 9 patients were evaluated. These were biopsy proven cases of prostate cancer and presented with biochemical evidence of prostate cancer relapse. The age range was 48-81 years. The prostate specific antigen (PSA) range was 0.12-45.1 (Unit: $\mu\text{g/L}$; normal range 0.00-4.00; Roche Modular method). All patients consented prior to the administration of radioisotope for PET/CT examination.

Radiopharmaceutical:

^{18}F -Fluoroethylcholine ^{18}F -FECH was provided by Erigal (Erigal Limited, Downs Road, Sutton, Surrey, UK), synthesized as described by Hara et al. (11). All QC parameters were fulfilled during the commercial preparation.

PET Imaging:

For setting up new ^{18}F Choline PET-CT protocol, Administration of Radioactive Substances Advisory Committee (ARSAC) guidance was obtained and following approval a diagnostic reference level (DRL) of 370MBq intravenously was approved (Effective Dose ED: 12.95 mSV (DeGrado 2002)). On arrival to the department, the patient was asked to change into a gown and check for metal objects. The dynamic images were acquired involving the injection of tracer while the patient was on the couch. The operator positioned centre of field of view over the prostate, which was often found posterior to the symphysis pubis. Prior to the imaging we asked the patient to empty the bladder. With the patient on the couch, we performed the scout. The prostate was aimed to be positioned in the centre of the field of view.



Scout view with blue lines indicating the desired field of view



Zoomed view of the pelvis covering the field of view for dynamic choline PET study.

The following scanning parameters were used

a) DYNAMIC STUDY

Landmark: Symphysis Pubis, CT Acquisition parameters

Scout 120 kVp, 10mA

CT 140 kVp, 80mA, 0.8s, Pitch 1.75 (1.375 (DVCT))

CT Slices 5mm (70 cm FoV PET AC)

2.5 mm (50 cm FoV Std)

2.5 mm (50 cm FoV Lung)

PET Acquisition Protocol: ^{18}F FECH Prostate Dynamic 3D

PET Acquisition Parameters

10 X 1 MIN & 5 X 2 min frames (List mode), Randoms from Singles

AC_3D

PET Recon Parameters

Iterative, 21 (20) subs, 2 iterations

Z-axis filter: Heavy

Post-Filter: 6 mm

Slice Thickness 3.27 mm

Recon. Diameter 70 cm

NAC_2D

Iterative, 21 Subs, 2 iterations

Z-axis filter: Heavy

Post-filter: 5.4 mm

Slice Thickness 3.27 mm

Recon. Diameter 70 cm

Z-axis filter: Heavy

Post-Filter: 6mm

Slice Thickness 3.27 mm

Recon. Diameter 70cm

NAC_2D

Iterative, 21 Subs, 2 iterations

Z-axis filter: Heavy

Post-filter: 5.4 mm

Slice Thickness 3.27 mm

Recon Diameter 70cm

^{18}F FECH was injected intravenously into the patient and dynamic scan was started. The patient was instructed not to move during the examination. For late scanning at 60 minutes post injection, the venflon was removed. The patient emptied the bladder prior to the examination. At 90 minutes post injection delayed pelvic views were obtained.

PET Analysis:

Choline is excreted rapidly into the urinary bladder and we aimed to do kinetic analysis as the tracer reaches the prostate and before there is excretory activity in the urinary bladder. For quantitative analysis ROIs were drawn on a metabolically active focus of the prostate (that represented areas of highest ^{18}F Choline accumulation in the prostate gland). For semi-quantitative analysis the tracer accumulation in the ROIs was measured using the SUV, which is the radioactivity concentration in an ROI divided by the injected dose and the patient's weight.

Technical Challenges:

^{18}F Choline PET-CT protocol was set up and dynamic curves were analysed prospectively. Due to several system and server upgrades at University College London Hospital NHS Trust, we had difficulty retrieving the list mode data. To address this issue, an alternative approach was adopted. We located the DICOM data and converted it to NIFTI format. This format enabled us to do Patlak analysis on the selected cases.

The PET data consisted of 15 time frames: 10x1 min, 5x2 min, voxel size 5.5 x 5.5 x 3.27 mm. The arteries were clearly visible on the initial frame and were used to derive an input function. Full kinetic analysis required short initial time frames (~10 s), which were not available. However, as the tracer binds irreversibly, it was possible to do a Patlak analysis, which did not require such short time-frames. This produced two outcome values, influx rate (K_i) and volume of distribution (V_D). The analysis was done on a VOI-basis or voxel-by-voxel, although the latter was affected by anatomical changes during the scan related to bladder filling. The following was the step-by-step process.

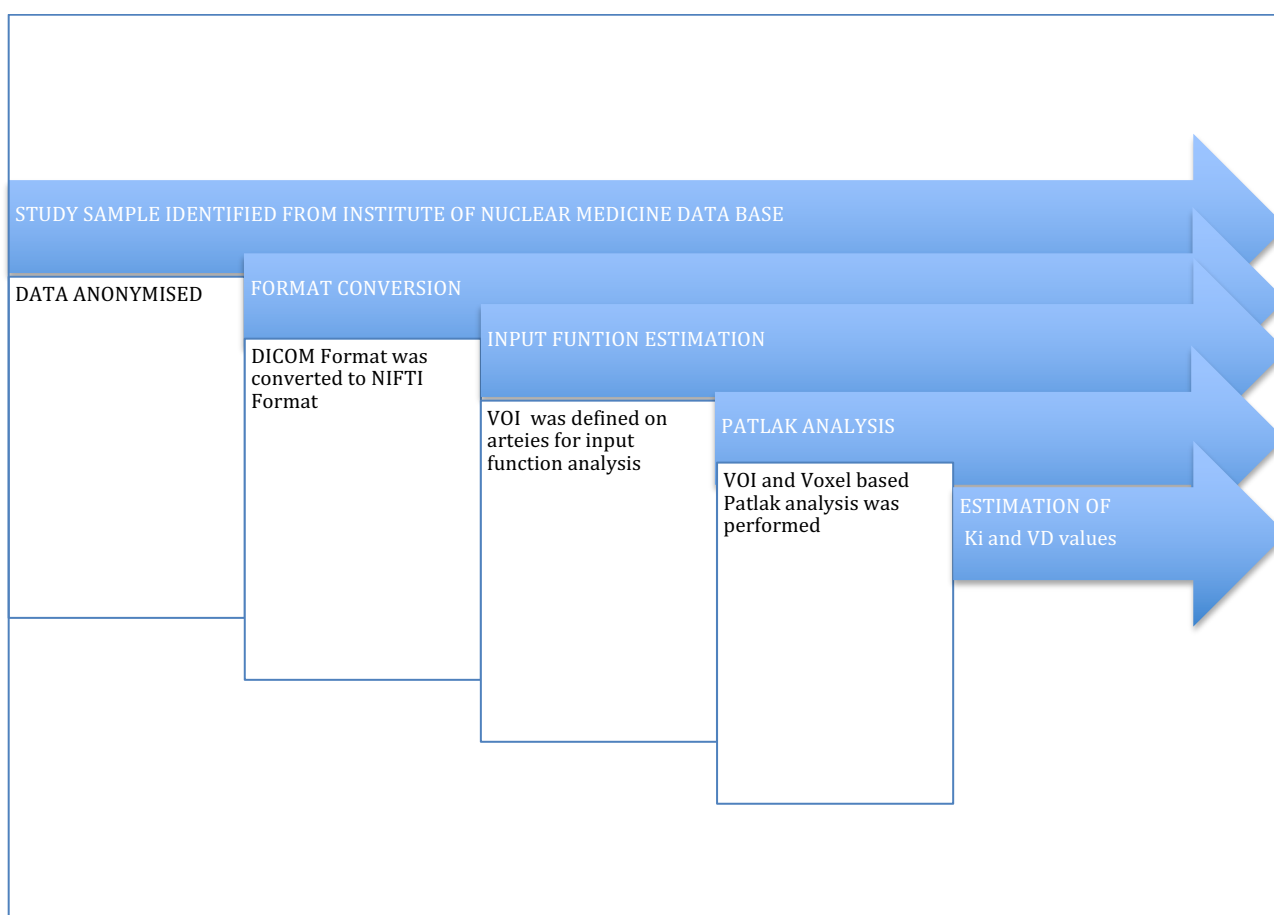


Fig: Step by step approach for arterial input function analysis of ^{18}F Choline PET data set.

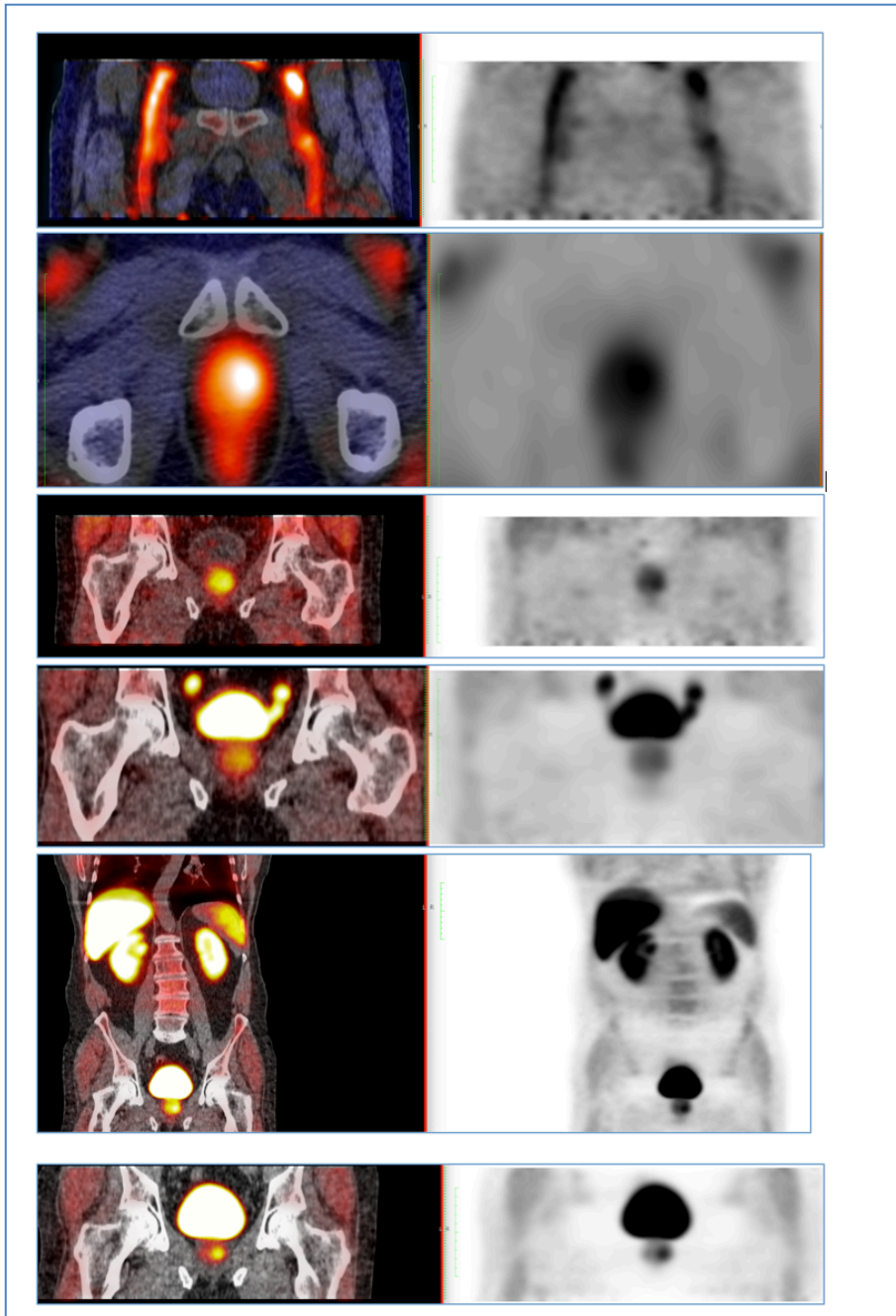


Fig: Fused PET & CT (left side) and PET reconstruction from top to bottom demonstrating flow to tracer in the vessels, perfusion to the prostate before the tracer has entered urinary bladder, excretion into the urinary bladder and prostate tracer retention on 60 minutes whole body and 90 minutes pelvic images.

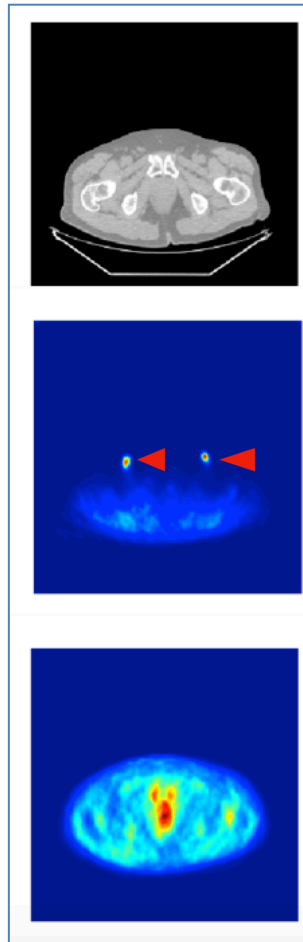


Fig: CT and PET Data (1st, 8th Frame) from ¹⁸F Choline PET CT Study. Red arrows on the second image represents the arterial activity.

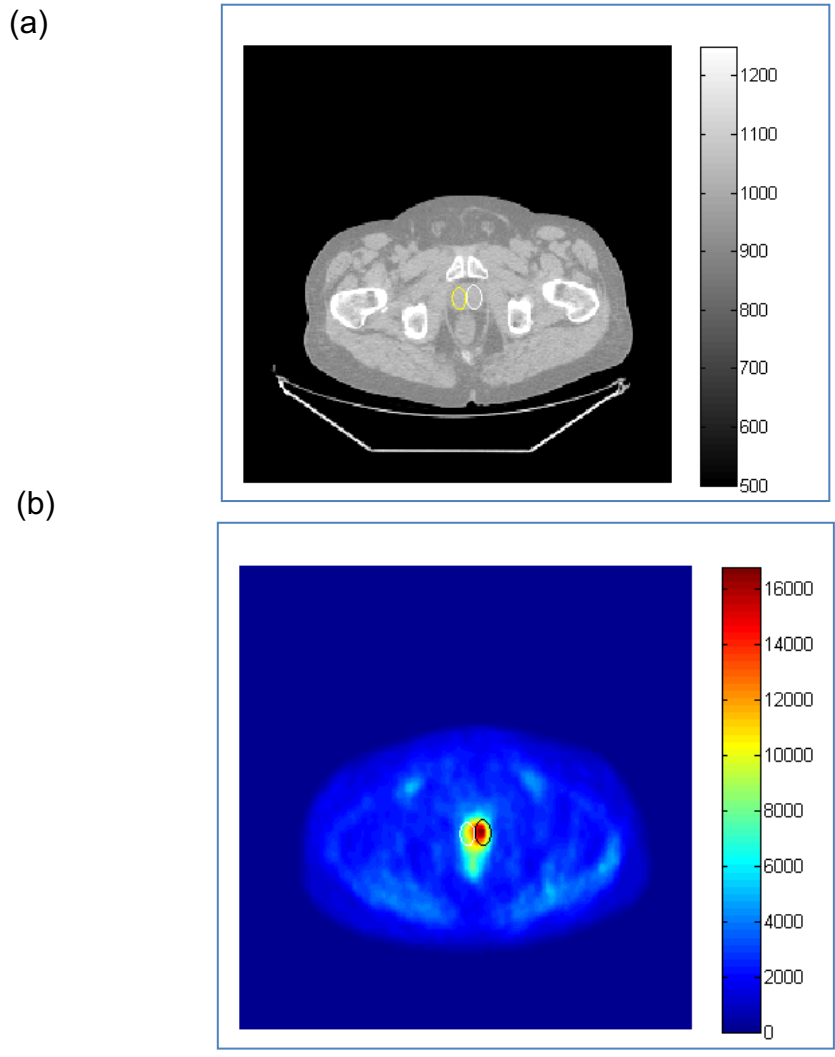


Fig: Axial Low dose CT and axial PET images of the pelvis. Regions of interest were drawn on both lobes of the prostate gland.

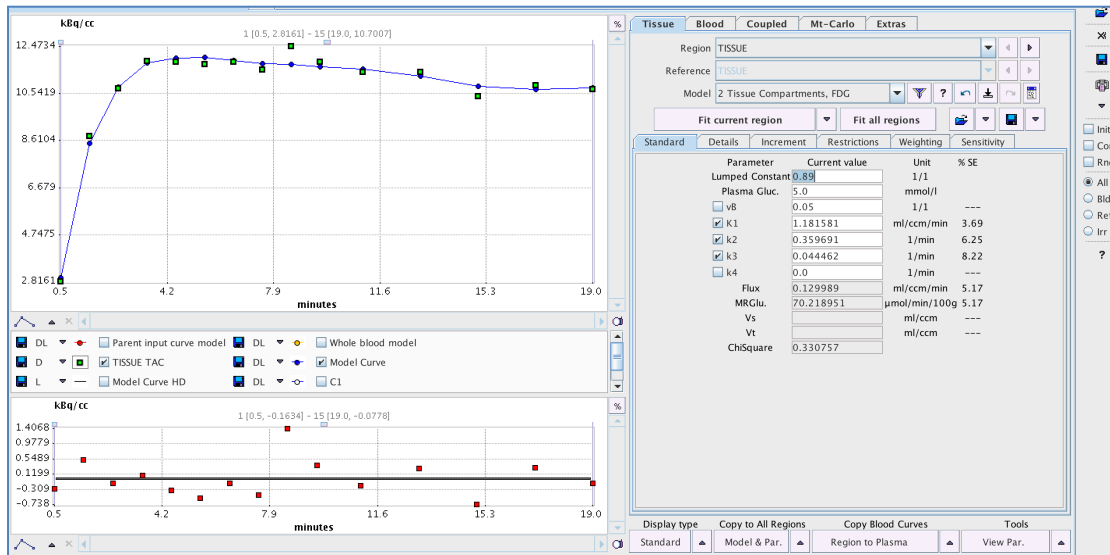


Fig: Left panel shows Time activity curve (TAC) with region of interest (ROI) placed over prostate. The left panel shows results of the compartmental model.

Fractional Rate of Tracer Transport:

The slope of the linear plot was equal to the utilization constant of ^{18}F Choline i.e. Influx constant, K_i , which represents the ***Fractional rate of tracer transport per unit time***. The first 10 data points representing the time from 1 to 5 min after the tracer injection were used to determine the slope for further analysis.

Statistical Analysis: Spearman's correlation coefficients were calculated to assess the possible association between ^{18}F Choline uptake and clinical and histopathological characteristics of prostate growth.

Results:

Data from nine patients were analysed. Volumes of interest (VOIs) were generated for blood, left and right lobes and bladder. Time-activity curves (TACs) were produced. The L- and R-lobe data were analysed with the Patlak method

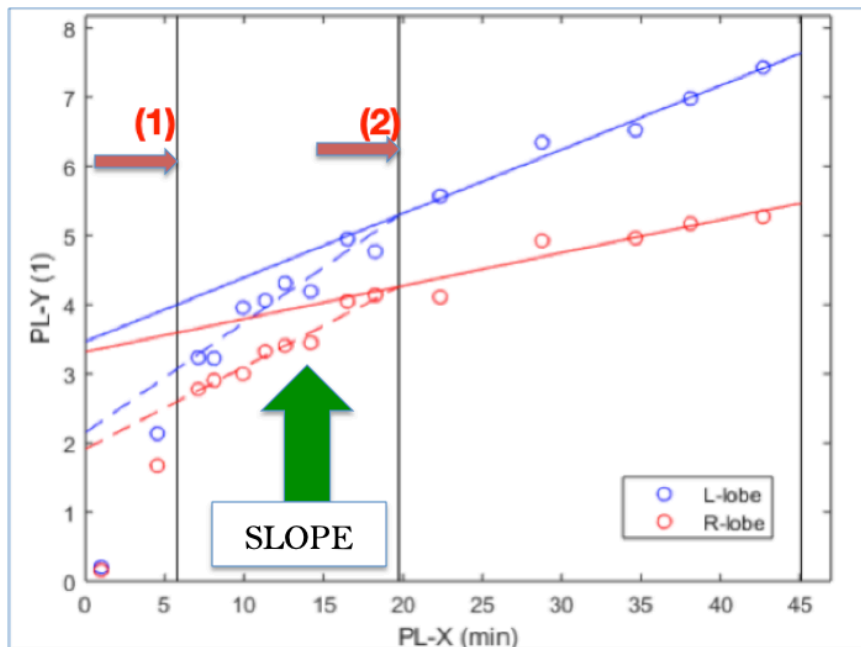
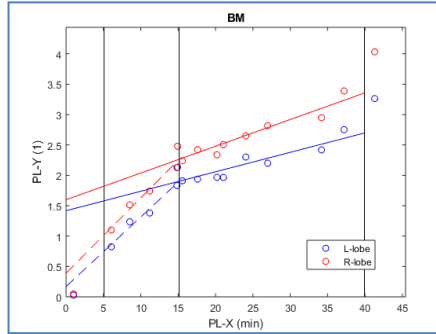
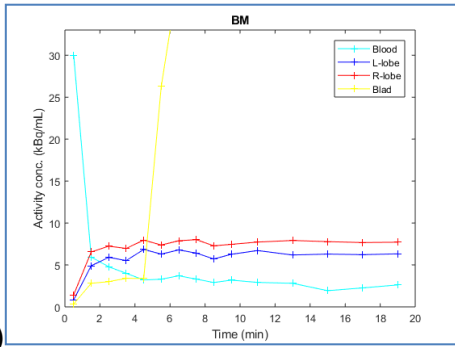


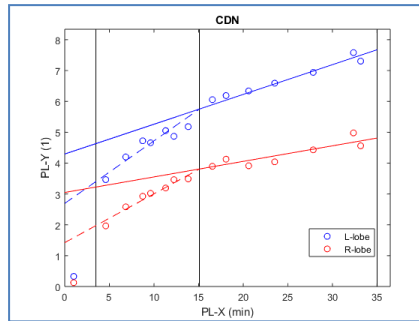
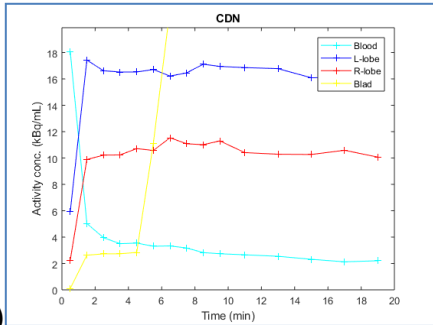
Fig: Patlak analysis with the first line abbreviated as **(1)** represents “perfusion”. The second line abbreviated as **(2)** represents irreversible tracer “binding”. The slope is “the influx rate” and the “intercept” represents volume of distribution V_D .

TACs and Patlak plots for all nine patients are shown below

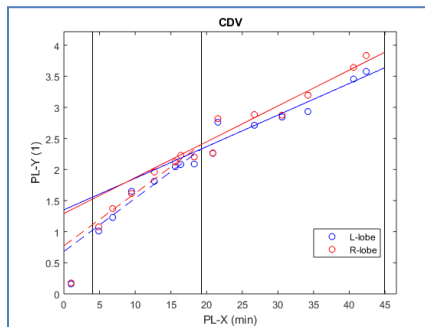
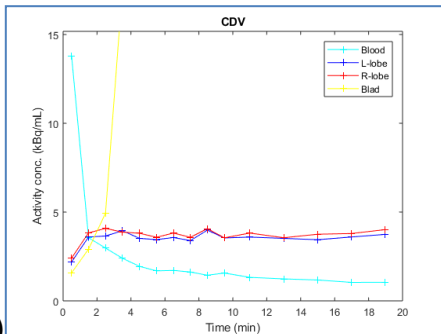
(1)



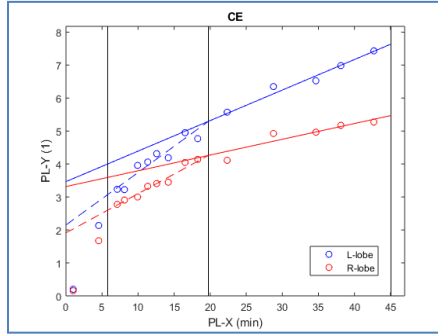
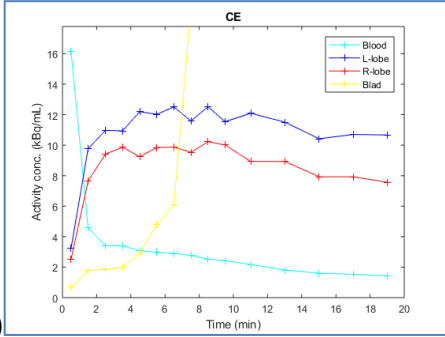
(2)



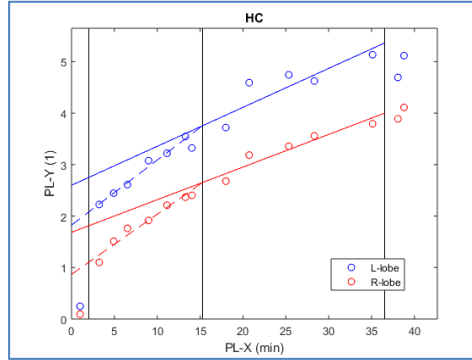
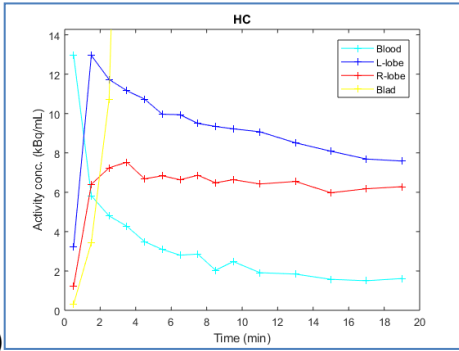
(3)



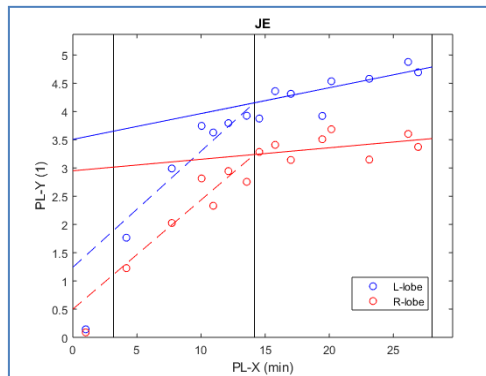
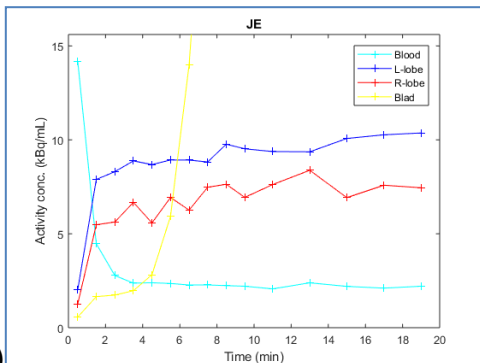
(4)



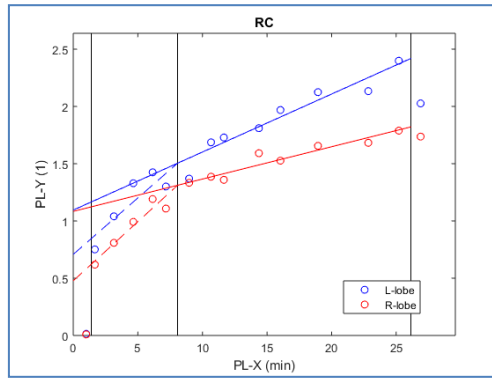
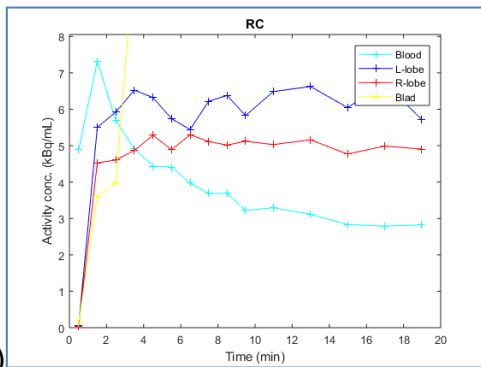
(5)



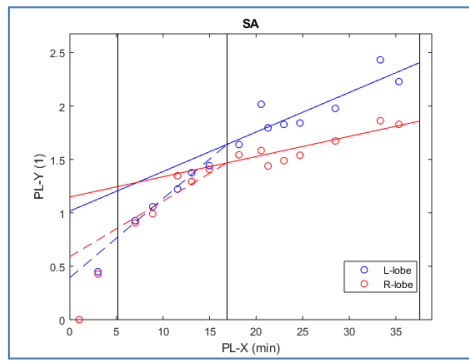
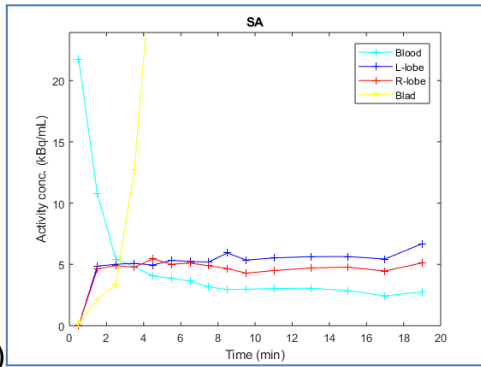
(6)



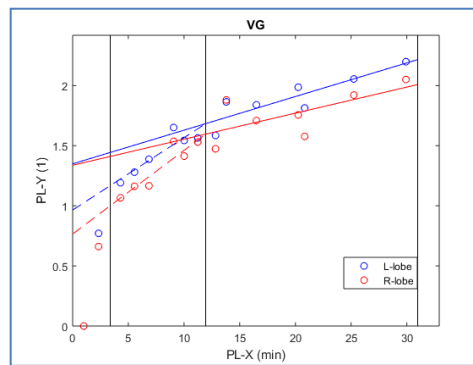
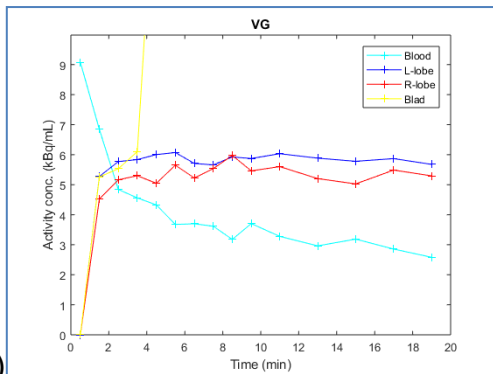
(7)



(8)



(9)



In general the TACs for the lobes seem to plateau after 1-2 min. The bladder TAC starts to increase suddenly after ~5 min, but this does not seem to affect the shape of the lobe-TACs, suggesting that the VOIs were sufficiently far away. All Patlak plots seem to exhibit a bi-linear behaviour. The K_i -values are also presented in a Left (L) vs right (R) scatter-plot.

In 4 cases, the L- and R (K_i) values are similar, and the points are close to the line of identity. In 5 cases, the L-values are clearly higher than the R-values and, curiously, seem to lie on a straight line with a slope of 1.8.

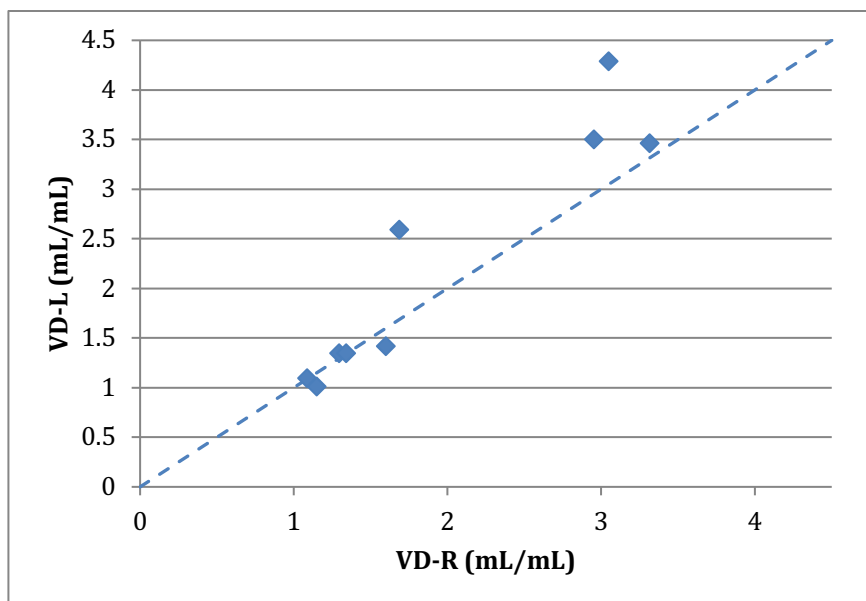
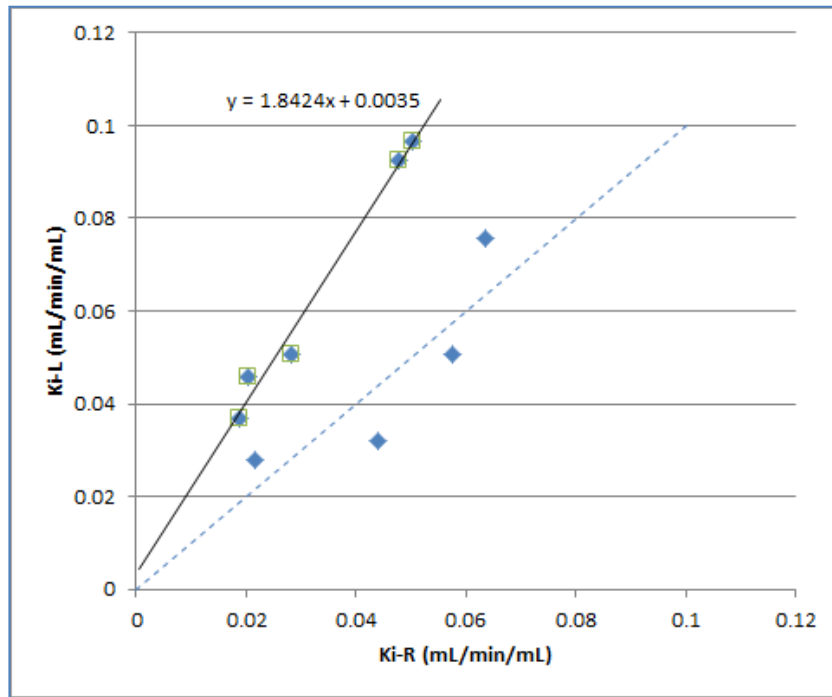
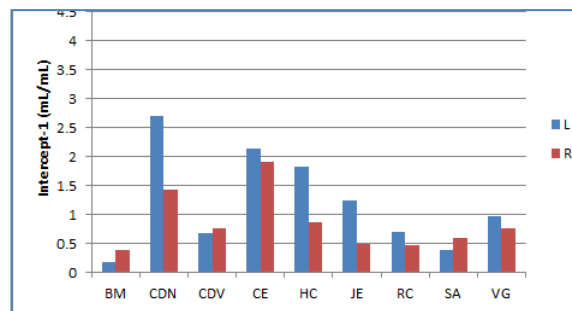
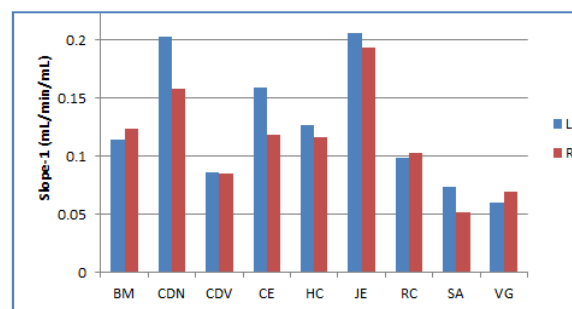
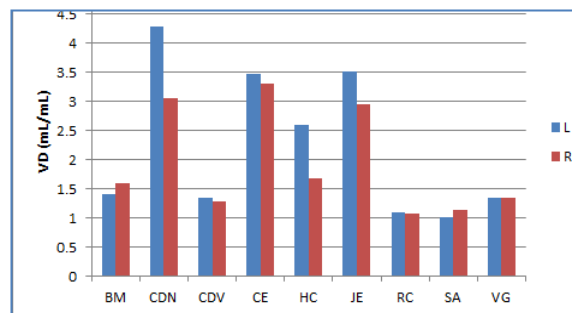
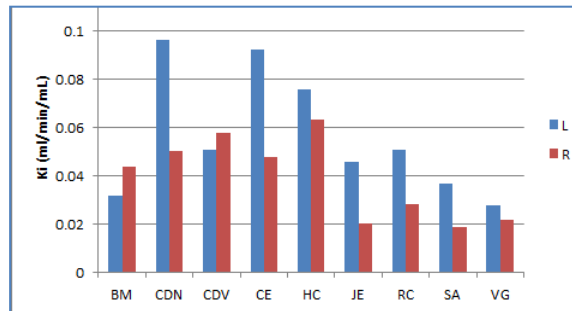


Fig: The K_i -values are also presented in Left (L) vs. Right (R) scatter-plot. In 4 cases, the L- and R- K_i values are similar, and the points are close to the line of identity. In 5 cases, the L-values are clearly higher than the R-values and, curiously, seem to lie on a straight line with a slope of 1.8.

The results including K_i , V_D , slope and intercept are presented in the bar charts below



	PSA	GLEASON	RIGHT LOBE OF THE PROSTATE					
			Ki	V _D	SLOPE	INTERCEPT	60 min SUVmax	90 min SUVmax
1	6.3	3+4	0.044	1.5986	0.124	0.3885	8.7	5.9
2	45.1	3+4	0.0504	3.0479	0.1582	1.4222	5.7	7.5
3	6	3+4	0.0577	1.2925	0.0846	0.7731	5.3	4.1
4	10	4+5	0.0478	3.3156	0.1189	1.9106	3.5	1.8
5	4.7	4+5	0.0634	1.6836	0.1167	0.8686	1.4	1.4
6	0.7	4+5	0.0203	2.9507	0.1933	0.5001	2.3	3.4
7	8.2	3+4	0.0282	1.0838	0.1033	0.4776	1.6	1.1
8	17	4+3	0.0189	1.1488	0.0519	0.5911	2.3	2.1
9	2.8	3+3	0.0217	1.3374	0.0695	0.7656	0.9	0.7

	PSA	GLEASON	LEFT LOBE OF THE PROSTATE					
			Ki	V _D	SLOPE	INTERCEPT	60 min SUVmax	90 min SUVmax
1	6.3	3+4	0.032	1.4179	0.1145	0.1698	7.8	5.2
2	45.1	3+4	0.0966	4.2939	0.2026	2.6949	3.6	1.19
3	6	3+4	0.0508	1.351	0.0856	0.6816	7.6	5.7
4	10	4+5	0.0926	3.4651	0.1592	2.1496	5.1	4.3
5	4.7	4+5	0.0757	2.5984	0.1263	1.825	2.8	1.7
6	0.7	4+5	0.0457	3.5068	0.2056	1.2415	2.3	6.6
7	8.2	3+4	0.0507	1.0952	0.0986	0.7083	2.03	1.5
8	17	4+3	0.037	1.0168	0.0739	0.3937	2.2	2.4
9	2.8	3+3	0.028	1.3492	0.0602	0.965	1.01	0.8

Table: 1: Biochemical, histological and kinetic modelling parameters in 9 patients.

Ki= Initial slope of tracer uptake related to blood flow (perfusion).

V_D= Volume of distribution related to reversible uptake.

Slope= delayed uptake rate of tracer related to irreversible binding

I =Intercept

	PSA (R_s)	GLEASON GRADE (R_s)	SUVmax@60 Minutes (R_s)	SUVmax@90 Minutes (R_s)
Ki	0.236	0.389	0.355	0.125
VD	-0.033	.584*	0.371	0.319
Slope	-0.033	.677**	0.369	0.395
Intercept	0.120	0.343	-0.030	-0.139

*. Correlation is significant at the 0.05 level (2-tailed).

**. Correlation is significant at the 0.01 level (2-tailed)

R_s Spearman Correlation coefficients

Ki- Influx rate

VD-Volume of distribution

The strength of correlation is described by the following values

(0.00-0.19-Very Weak; 0.20-0.39-Weak; 0.40-0.59-moderate; 0.60-0.79-strong

0.80-1.0-very strong)

Table: Spearman correlation coefficients (**R_s**) between Kinetic variables vs PSA, Gleason Grade, SUVmax at 60 Minutes and SUVmax at 90 minutes

Discussion

This pilot study demonstrates the ability of dynamic ^{18}F Choline PET/CT to provide quantitative variables which reflect perfusion of cancerous prostate tissue.

Majority of Choline PET-CT studies rely on static parameters such as SUVmax obtained as part of the whole body and/or pelvic acquisition. While SUVmax can provide information about end product of multiple reactions that occur as part of tracer uptake mechanism, the addition of dynamic acquisition facilitates sequential molecular functional information, which may help in characterizing and predicting the cellular morphology of examined tissue. Takesh et al (12) have done preliminary work and concluded that mean dynamic constants (transport and rate) as well as SUVmax may differ between the benign and malignant prostate tissue. Tracer uptake in their work was found to be more rapid and intense in cancerous tissue. Their work is limited by inclusion of primary and post treatment disease scenario while we have only selected cases, which presented with history of biochemical relapse of prostate cancer.

^{18}F Choline is known for higher urinary excretion and this property act as potential confounder as this masks the background activity (13). We have been able to demonstrate that dynamic ^{18}F Choline can provide information about perfusion of prostate and image acquisition of earlier part of examination can be performed clinically before tracer is excreted into the urinary bladder via the ureters.

We have noticed fast uptake of ^{18}F Choline in cancerous tissue. This correlates with the work done by Contracter et al (14) who showed correlation between increased ^{11}C uptake and choline kinase overexpression. They highlighted that cancerous lesions overexpressed choline kinase in cytoplasm and nucleus and SUVmax was strongly associated with Choline Kinase staining .

We did not see strong associating between the PSA level, Gleason score and Kinetic parameters. This is most likely because of small sample number of patients with high Gleason score on histology (n=3/9). Another possible explanation can be that intracellular choline levels are determined by two factors

1. Rate of Choline uptake
2. Rate of phosphatidylcholine synthesis and degradation.

It has been shown in laboratory studies (15) that a large proportion of intracellular choline can still be non-metabolized choline suggesting choline transport and not phosphorylation is the key factor in choline uptake by cancer cells. It is only at “longer” incubation times, choline phosphorylation becomes the dominant step in cellular enrichment. Thus variation in transport rates and cellular enrichment can be a contributory factor.

Prostatitis, benign prostate tissue hyperplasia and prostate cancer can produce SUVmax on whole body 60 minutes and 90 minutes imaging which may be similar as there is an overlap in metabolic expression of these lesions (16). Our study, despite of small sample size suggests that pharmacokinetics may provide information about perfusion of abnormal focus in the prostate gland and this can help patients in whom invasive tests like ultrasound guided biopsy or template guided biopsies may be difficult due to comorbidities.

Our finding related to analysis of time-activity-curves showed that there is gradual increase in tracer concentration after an initial plateau is reached. This observation is similar to other studies (14).

The dynamic scans are clinically less feasible, longer and less suited to a busy clinical work list with time pressure to scan more and more patients. We have omitted dynamic acquisition

as part of standard operating procedure in our department and only restricted it to clinical research studies.

Another limitation of this study is that arterial blood was not collected from the subjects hence precise information about radiolabelled metabolites was not possible.

No adverse events related to ^{18}F Ethyl Choline were reported during or as part of the follow up of patients in this pilot study.

Conflict of interest:

None declared.

Conclusion

It is clinically feasible to perform dynamic Choline PET study. We can quantify uptake with standardised uptake value (SUV) and evaluate tracer kinetics. We were able to obtain perfusion information before the excreted activity reached the urinary bladder and demonstrated that cancerous tissue show abnormal perfusion. From these observations we conclude that ^{18}F Choline can act as a biomarker to assess angiogenesis in prostate cancer. We were unable to demonstrate correlation between ^{18}F Choline kinetic variables, histological grade (Gleason Score) and biochemical parameter (Serum PSA) and larger studies are required to validate this further.

References

1. About prostate cancer | Prostate cancer | Cancer Research UK [Internet]. [cited 2019 Mar 9]. Available from: <https://www.cancerresearchuk.org/about-cancer/prostate-cancer/about>
2. Sutinen E, Nurmi M, Roivainen A, Varpula M, Tolvanen T, Lehtikainen P, et al. Kinetics of [(11)C]choline uptake in prostate cancer: a PET study. *Eur J Nucl Med Mol Imaging*. 2004 Mar;31(3):317–24.
3. Yu KK, Hricak H. Imaging prostate cancer. *Radiol Clin North Am*. 2000 Jan;38(1):59–85, viii.
4. Negendank W. Studies of human tumors by MRS: a review. *NMR Biomed*. 1992 Oct;5(5):303–24.
5. Ackerstaff E, Pflug BR, Nelson JB, Bhujwala ZM. Detection of increased choline compounds with proton nuclear magnetic resonance spectroscopy subsequent to malignant transformation of human prostatic epithelial cells. *Cancer Res*. 2001 May 1;61(9):3599–603.
6. Hernández-Alcoceba R, Saniger L, Campos J, Núñez MC, Khaless F, Gallo MA, et al. Choline kinase inhibitors as a novel approach for antiproliferative drug design. *Oncogene*. 1997 Nov 6;15(19):2289–301.
7. Folkman J. Angiogenesis in cancer, vascular, rheumatoid and other disease. *Nat Med*. 1995 Jan;1(1):27–31.
8. Tilki D, Seitz M, Singer BB, Irmak S, Stief CG, Reich O, et al. Molecular Imaging of Tumor Blood Vessels in Prostate Cancer. *ANTICANCER RESEARCH*. 2009;7.
9. Niu G, Chen X. PET Imaging of Angiogenesis. *PET Clin*. 2009 Jan 1;4(1):17–38.
10. Jones T. The imaging science of positron emission tomography. *Eur J Nucl Med*. 1996 Jul;23(7):807–13.
11. Hara T, Kosaka N, Kishi H. Development of (18)F-fluoroethylcholine for cancer imaging with PET: synthesis, biochemistry, and prostate cancer imaging. *J Nucl Med*. 2002 Feb;43(2):187–99.
12. Takesh M. Kinetic Modeling Application to 18 F-fluoroethylcholine Positron Emission Tomography in Patients with Primary and Recurrent Prostate Cancer Using Two-tissue Compartmental Model. *World Journal of Nuclear Medicine*. 2013 Jan 9;12(3):101.
13. Pantaleo MA, Nannini M, Maleddu A, Fanti S, Ambrosini V, Nanni C, et al. Conventional and novel PET tracers for imaging in oncology in the era of molecular therapy. *Cancer Treat Rev*. 2008 Apr;34(2):103–21.
14. Contractor K, Challapalli A, Barwick T, Winkler M, Hellawell G, Hazell S, et al. Use of [11C]choline PET-CT as a noninvasive method for detecting pelvic lymph node status from prostate cancer and relationship with choline kinase expression. *Clin Cancer Res*. 2011 Dec 15;17(24):7673–83.

15. Henriksen G, Herz M, Hauser A, Schwaiger M, Wester H-J. Synthesis and preclinical evaluation of the choline transport tracer deshydroxy-[18F]fluorocholine ([18F]dOC). *Nuclear Medicine and Biology*. 2004 Oct 1;31(7):851–8.
16. Haroon A, Ahmed HU, Cathcart P, Almuhaideb A, Kayani I, Dickson J, et al. 18F-FECH PET/CT to Assess Clinically Significant Disease in Prostate Cancer: Correlation With Maximum and Total Cancer Core Length Obtained via MRI-Guided Template Mapping Biopsies. *AJR Am J Roentgenol*. 2016 Dec;207(6):1297–306.

CHAPTER 4 : ^{18}F -Choline PET-CT for assessment of Clinically significant Prostate Cancer.

Abstract

Objective

Detection of clinically significant and insignificant prostate cancer on ^{18}F -FECH PET/CT and to correlate findings with Transperineal template guided prostate mapping biopsy (TPM).

Method

Fifty-six lobes of the prostate were analysed in 28 men who underwent ^{18}F -FECH PET/CT and TPM. Whole body images and pelvic images were acquired at 60 and 90 minutes. Correlation was made with TPM. Sensitivity, specificity, positive, negative predictive values and AUC of dual-phase ^{18}F -FECH PET/CT were calculated.

Results

Mean age of the patients was 68.8 years (range 53-79 years) and mean PSA was 12.1 $\mu\text{g/L}$ (range 0.6-45 $\mu\text{g/L}$). Mean maximum cancer core length was 4.4 mm (median 4 mm, range 1-14 mm) and mean total cancer core length, 14.6 mm (median 14.6 mm, range 1-82 mm). The Gleason grade was 6 in 5 lobes (13%), 7 in 27 lobes (71%) and 8-10 in six lobes (16%). ^{18}F -FECH PET/CT was positive in 46/56 lobes (82%). SUVmax range for 60- and 90-min ^{18}F -FECH PET/CT was 1.3-11.4 and 1.2-10.9 respectively. Clinically significant cancer was seen in 30/38 positive lobes while 8 had clinically insignificant disease. For 60 minute imaging the sensitivity, specificity and ROC (AUC) were 75%, 75%, 0.746 (95% CI 0.612, 0.853). For 90 minutes imaging the sensitivity, specificity and ROC (AUC) were 73.7%, 58.3% and 0.646(95% CI 0.498, 0.776). Overall sensitivity, specificity, positive predictive value, negative predictive value were 95%, 50%, 82.6%, 80% respectively.

Conclusion

¹⁸F-FECH PET/CT can detect prostate cancer and localizes TPM biopsy proven clinically significant prostate cancer with sensitivity of greater than 89.7%. 60 minutes imaging is more sensitive and specific than 90 minutes imaging.

Introduction

Prostate cancer is a commonly diagnosed malignancy in men, and recurrence following treatment is common: within 10 years of prostatectomy, recurrence is documented in 20-50% of cases ¹ and rates in excess of 50% have been reported following external beam radiation therapy ¹. A progressive rise in prostate-specific antigen (PSA) can precede clinically detectable disease by months or years ². Furthermore, it may be difficult to confirm disease on biopsy, particularly when recurrence is suspected after surgery ³. While there has been increased interest in the role of imaging within the setting of recurrent prostate cancer, the presence of scar tissue and late radiation effects render image interpretation a challenge ⁴. PET/CT imaging offers a novel option that may help to overcome some of the current deficiencies, as it is reliant on both anatomy and function.

During the past decade there has been increasing use of new PET tracers, namely ¹¹C- and ¹⁸F-labeled choline analogues, in prostate cancer ⁵. Choline acts as a precursor for the biosynthesis of phosphatidylcholine and other phospholipids. Since there is an increased cell proliferation rate in cancers, the demand for phospholipids is high. This high content of phosphorylcholine in prostate cancer has been demonstrated with ³¹P nuclear magnetic resonance studies, while the normal tissues have low levels ⁶. The uptake and phosphorylation of fluorocholeline is similar to that of ¹¹C-labeled choline and superior to that of other choline analogues ⁷. It has been suggested that ¹⁸F-FECH may be superior to ¹¹C-choline PET in terms of sharpness of image ⁸. Moreover, ¹¹C-choline studies are restricted to centres with an onsite cyclotron, while ¹⁸F-FECH can be delivered to sites without a cyclotron unit. Unlike the methylated form of ¹⁸F-fluorocholeline, which might otherwise have been used, the ethylated form (¹⁸F-FECH) has the advantage of commercial availability. For these reasons, ¹⁸F-FECH was chosen as the tracer for this study.

Materials and methods

Patients

This pilot study involved evaluation of 56 prostate lobes in 28 patients (age range 53-79 years; median 68.5 years) who had no evidence of metastatic disease on ¹⁸F-FECH PET/CT and underwent TPM for evaluation of disease burden in the prostate gland. As this pilot study was prospective, the sample population was heterogeneous and included 11 out of 28 patients who were being investigated for suspected prostate cancer and 17 patients who were referred with biochemical relapse after treatment for possible salvage therapy.

The previous treatments were categorised in two main divisions i.e. single mode of treatment or multiple. Single treatment consisted of HIFU (high frequency focussed ultrasound), radiotherapy or brachytherapy (7 patients). The second group consisted of patients who were referred for ¹⁸F-FECH PET/CT after different lines of treatment were given and presented with biochemical relapse. These treatments consisted of radiotherapy, HIFU, hormones and brachytherapy in varying combinations (10 patients) and these have been listed in Table 1.

Table 1: Patients with suspected relapse had two broad groups i.e. those patients who received single mode of treatment and those who received treatment in varying combination.

MODE OF TREATMENT	NO: OF PATIENTS
SINGLE	
HIFU	2
RADIOTHERAPY	3
BRACHYTHERAPY	2
SUM	7 patients
COMBINED	
RADIOTHERAPY AND HIFU	2
RADIOTHERAPY AND HORMONES	4
RADIOTHERAPY, HORMONES, HIFU	2
HORMONES, BRACHYTHERAPY AND RADIOTHERAPY	1
HORMONES, RADIOTHERAPY AND HIFU	1
SUM	10 patients
TOTAL	17 PATIENTS

¹⁸F-Fluoroethylcholine

¹⁸F-FECH was provided by Erigal (Erigal Limited, Downs Road, Sutton, Surrey, UK), synthesized as described by Hara et al. ⁸. All QC parameters were fulfilled during the commercial preparation.

The index test

Patients were injected with 300-370 MBq of ¹⁸F-FECH [effective dose 12.95 mSv (7)]. Whole-body PET/CT images were acquired 60 min after tracer injection. Owing to the rapid excretion of FECH in urine, the patients were asked to empty their bladder prior to imaging. At approximately 90 min, a limited (one bed position, PET/CT) pelvic view was obtained with the prostate in the field of view. The CT acquisition parameters included: scout 120 kVp, 10 mA; CT 140 kVp, 80 mA, 0.8 s, pitch 1.75; CT slices 5 mm (70-cm FOV PET AC), 2.5 mm (50-cm FOV Std), 2.5 mm (50-cm FOV Lung). PET acquisition parameters were: 3D attenuation-corrected and non-attenuation-corrected images, 20 subsets with iterative reconstructions. CT images were used to produce attenuation correction values for PET emission reconstruction and fused PET/CT presentation.

The ¹⁸F-FECH PET/CT images were interpreted by two of the authors (J.B., A.H.) who were blinded to the histological outcomes. They had access to the CT component of the PET/CT. These studies were typically read within 24 h (maximum 72 h) after the performance of the study by using advanced PET/CT review software (Advantage, version 4.2, GE Medical Systems) with inbuilt capability to scroll through the corresponding PET, CT, and fused images in transverse, coronal, and sagittal planes and the MIP (maximum intensity projection) images.

¹⁸F-FECH activity was expressed as maximum standardized uptake value (SUV_{max}) based on the patient's body weight and the dose of injected ¹⁸F-FECH within the region of interest.

The reference test

After imaging, Transperineal MR template-guided prostate mapping (TPM) biopsy was performed in 28 patients in whom the disease was confined to the prostate gland on imaging and there was no evidence of nodal or metastatic disease. These men were eligible for salvage therapy. TPM involves 5-mm sampling of the whole prostate using a brachytherapy template grid placed against the perineum. It overcomes the random and systematic sampling errors inherent in transrectal ultrasound-guided (TRUS) biopsies ^{9, 10}. Biopsies were plotted into 20 zones (modified Barzell zones): 1, left parasagittal anterior apex; 2, left parasagittal anterior base; 3, right parasagittal anterior apex; 4, right parasagittal anterior base; 5, midline apex; 6, midline base; 7, left medial anterior apex; 8, left medial anterior base; 9, right medial anterior apex; 10, right medial anterior base; 11, left lateral; 12, right lateral; 13, left parasagittal posterior apex; 14, left parasagittal posterior base; 15, right parasagittal posterior apex; 16, right parasagittal posterior base; 17, left medial posterior apex; 18, left medial posterior base; 19, right medial posterior apex; 20, right medial posterior base.

We measured the following two variables on TPM:

- a) Maximum cancer core length (MCCL)
- b) Total cancer core length (TCCL)

For instance, if a cluster of three positive adjacent biopsies showed a cancer core length of 2, 2, and 4 mm respectively, the MCCL would be 4 mm and the TCCL would be 8 mm. The histopathology generated by the biopsies was analysed and reported by a uropathologist (A.F.) with 10 years' experience.

The target condition

Pathology in the prostate represents a spectrum of disease in terms of risk. We used a previously published classification system. It has been validated for use in samples obtained using TPM ¹⁰ (Fig. 1) By using a uniform method of risk classification, we were able to incorporate the output of the TPM biopsy into those cases with clinically significant disease and clinically insignificant disease.

Measuring agreement

Paired ¹⁸F-FECH activity and histopathology outputs were analysed on a case-by-case basis using a consensus approach. The pathology outputs were limited to clinically insignificant disease (green) and clinically significant disease (yellow and red) as shown in Fig. 1. The imaging outputs were limited to positive or negative.

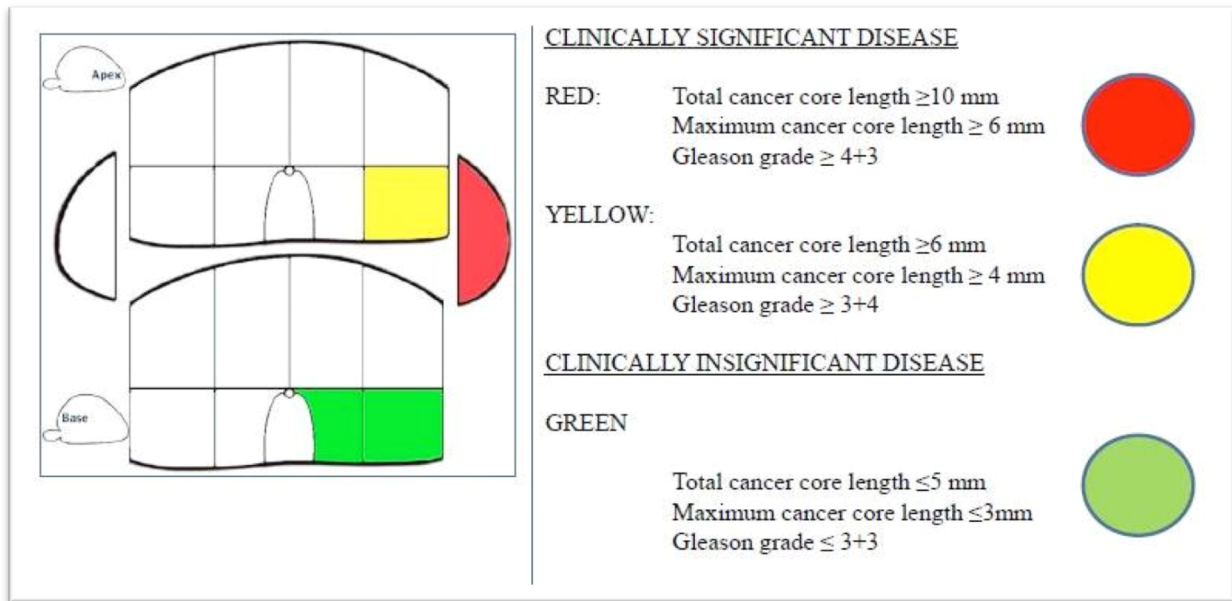


Fig. 1. Definitions of clinically significant (*red and yellow shapes*) and clinically insignificant (*green shape*) localized prostate cancer.

Planned analysis

Based on histopathology results, the specificity, sensitivity, positive predictive value, negative predictive values, and AUC (area under the ROC curve) of dual-phase ^{18}F -FECH PET/CT were calculated separately for early (60 min), delayed (90 min) imaging for detection of prostate cancer. In addition to that we also evaluated the performance of ^{18}F -FECH PET/CT in those TPM proven lobes where histopathological analysis demonstrated clinically significant disease. The STARD flow chart illustrates the study outline in Figure 2

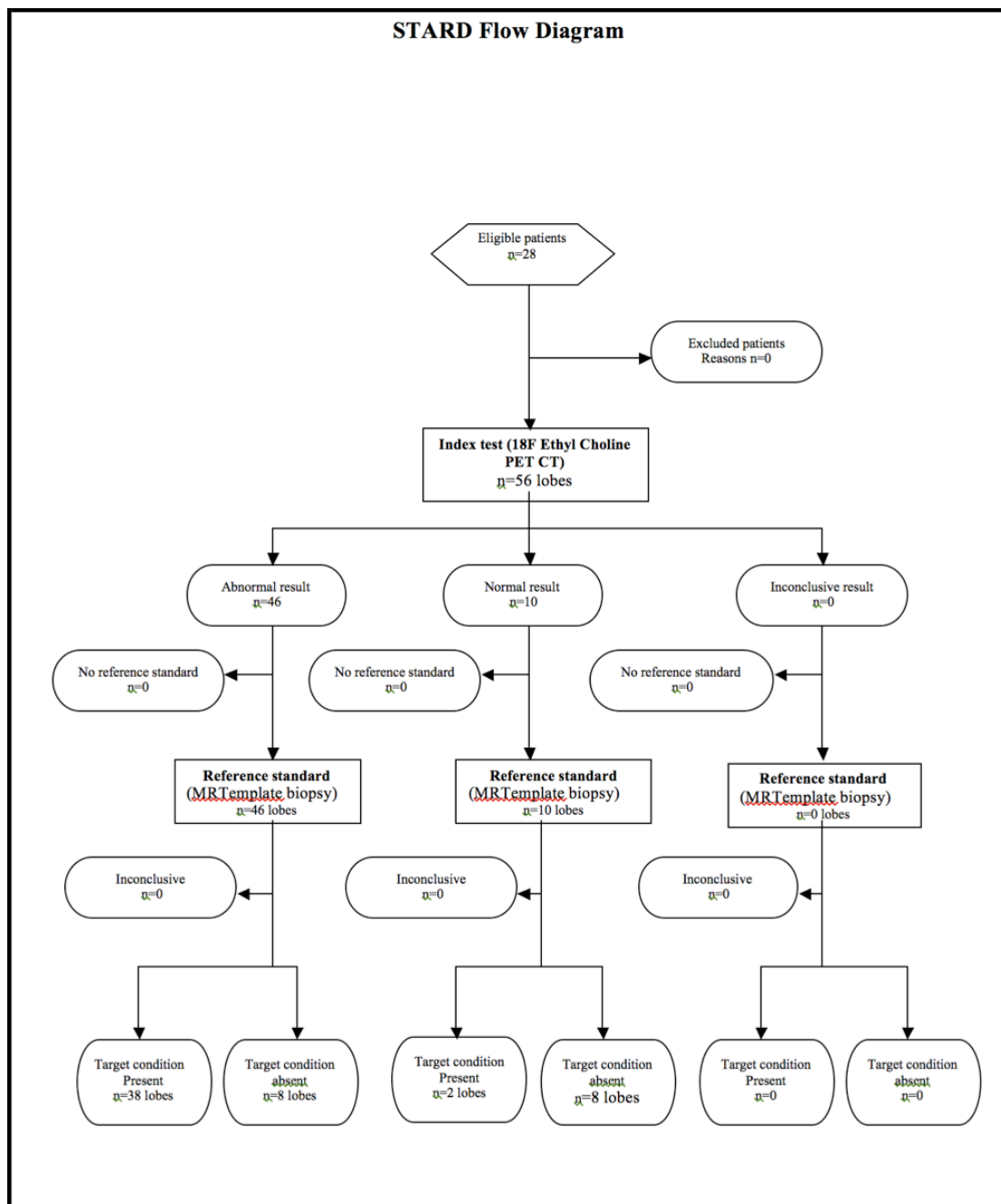


Fig 2: STARD flow diagram

Results

The mean age of the patients was 68.8 years (median 68.5 years, range 53-79 years) and mean PSA was 12.1 µg/L; median 9.1, range 0.6-45 µg/L; Roche Modular method. The SUV_{max} range for 60 and 90-min ¹⁸F-FECH PET/CT was 1.3-11.4 and 1.2-10.9 respectively (Table 2). The mean MCCL was 4.4 mm (median 4 mm, range 1-14 mm) and the mean TCCL was 14.6 mm (median 14.6 mm, range 1-82 mm). Prostate cancer was identified in 38 lobes with Gleason grade 6 in 5 lobes (8.9%), 7 in 27 lobes (48.2%), and 8 in 4 lobes (7.1%) and 9 in 2 lobes (3.5%).

^{18}F -FECH PET/CT demonstrated uptake in 46 (82%) of the 56 lobes examined (Fig 3). Of the positive 38 cases, a total of 30 had clinical significant disease and 8 had clinically insignificant disease. ^{18}F -FECH PET/CT detected clinically significant and insignificant cancer in all 38 cases.

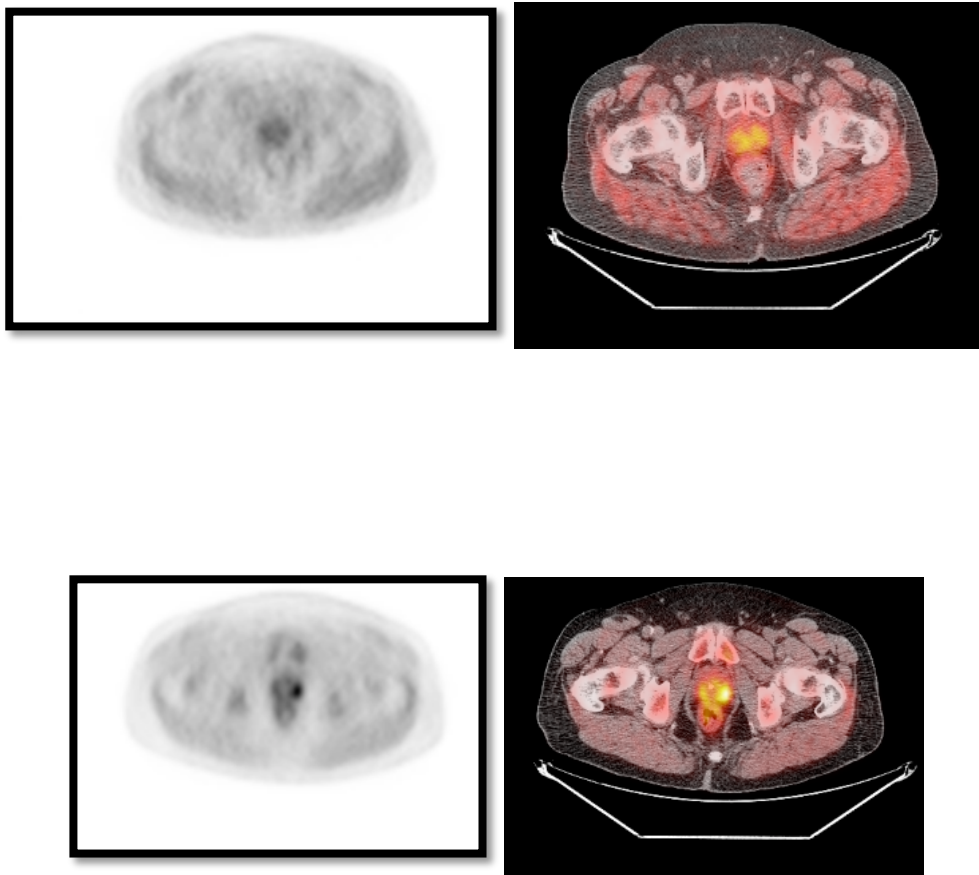


Fig. 3. Axial PET and fused ^{18}F -FECH PET/CT) images (Top row 60 minutes and bottom row 90 minute images) in a 75 years old patient , PSA 19.3 with biochemical relapse of prostate cancer. The 60 minute images show mild to moderate intensity uptake in both lobes of the prostate gland. The 90 minute image show focal intense uptake in the left lobe (4 o'clock position) and low grade uptake on the contralateral side. The biopsy showed Gleason 4+4 adenocarcinoma on the left and 3+4 on the right.

Histologically prostate cancer was identified in 38 lobes while in 8 cases there was no evidence of neoplasia. Lobes which were negative histologically but positive PET findings (false positive) consisted of normal prostate tissue in 1 case, radiotherapy effect in 1 case with 6 cases of fibrosis. ¹⁸F-FECH PET/CT was negative (Fig 4) in 10 lobes out of which 2 lobes had clinically insignificant disease. The histopathological features of the remainder of the 8 lobes consisted of normal prostate tissue in 7 and atypical acini in 1 lobe only.

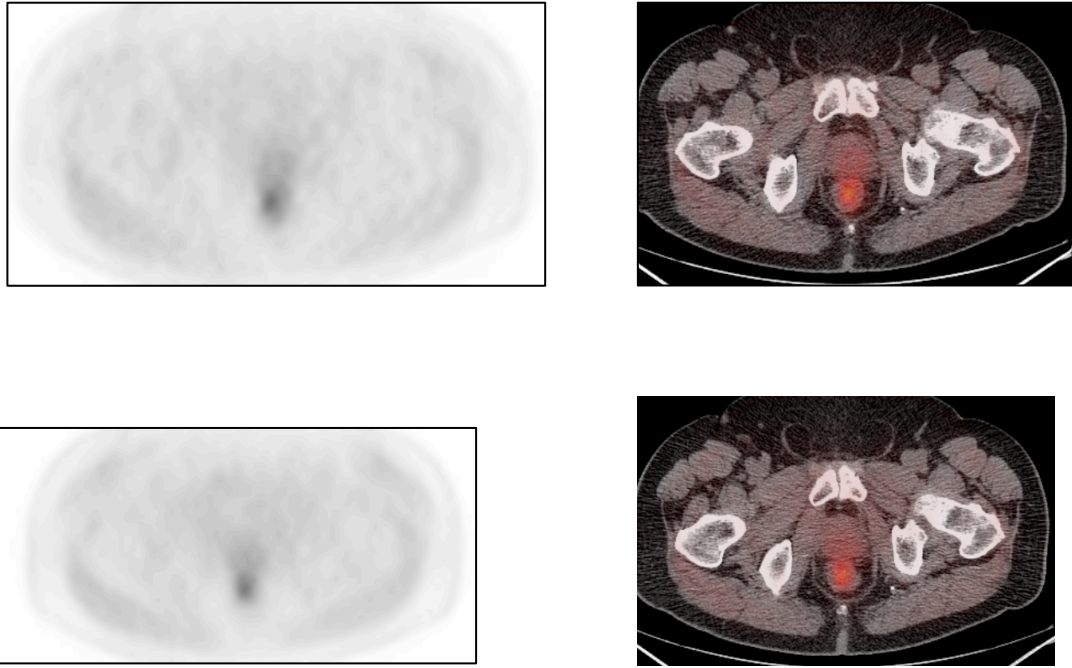


Figure 4: Axial PET and fused ^{18}F -FECH PET/CT images (Top row 60 minutes and bottom row 90 minute images) in a 58 years old patient , PSA 3.36 and previous history of radiotherapy showing no evidence of tracer avid disease. There was no evidence of malignancy on biopsy.

We evaluated the correlation (p value) between MCCL, TCCL and SUV_{max} (on 60 minutes and 90 minutes) ¹⁸F-FECH PET/CT by univariable and multivariable analysis (Table 3). For 60 minutes SUV_{max} and MCCL the p values by univariable analysis was 0.026 and by multivariable analysis it was 0.11. The corresponding values for 90 minutes SUV_{max} were 0.400 and 0.90. For TCCL and 60 minutes SUV_{max} the p value was 0.005 by univariable analysis and 0.022 by multivariable analysis. For TCCL and 90 minutes SUV_{max}, the corresponding values were 0.626 and 0.804. Overall, 60 min SUV_{max} predicted the risk of harbouring clinically significant prostate cancer on TPM (OR 1.36, p=0.016). This relationship was weakened at 90 min (OR 1.38, p=0.110). For 60 minute imaging the sensitivity, specificity and ROC (AUC) were 75%, 75%, 0.746 (95% CI 0.612, 0.853). For 90 minutes imaging the sensitivity, specificity and ROC (AUC) were 73.7%, 58.3% and 0.646(95% CI 0.498, 0.776), Fig 5. The overall sensitivity, specificity, positive predictive value, negative predictive value were 95%, 50%, 82.6%, 80% respectively.

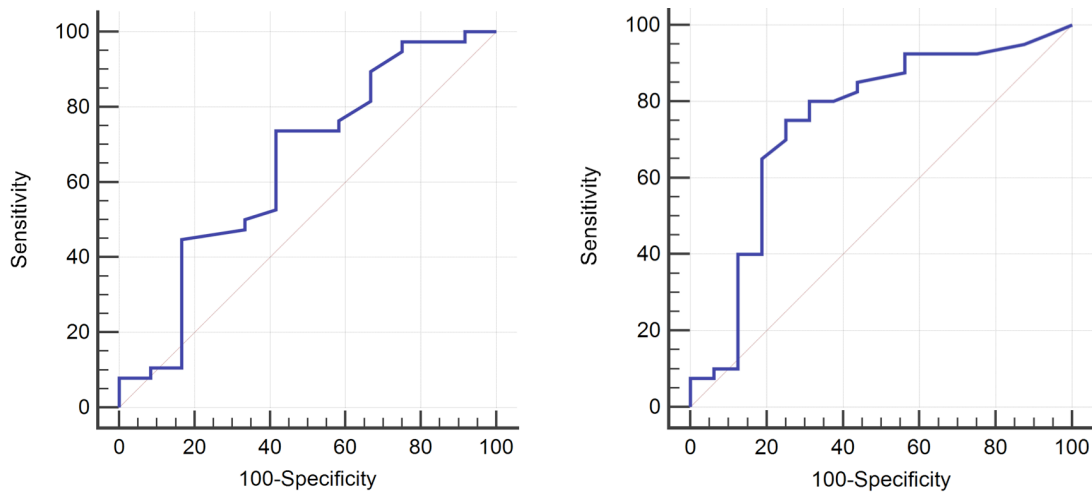


Figure 5: Receiver operating characteristic curve of tumour involvement on the bases of maximum standard uptake value (SUVmax) on the left is for 60 minutes and on the right for 90 minute images. ROC (AUC) for 60 min 0.746, 95%CI 0.612, 0.853 and for 90 minutes ROC (AUC) 0.646, 95% CI 0.498, 0.776.

The outcome of ^{18}F -FECH PET/CT in patients with different treatment types are shown in Fig6, Fig 7 and Fig 8. These 3 STARD flow charts show patients who received single treatment and multiple treatments.

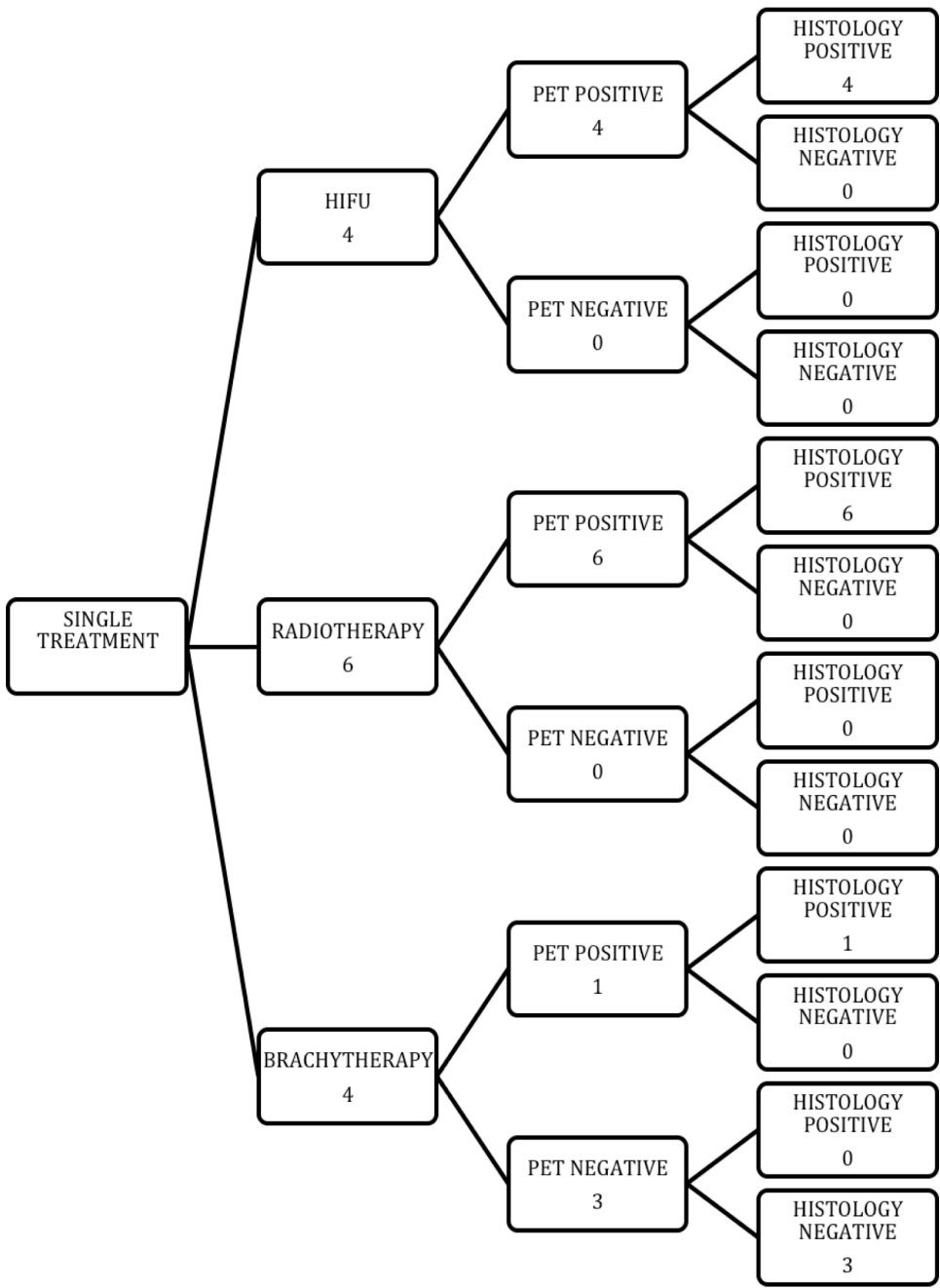


Fig 6:

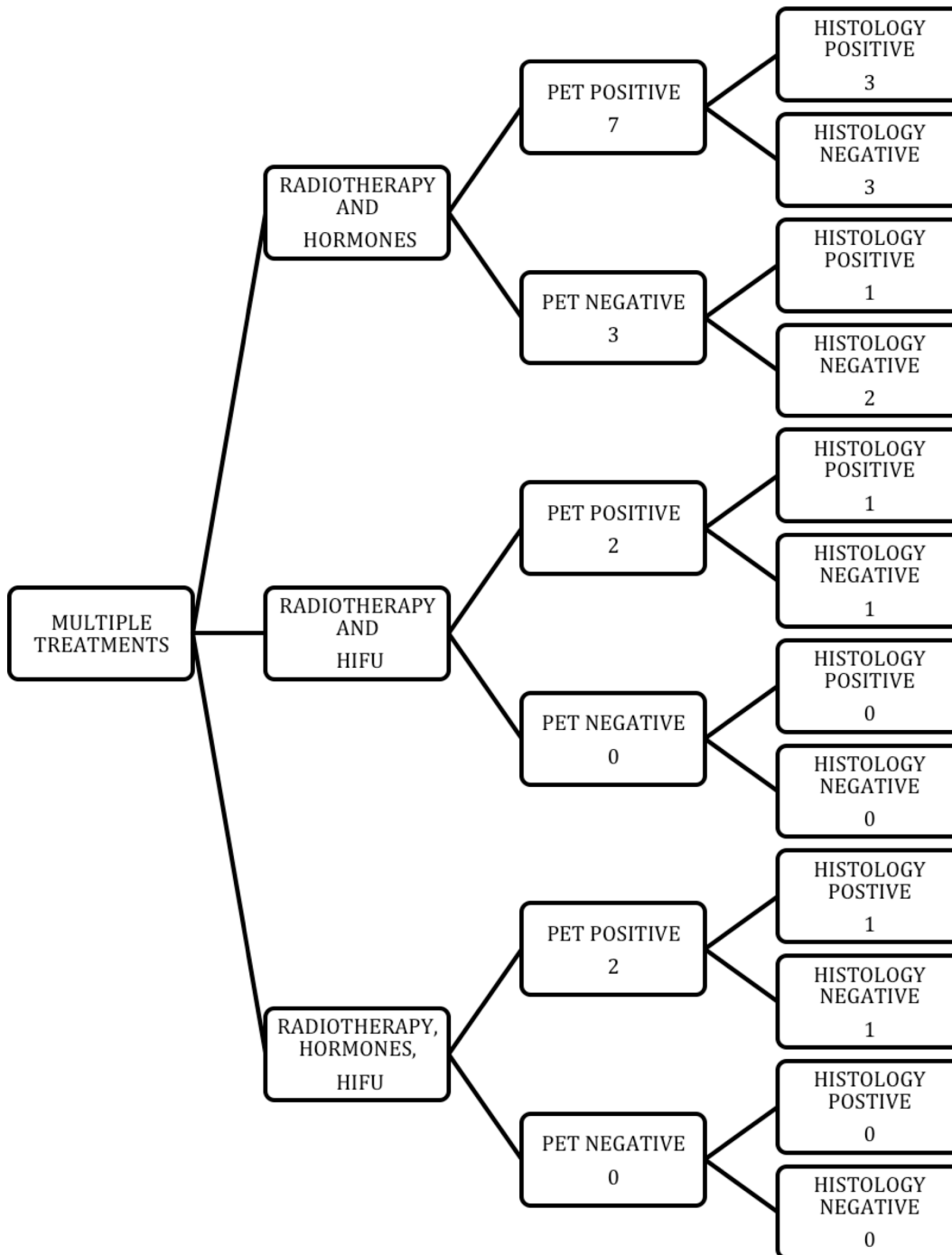


Fig 7:

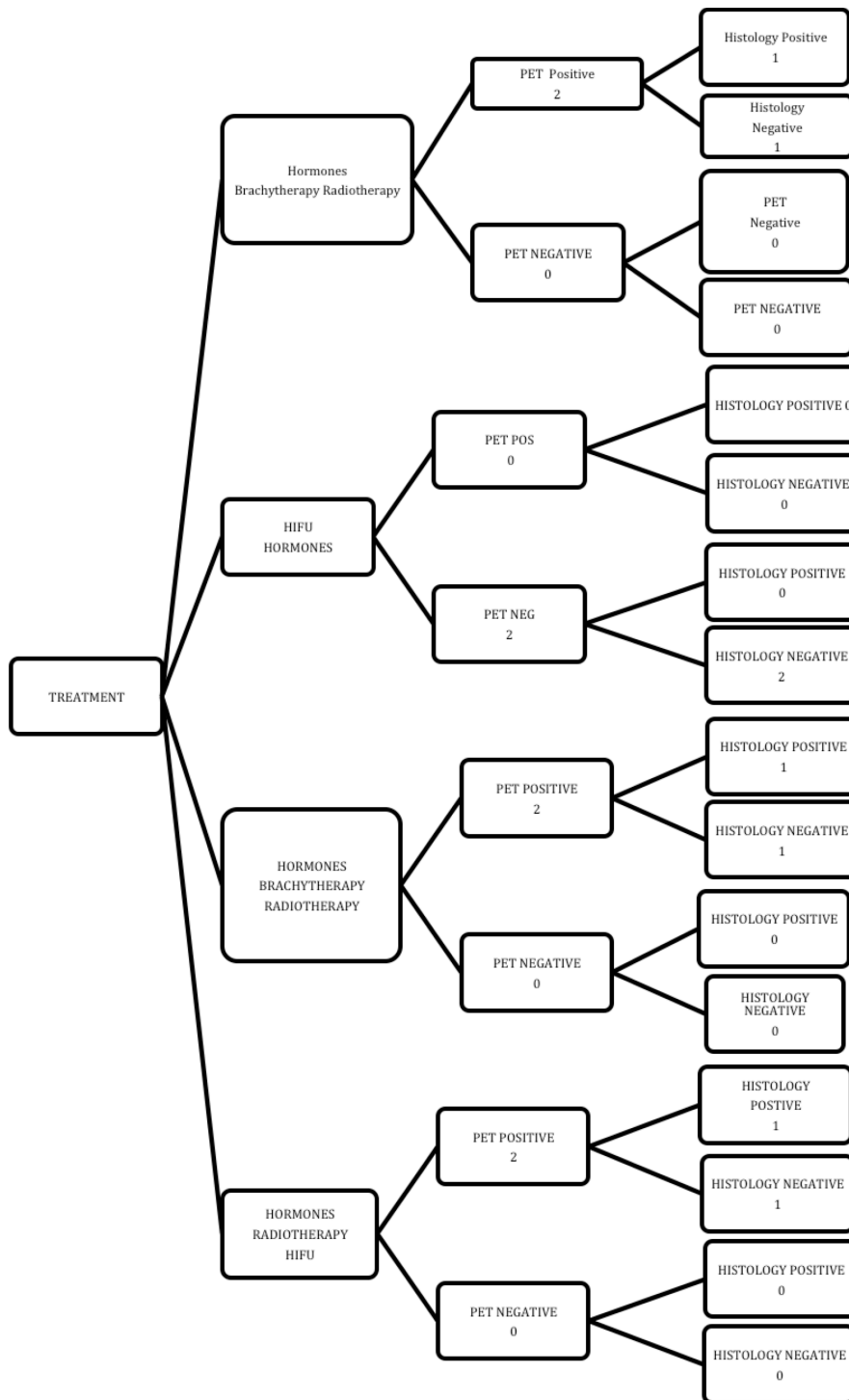


Fig 8

Discussion

This is the first study to demonstrate the correlation between TPM and ^{18}F -FECH PET/CT in patients with prostate cancer. We have thereby succeeded in showing with this pilot study that ^{18}F -FECH PET/CT can detect clinically significant disease.

There is diverse clinical course and natural history of prostate cancer as the prostatic lesions may vary from small indolent foci to highly aggressive and disseminated disease. Prostate carcinogenesis is underpinned by molecular imaging, which is non-invasive and demonstrates biologic interactions. The biomarkers which are used to evaluate the biological heterogeneity fall in different groups i.e. imaging of cell metabolism, imaging of prostate cancer specific membrane proteins and receptor molecules and those that bind to the bone matrix adjacent to the bone. Thus imaging of different phenotypes associated with varying stages of prostate cancer requires knowledge of underlying biological process ¹¹.

The study adds to the developments in the field of molecular imaging of the prostate and forms part of the pilot programme to synchronise local practice with international centres. As part of the first phase we evaluated the visceral localisation of ^{11}C Choline, ^{18}F Ethyl Choline and ^{18}F Methyl Choline as part of multicentre study ¹² in disease-free patients studying extra-prostatic sites. In the second phase we studied the prostate gland.

We have shown that ^{18}F Ethyl Choline can detect both clinically significant and insignificant cancer with sensitivity of 97.4%. In this pilot study we noted the specificity to be low (52.5%). We evaluated this group further and noted that majority of the cases which were negative histologically but with positive PET findings consisted of patients having effects of previous radiotherapy or fibrotic reaction histologically. This suggests complex relationship between

choline kinase activity and cell healing response post-radiotherapy. We do not know how long after radiotherapy, ^{18}F Ethyl Choline PET keeps demonstrating avidity making it indistinguishable from prostate cancer.

We do know from previous work that at cellular level the post-radiotherapy effect differs between the benign and malignant cells. A degree of atrophy and cytological atypia is seen in benign glands post-radiotherapy and this is related to radiation dose. Patients who received 64.8Gy to 81.0 Gy were found to have these findings in 99% and 98% on post-radiotherapy biopsies ¹³. Sheaff and Baithun ¹⁴ evaluated cystoprostatectomy specimen (dose 55 Gy) and they noted findings atrophic and cytological atypia in 80% of cases. The relationship is variable on prostate cancer cells with marked radiotherapy effect characterised by diminution of neoplastic glands, poorly formed glands and cytoplasmic vacuolization with majority of cases with little biological activity left.

We optimised our protocol by asking the patients to empty their bladder before the start of the PET CT exam. The whole body was started at the pelvis as compared to normal FDG exam where majority of the exams start from the head. This was aimed primarily to address the limitations in image interpretation associated with rapid excretion of ^{18}F -FECH as highlighted by Hara et al. ⁸ who developed the ^{18}F -labeled Choline analogue ^{18}F -FECH. The authors described superior image quality of ^{18}F -FECH compared with ^{11}C -choline but rapid excretion of radioactivity into urine, which they identified as a technical limitation of ^{18}F -FECH ⁸, rendering it less suitable for visualization of prostate cancer.

Our work is also different in that we confirmed positive ^{18}F -FECH PET/CT scans using a risk classification system based on the combination of total cancer core length, maximum cancer core length, and Gleason grade obtained via TPM. To our knowledge such biopsy proven rigor has not been applied to ^{18}F -FECH PET/CT imaging previously. Cimitan et al. ¹⁵ evaluated ^{18}F -

fluoromethylcholine in the assessment of suspected recurrence of prostate cancer after treatment. They obtained promising results, with most positive PET/CT findings (43/54) being observed in patients with PSA >4 µg/L and almost all negative PET/CT scans (41/46) being seen in patients with a post-treatment PSA of <4 µg/L. However, only 6% of patients (6/100) in Cimitan et al.'s study¹⁵ had biopsy confirmation of the findings. Our work is unique as it involved detailed histopathological analysis of all the lobes with a validated technique without relying on gross histopathology specimen obtained via radical prostatectomy.

From a clinician's point of view, it is difficult to define prostate cancer risk with any degree of precision. If TRUS biopsy is repeated in men under active surveillance, the diagnosis can change from positive to negative in up to two-thirds of cases¹⁶. At least 50% of men are misclassified by disease burden and at least a third are incorrectly classified by Gleason grade at diagnosis^{9, 17}. TPM biopsies can overcome systematic and random errors by sampling the entire prostate at 5-mm intervals¹⁸. Ahmed HU et al¹⁰ showed the advantage of TPM biopsies in a computer simulation study and concluded that Transperineal prostate mapping may provide an effective method to risk stratify men with localised prostate cancer.

A criticism to our work might be that the reference test (TPM) can detect very small lesions¹⁰ e.g. detection of a 1 mm focus in combination with low Gleason grade (3+3 or below) may be considered for surveillance only but labels the patient as having prostate cancer. However, detection of clinically significant disease in the prostate in the absence of tracer-avid metastatic disease elsewhere can guide clinicians in deciding between active surveillance, systemic treatment and focal treatment. For example treatment of organ-confined disease with modern techniques like HIFU can allow avoidance of aggressive procedures, especially in patients with co-morbidities. Another criticism to this study would be the heterogeneous study population.

Patients treated by radiotherapy and/or HIFU may be grouped together as these patients may be treated by salvage HIFU ablation (and ideally a focal HIFU ablation). Patients on hormones do not raise the same issues in terms of management and they constitute a heterogeneous population by themselves hence the reason why they were treated by hormone manipulation in the first place may be quite variable. This is a preliminary study and more precise assessment of the TPM data in a well defined population should be evaluated in future studies.

The mean PSA is very high (12.1ug/L) in this study and not representative of the patients with a relapse after radiotherapy or HIFU and who are candidates to a salvage treatment. If one takes into account the Phoenix criteria (PSA nadir +2ug/L) the post-radiotherapy recurrences must be detected at an earlier stage. It is the same thing for post HIFU recurrences (Stuttgart criteria + 1.2ug/L). We included all patients who were prospectively enrolled who had TPM and Choline PET/CT exam irrespective of the mean PSA values. Our institute is also a tertiary referral centre with a case mix from different regions.

Those patients who had increased avidity on 90 minutes imaging were found to have a Gleason score of 7. On the other hand increased avidity with 60 minutes imaging compared to 90 minute imaging showed a variable Gleason Grade pattern. We do not know the exact cause of this and this may be related to complex biological behaviour of prostate cancer. In this study we found 60 minutes imaging to be more sensitive and specific than 90 minutes imaging. Further larger studies are warranted to confirm these findings.

The recent introduction of PET/MRI may address some of these limitations and may guide urologists and radiologists in simultaneously targeting metabolically active sites on PET and foci of abnormal signal intensity on MRI. This would facilitate rapid diagnosis and staging of prostate

cancer by offering a “one-stop test.” In addition, co-registration via multimodal approach, navigation via synchronization and combined assessment with Choline PET, ultrasound and mpMRI has been shown to be valuable in planning and real time guidance of biopsy procedures¹⁹. As multi-parametric MRI is increasingly used, there have been developments in quantification parameters obtained via PET. Vermer et al²⁰ have demonstrated that a clinical compromise could be SUVAUC derived from 2 consecutive PET Scans. Their recommendation is to obtain a large blood pool scan by doing dynamic imaging and a whole body scan after injection to obtain lymph node activity concentration. At present MRI and choline positron emission tomography are giving encouraging results in detection of local, nodal and distant metastatic disease even at low PSA level¹⁹.

We are prospectively collecting data in a larger group of patients to evaluate the impact of ¹⁸F-FECH PET/CT imaging on patient management pathway. We postulate that focal salvage therapy may cause less morbidity if the intra- and extra-prostatic disease is detected accurately²¹. Further studies are required to ascertain the relationship between tracer avid clinically significant disease on ¹⁸F-FECH PET/CT, TPM biopsy, subsequent radical prostatectomy and long term cost-effective treatment outcome strategies.

Conclusion

Our results suggest that the data obtained with the ¹⁸F-FECH PET/CT can detect prostate cancer and localize TPM biopsy proven clinically significant prostate cancer with sensitivity of greater than 89.7%. ¹⁸F-FECH PET/CT performed at 60 minutes is more sensitive and specific than 90 minutes imaging.

Acknowledgments

This work was undertaken in the University College London Hospital, which receives a proportion of funding from the UK Department of Health's NIHR Comprehensive Biomedical Research Centres funding scheme and from Cancer Research, United Kingdom. Mark Emberton receives research support from UCLH/UCL Comprehensive Biomedical Research Centre. I am grateful to Shaun Casey from Erigal for providing the biochemical background of ^{18}F -FECH manufacture and Rebecca Gillibrand for assisting with the histopathology image.

References

1. Chism, D. B., Hanlon, A. L., Horwitz, E. M., Feigenberg, S. J. & Pollack, A. A comparison of the single and double factor high-risk models for risk assignment of prostate cancer treated with 3D conformal radiotherapy. *Int. J. Radiat. Oncol. Biol. Phys.* 59, 380–385 (2004).
2. Roberts, S. G., Blute, M. L., Bergstralh, E. J., Slezak, J. M. & Zincke, H. PSA doubling time as a predictor of clinical progression after biochemical failure following radical prostatectomy for prostate cancer. *Mayo Clin. Proc.* 76, 576–581 (2001).
3. Djavan, B. *et al.* Optimal predictors of prostate cancer on repeat prostate biopsy: a prospective study of 1,051 men. *J. Urol.* 163, 1144–1148; discussion 1148–1149 (2000).
4. Schmid, D. T. *et al.* Fluorocholine PET/CT in patients with prostate cancer: initial experience. *Radiology* 235, 623–628 (2005).
5. Sutinen, E. *et al.* Kinetics of [(11)C]choline uptake in prostate cancer: a PET study. *Eur. J. Nucl. Med. Mol. Imaging* 31, 317–324 (2004).
6. De Certaines, J. D. *et al.* In vivo ³¹P MRS of experimental tumours. *NMR Biomed* 6, 345–365 (1993).
7. DeGrado, T. R. *et al.* Synthesis and evaluation of (18)F-labeled choline analogs as oncologic PET tracers. *J. Nucl. Med.* 42, 1805–1814 (2001).
8. Hara, T., Kosaka, N. & Kishi, H. Development of (18)F-fluoroethylcholine for cancer imaging with PET: synthesis, biochemistry, and prostate cancer imaging. *J. Nucl. Med.* 43, 187–199 (2002).
9. Onik, G., Miessau, M. & Bostwick, D. G. Three-dimensional prostate mapping biopsy has a potentially significant impact on prostate cancer management. *J. Clin. Oncol.* 27, 4321–4326 (2009).
10. Ahmed, H. U. *et al.* Characterizing clinically significant prostate cancer using template prostate mapping biopsy. *J. Urol.* 186, 458–464 (2011).
11. Wibmer, A. G. *et al.* Molecular Imaging of Prostate Cancer. *Radiographics* 150059 (2015). doi:10.1148/rg.2016150059
12. Haroon, A. *et al.* Multicenter study evaluating extraprostatic uptake of ¹¹C-choline, ¹⁸F-methylcholine, and ¹⁸F-ethylcholine in male patients: physiological distribution, statistical differences, imaging pearls, and normal variants. *Nucl Med Commun* 36, 1065–1075 (2015).
13. Gaudin, P. B., Zelefsky, M. J., Leibel, S. A., Fuks, Z. & Reuter, V. E. Histopathologic effects of three-dimensional conformal external beam radiation therapy on benign and malignant prostate tissues. *Am. J. Surg. Pathol.* 23, 1021–1031 (1999).
14. Sheaff, M. t. & Baithun, S. i. Effects of radiation on the normal prostate gland. *Histopathology* 30, 341–348 (1997).

15. Cimitan, M. *et al.* [18F]fluorocholine PET/CT imaging for the detection of recurrent prostate cancer at PSA relapse: experience in 100 consecutive patients. *Eur. J. Nucl. Med. Mol. Imaging* 33, 1387–1398 (2006).
16. Van As, N. J. & Parker, C. C. Active surveillance with selective radical treatment for localized prostate cancer. *Cancer J* 13, 289–294 (2007).
17. Scattoni, V. *et al.* Extended and saturation prostatic biopsy in the diagnosis and characterisation of prostate cancer: a critical analysis of the literature. *Eur. Urol.* 52, 1309–1322 (2007).
18. Kepner, G. R. & Kepner, J. V. Transperineal prostate biopsy: analysis of a uniform core sampling pattern that yields data on tumor volume limits in negative biopsies. *Theor Biol Med Model* 7, 23 (2010).
19. Paparo, F. *et al.* Value of bimodal 18F-choline-PET/MRI and trimodal 18F-choline-PET/MRI/TRUS for the assessment of prostate cancer recurrence after radiation therapy and radical prostatectomy. *Abdominal Imaging* 40, 1772–1787 (2015).
20. Verwer, E. E. *et al.* Quantification of 18F-fluorocholine kinetics in patients with prostate cancer. *J. Nucl. Med.* 56, 365–371 (2015).
21. Kanthabalan, A. *et al.* The FORECAST Study - Focal Recurrent Assessment and Salvage Treatment for Radiorecurrent Prostate Cancer. *Contemp Clin Trials* (2015).
doi:10.1016/j.cct.2015.07.004

Chapter 5 : Validating ^{18}F Choline PET/MR with Template Biopsy as Gold Standard

Overview:

In this chapter the accuracy of ^{18}F Choline PET/MR is compared to the reference standard MRI-guided Template mapping biopsies for evaluation of biochemical relapse of prostate cancer

Research questions:

This is a proof of concept study with following research questions

- 1: How ^{18}F Choline PET/MR performs compared to specialized biopsy technique (Template Mapping Biopsies) for evaluation of recurrent prostate cancer?
- 2: Can ^{18}F Choline PET/MR detect clinically significant prostate cancer with good accuracy?

Rationale:

Current imaging gold standard for assessment of prostate cancer relapse is multi-parametric MRI (mpMRI) in combination with conventional imaging techniques such as CT Scan and ^{99}Tc MDP Bone Scan. However, for evaluation of metastatic disease the sensitivity and specificity of these tests is not good. ^{18}F Choline PET/MR, combining anatomical and functional MRI sequences, might provide a novel imaging technique for assessment of biochemical relapse of prostate cancer.

Aims:

1: To compare diagnostic accuracy of ^{18}F Choline PET/MR against reference standard Template Mapping biopsies.

2: To compare the performance and accuracy of ^{18}F Choline PET/MR for clinically significant and insignificant disease.

Author declaration

All of the work in this chapter was conceived, analysed and written by myself, under the supervision of Professor Jamshed Bomanji Consultant Nuclear Medicine and Clinical Head at the Institute of Nuclear Medicine , University College London Hospital. Clinical data input was provided by Dr. Laura May Davis. Scan retrieval was facilitated by Raymond Endozo. Dr Asim Afaq provided input into analysis technique of ^{18}F Choline PET/MR.

Abbreviation Key:

PET: Positron Emission Tomography

MRI: Magnetic Resonance Imaging

CT: Cross-sectional Tomography

mpMRI: multiparametric Magnetic Resonance Imaging

PI-RADS: Prostate Imaging Reporting and Data system

TPM: Template Mapping biopsy

HIFU: High Frequency Focussed Ultrasound

MBq: Megabecquerels

SOP: Standard Operating Procedure

MCCL: Maximum Cancer Core Length

TCCL: Total Cancer Core Length

ROC: Receiver Operator Characteristics

AUC: Area under the curve

CI: Confidence Interval

SUVmax: Maximum Standardised Uptake Value

PACS: Picture Archive Communication System

DWI: Diffusion Weighted Images

Introduction

A useful tool for the detection and risk stratification of primary prostate cancer is multiparametric MRI (mpMRI). It is cost effective, identifies and minimizes the errors caused by standard biopsy (1) (2). Over diagnosis of primary prostate cancer and overtreatment can be avoided by using an imaging technique which facilitates accurate risk stratification (3) (4). MRI is easily available and most of the static and mobile units can offer a service for diagnosis of primary prostate cancer. There are limitations associated with the use of mpMRI such as steep learning curve (5), false positive results (6)(7) and moderate inter-rater agreement (8) . These trigger unnecessary biopsies, which are also associated with complications and detection of low risk disease, which does not require treatment. In order to reduce the reporting errors several image-reporting systems have been introduced. One of the most commonly used reporting systems is Prostate Imaging Reporting and Data system (PI-RADS). The positive predictive value is low for the commonly detected lesions e.g. 15% of PI-RADS and 45% for PI-RADS 4 (6)(9)(10). Moreover 60-70% of mpMRI reports contain at least 1 lesion as PI-RADS 3 or higher (8) This implies that those patients undergoing multiparametric MR also have a targeted biopsy. Since the staging system in majority of the hospitals rely on CT scans and Bone Scans, which can under or over estimate burden of metastatic disease. Therefore unnecessary biopsies can be avoided in patients with metastatic disease by improving the staging work up.

Integration of PET with MRI as simultaneous PET/MR has added advantage of providing complementary anatomical and biological information. This technique can broaden the horizon of molecular imaging however this novel imaging technology may not be used for routine clinical examinations of prostate cancer until the accuracy and impact on diagnostics has been validated with reference tests such as biopsy. We have validated our results of ^{18}F

Choline PET-CT (11) and now we present our analysis of using the same biomarker but with PET/MR technique. To improve the validation standard, we compared our results with Template Mapping biopsies (TPM) which are more accurate in detection of clinically significant disease (12).

Materials and Methods

Patients

This pilot study involved evaluation of 26 prostate lobes in 13 patients (age range 56-79; median 66 years) who had no evidence of metastatic disease on ^{18}F Choline PET/MR and underwent TPM for evaluation of disease burden in the prostate gland and presence or absence of metastatic disease. The sample population consisted of 12 patients who were referred for suspected biochemical relapse of Prostate cancer following treatment while 1 patient was on active surveillance and underwent ^{18}F Choline PET/MR following rise in serum PSA. The previous treatments were subdivided in two main groups: single or multiple modes of treatments. Single treatment consisted of high-intensity focused ultrasound (HIFU) or radiotherapy. The second group consisted of patients who had received different lines of treatment in varying combinations (radiotherapy, HIFU, hormones and brachytherapy). Treatment groups have been listed in Table 1.

Mode of Treatment	No: of Patients
Active Surveillance	1
Single (n=5)	
Radiotherapy	3
HIFU	2
Multiple Treatments (n=7)	
Radiotherapy, Hormones	4
Radiotherapy, HIFU	1
Radiotherapy, Brachytherapy	1
Radiotherapy, Hormones, Brachytherapy	1
Total No: of Patients	13

Table 1: Treatment distribution in 13 patients who had ¹⁸F Choline PET/MR and TPM.
Note-HIFU=High Intensity Focused Ultrasound

The Radiopharmaceutical ^{18}F Choline

^{18}F Choline was provided by PETNET. All quality control parameters were fulfilled during the commercial preparation.

The Index Test

Patients were injected intravenously with 370MBq \pm 10% of ^{18}F Choline (effective dose 12.95mSv). Whole body PET/MR images were acquired 60 minutes after tracer injection. The patients were asked to empty their bladder before imaging. PET and MR sequences acquired are summarised in Table 2. Detailed SOP for ^{18}F Choline PET/MR is provided as supplementary material.

Acquisition Technique

Scanning Parameters

Landmark	Forehead	
MR Acquisition Protocol	INVPM106	
MR Sequences	Survey T1 Dixon Coronal MRAC – 5 bed T2 HASTE Axial T1 Dixon Axial MRAC Pelvis – 1 bed	Diffusion Pelvis Region Specific Sequences as appropriate
PET Acquisition Parameters	3D, 3Minutes / Bed, Randoms from Singles	
PET Recon Parameters	Iterative reconstructions 3 Iterations 21 subsets 172 matrix, Smooth: Gaussian FWHM 5 mm	

Table 2: Acquisition technique and scanning parameters for ^{18}F Choline PET/MR of the Prostate.

^{18}F Choline PET-MR images were initially reported prospectively as per departmental SOP and a second reading was done by AH retrospectively who was blinded to the histologic outcomes. These studies were read using OsiriX, an open source software for navigating in multi-dimensional DICOM images with built-in capacity to scroll through PET, MR and fused images.

The Reference Test

After imaging, Transperineal MR TPM biopsy was performed in 13 patients in whom disease was confined to the prostate gland on imaging who showed no evidence of nodal or metastatic disease. These men were eligible for salvage therapy. TPM involved 5mm sampling of the whole prostate (**Fig 1**) using a brachytherapy template grid placed against the perineum. To overcome the random and systemic sampling error inherent in transrectal ultrasound (TRUS)-guided biopsies (13) (14). Biopsies were plotted into 20 zones (modified Barzell zones) summarised in **Fig 2**.



Fig 1: Template Mapping Biopsy machine at UCLH which is used in theatre and biopsies are obtained under general anaesthesia as day case procedure

Left parasagittal anterior apex

Left parasagittal anterior base

Right parasagittal anterior apex

Right parasagittal anterior base

- Midline apex
- Midline base
- Left medial anterior apex
- Left medial anterior base
- Right medial anterior apex
- Right medial anterior bas
- Left lateral
- Right lateral
- Left parasagittal posterior apex
- Left parasagittal posterior base
- Right parasagittal posterior apex
- Right parasagittal posterior base
- Left medial posterior apex
- Left medial posterior base;
- Right medial posterior apex
- Right medial posterior base

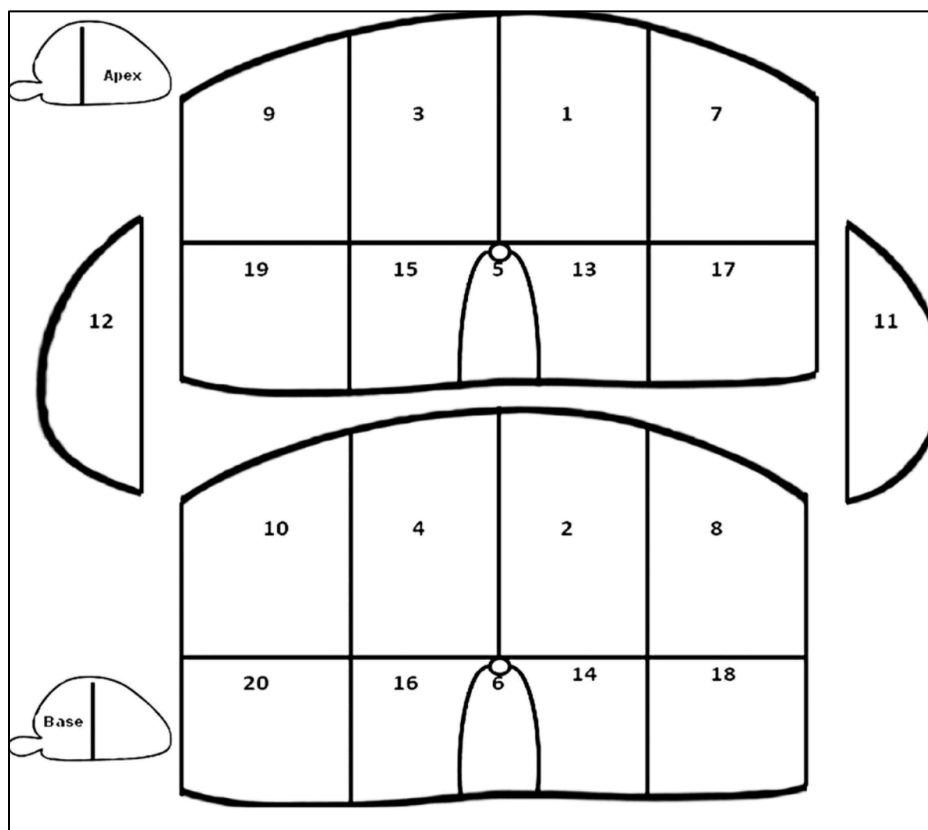


Fig 2: Modified Barzell zones used in Transperineal MR TPM biopsy.

Two variables, which were measured on TPM, were

Maximum cancer core length (MCCL)

Total cancer core length (TCCL).

For instance, if a cluster of three positive adjacent biopsies showed cancer core lengths of 2, 2, and 4 mm, the MCCL will be 4 mm and the TCCL would be 8 mm. The histopathology generated by the biopsies was analysed and reported by a uropathologist with 10 years' experience.

The Target Condition

Prostate cancer was categorized into clinically significant or insignificant disease. This definition was based on previous work by Ahmed HU (14) on computer based simulation. TCCL thresholds of 10 mm or greater and 6 mm or greater provided 95% or greater sensitivity to predict lesions 0.5 mls or greater and 0.2 mls or greater respectively. MCCL of 6mm or greater and 4 mm or greater provided 95% or greater sensitivity to predict lesion 0.5 mls or greater and 0.2 mls or greater, respectively. These definitions have been validated and illustrated in **Fig 3**.

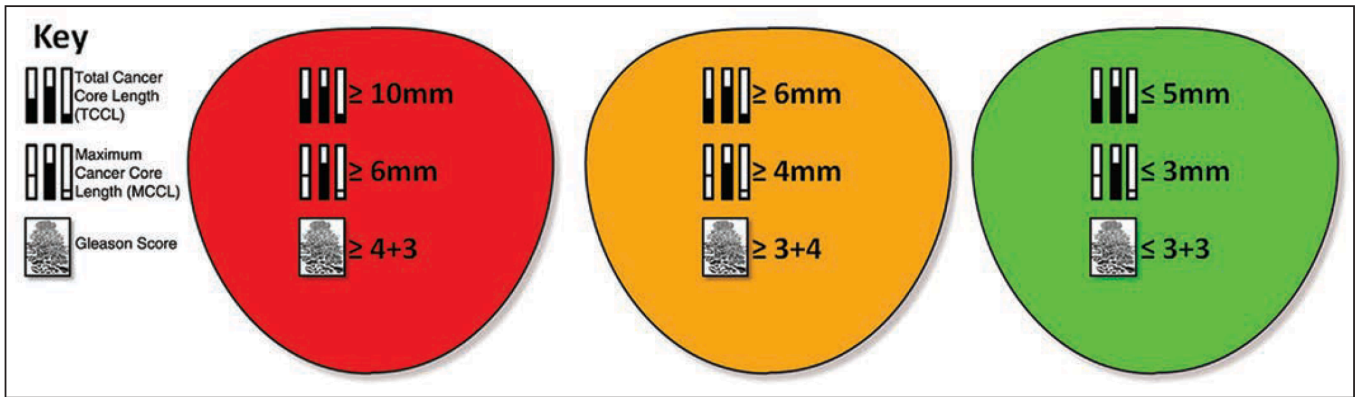


Fig 3: University College London Hospital definition of clinically significant (red and orange) and green (insignificant disease). Ahmed HU et al, Characterizing clinically significant prostate cancer using template prostate mapping biopsy. J Urol. 2011 Aug;186(2):458–64

Measuring Agreement

Paired ^{18}F Choline activity and histopathology output were analysed on a case-by-case basis using a consensus approach. The pathology outputs were limited to clinically insignificant disease (green) and clinically significant disease (yellow and red) as shown in Fig 3. Imaging outputs were limited to positive or negative.

Planned Analysis

On the basis of the histopathology results, the specificity, sensitivity, positive predictive values, negative predictive values, and ROC AUC of ^{18}F Choline PET/MR were calculated for 60 minutes images for detection of prostate cancer. We also evaluated the performance of ^{18}F Choline PET/MR in TPM-proven cases in which histopathology analysis showed clinically significant disease. **Fig 4** provides a flowchart outlining the study population.

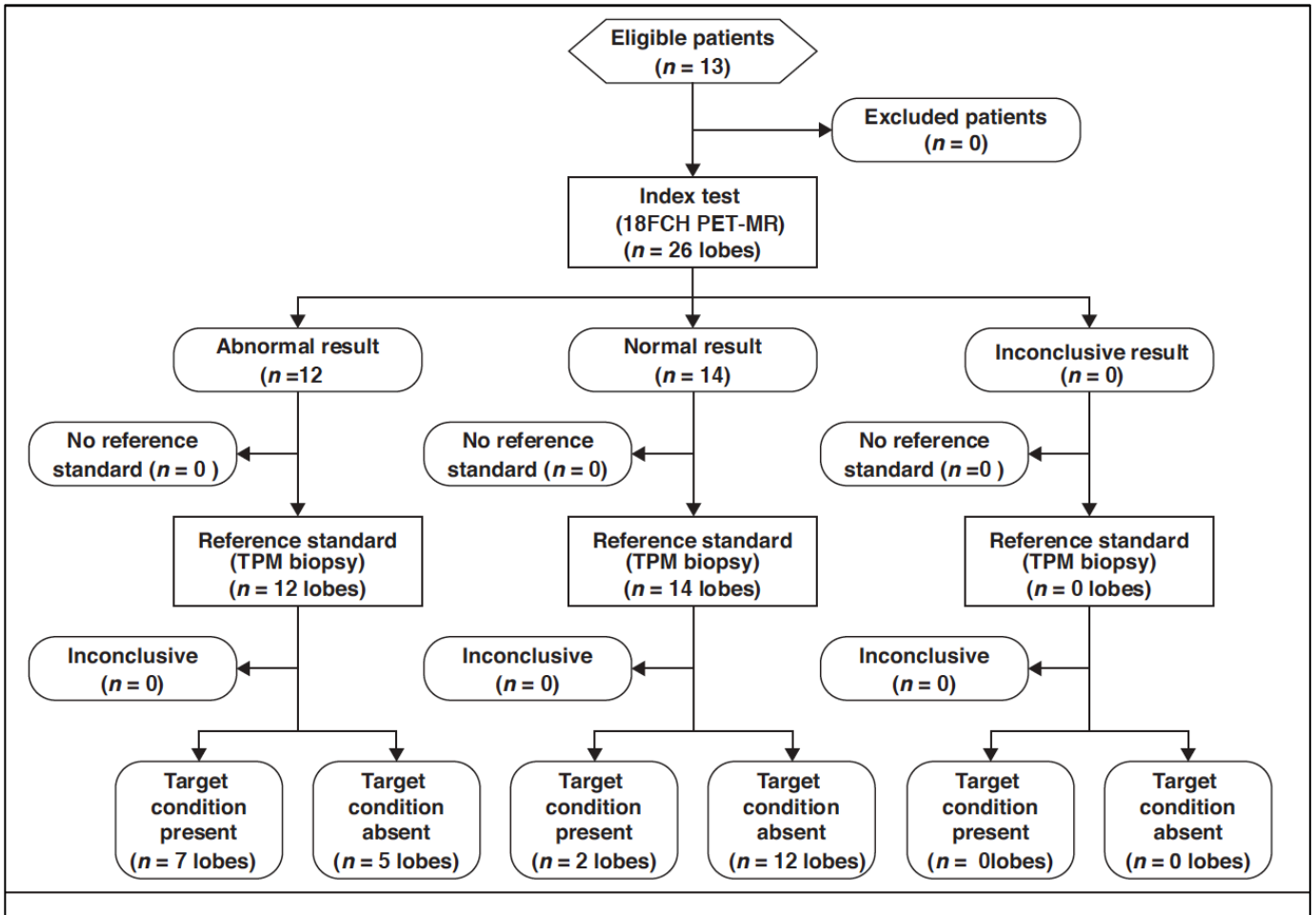


Fig 4: Standards for Reporting of Diagnostic Accuracy flow diagram for full study population. TPM=Template guided prostate mapping biopsy

Results

The mean age of the patients was 66 years (median 66; range 56-79 years) and mean PSA level was 5.17 ng/mL (Median 4.40 ng/mL; range 1.0-11.1 ng/mL; Roche Modular method method). The mean SUV_{max} was 3.18 (median 2.3; range 0.6-12.3). The mean MCCL was 1.5 mm (range 1-9 mm) and the mean TCCL was 3.1 mm (range 1-28 mm). These have been listed in Table 2.

Patient number	Side	Age (years)	PSA (ng/mL)	MCCL (mm)	TCCL (mm)	Gleason Score	Maximum Standardised Uptake Value (SUVmax)
1	Left	66	4.29	0	0	0	3.3
1	Right	66	4.29	0	0	0	6.8
2	Left	56	2.67	7	14	7	3.4
2	Right	56	2.67	0	0	0	1.8
3	Left	76	6.90	0	0	0	1.7
3	Right	76	6.90	0	0	0	1.9
4	Left	78	1.60	2	2	7	0.8
4	Right	78	1.60	0	0	0	1.1
5	Left	60	4.18	0	0	0	1.8
5	Right	60	4.18	9	28	7	3.2
6	Left	58	1.10	2.5	2.5	6	3.5
6	Right	58	1.10	0	0	0	12.3
7	Left	79	1.00	0	0	0	0.6
7	Right	79	1.00	0	0	0	1.3
8	Left	67	5.50	0	0	0	4.3
8	Right	67	5.50	0	0	0	1.6

9	Left	66	9.82	0	0	0	2
9	Right	66	9.82	2	3	7	1.8
10	Left	67	9.26	0	0	0	5
10	Right	67	9.26	3	6	7	2.6
11	Left	56	4.40	4	5	6	3.9
11	Right	56	4.40	1	1	6	4.2
12	Left	56	5.40	0	0	0	1.6
12	Right	56	5.40	0	0	0	1.2
13	Left	77	11.11	0	0	0	4.2
13	Right	77	11.11	4	11	7	6.8

Table 2: Lobe based MR Template Guided Biopsy and ¹⁸F Choline PET/MR data in 13 patients

(26 lobes) lobes). Note—PSA = prostate-specific antigen, MCCL = maximum cancer core length, TCCL = total cancer core length,

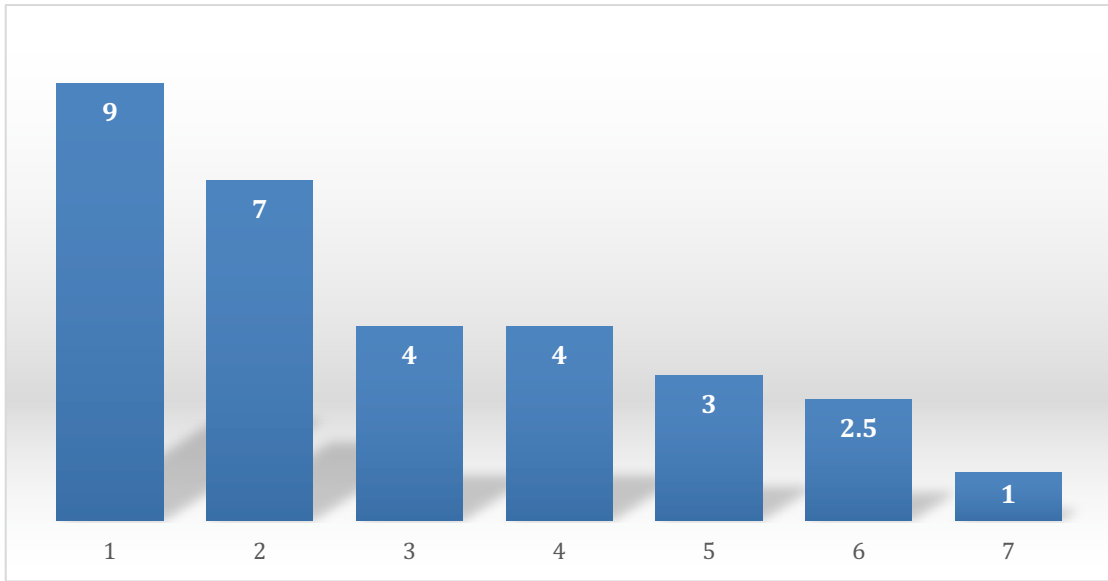
Prostate cancer was identified in 9 lobes with a Gleason of 6 in 3 lobes, Gleason score of 7 in 6 lobes. No tumour had a Gleason score of 7 or higher. In 17 lobes there was no evidence of cancer, clinically significant disease was seen in 4 lobes, and clinically insignificant disease

in 5 lobes. ^{18}F Choline PET/MR detected cancer in all 9 lobes containing either clinically significant or insignificant cancer.

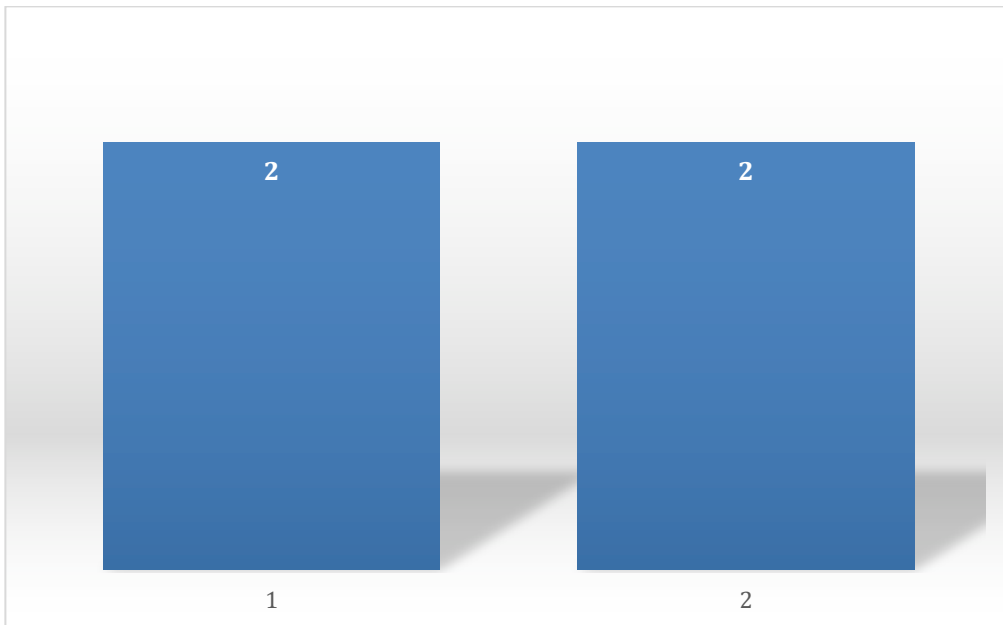
Of the 26 lobes examined, 12 lobes demonstrated increased tracer uptake while ^{18}F Choline PET/MR did not show any pathological uptake in 14 lobes. The 12 lobes, which were positive on PET, had cancer in 7 lobes (True positive) while in 5 lobes there was no evidence of malignancy on histology. Of the 14 lobes reported as normal, 2 had cancer on histology while in 12 lobes (True negative) there was concordance between histology and ^{18}F Choline PET/MR i.e. both histology and ^{18}F Choline PET/MR showed no evidence of malignancy.

False positive findings on ^{18}F Choline PET/MR were detected by identifying lobes that were negative histologically but showed positive findings on ^{18}F Choline PET/MR. The histological features of these lobes consisted of radiotherapy related fibrosis in 1, focal high grade PIN (prostate intra-epithelial neoplasia) in 3 while in 1 cases the histology did not show any pathological features.

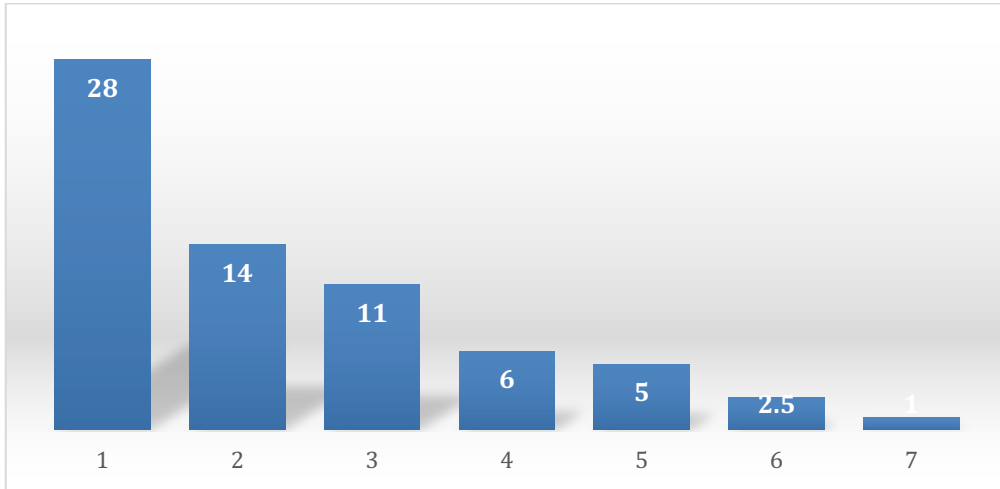
False negative findings on ^{18}F Choline PET/MR were detected by identifying lobes that were reported normal on ^{18}F Choline PET/MR and correlating with histology results, which demonstrated evidence of malignancy. Of 14 lobes reported as normal on ^{18}F Choline PET/MR, only 2 lobes contained evidence of malignancy and in both of these lobes, there was clinically insignificant disease. The MCCL and TCCL in true positive and false positive cases have been illustrated in **Fig 5**



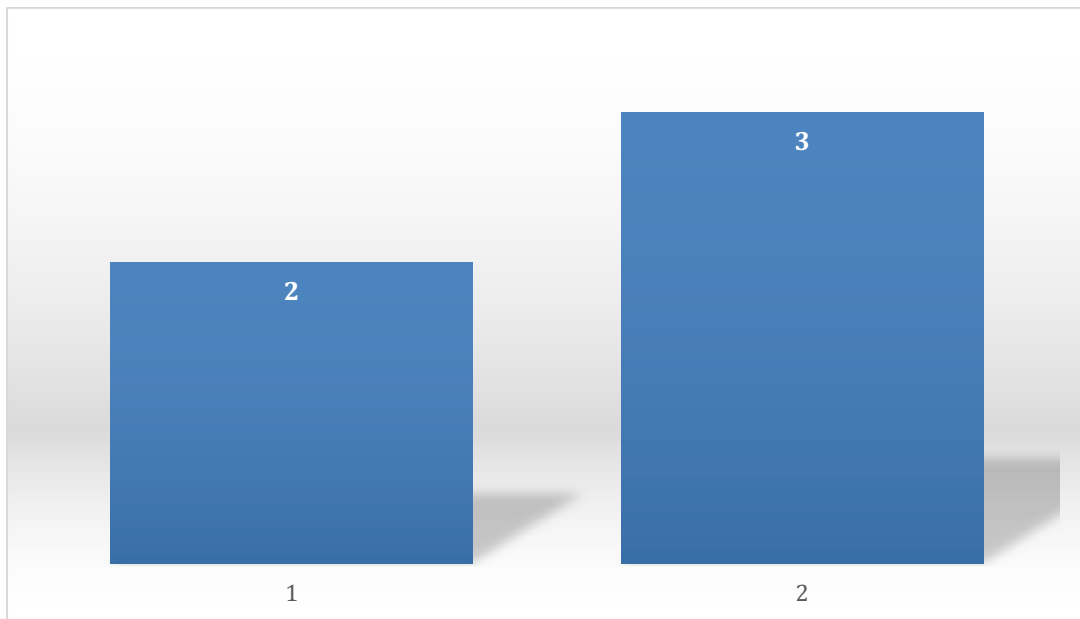
(a) Maximum Cancer Core Length-MCCL (mm) in True positive cases



(b) Maximum Cancer Core Length-MCCL (mm) in false negative cases



(c) Total Cancer Core Length-TCCL (mm) in True positive cases



(d) Total Cancer Core Length-TCCL in False negative cases

Fig 5 (a-d): Graphical representation of Maximum Cancer Core Length MCCL (mm) and Total Cancer Core Length TCCL (mm) in True positive and True negative ¹⁸F Choline PET/MR cases. False negative and false positive cases the MCCL and TCCL would be zero hence those have not been represented in graphs.

As per UCLH histological grading of clinically significant and insignificant disease, the clinically significant disease was seen in 4 lobes and all of these 4 lobes were avid on ¹⁸F Choline PET/MR. Clinically insignificant disease was seen in 5 lobes and out of these 3 lobes were avid on ¹⁸F Choline PET/MR and in 2 lobes PET/MR did not detect disease.

In 17 lobes no malignancy was found and out of these 12 were reported as normal on PET/MR and 5 lobes were reported as abnormal (**Fig 6**)

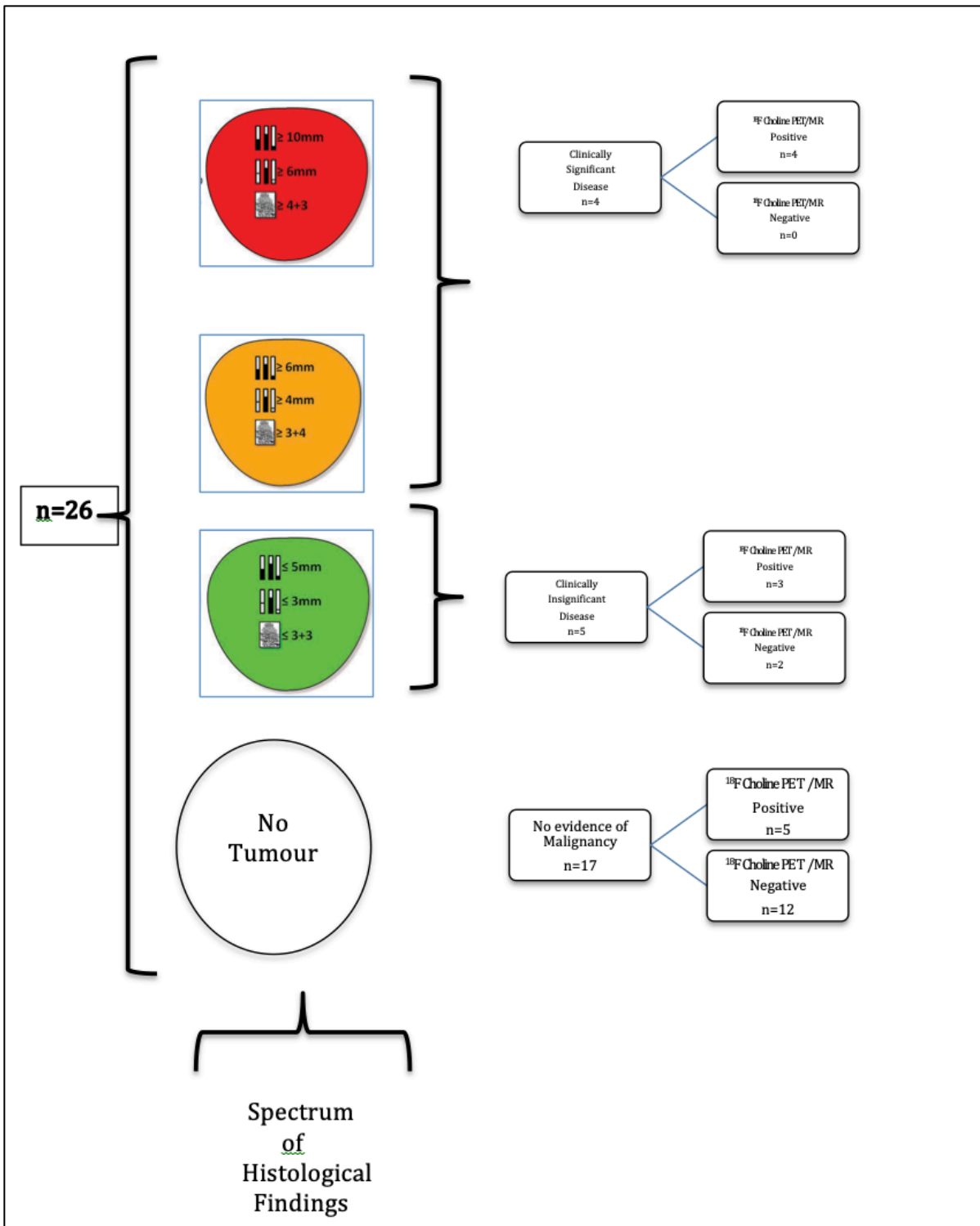


Fig 6: Flow chart illustrating the distribution of case mix based on the UCLH histological definition of **Clinically Significant** (red and yellow) and **Clinically Insignificant disease** (Green). White circle represents **Normal prostate** tissue obtained via template mapping biopsies. (n= number of lobes). In red, yellow and green diagrams the top row represents **TCCL**=Total Cancer Core Length, middle row represents **MCCL**=Maximum Cancer Core Length and lower row represents **Gleason Score**.

We evaluated the correlation (p value) between MCCL, TCCL and SUV_{max} on ¹⁸F Choline PET/MR with univariate analysis. The p value for MCCL was 0.078 and for TCCL 0.093.

Overall the sensitivity, specificity, positive predictive value, negative predictive value and AUC were 77%, 70%, 58%, 85% and 0.621(95% CI, 2.16-4.19)-**Fig 7**.

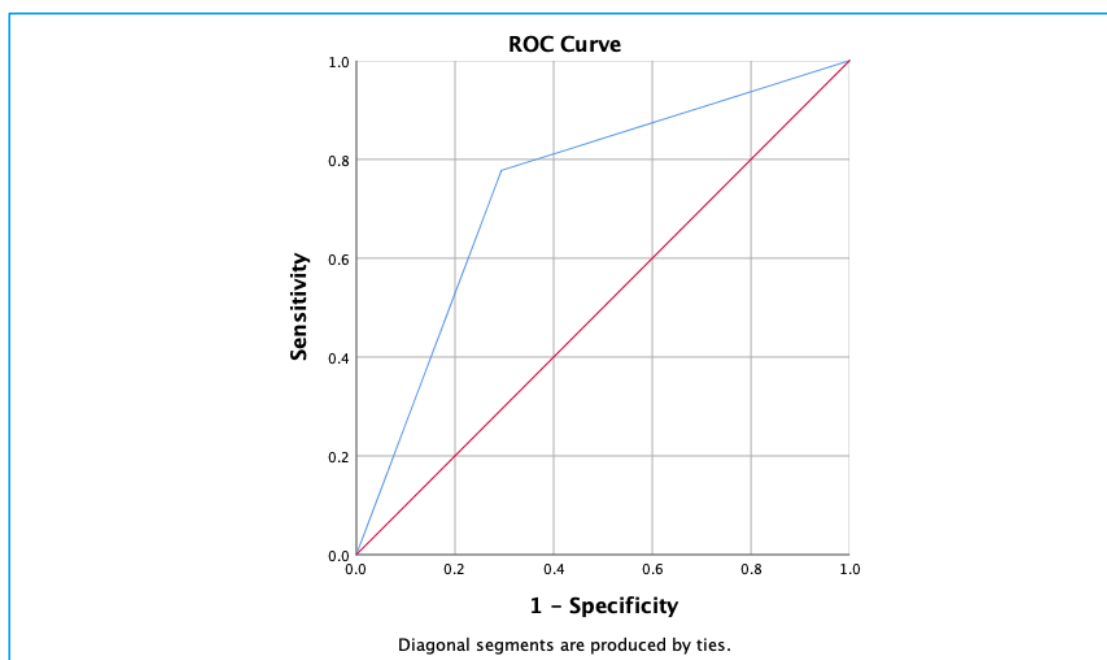


Fig 7: ROC curves of tumour involvement on the basis of maximum standard uptake value (SUVmax) obtained with ¹⁸F Choline PET/MR -AUC=0.742 (95% CI, 0.537-0.947)

The patient who was under active surveillance had ^{18}F Choline PET/MR positive in both lobes on visual assessment. The histology detected malignancy in one lobe only. The outcome of ^{18}F Choline PET/MR inpatient with different treatment types is shown in **Fig 8- Fig 9**.

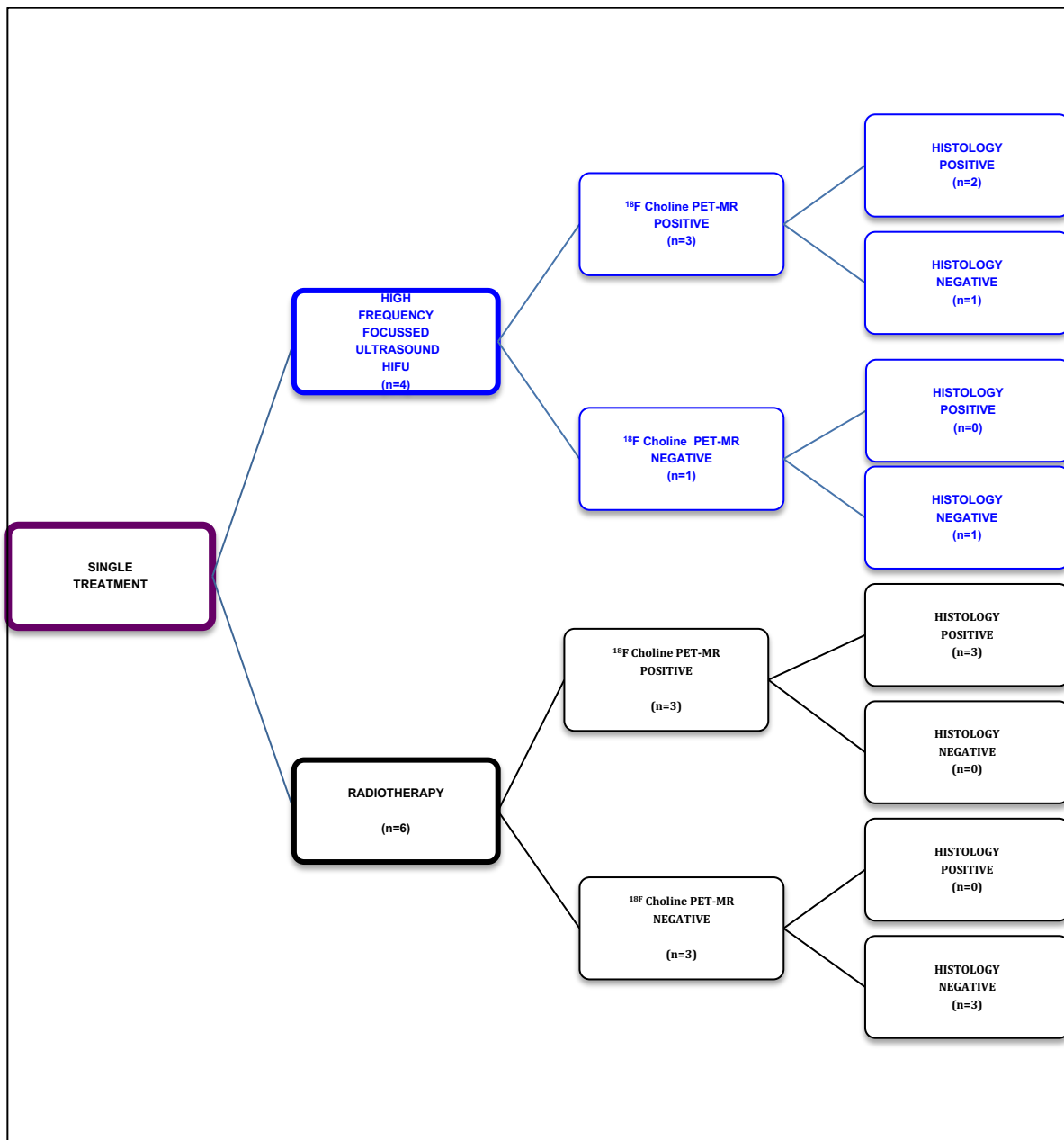


Fig.8-Standards for Reporting of Diagnostic Accuracy flowchart of patients who had single treatment (HIFU or Radiotherapy). n=number of lobes.

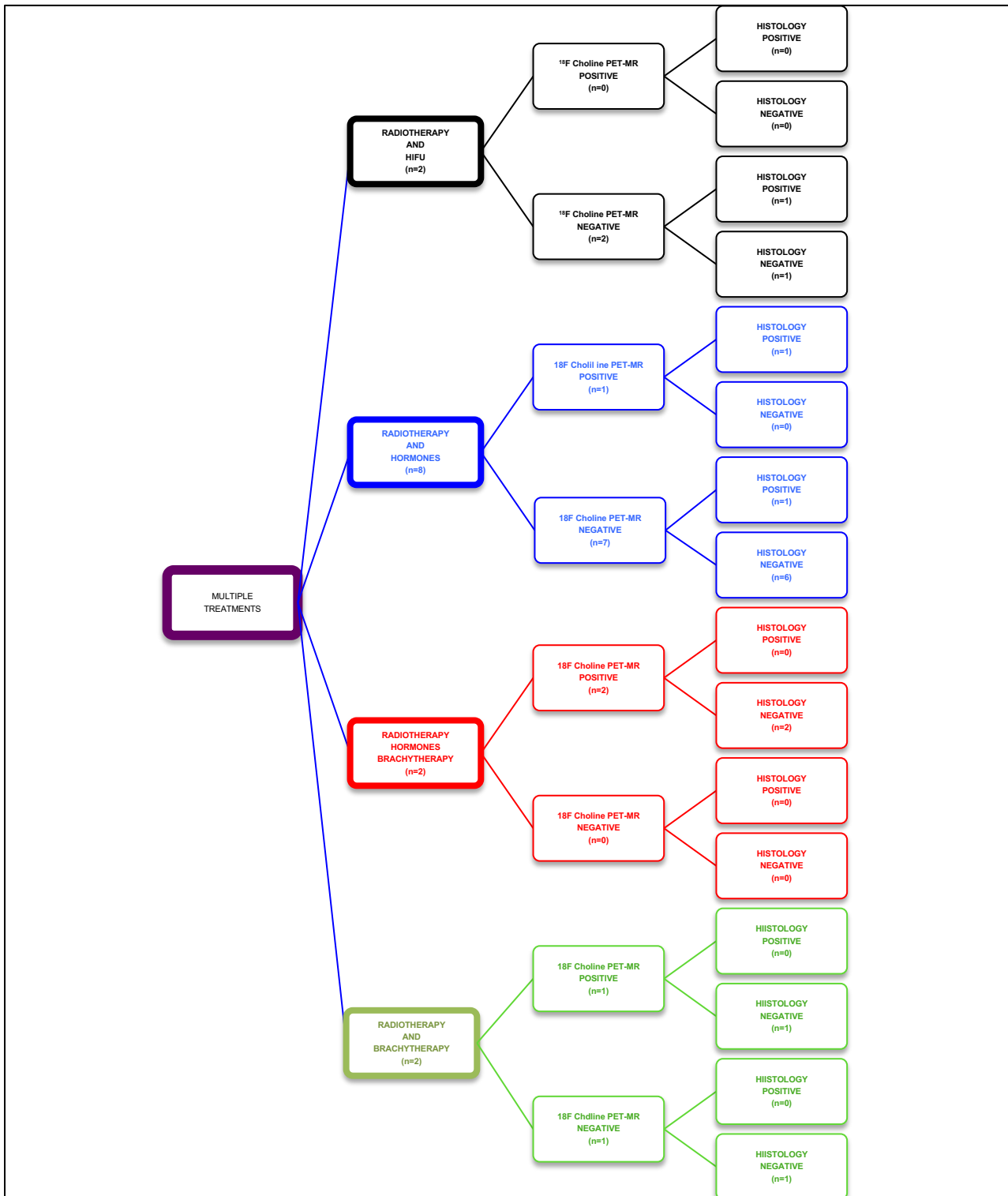


Fig.9-Standards for Reporting of Diagnostic Accuracy flowchart of patients who had multiple treatments (n= number of lobes; HIFU=High Frequency Focused Ultrasound).

Discussion

This study is the first to consider the correlation between TPM (reference test) and ^{18}F Choline PET/MR (index test) which builds on previous work with PET/CT (11). Our results show that

- 1- ^{18}F Choline PET/MR can detect clinically significant and clinically insignificant disease.
- 2- Incidence of false positive ^{18}F Choline PET/MR is higher in patients receiving multiple treatments.
- 3- In patients who have undergone HIFU treatment ^{18}F Choline PET/MR has higher accuracy compared to PET/CT due to better anatomical delineation of post-HIFU changes.
- 4-False negative cases of ^{18}F Choline PET/MR had very small volume disease ($\leq 2\text{mm}$ MCCL and TCCL)

PET-MR is a potentially useful imaging tool for characterization, localization and detection of metastatic spread of disease for Prostate cancer. For clinical setting of biochemical relapse of Prostate cancer ^{18}F Choline PET-MR offers a high negative predictive value of $>85\%$. High grade and clinically significant disease detection in the absence of metastatic disease can help guide local therapy based on risk stratification. Risk stratification is important to facilitate various treatment options based on current guidelines and this includes prostate specific antigen (PSA), Gleason score on biopsy and T score based on diagnostics (15) and all of these have limitations e.g. mpMRI enables improved identification of clinically significant disease however there are false positive rates of low and intermediate risk lesions (16) and this results in further unnecessary biopsies. Although there are a number of studies conducted with ^{18}F Choline PET/CT, we know that CT component does not provide adequate

soft tissue contrast of the prostate. To overcome this, advanced fusion technique can be utilized and this can be in the form of different models such as simultaneous ^{18}F Choline PET/MR or sequential ^{18}F Choline PET/MR. In either case the diagnostic accuracy for detection of prostate cancer will increase.

Our work is also different in that we confirmed positive ^{18}F Choline PET/MR scans using a risk classification system that is based on the combination of total cancer core length, maximum cancer core length, and Gleason grade obtained via TPM.

To our knowledge, a biopsy-proven rigor has not been applied to ^{18}F Choline PET/MR. Our initial work with ^{18}F Choline PET/MR was not restricted to Gleason 3+4 cases and as the results of TPM biopsy shows, there are low, intermediate and high-risk lesions. This was not intentional or part of the study design. We prospectively recruited cases in which both ^{18}F Choline PET/MR and TPM biopsies were done so that we could have a detailed analysis of prostate tissue and correlate the uptake (SUVmax) with the cancer core lengths.

We have observed that the incidence of false positive results is higher in patients with multiple treatments. ^{18}F Choline is known to give false positive results such as benign prostatic hyperplasia and inflammatory foci (11) and the MR component helps to exclude physiological variants. In this study increased uptake was noted in 2 lobes of patient who had received radiotherapy, hormones and then brachytherapy, in 1 lobe of patient who had radiotherapy and hormones, and 1 lobe of patient who had radiotherapy and brachytherapy. The TPM did not reveal any malignancy in these cases.

Interestingly, our results in cases where radiotherapy and HIFU were used did not demonstrate any false positive results. This is contrary to our experience with ^{18}F Choline PET/CT (11) in which we noticed maximum false positive results in patients receiving HIFU treatment. This can be explained by anatomical changes which happen following HIFU (17) such as increased volume of prostate at 1 month (with heterogeneous periprostatic fat signal intensity), at 1-3 months there is formation of “double rim” and at 6 months the volume of prostate reduces by approximately 45% with low signal prostate surrounded by a capacious prostatic cavity. With increased urinary excretion of tracer, this can be easily mistaken as tumour on PET component. MR component of the PET/MR helps identify these changes (**Fig 14**).

Our work is unique in that it is the first study which evaluates simultaneous ^{18}F Choline PET/MR and TPM which provides detailed histopathological analysis of the prostate. TPM biopsies can overcome systematic and random errors by sampling the entire prostate at 5-mm intervals (18) and this can provide an effective way to stratify risk in men with localized prostate cancer (14).

We did in-depth analysis of histopathology of cases where ^{18}F Choline PET/MR findings were false negative. In our cohort, there were 14 lobes, which were reported as normal on ^{18}F Choline PET/MR and out of these there were two lobes where there was evidence of malignancy on histology. None of these had clinically significant disease. The detailed microscopic features of these lobes consisted of minor treatment effect in 1 lobe with small focus of cancer at the right anterior apex (modified Barzell Zones) and these foci were just

sufficient enough to allow Gleason grading on histology with MCCL of 2 mm and TCCL of 3 mm. The other case had radiotherapy related fibrosis and focus of cancer with MCCL and TCCL of 2 mm (Gleason Grade 7) at left medial posterior base (modified Barzell zones).

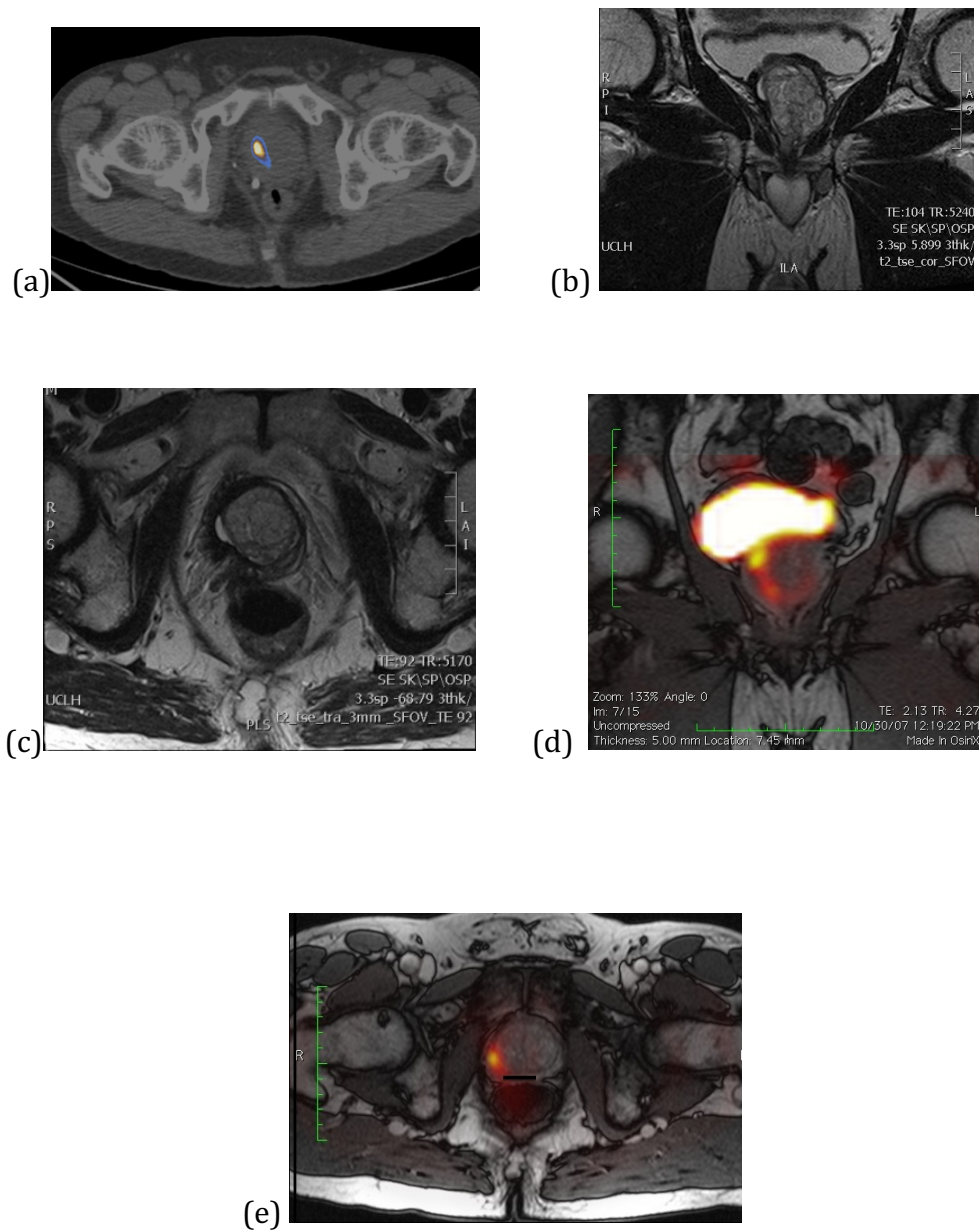


Fig 14 (a-e): (a) axial ^{18}F Choline PET/CT (b-c) coronal and axial MRI prostate (d-e) fused ^{18}F Choline PET/MR prostate. HIFU can alter the anatomical configuration of prostate with cavitation, reduction in volume and periprostatic stranding. The uptake seen in (a) was noted to be a false positive finding as the appearances represent post HIFU cavity with excretory activity easily identified on PET/MR.

LIMITATIONS

- The sample size is small.
- False positive results in lobes with Radiotherapy effect.
- SUVmax overestimation due to rapid excretion of ^{18}F Choline in the urinary bladder.
- Increased detection of microscopic foci of cancer with the chosen reference test (TPM Biopsy)
- Heterogeneous study population
- Mean PSA is high

The study sample size is small mainly because there were logistical problems, having a cohort of patients who had both TPM and ^{18}F Choline PET/MR and patient's refusal to undergo TPM. However it is encouraging to see that both clinically significant and insignificant disease was detected with ^{18}F Choline PET/MR, one would question the number of false positive findings in 5/17 lobes when histology did not reveal any prostate cancer. We have explained that inflammatory tissue can cause false positive findings (11) but another variable, which can help improve the outcome, would be optimization of PET/MR sequences.

Current routine clinical mpMRI procedure includes diffusion-weighted images and dynamic contrast enhanced images in addition to other routine MR sequences. For PET/MR a range of sequences were acquired initially, however over time, based on the feedback of each modality we gradually improved organ based PET/MR image optimization. The attenuation correction maps in clinical PET/MR studies were derived from Dixon sequence, which

provides attenuation correction for different tissue classes (air, fat, lungs, bones and soft tissues). This approach results in improvement in accuracy of SUVmax estimation in the prototype model we followed at UCLH. The Dixon sequence was less than ideal therefore sequence improvement was carried out with diffusion weighted images (DWI) and have been included as part of the standard operating PET/MR procedures for ^{18}F Choline, ^{68}Ga PSMA and ^{18}F PSMA PET /MR imaging. **Fig 15** demonstrates the heterogeneity in MR sequences in 13 patients (26 lobes).

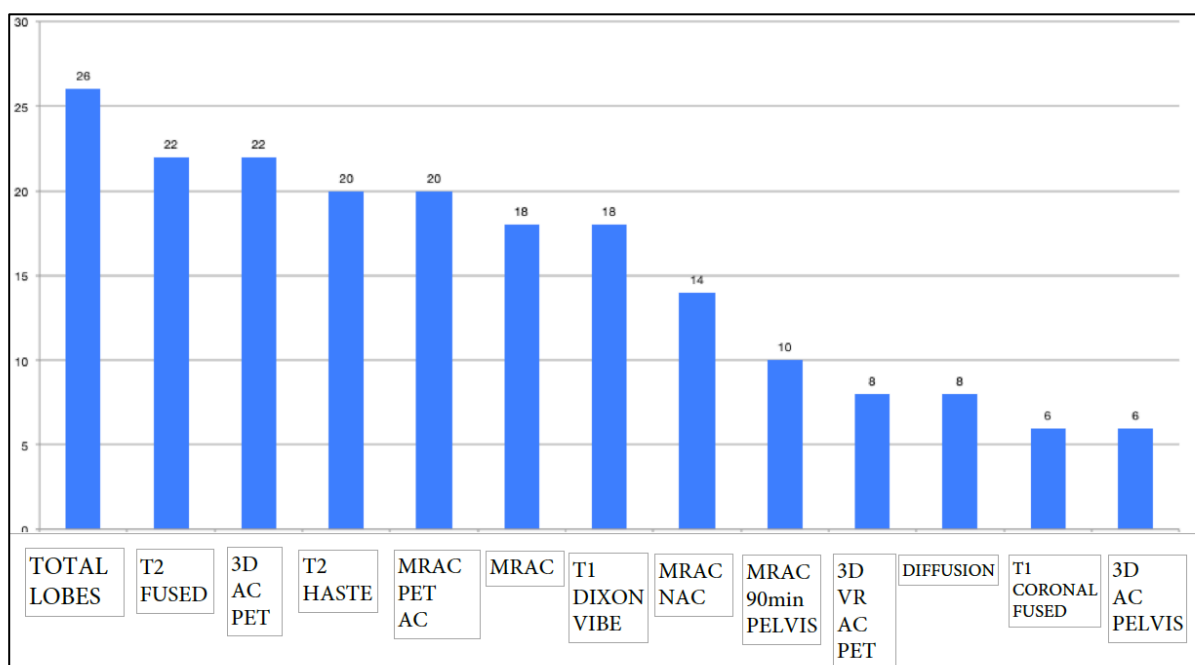


Fig 15: Range of different MR sequences (as part of simultaneous ^{18}F Choline PET/MR acquisition) available on PACS (Picture Archive Communication System) for 13 patients included in this analysis.

Radiotherapy related fibrosis is a complex entity and causes both false positive and false negative findings. It is possibly due to a complex relationship between choline kinase activity and cell healing response after radiotherapy. It is unknown how long after radiotherapy ^{18}F Choline continues to show avidity, making it indistinguishable from prostate cancer. At the cellular level, radiotherapy affects benign and malignant cells differently. Atrophy and cytological atypia is seen in benign glands after radiotherapy that is radiotherapy dose dependent (19). In prostate cancer cells (20) there is marked diminution of neoplastic glands, poorly formed glands, and cytoplasmic vacuolization, with the majority of cases having little biologic activity left. We do not know whether a choline avid site but histologically atrophic tissue actually represents some degree of viability at cellular level and results in future biochemical relapse if there is incomplete scar formation. This would require a retrospective analysis to see the biochemical effect of this phenotypic-genotypic (PET/MR imaging) and histological discordance.

Despite using Dixon sequence for attenuation correction we anticipate some degree of SUVmax overestimation due to excretory activity. We optimized our protocol by asking patient to empty their bladder before the start of the PET/MR examination. The whole body scan was started at the pelvis. This difference was intended primarily to address limitations within image interpretation associated with rapid excretion of ^{18}F Choline Hara et al (21).

The reference test (TPM) can detect microscopic lesions, which may be considered for surveillance only but labels the patient as having prostate cancer. On the other side,

exclusion of metastatic disease by ^{18}F Choline PET-MR and correct risk stratification of localized prostate cancer can allow clinicians to use modern techniques like HIFU. This allows avoidance of aggressive procedures, especially in patients with comorbidities.

Another limitation of this study would be the heterogeneous study population and elevated mean PSA. These two problems could be avoided by defining a trigger PSA at which the index test could be requested at an early stage of biochemical relapse and avoiding cases where radiotherapy has been used more recently. Cases, which have been included in this study, have received a variety of treatments. To simplify, we have divided the patient cohort into groups such as active surveillance, single treatment and multiple treatments. We have also provided output according to STARD flow chart to delineate the performance in each group. Despite heterogeneity, we have observed that radiotherapy causes false positive results and when used in combination with treatments there is increased incidence of false positive ^{18}F Choline PET/MR results. **Fig 16-Fig 20** demonstrates different examples of ^{18}F Choline PET/MR findings with histopathology results.

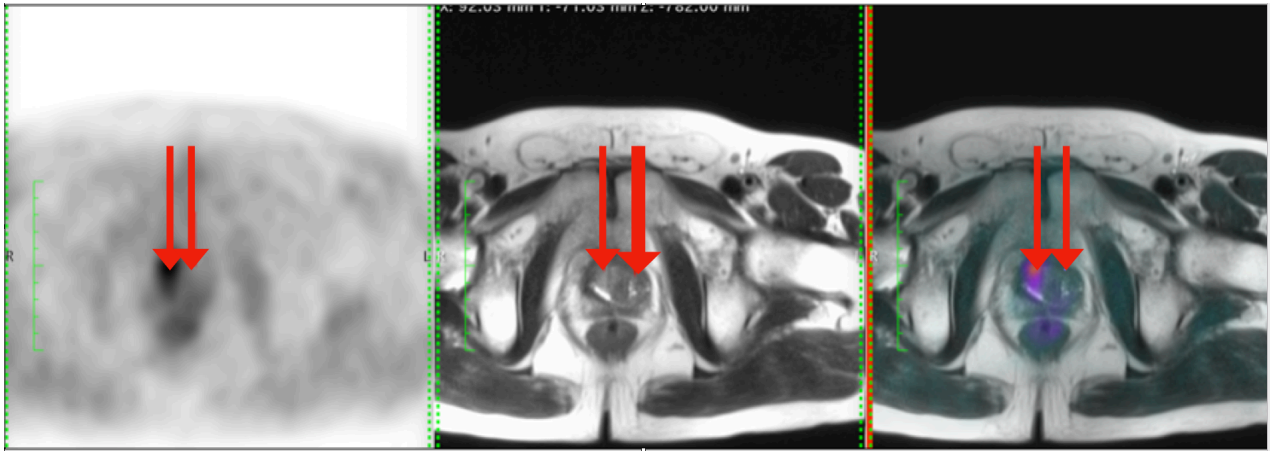


Fig 16: ^{18}F Choline PET/MR (from left to right) axial PET, MR and fused axial PET/MR. The patient had previous history of radiotherapy, hormones and brachytherapy and presented with PSA of 4.29. Increased uptake in the right lobe was detected. Physiological uptake was seen in the left lobe. TPM revealed focal high grade PIN and no adenocarcinoma.

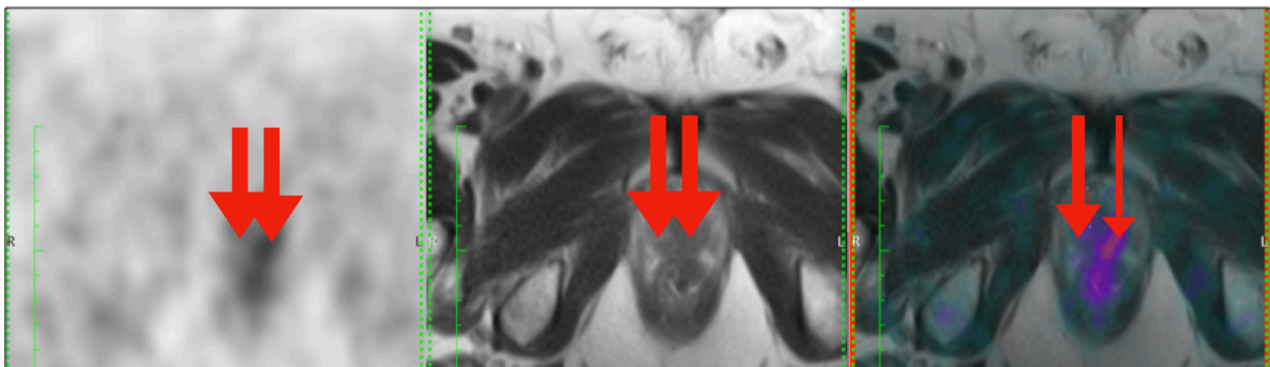


Fig 17: ^{18}F Choline PET/MR (from left to right) axial PET, MR and fused axial PET/MR. This patient presented with history of biochemical relapse following radiotherapy (PSA 2.67). There is asymmetrical increased tracer uptake in the left lobe of the prostate (SUVmax left lobe 3.6 and right lobe 1.8). TPM revealed adenocarcinoma in the left lobe with MCCL of 7mm and TCCL of 14mm. No evidence of malignancy in the right lobe.

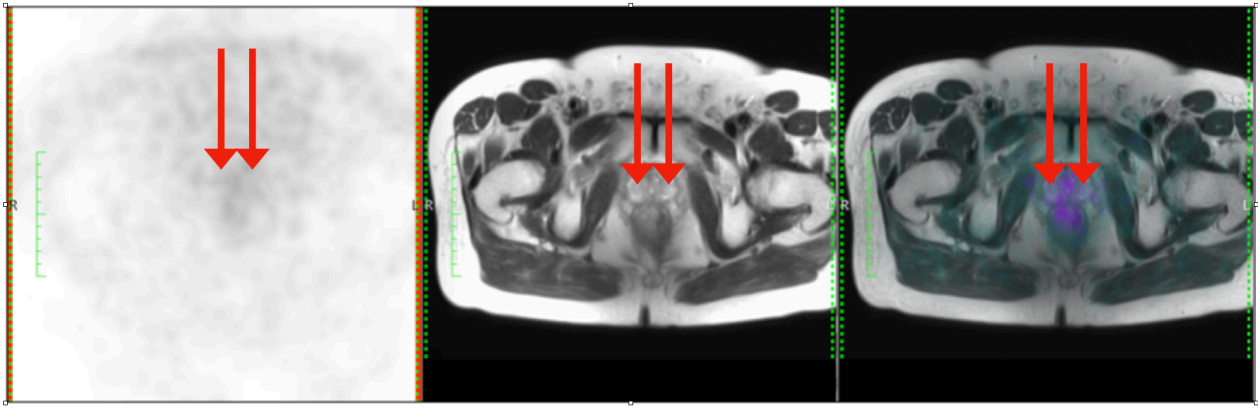


Fig 18: ^{18}F Choline PET/MR (from left to right) axial PET, MR and fused axial PET/MR. The patient had previous history of radiotherapy. The serum PSA was 6.9. No pathological uptake was noted on PET/MR and TPM did not reveal any evidence of malignancy.

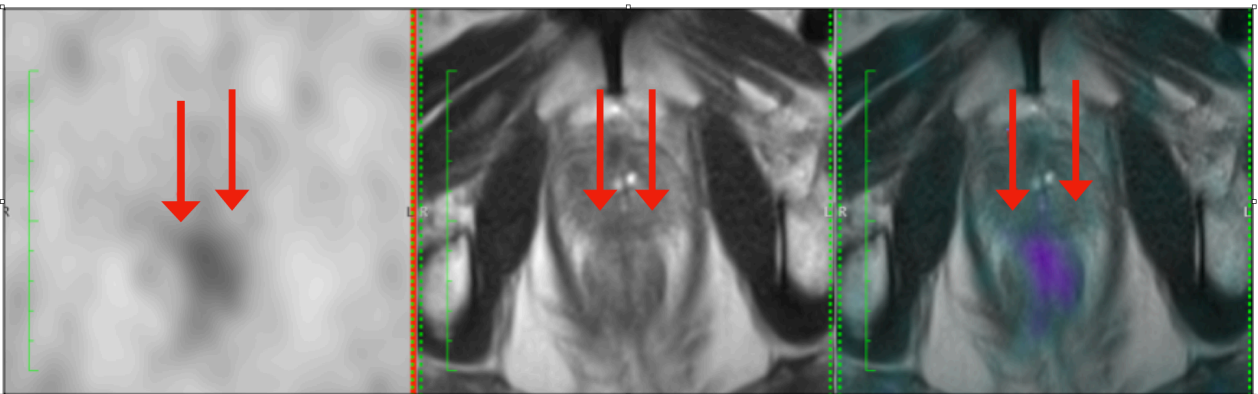


Fig 19: ^{18}F Choline PET/MR (from left to right) axial PET, MR and fused axial PET/MR. This patient had previous history of radiotherapy and hormones, serum PSA 1.6. The PET/MR was reported as normal. TPM showed radiotherapy effect with adenocarcinoma MCCL and TCCL of only 2 mm (Gleason 7) prostate cancer.

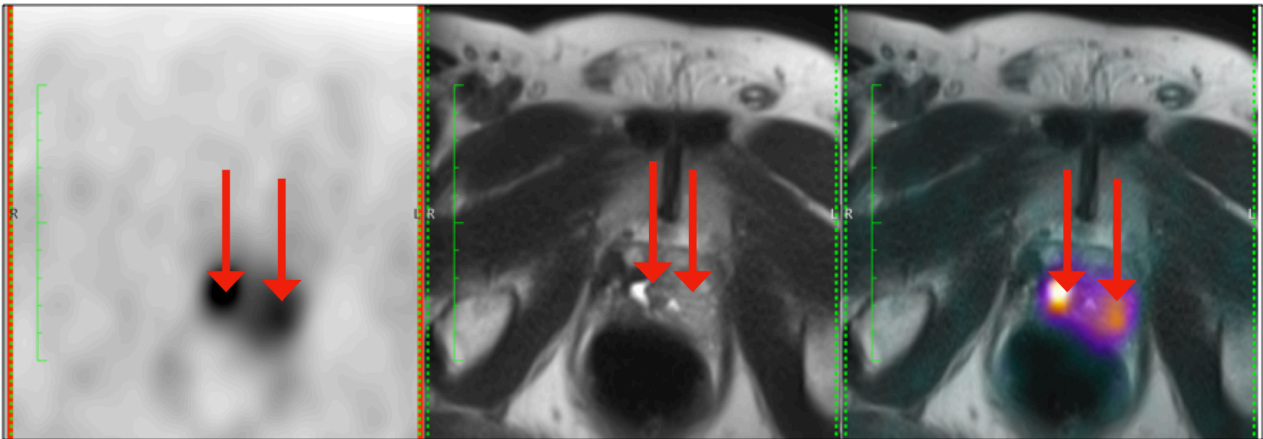


Fig 20: ^{18}F Choline PET/MR (from left to right) axial PET, MR and fused axial PET/MR. Post HIFU cavity in the right lobe with urinary excretion. MR component of the PET/MR helps identify these features. ^{18}F Choline uptake in the left lobe on TPM was found to be acinar adenocarcinoma MCCL and TCCL 2.5 mm (Gleason Score 6) which was clinically insignificant as per UCLH definition.

Another reason for heterogeneous study is that the inclusion criteria for this pilot work were based on selection of patients who had both index test (^{18}F Choline PET/MR) and reference test (TPM). This work is a preliminary study and patients were enrolled irrespective of the treatment they had or PSA levels. Further studies are required to ascertain the relationship among tracer-avid, clinically significant disease on ^{18}F Choline PET/MR, TPM biopsy, subsequent radical prostatectomy, and long-term, cost-effective treatment strategies.

Conclusion:

Our results suggest that data obtained from ^{18}F Choline PET/MR can allow detection of clinical significant and insignificant prostate cancer. Multiple previous treatments can give false positive results and ^{18}F Choline PET/MR is imaging investigation of choice post HIFU. Moreover, false negative results with ^{18}F Choline PET/MR can be due to very small volume (≤ 2 mm) disease.

References

1. Siddiqui MM, Rais-Bahrami S, Turkbey B, George AK, Rothwax J, Shakir N, et al. Comparison of MR/ultrasound fusion-guided biopsy with ultrasound-guided biopsy for the diagnosis of prostate cancer. *JAMA*. 2015 Jan 27;313(4):390–7.
2. Barnett CL, Davenport MS, Montgomery JS, Wei JT, Montie JE, Denton BT. Cost-effectiveness of magnetic resonance imaging and targeted fusion biopsy for early detection of prostate cancer. *BJU Int*. 2018;122(1):50–8.
3. Aizer AA, Gu X, Chen M-H, Choueiri TK, Martin NE, Efstathiou JA, et al. Cost implications and complications of overtreatment of low-risk prostate cancer in the United States. *J Natl Compr Canc Netw*. 2015 Jan;13(1):61–8.
4. Rosenkrantz AB, Taneja SS. Prostate MRI can reduce overdiagnosis and overtreatment of prostate cancer. *Acad Radiol*. 2015 Aug;22(8):1000–6.
5. Rosenkrantz AB, Ayoola A, Hoffman D, Khasgiwala A, Prabhu V, Smereka P, et al. The Learning Curve in Prostate MRI Interpretation: Self-Directed Learning Versus Continual Reader Feedback. *AJR Am J Roentgenol*. 2017 Mar;208(3):W92–100.
6. Ahmed HU, El-Shater Bosaily A, Brown LC, Gabe R, Kaplan R, Parmar MK, et al. Diagnostic accuracy of multi-parametric MRI and TRUS biopsy in prostate cancer (PROMIS): a paired validating confirmatory study. *Lancet*. 2017 25;389(10071):815–22.
7. Abd-Alazeez M, Ahmed HU, Arya M, Charman SC, Anastasiadis E, Freeman A, et al. The accuracy of multiparametric MRI in men with negative biopsy and elevated PSA level--can it rule out clinically significant prostate cancer? *Urol Oncol*. 2014 Jan;32(1):45.e17-22.
8. Muller BG, Shih JH, Sankineni S, Marko J, Rais-Bahrami S, George AK, et al. Prostate Cancer: Interobserver Agreement and Accuracy with the Revised Prostate Imaging Reporting and Data System at Multiparametric MR Imaging. *Radiology*. 2015 Dec;277(3):741–50.
9. Shankar PR, Kaza RK, Al-Hawary MM, Masch WR, Curci NE, Mendiratta-Lala M, et al. Impact of Clinical History on Maximum PI-RADS Version 2 Score: A Six-Reader 120-Case Sham History Retrospective Evaluation. *Radiology*. 2018 Jul;288(1):158–63.
10. Zhang L, Tang M, Chen S, Lei X, Zhang X, Huan Y. A meta-analysis of use of Prostate Imaging Reporting and Data System Version 2 (PI-RADS V2) with multiparametric MR imaging for the detection of prostate cancer. *Eur Radiol*. 2017 Dec;27(12):5204–14.
11. Haroon A, Ahmed HU, Cathcart P, Almuhaideb A, Kayani I, Dickson J, et al. (18)F-FECH PET/CT to Assess Clinically Significant Disease in Prostate Cancer: Correlation With Maximum and Total Cancer Core Length Obtained via MRI-Guided Template Mapping Biopsies. *AJR Am J Roentgenol*. 2016 Dec;207(6):1297–306.
12. Ahmed HU, Hu Y, Carter T, Arumainayagam N, Lecornet E, Freeman A, et al. Characterizing clinically significant prostate cancer using template prostate mapping biopsy. *J Urol*. 2011 Aug;186(2):458–64.

13. Onik G, Miessau M, Bostwick DG. Three-dimensional prostate mapping biopsy has a potentially significant impact on prostate cancer management. *J Clin Oncol*. 2009 Sep 10;27(26):4321–6.
14. Ahmed HU, Hu Y, Carter T, Arumainayagam N, Lecornet E, Freeman A, et al. Characterizing clinically significant prostate cancer using template prostate mapping biopsy. *J Urol*. 2011 Aug;186(2):458–64.
15. Thompson I, Thrasher JB, Aus G, Burnett AL, Canby-Hagino ED, Cookson MS, et al. Guideline for the management of clinically localized prostate cancer: 2007 update. *J Urol*. 2007 Jun;177(6):2106–31.
16. Davenport MS, Montgomery JS, Kunju LP, Siddiqui J, Shankar PR, Rajendiran T, et al. 18F-Choline PET/mpMRI for Detection of Clinically Significant Prostate Cancer: Part 1. Improved Risk Stratification for MRI-Guided Transrectal Prostate Biopsies. *J Nucl Med*. 2020 Mar;61(3):337–43.
17. Kirkham APS, Emberton M, Hoh IM, Illing RO, Freeman AA, Allen C. MR imaging of prostate after treatment with high-intensity focused ultrasound. *Radiology*. 2008 Mar;246(3):833–44.
18. Kepner GR, Kepner JV. Transperineal prostate biopsy: analysis of a uniform core sampling pattern that yields data on tumor volume limits in negative biopsies. *Theor Biol Med Model*. 2010 Jun 17;7:23.
19. Gaudin PB, Zelefsky MJ, Leibel SA, Fuks Z, Reuter VE. Histopathologic effects of three-dimensional conformal external beam radiation therapy on benign and malignant prostate tissues. *Am J Surg Pathol*. 1999 Sep;23(9):1021–31.
20. Sheaff MT, Baithun SI. Effects of radiation on the normal prostate gland. *Histopathology*. 1997;30(4):341–8.
21. Hara T, Kosaka N, Kishi H. Development of (18)F-fluoroethylcholine for cancer imaging with PET: synthesis, biochemistry, and prostate cancer imaging. *J Nucl Med*. 2002 Feb;43(2):187–99.

Chapter 6: Mapping the phenotypic appearances of Prostate on PET-CT and PET-MR

This work was undertaken at Barts Health NHS Trust, University College London Hospital, Great Ormond Street Hospital London and Aurora Health Care, Milwaukee WI, USA. The work carried out in UK was in collaboration with funding from UK Department of Health's NIHR Comprehensive Biomedical Research Centres and Cancer Research, United Kingdom. An abstract of this work was presented at the Society of Nuclear Medicine and Molecular Imaging (SNMI) annual meeting in 2012 in Texas, USA.

Abstract

Objective:

To highlight the role of multimodality imaging and present differential diagnosis of abnormal tracer accumulation in the Prostate and periprostatic tissue.

Method:

Our departments have performed molecular imaging of the prostate utilising PET-CT and PET-MR with a range of biomarkers including ^{18}F FDG, radiolabelled Choline, ^{68}Ga DOTATATE PET-CT and ^{68}Ga PSMA images. We retrospectively reviewed the varying appearances of the prostate gland in different diseases and incidental findings in periprostatic region.

Results:

The differential diagnosis of pathologies related to prostate and periprostatic tissue on multimodality imaging include

1. Malakoplakia
2. Rhabdomyosarcoma
3. Lymphoma
4. Prostate Cancer
5. Neuroendocrine tumours
6. Uchida changes

7. Recto-prostatic fistula
8. Synchronous malignancies
9. Lymphocele
10. Schwannoma

Conclusion:

There exists a wide differential for abnormal tracer accumulation in the prostate gland. As a radiologist and nuclear medicine physician it is important to be aware of range of prostatic and periprostatic pathologies.

Introduction

Prostate cancer has a diverse range of findings and it can present as small indolent intra-prostatic lesion to highly aggressive disseminated disease. Biological heterogeneity presents a diagnostic challenge and it is important to understand the underlying mechanism of spread of prostate cancer. A reporting radiologist or nuclear medicine physician should be aware of varying appearances of prostate at different stages and spectrum of findings with different biomarkers utilizing PET-CT or PET-MRI. We validated our findings on the PET-CT appearances of prostate cancer presenting as focal or diffuse uptake (1) (2) (3). This article relates to the phenotypic appearances of the prostate with a range of biomarkers which facilitate diagnosis of prostate cancer and these can be categorized into different groups:

- 1-Increased choline kinase activity (¹⁸F Methyl Choline, ¹⁸F Ethyl Choline and ¹¹C Choline)
- 2-Prostate specific membrane proteins (⁶⁸Ga PSMA)
- 3-Receptor imaging (⁶⁸Ga DOTATATE)
- 4-Glucose imaging (¹⁸F FDG)

Biomarkers

1-Radiolabelled Choline

There is increased proliferation of cells in cancer with increased Choline Kinase activity. This enzyme is important for phosphorylation and choline uptake is increased as a result of this. There are three radiolabelled sub-types of Choline (^{18}F Methyl Choline, ^{18}F Ethyl Choline and ^{11}C Choline). Normal biodistribution of these three subtypes of radiolabelled Choline has been described by Athar Haroon et al (4). Visceral localization of radiolabelled Choline is the same for all subtypes. There are only minor differences which fall in the category of statistically significant or non significant differences. Range of SUVs for various organs for the three tracers was also evaluated in this study. The main utility of radiolabelled Choline PET is in detection of biochemical relapse of prostate cancer (2).

2- ^{68}Ga Prostate Specific Membrane Antigen (PSMA)

PSMA is present in prostate epithelial cells, salivary glands, renal tubular cells, small intestine and coeliac ganglia. Three properties of PSMA makes it a highly attractive target for imaging (a) Increased expression in Prostate cancer cells (b) Cell membrane anchorage (c) Internalization. ^{68}Ga PSMA is more sensitive and specific than radiolabelled Choline in patients with recurrent prostate cancer (5).

3- 2-[^{18}F]-fluoro-2-deoxy-D-glucose (^{18}F -FDG)

^{18}F FDG is a radiolabelled analogue of glucose and it also uses transmembrane glucose transporters to enter a cell which is phosphorylated by hexokinase. As ^{18}F FDG demonstrates low uptake in newly diagnosed prostate cancer, it is of only limited value for local staging of prostate cancer.

4- ⁶⁸Ga-DOTATATE

Somatostatin is a cyclic neuropeptide and it is found in neurons and endocrine cells. There are five subtypes of somatostatin receptors which may frequently co-exist in same cell. There is overexpression of sstr in prostate cancer and 30% of prostate cancer cells (6) express sstr. ⁶⁸Gallium (⁶⁸Ga) 1,4,7,10-tetraazacyclododecane-1,4,7,10-tetraacetic acid (DOTA)-octreotate (DOTATATE, GaTate) PET-CT allows cell surface expression of somatostatin receptors (SSRRs).

Differential diagnosis

1-Malakoplakia:

Malacoplakia is derived from Greek words “malakos” meaning “soft” and “plakos” meaning “plaque” and the first person to coin this term was Von Hansemann. Malakoplakia is a chronic inflammatory condition with different etiologies including tuberculosis, tumors, fungal infections, parasitic infestations, sarcoidosis, ectopic rests of adrenal cortical cells and coliform infections. Histological hallmark are Von Hansemann cells and Michaelis-Gutmann bodies. Clinically, genitourinary tract is the most common site with 80-90% of patients having coliform infection.

CASE STUDY:

A 71 years old man of Caribbean origin presented with proximal muscle weakness and sensory loss in all four limbs. His ESR was 100. His treponemal antibody enzyme-linked immunosorbent assay (*ELISA*) was positive (syphilis), rapid plasma reagin (RPR) was positive at a titre of 4 and treponema pallidum particle agglutination assay (TPPA) was also positive. Sural nerve biopsy was in keeping with segmental demyelination with axonal degeneration. A diagnosis of chronic inflammatory demyelinating neuropathy was made. ¹⁸F

FDG PET-CT (FIG 1) showed a non-avid lung lesion. There was a single focus of FDG uptake at the right lateral aspect of the prostate and on biopsy malakoplakia was confirmed.

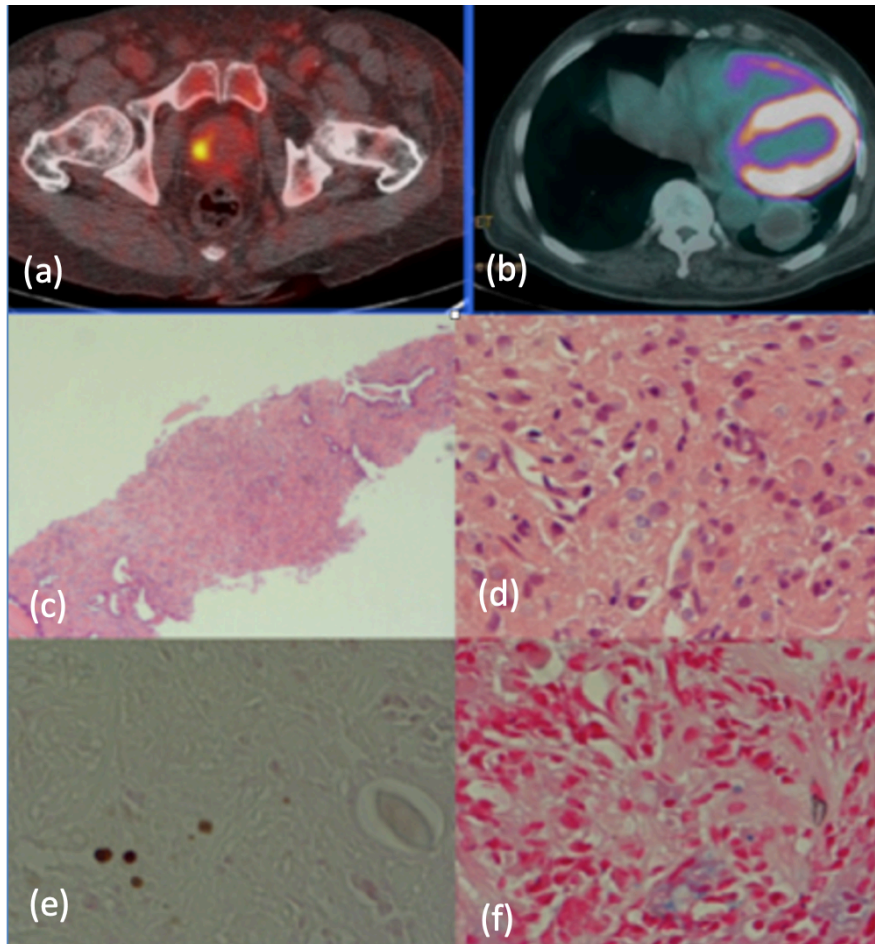


Fig: 1 (a) ^{18}F FDG Axial fused PET/CT showing a focal area of increased uptake involving the right lobe of the prostate gland. **(b)** A well-circumscribed area of peripheral increased soft tissue density and only faint uptake at the left lung base. **(c)** H&E stain x 40 magnification **(d)** H&E stain with Michaelis-Guttman body x 400 magnification **(e)** von Kossa stain for calcium x 400 magnification **(f)** Perls stain for iron x400 magnification

2-Rhabdomyosarcoma

Prostatic sarcomas are rare and arise from mesoderm and constitute 0.7% of the primary tumours of the prostate (7). There is increased risk of local recurrence in patients with genitourinary sarcomas when compared with sarcomas of the soft tissues (8) (9). In paediatric population RMS with localised and metastatic disease have better prognosis (10). AJCC has re-categorized nodal involvement from stage IV to stage III due to better prognosis (10). MRI with superior anatomical resolution and PET providing additional information about the nodal and distant status of disease can help triaging patients for surgery.

CASE STUDY:

An 18 months old boy presented with urinary outflow obstruction and bilateral hydronephrosis. MRI and ¹⁸F FDG PET-CT scan (FIG 2) demonstrated soft tissue mass bulging into the bladder displacing it anteriorly and was adherent to the rectum. Histology demonstrated embryonic rhabdomyosarcoma with anaplasia localised to the bladder neck and prostate. He was treated with chemotherapy and follow-up PET-CT scan short residual low-grade uptake in the primary mass lesion with no evidence of metabolically active metastatic disease.

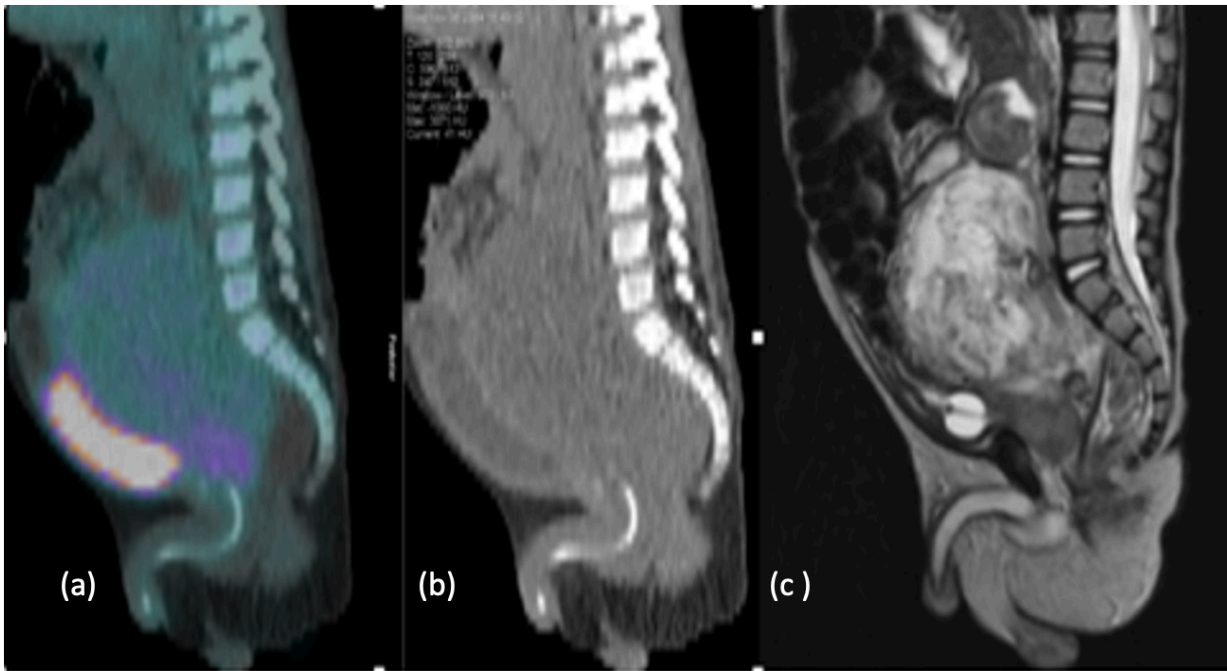


Fig 2: (a) Sagittal fused PET CT and low dose CT image showing a heterogenous mass infiltrating the superior aspect of the prostate gland and extending to the presacral region. The urinary bladder is compressed (catheter balloon insitu). The mass demonstrates low-grade metabolic activity and compresses the urinary bladder anteriorly. Sagittal T2 weighted image show heterogenous signal intensity. Histology confirmed this to be rhabdomyosarcoma.

3- Lymphoma

These are low-grade malignancies and the incidence is highest in the seventh decade (11) (12) (3) (4).

Following features raise the possibility of primary lymphoma of the prostate (11)

(a) Symptoms related to prostatic enlargement.

(b) Predominant site of involvement is prostate.

(c) Absence of involvement of liver, spleen and lymph nodes (1 month of diagnosis)

¹⁸F FDG PET-CT provide additional information as it is possible to differentiate these from Diffuse large B cell lymphoma (13) on histology.

a) High grade adenocarcinoma shows nuclear pleomorphism, cellular cohesion with large sheets of tumour cells. On the other hand infiltrative adenocarcinoma are more difficult to distinguish. Most of the adenocarcinomas are negative for CD45, CD20 while diffuse large B cell lymphoma demonstrates positivity with such immunoprofile (12).

b) Urothelial carcinomas show cellular cohesion including solid tumour nests and non invasive carcinoma on the surface urothelium. There exists an overlap with diffuse large B cell lymphoma with extreme morphological diversity, invasive, discohesive tumour cells. Urothelial carcinomas are positive for pancytokeratin, CK903/34BE12, p63 and GATA3 5-7. These are negative for CD45 and CD20.

c) Small cell carcinoma show sheet like growth, small blue cells with scant cytoplasm, high nuclear to cytoplasmic ratio, salt and pepper chromatin, nuclear molding, single cell or geographic necrosis. Small cell carcinomas express pancytokeratin, chromogranin and synaptophysin. These lack CD45 and CD20.

4-Prostate cancer

Acinar adenocarcinoma

Adenocarcinomas (FIG 3, FIG 4) are the most common type of prostate cancer. It develops in the gland cells that line the prostate (14). Ductal adenocarcinoma starts in the cells that line the ducts (tubes) of the prostate gland. It tends to grow and spread more quickly than acinar adenocarcinoma. When uptake pattern of ^{18}F Ethyl Choline PET-CT was correlated with MR Template guided mapping biopsies it was found that 60 minutes imaging was more sensitive than 90 minutes imaging for detection of clinically significant prostate cancer (2).

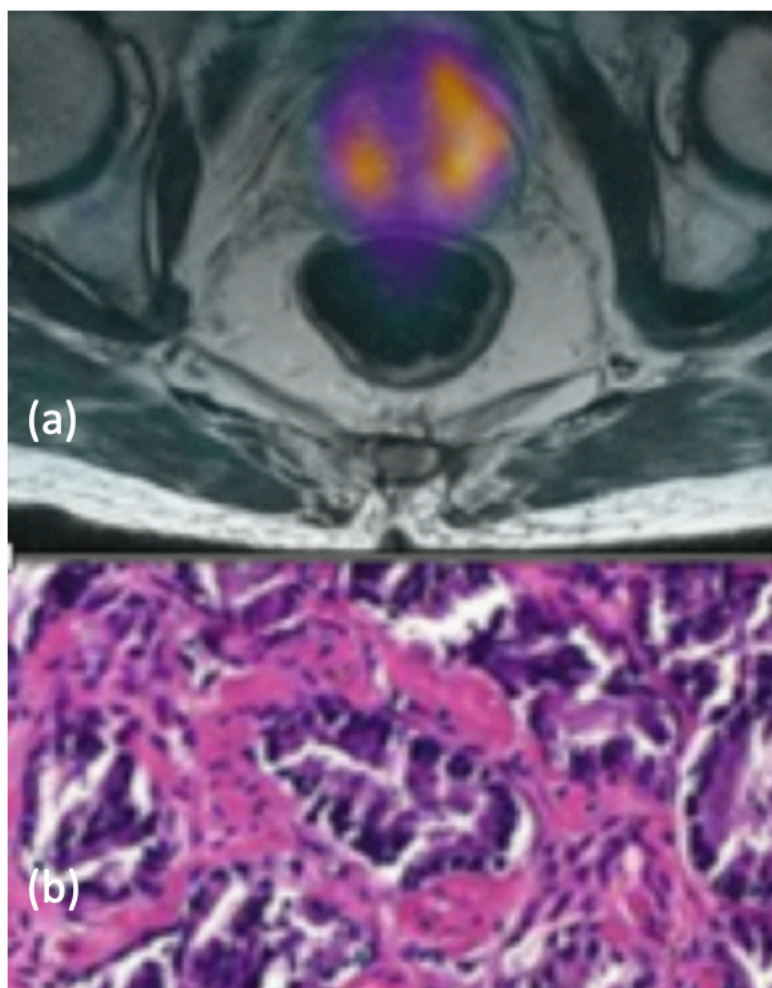


Fig 3: (a) ^{18}F Choline PET/MRI showing focal uptake in the right lobe and diffuse pattern is seen in the left lobe. Histology confirming poorly differentiated adenocarcinoma in abnormal areas of PET CT (Gleason 4+4).

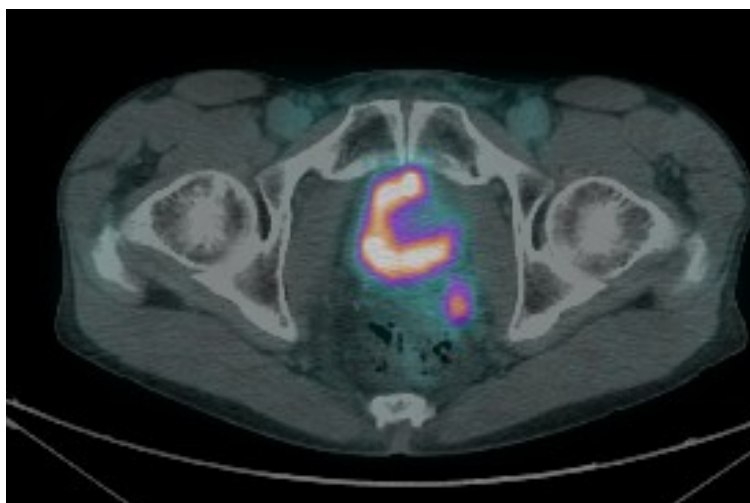


Fig 4: Rising PSA was noted in a patient with previous history of prostate cancer, left seminal vesicle involvement, which was removed at surgery and then treated with radiotherapy. ⁶⁸Gallium PSMA PET/CT showed focal area of uptake at the poster aspect of the bladder on the left side with soft tissue abnormality on the low dose CT. This is in keeping with disease relapse.

Transitional cell (or urothelial) cancer

Transitional cell cancer of the prostate starts in the cells that line the tube carrying urine to the outside of the body (the urethra). There is more than 50%, 5 year disease specific survival rate for patients with transitional cell carcinoma of the prostate (15) and it was found that the extent of loco-regional spread was the strongest rate predictor of patient survival outcome.

Squamous cell cancer

These cancers develop from flat cells that cover the prostate. They tend to grow and spread more quickly than adenocarcinoma of the prostate. These are extremely rare comprising only 0.5-1% of all prostatic carcinomas (16).

Small cell prostate cancer

Small cell prostate cancer is made up of small round cells. It's a type of neuroendocrine cancer (14). These are rare and can be mistaken for high-grade conventional prostate carcinoma. It has poor prognosis.

5- Neuroendocrine tumours of the Prostate

Primary neuroendocrine carcinomas are divided into two main types

- (a) High grade histological type (small cell carcinoma)
- (b) Low grade histological type (carcinoid tumours) (17).

Prostate carcinoid are associated with adenocarcinomas(18), trans-differentiation from adenocarcinomas (19) and multiple endocrine neoplasia (20). These lesions pose diagnostic challenge

due to several overlapping features such as adenocarcinomas may demonstrate neuroendocrine features (carcinoid like growth pattern) and may show positive immunostaining for neuroendocrine markers (21). It is of crucial importance to know whether the cancer is conventional adenocarcinoma with neuroendocrine differentiation or a true neuroendocrine carcinoma.

In a study by Shastry et al (22) distribution pattern of ^{68}Ga DOTATATE in disease free patients was evaluated and the uptake was found to be low grade and diffuse in the prostate. There is low density of sst2 receptors in normal prostate gland in the smooth muscles.

CASE STUDY

A male patient with calcified mass in the tail of the pancreas with intense somatostatin receptor expression was diagnosed as pancreatic neuroendocrine tumour on histology. There were multiple tracer avid metastatic deposits in the liver (FIG 5) and also periportal lymph nodes. The images of the pelvis showed heterogeneous tracer uptake in in the central gland of prostate.

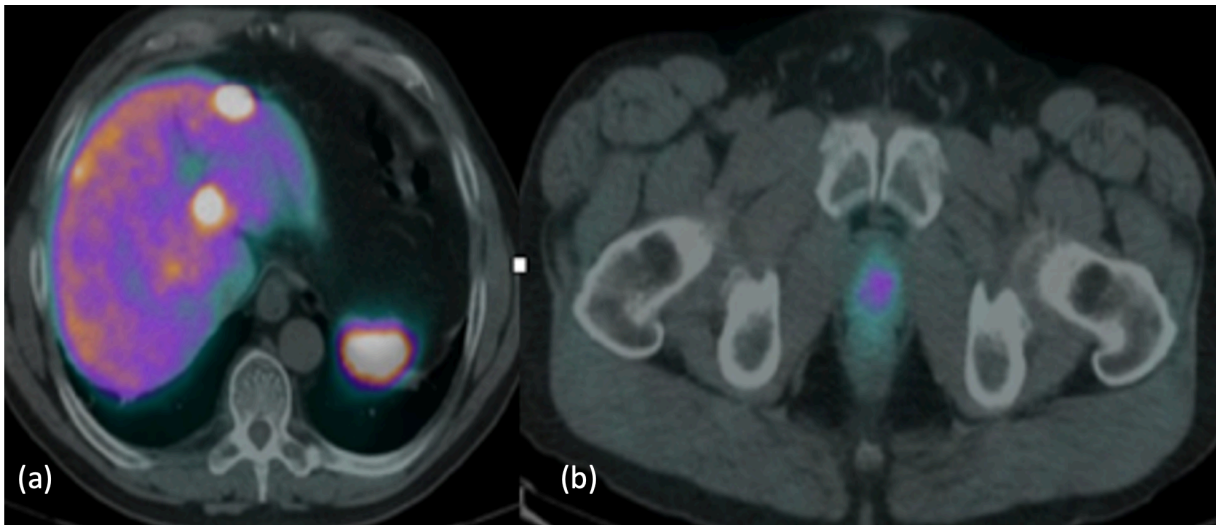


Fig 5: (a) ^{68}Ga Gallium Octreotate axial fused PET/CT (upper abdomen and pelvis) image in a patient with metastatic pancreatic neuroendocrine tumour. There are multiple tracer avid liver metastases. (b) In addition there is focal intense Somatostatin receptor expression in the prostate gland.

6- Uchida Changes

High frequency focused ultrasound (HIFU) utilizes the physical properties of ultrasound. When it is used for therapy it can be focused by an acoustic lens, a transducer or electronic phased array. This creates zones of high and low pressure through the tissues and this causes thermal coagulation and/or acoustic cavitation (23). On PET-CT scan it is difficult to identify changes on the low dose CT as the focal point is small (10mm x 1-2mm) and is situated along the long axis of the beam. These changes are called “Uchida changes” (24) and were described by Professor Toyoaki Uchida in Japan. There are three grades I- changes identified within the treatment zones. II-confluent between the adjacent treatment zones and III-migration outside the treatment zone. The changes are further sub-classified into three types based on the involvement of the focal regions. (a) <10% (b) 10-50% (c) >50%. The overall impact of treatment results in altered morphology of the gland, which are very difficult to recognise on the low dose PET-CT with formation of subsequent scar tissue. If MRI is available then anatomical alteration particularly “Uchida changes” should be evaluated. Cavitation, fistulation (FIG 6) and asymmetrical atrophic changes should be considered before labelling tracer avid disease site as tumour. Excreted activity due to focal small cavitation adjacent to the urethra may accumulate urinary activity and can be misdiagnosed as a metabolically active pathological lesion.

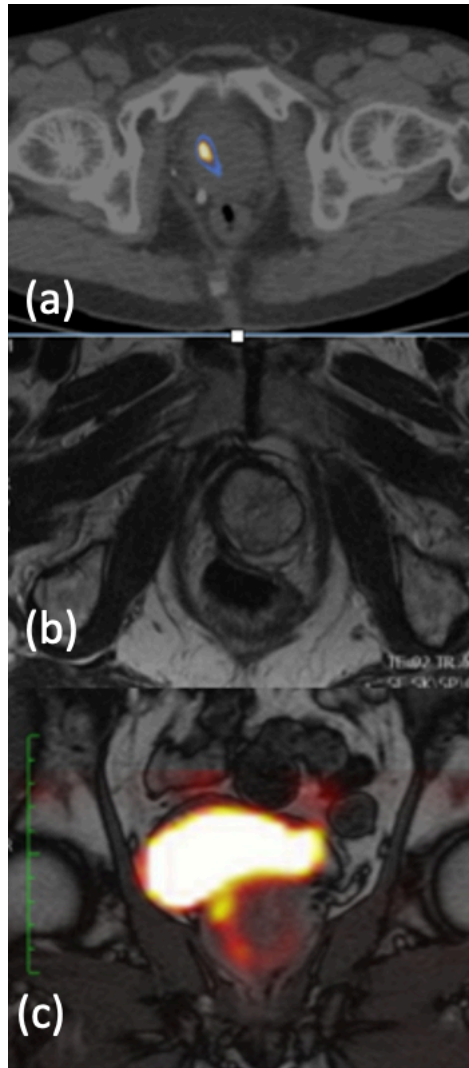


Fig 6: (a) Axial ^{18}F Choline PET/CT demonstrating focal area of apparent increased uptake in the right lobe of the prostate gland. Axial MRI showed post HIFU changes with marked atrophy of right lobe, hypertrophy of the left lobe. Coronal fused PET/MRI showed urethral tract with excreted activity and no evidence of tumour.

7- Post Radiotherapy

The main utility of PET is detection of early biochemical relapse. Novel biomarkers have the potential to discriminate viable disease versus postsurgical and post radiotherapy changes (25). In post radiotherapy scenario there is relatively poor yield of FDG and Choline with PSA less than 4 ng/ml (26). The most common reason for false positive result is post radiotherapy-related inflammatory change.

CASE STUDY:

A 72 years old man with history of prostate cancer presented with biochemical relapse (PSA 12.67). The patient underwent ¹⁸F Choline PET-CT which showed a moderate intensity focal uptake in the right lobe of the prostate gland and no evidence of tracer avid disease in the contralateral lobe. The patient underwent MR-Template guided biopsy of the prostate which showed only fibrosis on the right side and Gleason 3+4 adenocarcinoma of the prostate on the left side. The scan was false positive in the right lobe and false negative in the left lobe.

8-Post Hormones

Hormones suppress the choline uptake of prostate cancer. There are limited studies which have evaluated this effect. It is recommended that androgen deprivation therapy should be put on hold prior to Choline PET-CT to avoid false negative outcome (27). This is of utmost importance in clinical scenario of biochemical relapse of prostate cancer in hormone naïve patients.

9-Post Transurethral Resection of the Prostate (TURP)

Trans-urethral resection of the prostate causes increase in the diameter of the prostatic urethra. The prostatic urethra appears capacious with focal intense uptake when delayed imaging with ^{18}F FDG or when radiolabelled Choline is used. The intensity of uptake matches that of the excreted activity in the urinary bladder.

10- Post Prostatectomy

Radical prostatectomy is the removal of entire prostate gland. The modern methods encourage the use of nerve sparing surgery to preserve the erectile function. Prostatectomy involves partial or complete removal of the prostate. PET-CT readers should be aware of two surgical approaches, as postoperative scarring will alter the morphology of the prostate bed and perineum. Functional imaging helps to distinguish scar tissue from tumour recurrence or metastases (Fig 7).

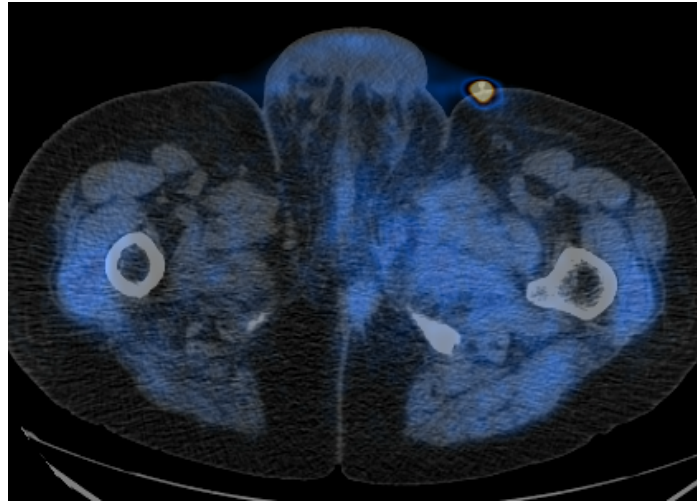


Fig 7: ^{18}F Choline axial fused PET/CT images in a patient post radical prostatectomy . There is a spiculated mildly avid soft tissue abnormality in the left ischio-rectal fossa, which was a metastatic deposit from prostate cancer. Focal intense uptake at the left inguinal region is excreted activity in the drainage tube of urinary catheter.

11-Recto-prostatic Fistula:

Recto-prostatic fistula are either due to inflammatory aetiologies (abscess formation, xanthogranulomatous prostatitis), iatrogenic (postsurgical, brachytherapy, high frequency focused ultrasound) or related to primary prostate cancer (28).

CASE STUDY:

A patient presented with left sided hydronephrosis and hydroureter. Investigations revealed left VUJ obstruction. MRI demonstrated a large prostate cancer with infiltration of the left lateral aspect of the pelvis and fistula formation with rectum. ¹⁸F Choline PET-CT showed a heterogenous appearing mass with photopenic areas (FIG 8). A right lower lobe lung nodule was demonstrated, and it was intensely avid on ¹⁸F FDG PET-CT. On original histology it was thought to be due to small cell carcinoma of the lung. On PSMA staining diagnosis of metastases from prostate cancer was confirmed. This patient demonstrated significant progression on bone scan with development of osteoblastic bone metastases within an interval of 6 months.

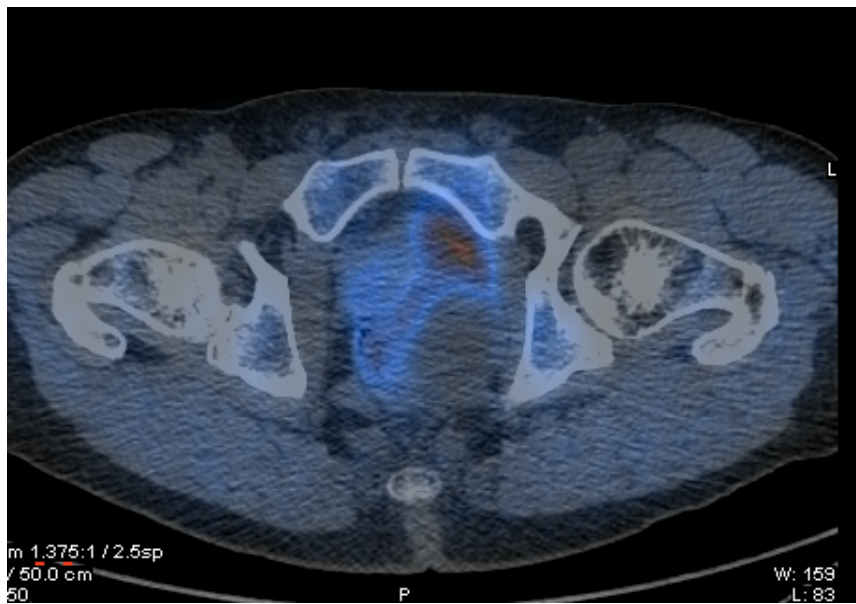


Fig 8: Axial fused ^{18}F Choline PET/CT showing heterogeneously avid soft tissue involving the prostate with multiple photopenic areas and soft tissue mass extending into the lateral aspect of the prostate gland.

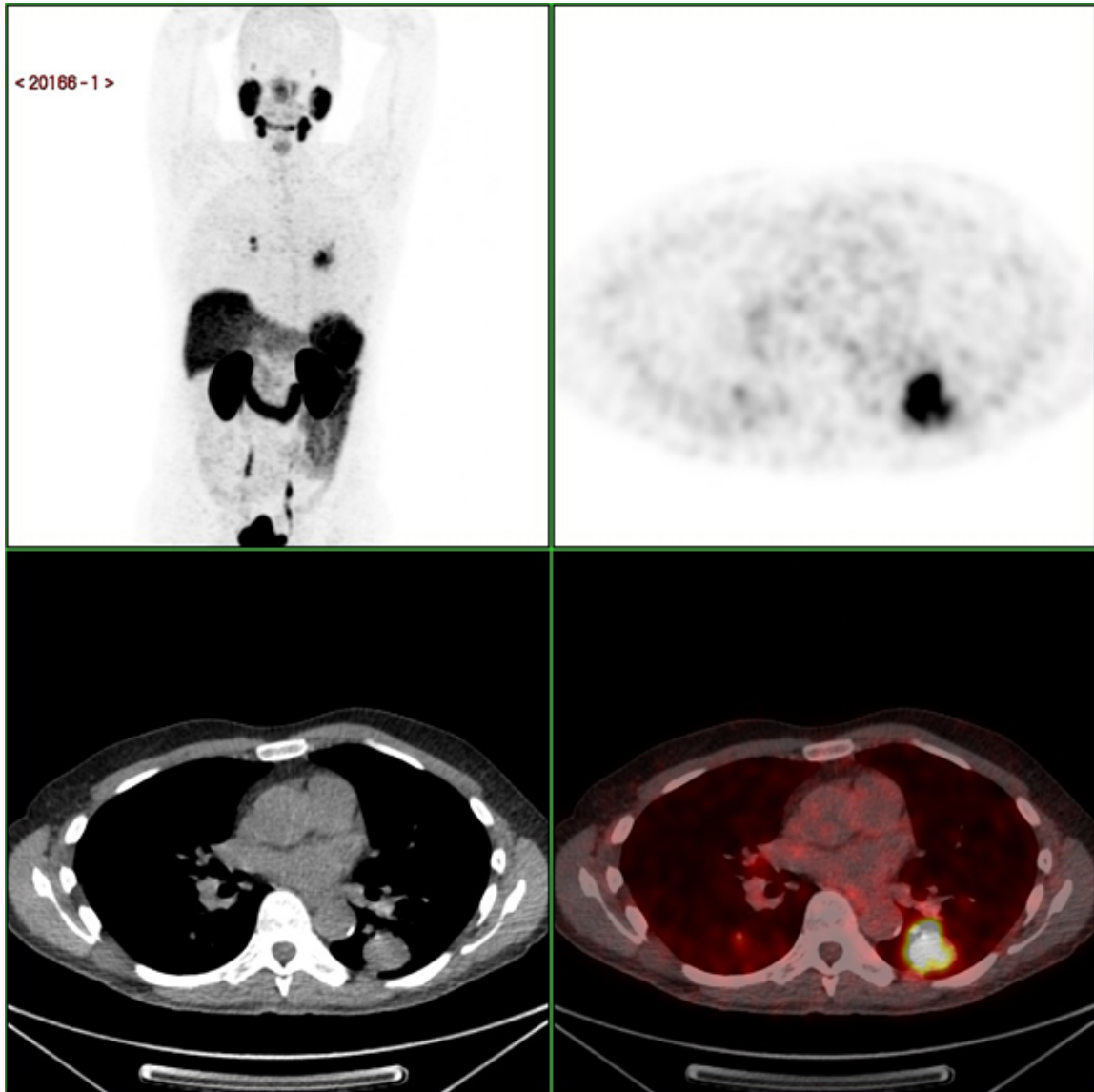


Fig 9: ^{68}Ga PSMA PET/CT MIP, axial PET, low dose CT and PET/CT in a 75 years old patient with biochemical relapse following radiotherapy (PSA 9.2). There are bilateral lung nodules, largest in the apical segment of the left lower lobe with intense tracer uptake. These findings are in keeping with metastatic disease

12-Synchronous Malignancies

(a) Prostate and Skin cancer

There is 1% incidence of skin metastases in patients with prostate cancer (29) and of note there is increased risk of melanoma after prostate cancer treatment (29). A patient who was being investigated for suspected relapse of the prostate cancer had ¹⁸F Choline PET-CT which demonstrated relapse at the mid gland and left lobe. An intensely avid nodule was noted at the left shoulder, which was clinically thought to be skin metastases from prostate cancer. The biopsy was confirmed to be squamous cell carcinoma of the skin.

(b) Prostate and Rectal Carcinoma

We came across a patient who had ¹⁸F Choline PET-CT as part of work up for prostate cancer relapse. There was focal area of intense uptake in the rectum at the left lateral wall. On retrospective review of the MRI, it was found to be a nodular lesion situated at the lateral wall of the rectum. It was difficult to detect it initially on zoomed narrow field of view images but on direct inspection it was found to be a rectal carcinoma incidentally detected on MRI and Choline PET-CT.

13-Schwannoma

Benign tumours originating from the neuronal sheath are known as neurilemmomas or schwannomas. These occur along the distribution of the cranial nerves and in the flexor surfaces of the upper and lower extremities. Most of these are incidentally detected as part of staging.

14- Lymphocele

These are collections of fluid secondary to disruption and surgical dissection of the lymphatics and lymph nodes. These are not metabolically active unless there is an inflammatory reaction. Low dose CT detects these as hypodense area with well defined margins.

Conclusion

It is concluded that there exists a wide differential for prostatic and periprostatic pathologies. As a nuclear medicine physician it is important to be aware of the range of prostatic and periprostatic pathologies. Biological heterogeneity presents a diagnostic challenge in detection of Prostate Cancer. Choline uptake in the cells can be due to inflammation, prostatic hyperplasia and malignancy. PSMA is present in prostate epithelial cells, renal tubular cells and coeliac ganglia. 30% of Prostate cancer show over-expression of Somatostatin receptors. Malacoplakia can be due to tuberculosis, sarcoidosis, tumours and fungal infections. When reporting PET for evaluation of prostate cancer, reporting nuclear medicine physician should evaluate morphology of the prostate gland particularly in cases where previous treatment has been given, check pelvis and other nodal stations for involvement and assess for the presence of incidental findings.

References

1. Haroon A, Almuhaideb A, Dickson J, Ahmed H, Syed R, Kirkham A, et al. Dual phase 18F-FDG PET-CT imaging in evaluation of “radio-recurrent” prostate cancer. *J Nucl Med*. 2011 May 1;52(supplement 1):1901–1901.
2. Haroon A, Ahmed HU, Cathcart P, Almuhaideb A, Kayani I, Dickson J, et al. (18)F-FECH PET-CT to Assess Clinically Significant Disease in Prostate Cancer: Correlation With Maximum and Total Cancer Core Length Obtained via MRI-Guided Template Mapping Biopsies. *AJR Am J Roentgenol*. 2016 Dec;207(6):1297–306.
3. Haroon A, Almuhaideb A, Dickson J, Emberton M, Kayani I, Ahmed H, et al. 18F Choline PET-CT for assessing disease recurrence: Correlation with TRUS, MR template-guided prostate mapping biopsies. *J Nucl Med*. 2012 May 1;53(supplement 1):1415–1415.
4. Haroon A, Zanoni L, Celli M, Zakavi R, Beheshti M, Langsteger W, et al. Multicenter study evaluating extraprostatic uptake of 11C-choline, 18F-methylcholine, and 18F-ethylcholine in male patients: physiological distribution, statistical differences, imaging pearls, and normal variants. *Nucl Med Commun*. 2015 Nov;36(11):1065–75.
5. Afshar-Oromieh A, Haberkorn U, Schlemmer HP, Fenchel M, Eder M, Eisenhut M, et al. Comparison of PET-CT and PET/MRI hybrid systems using a 68Ga-labelled PSMA ligand for the diagnosis of recurrent prostate cancer: initial experience. *European journal of nuclear medicine and molecular imaging*. 2014;41(5):887–97.
6. Luboldt W, Zöphel K, Wunderlich G, Abramyuk A, Luboldt H-J, Kotzerke J. Visualization of somatostatin receptors in prostate cancer and its bone metastases with Ga-68-DOTATOC PET-CT. *Mol Imaging Biol*. 2010 Feb;12(1):78–84.
7. Wang X, Liu L, Tang H, Rao Z, Zhan W, Li X, et al. Twenty-five cases of adult prostate sarcoma treated at a high-volume institution from 1989 to 2009. *Urology*. 2013 Jul;82(1):160–5.
8. Dotan ZA, Tal R, Golijanin D, Snyder ME, Antonescu C, Brennan MF, et al. Adult genitourinary sarcoma: the 25-year Memorial Sloan-Kettering experience. *J Urol*. 2006 Nov;176(5):2033–8; discussion 2038–9.
9. Sexton WJ, Lance RE, Reyes AO, Pisters PW, Tu SM, Pisters LL. Adult prostate sarcoma: the M. D. Anderson Cancer Center Experience. *J Urol*. 2001 Aug;166(2):521–5.
10. Edge SB, Compton CC. The American Joint Committee on Cancer: the 7th edition of the AJCC cancer staging manual and the future of TNM. *Ann Surg Oncol*. 2010 Jun;17(6):1471–4.
11. Bostwick DG, Mann RB. Malignant lymphomas involving the prostate. A study of 13 cases. *Cancer*. 1985 Dec 15;56(12):2932–8.
12. Chuang A-Y, demarzo AM, Veltri RW, Sharma RB, Bieberich CJ, Epstein JI. Immunohistochemical differentiation of high-grade prostate carcinoma from urothelial carcinoma. *Am J Surg Pathol*. 2007 Aug;31(8):1246–55.

13. Warrick JI, Owens SR, Tomlins SA. Diffuse large B-cell lymphoma of the prostate. *Arch Pathol Lab Med*. 2014 Oct;138(10):1286–9.
14. Types and grades | Cancer Research UK [Internet]. [cited 2016 Dec 26]. Available from: <http://www.cancerresearchuk.org/about-cancer/prostate-cancer/types-grades>
15. Cheville JC, Dundore PA, Bostwick DG, Lieber MM, Batts KP, Sebo TJ, et al. Transitional cell carcinoma of the prostate. *Cancer*. 1998 Feb 15;82(4):703–7.
16. Mohan H, Bal A, Punia RPS, Bawa AS. Squamous cell carcinoma of the prostate. *International Journal of Urology*. 2003 Feb 1;10(2):114–6.
17. Nelson EC, Cambio AJ, Yang JC, Ok J-H, Lara PN, Evans CP. Clinical implications of neuroendocrine differentiation in prostate cancer. *Prostate Cancer Prostatic Dis*. 2006 Oct 31;10(1):6–14.
18. Montasser AY, Ong MG, Mehta VT. Carcinoid tumor of the prostate associated with adenocarcinoma. *Cancer*. 1979;44(1):307–10.
19. Stratton M, Evans DJ, Lampert IA. Prostatic adenocarcinoma evolving into carcinoid: selective effect of hormonal treatment? *Journal of clinical pathology*. 1986;39(7):750–6.
20. Whelan T, Gatfield CT, Robertson S, Carpenter B, Schillinger JF. Pediatric Articles: Primary Carcinoid of the Prostate in Conjunction With Multiple Endocrine Neoplasia iib in a Child. *The Journal of urology*. 1995;153(3):1080–2.
21. Almagro UA, Tieu TM, Remeniuk E, Kueck B, Strumpf K. Argyrophilic,'carcinoid-like'prostatic carcinoma. An immunocytochemical study. *Archives of pathology & laboratory medicine*. 1986;110(10):916–9.
22. Shastry M, Kayani I, Wild D, Caplin M, Visvikis D, Gacinovic S, et al. Distribution pattern of 68Ga-DOTATATE in disease-free patients: *Nuclear Medicine Communications*. 2010 Oct;1.
23. Illing RO, Leslie TA, Kennedy JE, Calleary JG, Ogden CW, Emberton M. Visually directed high-intensity focused ultrasound for organ-confined prostate cancer: a proposed standard for the conduct of therapy. *BJU International*. 2006 Dec 1;98(6):1187–92.
24. Uchida T, Ohkusa H, Nagata Y, Hyodo T, Satoh T, Irie A. Treatment of localized prostate cancer using high-intensity focused ultrasound. *BJU Int*. 2006 Jan;97(1):56–61.
25. Boukaram C, Hannoun-Levi J-M. Management of prostate cancer recurrence after definitive radiation therapy. *Cancer Treatment Reviews*. 2010 Apr;36(2):91–100.
26. Greco C, Cascini GL, Tamburrini O. Is there a role for positron emission tomography imaging in the early evaluation of prostate cancer relapse? *Prostate Cancer Prostatic Dis*. 2008 Jan 8;11(2):121–8.
27. Dost RJ, Glaudemans AWJM, Breeuwsma AJ, Jong IJ de. Influence of androgen deprivation therapy on choline PET-CT in recurrent prostate cancer. *Eur J Nucl Med Mol Imaging*. 2013 Jul 1;40(1):41–7.
28. Xing L, Liu Z, Deng G, Wang H, Zhu Y, Shi P, et al. Xanthogranulomatous prostatitis with prostatico-rectal fistula: a case report and review of the literature. *Res Rep Urol*. 2016 Sep 16;8:165–8.

29. Brownstein MH, Helwig EB. Metastatic tumors of the skin. *Cancer*. 1972 May;29(5):1298–307.

CHAPTER 7:COMPARISON OF BONE SCAN AND ¹⁸F CHOLINE PET-CT

ABSTRACT

The aim of this study was to evaluate the spectrum of skeletal findings on dual-phase ^{18}F -Fluoroethylcholine (FECH) PET/CT performed during the work-up of patients referred for suspected prostate cancer relapse.

Methods: Three hundred ^{18}F -FECH PET/CT scans were prospectively evaluated. The low-dose CT features of all cases were categorized as isodense, sclerotic, lytic, or mixed lytic/sclerotic and SUV_{max} values were calculated. Findings on ^{18}F -FECH PET/CT were correlated with $^{99\text{m}}\text{Tc}$ -MDP planar bone scans and serum PSA.

Results: Patient age range was 50–90 years (median 71) and PSA values, 0.04–372 ng/mL (Roche Modular method). Seventy-two lesions were detected on ^{18}F -FECH PET/CT in 45 patients, including 31 (43%) in the pelvis, 17 (23%) in the spine {cervical 3, thoracic 8 and lumbar spine 6}, and 10 (13%) in ribs. Evaluation of low-dose CT in combination with PET helped to characterize benign findings in 21 (29%) lesions. The SUV_{max} for all except one benign lesion ranged from 0.49 to 2.15. In 51 lesions (71%) due to metastatic disease, SUV_{max} was 0.6–11.6 for those classified as sclerotic on low-dose CT, 0.7–8.58 for lytic lesions, 1.1–7.65 for isodense lesions, and 1.27–3.53 for mixed lytic/sclerotic lesions. Of the 56 ^{18}F -FECH avid lesions, 21 lesions showed avidity on bone scan {3 (23%) of the 13 isodense lesions, 14 (40%) of the 35 sclerotic lesions, 2 (50%) of the lytic lesions, and 2 (50%) of the mixed sclerotic/lytic lesions}.

Conclusion: ^{18}F -FECH PET/CT identified bone lesions in 15% of patients with suspected prostate cancer relapse. SUV_{max} in isolation cannot be used to characterize these lesions as benign or malignant. Minimal overlap of benign and malignant lesions was seen above SUV_{max} of 2.5. Low-dose CT of PET/CT is a useful tool to assist characterization.

Introduction

Biochemical recurrence after radical prostatectomy or radiation therapy has been reported in 27%–53% of patients [1]. Radiology and nuclear medicine techniques play an important role in the detection of local relapse and lymph node and skeletal metastases. Most institutes rely on magnetic resonance imaging (MRI) for this purpose, with increasing emphasis on the multiparametric technique. The main advantage of MRI is its excellent anatomic resolution. Nevertheless, positron emission tomography/computed tomography (PET/CT) offers benefits due to its increasing ability to demonstrate functional characteristics thereby facilitating differentiation between benign and malignant lesions. PET imaging is based on labelling of small, biologically and clinically significant molecules with positron-emitters. A variety of compounds have been used for this purpose, e.g., sugar, amino acids, nucleic acids, receptor binding ligands, water, and oxygen. Physiological maps of functions or processes relevant to the labeled molecules can be created in real time by imaging the temporal distribution of these compounds [2].

In the past decade, tremendous work has been done in elucidating the potential role of PET biomarkers in supplementing MRI for the detection of metastatic disease, including in morphologically normal lymph nodes, the bone marrow, and the skeleton. While ^{18}F -Fluorodeoxyglucose (FDG) is the most common PET/CT tracer worldwide, the results in respect of prostate cancer detection are not very good [3]. Consequently, other tracers have been investigated for this purpose, and radiolabelled Choline has emerged as one of the most common non-FDG PET biomarkers for the evaluation of prostate cancer [4].

In a meta-analysis [5], it was found that MRI and choline PET/CT were more accurate than bone single-photon emission computed tomography (SPECT) and bone scintigraphy (BS) for detecting bone metastases in patients with prostate cancer. The sensitivity and specificity of MRI on a per-patient basis were 95% and 96%, respectively, while those of choline PET/CT

were approximately 87% and 97%, respectively. Though choline PET/CT had the highest specificity on a per-patient basis, MRI was significantly better than choline PET/CT ($p < 0.05$) and BS ($p < 0.05$) for the detection of bone metastases from prostate cancer. The area under the curve (AUC) estimate for MRI (0.9870) on a per-patient basis was also significantly higher than those for choline PET/CT (0.9541, $p < 0.05$) and BS (0.8876, $p < 0.05$). On a per-lesion basis, choline PET/CT had a higher AUC (0.9494) than bone SPECT (0.9381) and BS (0.7736).

In vitro data have demonstrated greater ^{18}F -fluorocholine than FDG uptake in androgen-dependent (LNCaP) and androgen-independent (PC-3) prostate cancer cells [6]. A meta-analysis by Shen G et al demonstrated that on a per patient basis MRI was better than choline PET/CT and bone scan. Choline PET/CT was found to have highest diagnostic odds ratio compared to bone SPECT and bone scan.

There are three commonly used choline-based tracers, namely ^{18}F -fluoroethylcholine (^{18}F -FECH), ^{18}F -methylcholine, and ^{11}C -choline, which have a similar physiological biodistribution [7]. The purpose of the current study was to evaluate the spectrum of skeletal findings on ^{18}F -FECH PET/CT in patients undergoing investigation for biochemical relapse of prostate cancer.

Materials and methods

A total of 300 ^{18}F -FECH PET/CT scans were prospectively evaluated for detection of skeletal findings in patients with suspected prostate cancer relapse. ^{18}F -FECH was provided by Erigal (Erigal Limited, Downs Road, Sutton, Surrey, UK), synthesized as described by Hara et al. [8]. All QC parameters were fulfilled during the commercial preparation. Patients were

injected with 300–370 MBq of ^{18}F -FECH (effective dose 12.95 mSv). Whole-body PET/CT images were acquired 60 min after tracer injection. A 90-min post-injection dedicated view of the pelvis was also obtained. Owing to the rapid excretion of ^{18}F -FECH in urine, patients were asked to empty their bladder prior to imaging. The CT acquisition parameters included: scout 120 kVp, 10 mA; CT 140 kVp, 80 mA, 0.8 s, pitch 1.75; CT slices 5 mm (70-cm FOV PET AC), 2.5 mm (50-cm FOV Std), 2.5 mm (50-cm FOV Lung). PET acquisition parameters were: 3D attenuation-corrected and non-attenuation-corrected images, 20 subsets with iterative reconstructions. CT images were used to produce attenuation correction values for PET emission reconstruction and fused PET/CT presentation. The images were read by a nuclear medicine physician (with 20 years' experience) and a radionuclide radiologist (with 5 years' experience). The low-dose CT features of all cases were categorized into four groups (isodense, sclerotic, lytic, and mixed lytic/sclerotic) and maximum standardized uptake values (SUV_{max}) were calculated. Planar bone scan images were acquired after intravenous injection of $^{99\text{m}}\text{Tc}$ -methylene diphosphonate (MDP) and correlation was made with ^{18}F -FECH PET/CT for detection of skeletal lesions.

Benign lesions on PET/CT were those which were situated at sites of previous trauma, joints with arthritic changes (loss of disc space, peri-articular sclerosis, sub-articular cyst formation, peri-articular osteophytes), intervertebral discs with degenerative changes, facial sinuses with features of sinusitis, avascular necrosis, thickened cortex with bone expansion and coarse trabecular pattern (Paget's disease) and ground glass change (fibrous dysplasia). Malignant lesions had ^{18}F FECH avidity, intramedullary location and associated altered morphology i.e. sclerotic, lytic or mixed pattern. The identification of these lesions was based on subjective assessment.

If the lesion is not metabolically active but showed CT abnormality this either reflects a non viable lesion or apoptosis. Lesions which are found to be *suspicious* on PET/CT and there is

concordance with other imaging modalities are considered highly suspicious for metastatic disease. For the purpose of this study (in the absence of histology) we have relied on the avidity of the lesions on PET component as gold standard. At the same time we have highlighted the weakness of the gold standard. This reflects challenges faced by the radiologists and nuclear medicine physicians in multidisciplinary team settings.

Results

The age range of the 300 patients was 50–90 years (mean 71.3 years) and PSA values were 0.04–372 ng/mL (Roche Modular method). A total of 72 lesions were detected on ¹⁸F-FECH PET/CT in 45 patients (15%).

Anatomically the distribution of lesions was similar to what is seen in cases of metastatic prostate cancer. In our study of the 72 lesions, 31 were found in the pelvis, 17 in the spine (cervical 3, thoracic 8 and lumbar spine 6), 10 in ribs, 4 in the sternum, 3 in bone marrow, 3 in the skull, 2 in the scapula, 1 in the clavicle, and 1 in the femur.

The final interpretation of the lesions as benign or malignant on ¹⁸F FECH PET/CT was based on overall anatomical appearances of the lesions and avidity (Fig 1a). Benign findings (21/72) included bone island (13), avascular necrosis (1), fibrous dysplasia (1), Paget's disease (1), vertebral fractures (2), advanced focal degenerative changes (2), and inflammatory changes (maxillary sinus) (1). The SUV_{max} for vast majority of benign lesions ranged from 0.49 to 2.15. Only one case in this case cohort, with fibrous dysplasia, had very high SUV_{max} (10.8).

The malignant lesions were further subcategorized based on anatomical appearances on the low dose CT as isodense, sclerotic, lytic and mixed lytic or sclerotic lesions. A total of 51 lesions were considered to be of malignant etiology. The SUV_{max} values for the malignant lesions ranged from 0.6 to 11.6. The lytic lesions had SUV_{max} in the range of 2.36-8.58,

sclerotic lesions 0.6-11.6, isodense lesions 2-7.65 and mixed lytic/sclerotic lesions as 2.75-3.53. There were three cases of bone marrow uptake; two were attributed to metastatic disease and one, to recent treatment of leukaemia. Flow chart of SUVmax range of different skeletal lesions is demonstrated in Fig 1 (b)

¹⁸F FECH PET/CT data was further analysed based on avidity on PET component, detection of osteoblastic lesions on Bone Scan with a view to segregate lesions which are avid on one modality and non avid on the other and vice versa. A true matched analysis was possible in 59 /72 lesions, as cases where Tc99m MDP Bone Scan was not available were excluded from the analysis. A total of 56/59 lesions were found to be avid on 18F Choline PET/CT. The SUVmax value was 0.6-11.6. A total of 37.5% (21/56 lesions) demonstrated osteoblastic activity while 62.5% (35/56 lesions) were non avid on bone scan (Fig 1c).

The PSA value ranged from 0.04-372. Detailed analysis of the lesions as isodense, sclerotic, lytic, or mixed, SUVmax range, bone scan avidity and PSA values are listed in Table 1.

There were only 3 lesions which were non avid on ¹⁸F FECH PET/CT but were avid on Tc99m MDP Bone Scan. All of these three were sclerotic lesions, SUVmax range was 1.06-1.08 and PSA value was 3.6-240 (Table 2).

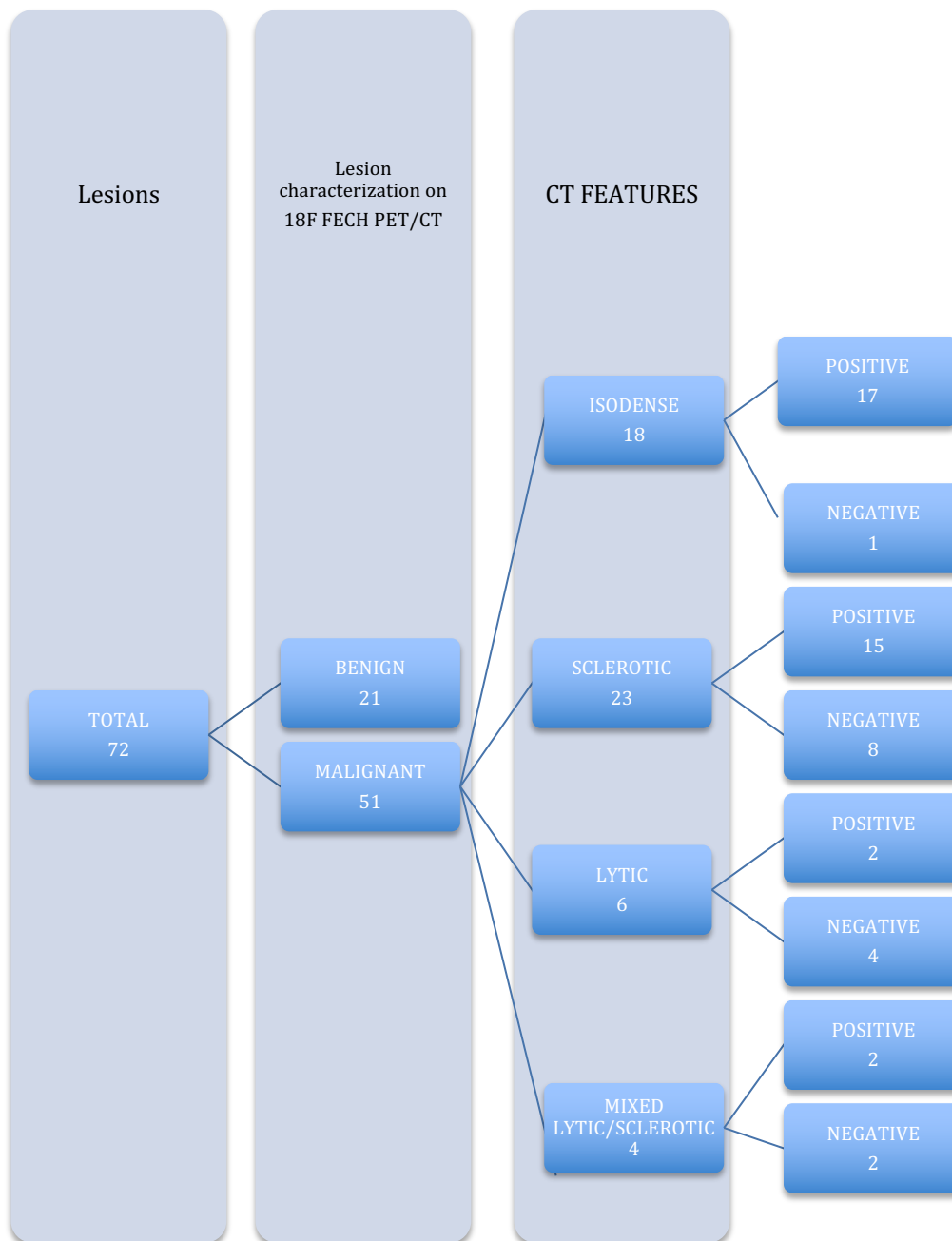


Figure 1 (a) Flow chart demonstrating distribution of the case mix in this analysis.

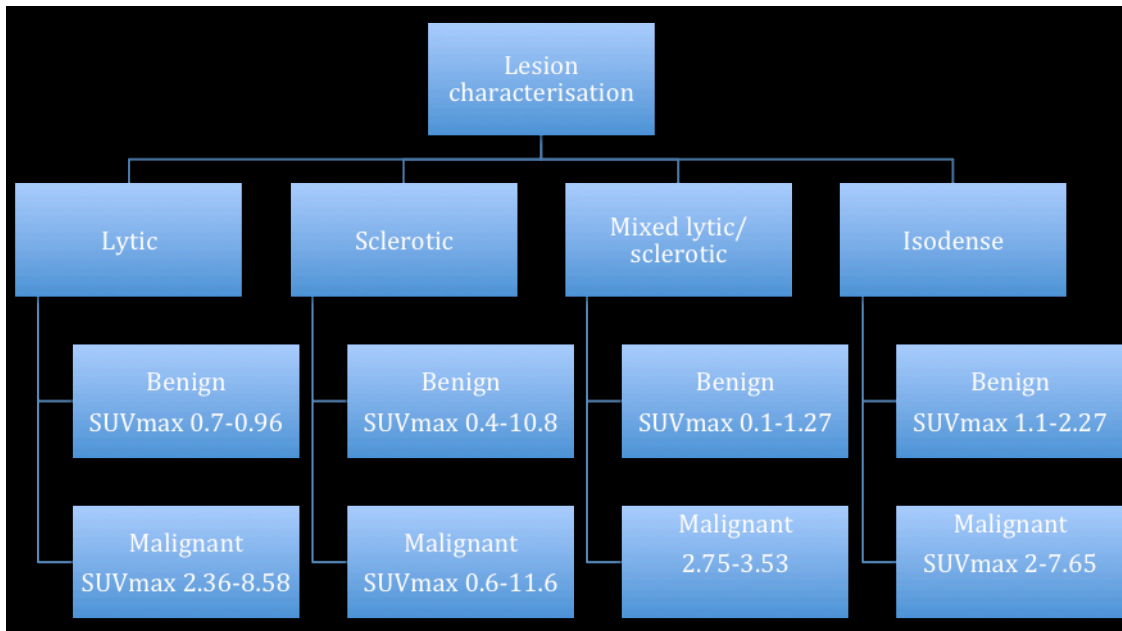


Fig 1(b) :

Flow chart of the SUVmax range of different skeletal lesions characterized as benign or malignant on the ^{18}F FECH PET/CT.

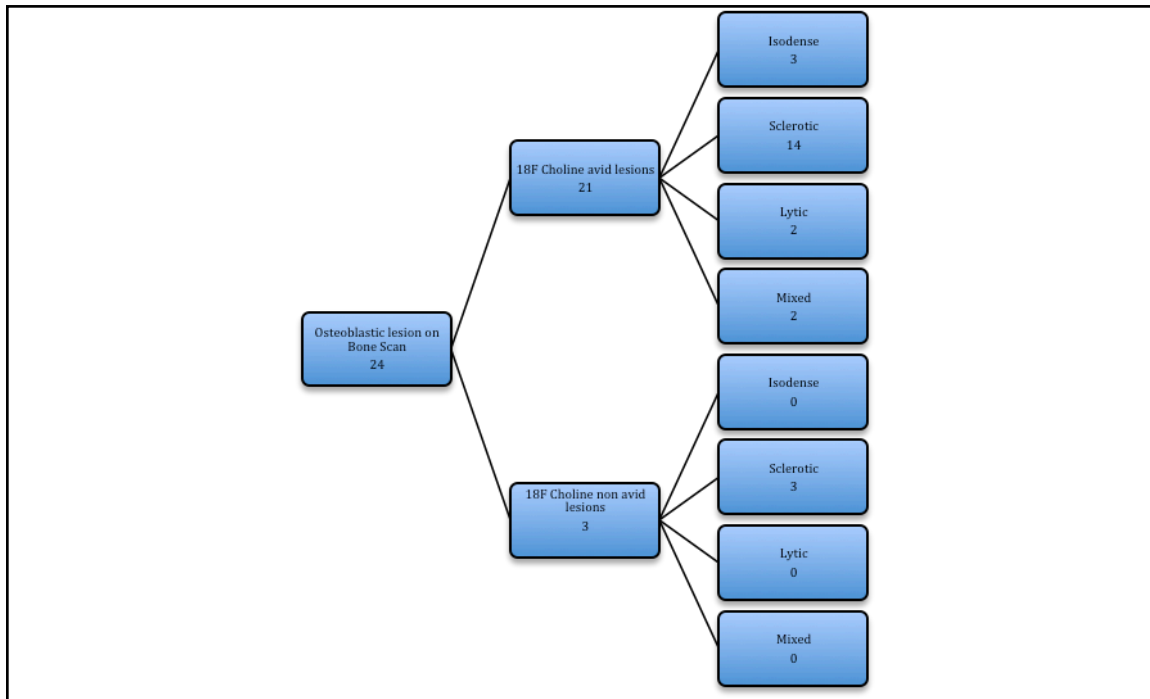


Fig 1(c):

Osteoblastic lesions and 18F Choline PET/CT. Only 3 lesions demonstrating osteoblastic activity were found to be non-avid on 18F Choline PET/CT. All three related to non -acute fractures (sternum, vertebra, rib).

Table 1

Low dose CT features of 18F FECH avid lesions	SUVmax range	Bone Scan positive	Bone Scan negative	PSA Range
Isodense 13	1.1-7.65	3 (23.07%)	10 (76.92%)	3.02-153
Sclerotic 35	0.6-11.6	14 (40%)	21 (60%)	2.81-372
Lytic 4	0.7-8.58	2 (50%)	2 (50%)	1.2-5.89
Mixed sclerotic/lytic 4	1.27-3.53	2 (50%)	2 (50%)	0.04-7
TOTAL 56	0.6-11.6	21 (37.5%)	35 (62.5%)	0.04-372

Table 2

Low dose CT Features of non avid 18F FECH Lesions showing osteoblastic activity on Bone Scan	SUVmax range	PSA
Isodense 0	NA	NA
Sclerotic 3	1.06-1.08	3.6-240
Lytic 0	NA	NA
Mixed sclerotic/lytic 0	NA	NA
TOTAL 3	1.06-1.08	3.6-240

Fig. 2 shows the scatter plot of SUV_{max} values in relation to lesion characterization as benign or malignant. We noted minimal overlap of benign and malignant lesions was seen above SUV_{max} of 2.5.

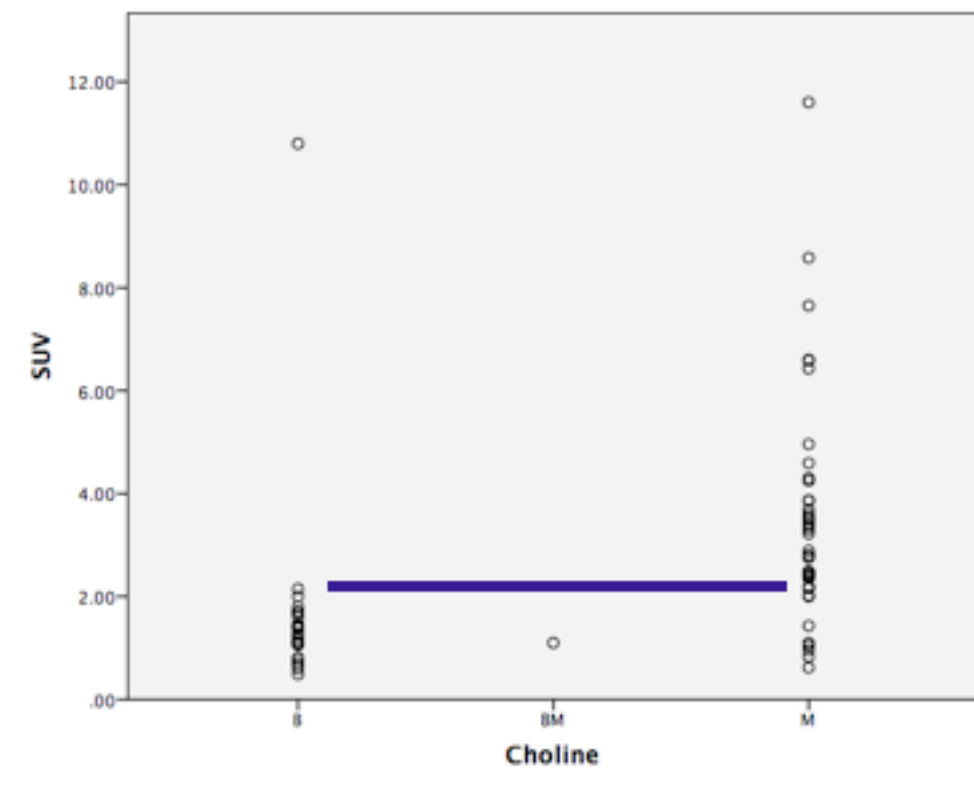


Figure 2- SUV_{max} values of benign lesions (*B*) and malignant lesions (*M*). There is an overlap of SUV_{max} values between benign and malignant lesions. The only outlier in the benign category with intense uptake was a case of fibrous dysplasia with SUV_{max} greater than 11. *BM*, bone marrow uptake.

Discussion

To our knowledge this is the first study to analyse the correlation between lesion-based analysis of skeletal findings on low-dose CT, bone scan, and quantification data obtained with ^{18}F -FECH PET/CT. It was observed that 29% of the ^{18}F -FECH PET/CT-positive lesions had a benign etiology. The study also demonstrates the superiority of ^{18}F -FECH PET/CT over bone scan, given that bone scan detected only 37.5% of the ^{18}F -FECH-avid lesions.

The skeleton is the second most frequent site (after lymph nodes) for metastases from prostate cancer, and the incidence of skeletal involvement is 65–75% among patients with advanced disease [9]. Among the 15% of patients with bone lesions in this study, 71% of the lesions were due to metastatic disease. The distribution of skeletal lesions overlapped with the sites of spread of prostate cancer, and 43% of the lesions were seen in the pelvis (31/72 lesions) and 23.6% in the spine (17/72 lesions), with scattered foci of uptake in the remainder of the skeleton. The anatomical area covered in bone scan (skull vertex to feet) exceeds that covered on ^{18}F -FECH PET/CT (skull vertex to mid thigh). Bone scan did not detect any lesion in the lower limbs, which were not covered on ^{18}F -FECH PET/CT.

A total of 23/51 (45%) malignant lesions were noted to be sclerotic and out of these, 20.83% (15) were avid on ^{18}F -FECH PET/CT. Isodense but avid lesions fall into the category of “*discordant lesions*” and pose a different diagnostic dilemma. Detection of isodense but “neoplastic lesions” is a real challenge faced while reporting oncology scans. The majority of these lesions have a Hounsfield unit value very similar to that of the adjacent bone matrix and these lesions are easily missed on diagnostic CT scans even when intravenous contrast is administered. Increased avidity of these lesions as detected by ^{18}F -FECH PET/CT helps

to distinguish them from surrounding bone. Bone metastases undergo osteoblastic healing response with treatment. The isodense lesions may become sclerotic and these lesions can be easily labelled as progressive disease. In this study there were 13 isodense lesions (SUV_{max} range 1.1–7.65). Interestingly, out of these only 3 were avid on bone scan (23.1%) while the majority (76.9%) were non-avid. Even on retrospective review of this specific cohort of patients we were not able to identify these lesions on the low-dose CT component of the PET/CT. Focal ^{18}F -FECH in isodense lesions reflects bone marrow infiltration (Fig 5). Caution should be exercised when monitoring isodense lesions. Reduction in choline uptake with sclerosis can distinguish osteoblastic healing response from progressive disease [10] . Figures 3–6 show different examples from this study.

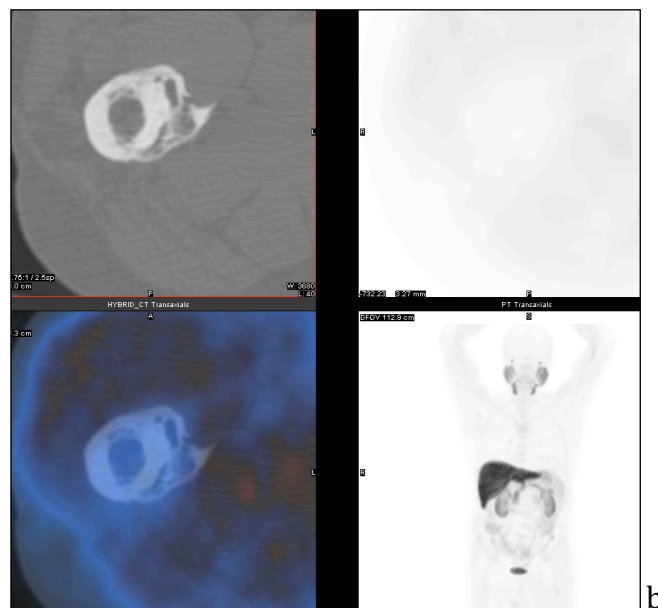
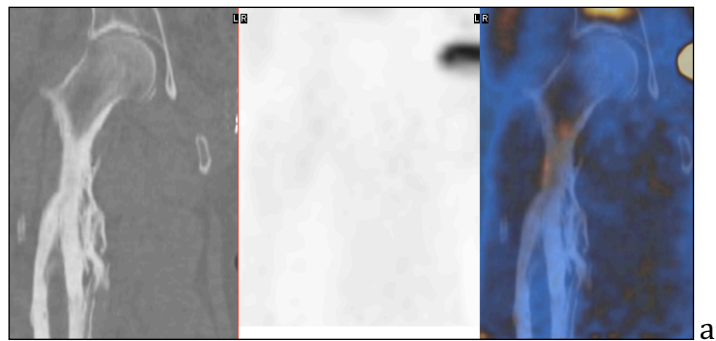


Figure 3a, b- Multiplanar ^{18}F -FECH PET/CT with coronal, axial, and MIP (maximum intensity projection) images showing sclerosis, periosteal thickening, and low-grade uptake at the proximal aspect of the right femur. This patient had a previous history of osteomyelitis.

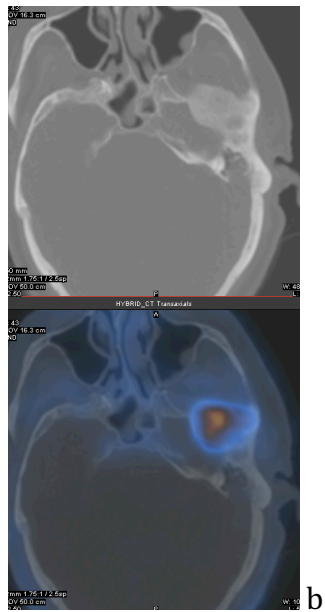
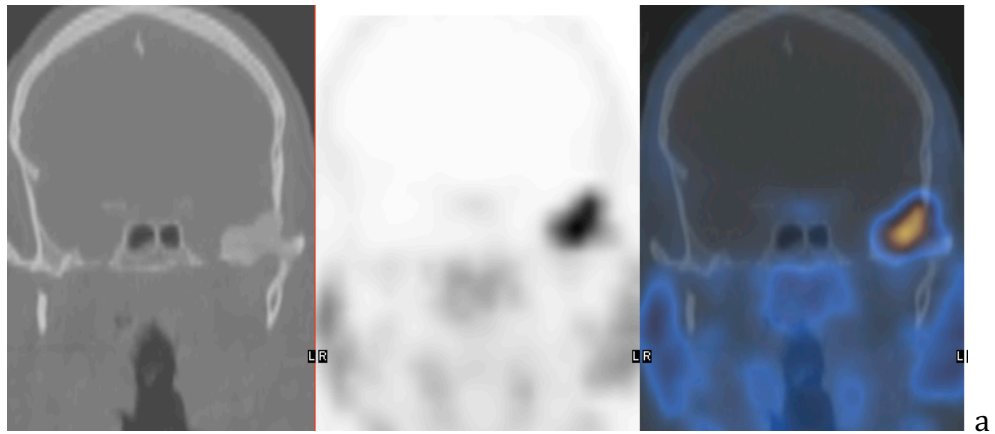


Figure 4. **a** - Coronal (low-dose CT, PET, and PET/CT) and **b** axial (low-dose CT and PET/CT) ^{18}F -FECH images showing an intensely avid area at the left skull base with ground glass appearances on low-dose CT. These findings are in keeping with fibrous dysplasia.

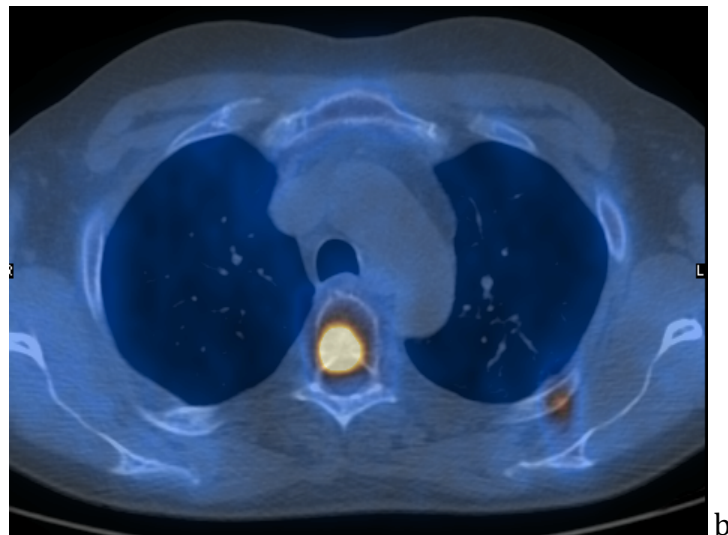
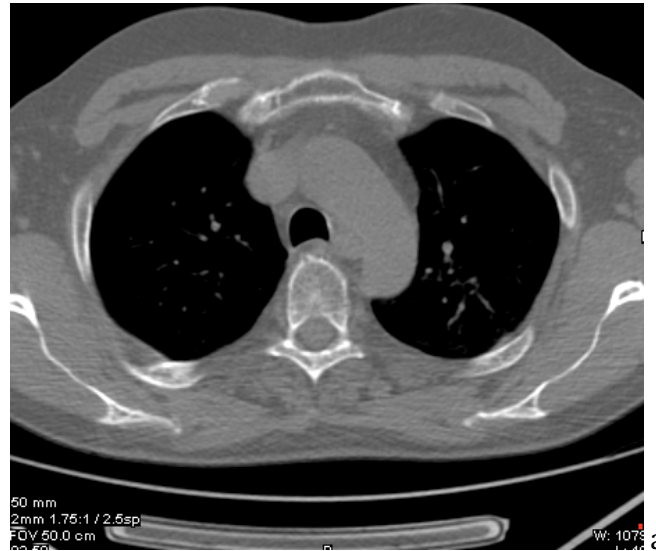


Figure 5: a, b On CT, there is no evidence of sclerotic, lysis, pedicular destruction, or pre- or paravertebral soft tissue abnormality to indicate metastatic disease. **b** Axial PET/CT and low-dose CT demonstrate an intensely avid lesion at the upper thoracic vertebra, which is in keeping with metastatic disease. In addition, there is an isodense metastatic deposit involving the left 4th rib.

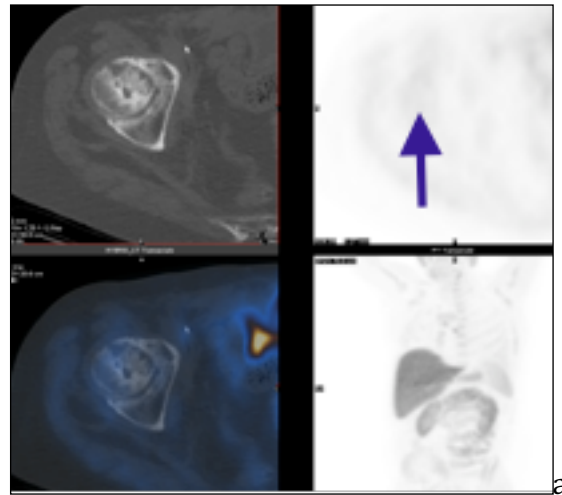


Figure 6. a ^{18}F -FECH PET/CT (multiplanar) demonstrating a very faintly avid area at the right femoral head with cystic appearances. **b** The coronal MRI scan demonstrates a focal area of low signal involving the right femoral head with loss of height. This patient had a previous history of avascular necrosis of the right femoral head.

There were three osteoblastic lesions on Tc99m MDP Bone Scan, which were non-avid on ^{18}F FECH PET/CT. These included old fractures undergoing osteoblastic healing response. These were situated at site of sternal fracture (SUVmax 1.7, PSA 3.6), superior end plate fracture at T12 vertebra (SUVmax 1.06, PSA 9.2) and right 10th rib fracture (SUVmax 1.08, SUVmax 240). The patient with rib fracture had close serial follow up. This patient was also found to have a fracture of the 8th rib on the same side which was only visible on the low dose CT component and non avid on Bone Scan and ^{18}F FECH PET/CT. Due to symmetrical nature but very high PSA a differential of fractures and metastatic disease was made. These were found to be stable on 3 serial Bone Scans over a period of 2 years and also on 2 serial CT Scans over 12 months. The patient was put on hormones with gradual decline of PSA from 240 to 29.79, 13.07 and 9.14.

Our cohort demonstrated that quantification of ^{18}F -FECH uptake cannot characterise skeletal lesions as benign or malignant in patients undergoing investigation for biochemical relapse of prostate cancer and furthermore does not correlate with the isodense, sclerotic, lytic, or mixed lytic/sclerotic status of the lesions.

A major limitation of our study is that the bone scan images were planar images and lacked SPECT/CT, which can help with lesion characterization. At our institution, staging investigations for prostate cancer include planar images as standard of care in the vast majority of prostate cancer patients.

Histopathological correlation was not available in all cases. Our institute is a tertiary referral centre to which a heterogeneous group of patients are referred for imaging from a variety of hospitals. We relied on the low-dose CT features to characterize the patients and correlated findings with available bone scans. This approach is suboptimal, but the study demonstrates that not all avid lesions on ^{18}F -FECH PET are due to a metastatic disease process.

Conclusion:

^{18}F -FECH PET/CT identified bone lesions in 15% of the patients with suspected prostate cancer relapse; 71% of the lesions were due to bone metastases and 29% due to benign etiology. ^{18}F -FECH PET/CT demonstrates a range of benign skeletal findings and caution should be exercised in labelling choline-avid lesions as metastatic disease. Quantification of ^{18}F -FECH PET/CT with SUV_{max} cannot be used to characterize lesions as benign or malignant. Minimal overlap of benign and malignant lesions was seen above SUV_{max} of 2.5. Low-dose CT acquired as part of the PET/CT may help to characterize tracer-avid lesions. Conventional $^{99\text{m}}\text{Tc}$ MDP bone scan detects only 37.5% of lesions detected by ^{18}F -FECH PET/CT.

References

- [1] A. Heidenreich *et al.*, “EAU Guidelines on Prostate Cancer. Part II: Treatment of Advanced, Relapsing, and Castration-Resistant Prostate Cancer,” *Eur. Urol.*, vol. 65, no. 2, pp. 467–479, Feb. 2014.
- [2] L. K. Griffeth, “Use of PET/CT scanning in cancer patients: technical and practical considerations,” *Proc. Bayl. Univ. Med. Cent.*, vol. 18, no. 4, pp. 321–330, Oct. 2005.
- [3] H. Jadvar, “Prostate Cancer: PET with 18F-FDG, 18F- or 11C-Acetate, and 18F- or 11C-Choline,” *J. Nucl. Med.*, vol. 52, no. 1, pp. 81–89, Jan. 2011.
- [4] S. Fanti *et al.*, “PET/CT with (11)C-choline for evaluation of prostate cancer patients with biochemical recurrence: meta-analysis and critical review of available data,” *Eur. J. Nucl. Med. Mol. Imaging*, Oct. 2015.
- [5] G. Shen, H. Deng, S. Hu, and Z. Jia, “Comparison of choline-PET/CT, MRI, SPECT, and bone scintigraphy in the diagnosis of bone metastases in patients with prostate cancer: a meta-analysis,” *Skeletal Radiol.*, vol. 43, no. 11, pp. 1503–1513, Nov. 2014.
- [6] D. T. Price, R. E. Coleman, R. P. Liao, C. N. Robertson, T. J. Polascik, and T. R. DeGrado, “Comparison of [18 F]fluorocholine and [18 F]fluorodeoxyglucose for positron emission tomography of androgen dependent and androgen independent prostate cancer,” *J. Urol.*, vol. 168, no. 1, pp. 273–280, Jul. 2002.
- [7] A. Haroon *et al.*, “Multicenter study evaluating extraprostatic uptake of 11C-choline, 18F-methylcholine, and 18F-ethylcholine in male patients: physiological distribution, statistical differences, imaging pearls, and normal variants,” *Nucl. Med. Commun.*, vol. 36, no. 11, pp. 1065–1075, Nov. 2015.
- [8] T. Hara, N. Kosaka, and H. Kishi, “Development of (18)F-fluoroethylcholine for cancer imaging with PET: synthesis, biochemistry, and prostate cancer imaging,” *J. Nucl. Med. Off. Publ. Soc. Nucl. Med.*, vol. 43, no. 2, pp. 187–199, Feb. 2002.
- [9] S. Halabi *et al.*, “Meta-Analysis Evaluating the Impact of Site of Metastasis on Overall Survival in Men With Castration-Resistant Prostate Cancer,” *J. Clin. Oncol. Off. J. Am. Soc. Clin. Oncol.*, vol. 34, no. 14, pp. 1652–1659, May 2016.
- [10] M. Beheshti *et al.*, “The use of F-18 choline PET in the assessment of bone metastases in prostate cancer: correlation with morphological changes on CT,” *Mol. Imaging Biol. MIB Off. Publ. Acad. Mol. Imaging*, vol. 11, no. 6, pp. 446–454, Dec. 2009.

Chapter 8: Role of ^{18}F Choline as a Novel Diagnostic Complex

Overview:

To establish the clinical utility of ^{18}F Choline we prospectively evaluated the role of ^{18}F Choline as novel imaging based diagnostic complex. A collaborative model was established between Uro-oncology, Nuclear Medicine and Radiology in the form of prospective clinical trial following peer review and ethical approval. Prospective Clinical Trial comparing ^{18}F Choline PET-CT and Whole Body MRI The FORECAST Study- FOcal RECurrent Assessment and Salvage Treatment for radio recurrent prostate cancer

Research question:

Which test among ^{18}F Choline PET/CT, Bone Scan and Whole Body MRI is more accurate for detection of burden of metastatic disease in radio-recurrent prostate cancer ?

Rationale:

Traditional Bone Scan only looks at osseous metastases therefore there is a need for a diagnostic modality which detects osseous and soft tissue metastases. ^{18}F Choline PET-CT and Whole Body MRI are two such modalities which can address this need.

Aims:

To compare ¹⁸F Choline PET/CT, Bone Scintigraphy and whole body MRI for detection of metastatic disease in radio-recurrent prostate cancer.

Author declaration

Professor Hashim Ahmed was the Chief investigator for FORECAST Study. Professor Jamshed Bomanji was the co-investigator and facilitated Nuclear Medicine aspects of the FORECAST Trial. Neil McCartan provided support as data manager. Malisha Maru helped with data collection. The MRI scans were reported by Shonit Punwani and Navid Ramachandran. The nuclear Medicine scans were read by Athar Haroon. Dr Ana Abhiramy Kanthabalan provided significant input into the evaluation of novel imaging based complex diagnostic pathway intervention for men who fail radiotherapy for prostate cancer and this collaborative work is also part of her PhD work with the Division of Surgery and Interventional Science at University College London.

Abbreviation Key:

PET: Positron Emission Tomography

MRI: Magnetic Resonance Imaging

CT: Cross-sectional Tomography

mpMRI: multiparametric Magnetic Resonance Imaging

PI-RADS: Prostate Imaging Reporting and Data system

TPM: Template Mapping biopsy

HIFU: High Frequency Focussed Ultrasound

MBq: Megabecquerels

SOP: Standard Operating Procedure

MCCL: Maximum Cancer Core Length

TCCL: Total Cancer Core Length

ROC: Receiver Operator Characteristics

AUC: Area under the curve

CI: Confidence Interval

SUVmax: Maximum Standardised Uptake Value

PACS: Picture Archive Communication System

DWI: Diffusion Weighted Images

Introduction

It is vital to establish whether the recurrent prostate cancer is organ confined, spread to the lymph nodes or there is extra nodal disease. Approximately 90% of patients with progressive CRPC will develop bone metastases, with another 20% developing soft tissue metastases in the lungs, liver or lymph nodes (1).

In order to evaluate the clinical impact of ^{18}F Choline PET-CT scan in comparison to other imaging modalities for detection of metastatic disease, it is important to define the following two terms:

Oligometastatic: The patient presents with disease in a limited number of distant regions, with or without control of the primary tumour(2).

Oligorecurrence: The patient presents one or more limited distant metastasis or recurrence is in one or more organs (with control of the primary tumour) (3).

PSA is used to monitor the biochemical relapse of prostate cancer, it is not useful to define the extent of disease. Cross-sectional imaging modalities such as CT scan, MRI, PET/CT and bone scintigraphy are the main imaging investigations for restaging of prostate cancer (4)(5).

Between PET/CT and full body MRI, there is no data to support the superiority of one technique over the other (6). Moreover there is no reproducible or precise imaging gold standard for detection of metastatic disease. One of the main reason for this is that sensitivity and specificity of the cross-sectional imaging techniques vary considerably (7).

For staging and follow up of patients with prostate cancer, positron emission tomography using ^{11}C Choline has shown promising results (8). PET is usually performed as hybrid imaging technique examination with CT and this facilitates full body molecular imaging survey in a single imaging session(9).

For detection of relapse, anatomical localisation of recurrent prostate cancer is improved when hybrid-imaging technique is used. The limitation of ^{11}C Choline is that it fails to identify relapse in patients with PSA less than 2 mg/ml(10). While developments in better biomarkers is underway, non-radiation imaging test such as MRI play a crucial role.

Whole body MRI can now be performed with high gradient amplitudes and high spatial resolution diffusion weighted imaging covering the whole body has also been introduced (11). It is possible to achieve high lesion to background contrast and the technique is actively used in detection of primary malignancy(12) . Diffusion weighted imaging can characterise lesions by quantitative apparent diffusion coefficient (ADC) values. ADC values are considered potential imaging biomarker compatible to the standardised uptake value (SUV) on ^{11}C Choline PET/CT (13). It has incremental value in detection of disease relapse in the lymph nodes and skeleton in patients with prostate cancer (14). There are still limited systematic reports validating the role of whole body MRI in prostate cancer.

Bone marrow is infiltrated before Bone metastases. Prostate cancer cells first seed into the normal haematopoietic marrow and its fat cells. Following this there is activation of osteoblastic and osteoclastic lines. It is the osteoblastic activity becomes visible on the bone scan (15). ^{18}F -choline PET CT can detect bone marrow infiltration due to its ability to detect cell proliferation. WB-MRI may detect prostate cancer cell masses in the normal haematopoietic marrow; before the bone marrow metastases are visible on bone scan(16) .

Methods and Materials

A total of 50 men were prospectively recruited to this study (between April 2014 to September 2015).

Inclusion Criteria

1. Previous external beam radiotherapy with or without new-adjuvant/adjuvant hormone therapy.
2. Biochemical failure as defined by the Phoenix Criteria (PSA nadir + 2ng/ml).
3. Men considering local salvage treatment for radio-recurrent disease.
4. Life expectancy of 5 years or more.

Exclusion criteria

1. Have taken any form of hormones (except 5-alpha reductase inhibitors) within the previous 6 months.
2. Unable to have MRI scan as defined by the standard of care practice.
3. Metallic implant likely to cause artefact and reduce scan quality.
4. PSA doubling time of 3 months or less.
5. PSA value 20ng/ml or greater
6. Prior prostate biopsies following biochemical failure
7. Any prior local intervention to the prostate (e.g. laser/electrical resection or incision, cryotherapy, HIFU, any other ablative modality, any other radiotherapy, any other prostate injection therapy for symptoms or cancer control.
8. Unable to have general or regional anaesthesia.
9. Unable to give informed consent.

MRI Scan:

All WB-MRI studies were performed on a single 3T MRI scanner (Ingenia, Phillips healthcare, Best, Netherlands). Multi-station acquisitions of contiguous body regions were performed using the manufacturers' head coil, two anterior surface coils and table-embedded posterior coils with the patient in supine position. Whole-body coronal pre-contrast mDixon imaging was complemented with axial T2- weighted turbo spin echo (TSE), axial DWI (b_0 and b_{1000}) and coronal contrast enhanced (CE) mDixon imaging. CE MRI was performed following 20 ml of hand injected intravenous (IV) gadoterate meglumine (Dotarem, Guebert, France). WBMRI protocol parameters are summarised in the following table.

	T2-TSE	MDixon (pre- and post-contrast)	DWI (b_0 , 1000)
Slice orientation	Transverse	Coronal	Transverse
TE (ms)	80	2.303	17
TR (ms)	1214.69	3.5	6304.5
Space between slices	5.5	2.5	5.5
Number of slices	40	120	40
Slice thickness (mm)	5	5	5
Acquisition matrix	500*497	240*238	124*118
ETL	89	2	39
Number of averages	1	1	2
Pixel bandwidth (Hz)	538	1847	3354
Pixel spacing	0.78/0.78	1.04/1.04	2.08
Flip angle	90	15	90

WB-MRI sequence parameters. T2-TSE, T2-weighted turbo spin echo; mDixon, modified Dixon; DWI, diffusion weighted imaging; TE, time of echo; TR, time of repetition; ETL, echo train length. Contrast agent 20 ml intravenous gadoterate meglumine, Dotarem®, Guerbet, Villepint, France.

The pre and post-contrast mDixon images were reconstructed into water only, fat only and in-phase and out of phase image datasets. The DWI images were used to generate ADC maps. The scans reviewed the unenhanced mDIXON and scored the suspicion of disease at each site using an a 1-6 ordinal scale. The score was specifically assigned at each site using the imaging features as follows on the pre-contrast mDIXON and DWI sequences

- 1- No lesion evident.
- 2- Poorly visible lesion evident on T1-weighted imaging only—low T1 signal bone focus or lymph node visible but not convincing for malignant involvement or < 5-mm short axis diameter (SAD).
- 3- Definite lesion visible on T1-weighted imaging but not DWI, lymph node 6–9 mm in SAD.
- 4- Definite lesion on T1 with mild increase in high b-value diffusion signal vs. background noise, lymph node 10-12 mm in SAD;
- 5- Definite lesion seen on T1 and DWI with moderate increase in high b-value DWI signal vs. background noise, lymph node 12–14 mm SAD.
- 6- Definite lesion seen on T1 and DWI with large increase in high b-value signal vs. background noise, lymph node ≥ 15 mm SAD.

On T2W images sites were rescored as negative or positive. A negative score was assigned where there was no lesion or where features favoured benignity (e.g. fatty nodal hilum or high T2 signal of haemangioma), and a positive score assigned for features that favour malignancy (rounded nodal morphology, low T2 signal in node or bone lesion). Positive T2 appearances were scored up a point on the initial 1–6 scale (e.g. 3/6 on mDixon/DWI becomes 4/6), and negative T2 appearances were scored down a point (3/6 on mDixon/DWI becomes 2/6). Lastly, post-contrast mDixon images were reviewed and a final WB-MRI score was assigned. Here, lesional enhancement was scored up a point on the 1–6 scale and down a point if there was no enhancement.

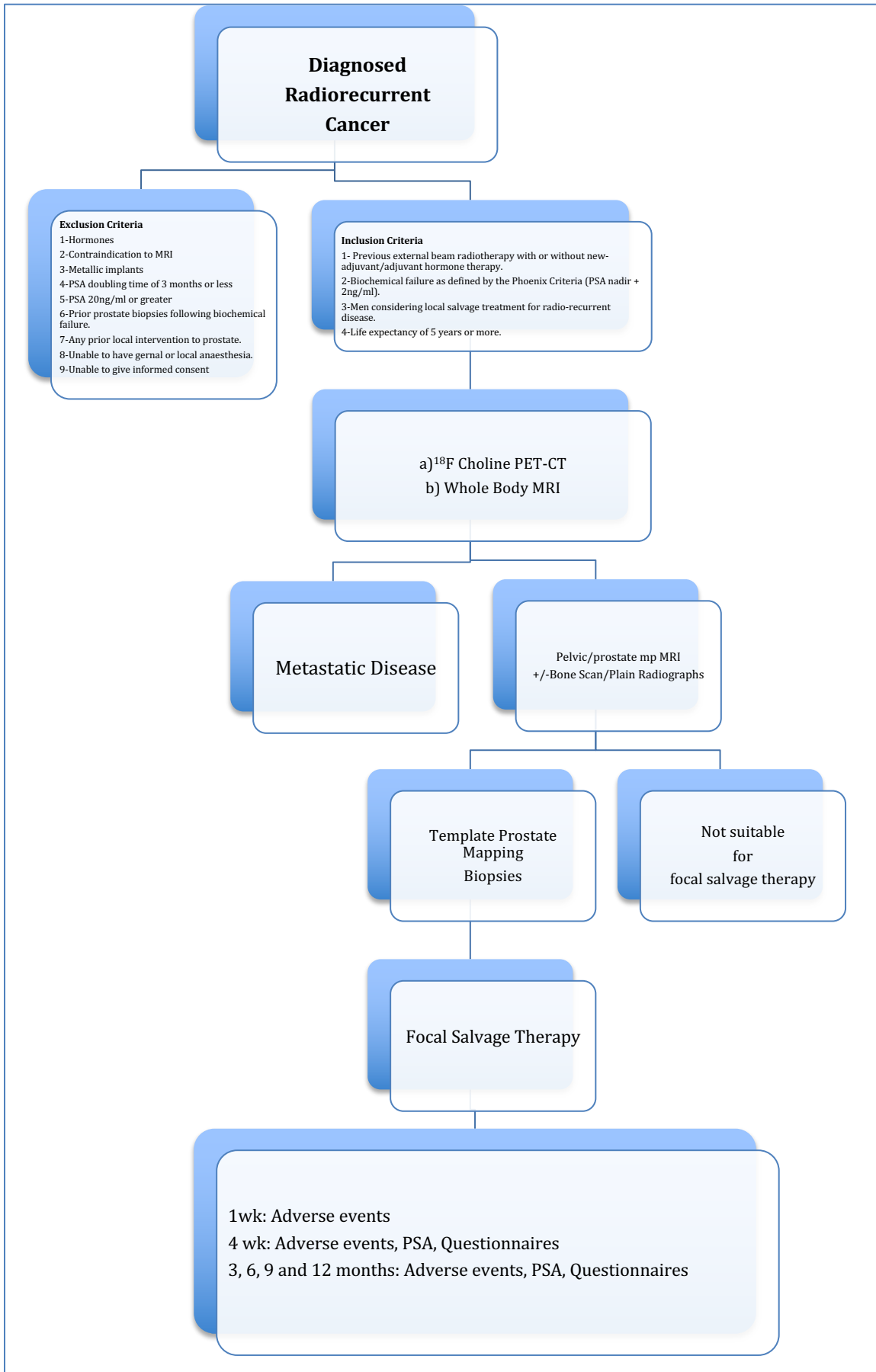
PET-CT scan:

Patients were injected with 300-370 MBq of ^{18}F -FECH [effective dose 12.95 mSv]. Whole-body PET/CT images were acquired 60 min after tracer injection. Owing to the rapid excretion of ^{18}F -FECH in urine, the patients were asked to empty their bladder prior to imaging. At approximately 90 min, a limited (one bed position, PET/CT) pelvic view was obtained with the prostate in the field of view. The CT acquisition parameters included: scout 120 kVp, 10 mA; CT 140 kVp, 80 mA, 0.8 s, pitch 1.75; CT slices 5 mm (70-cm FOV PET AC), 2.5 mm (50-cm FOV Std), 2.5 mm (50-cm FOV Lung). PET acquisition parameters were: 3D attenuation-corrected and non-attenuation-corrected images, 20 subsets with iterative reconstructions. CT images were used to produce attenuation correction values for PET emission reconstruction and fused PET/CT presentation. ^{18}F Choline uptake above the background (excluding normal physiological uptake) was considered as a positive lesion.

Bone Scan:

Technetium-99m labelled diphosphonates was administered through intravenous injection. Whole body imaging was performed with anterior and posterior views, 256 x 1024 matrix and energy window(s) of 140 KeV. Effective dose (ED) is 3mSv (or 5mSv for cancer patients) and Diagnostic Reference Level (DRL) is 600 MBq (Or 800 for cancer patients).

The trial flow chart is as follows:



FORECAST Trial flow chart

Statistical Analysis

Statistical analysis was performed using SPSS version 23.0 (SPSS, IBM Corporation, New York) and the R language environment (R Core Team 2015, version 3.2.1). SPSS was used for descriptive statistics and the rms package in R for the modelling process. Using univariable and multivariable logistic regression, odds ratios (ORs) with 95% confidence intervals (95% CIs) were obtained to assess the influence of clinical characteristics on the outcome of Choline PET/CT positivity. A two-tailed $p < 0.05$ was considered statistically significant. Factors with $p < 0.05$ were retained in the final model. Cohen's Kappa Score is useful for either inter rater or intra rater reliability testing. The score can range from -1 to $+1$, 1 represents perfect agreement between the raters and 0 represents the amount of agreement that can be expected from random chance. Typically, it is accepted that values $0.01-0.20$ as none to slight, $0.21-0.40$ as fair, $0.41-0.60$ as moderate, $0.61-0.80$ as substantial, and $0.81-1.00$ as almost perfect agreement.

Results

The median age was 69.5 years (range 54-85 years) and median PSA was 14.7 ng/ml (range 7.78 - 36 ng/ml). According to D'Amico classification (17) there were following three category of patients

- **Low risk** PSA < 10 , G < 6 , T1-2a
- **Intermediate risk** PSA 10 - 20, G7 or T2b
- **High-risk disease** High-risk: PSA > 20 , G > 8 , T2c-3a

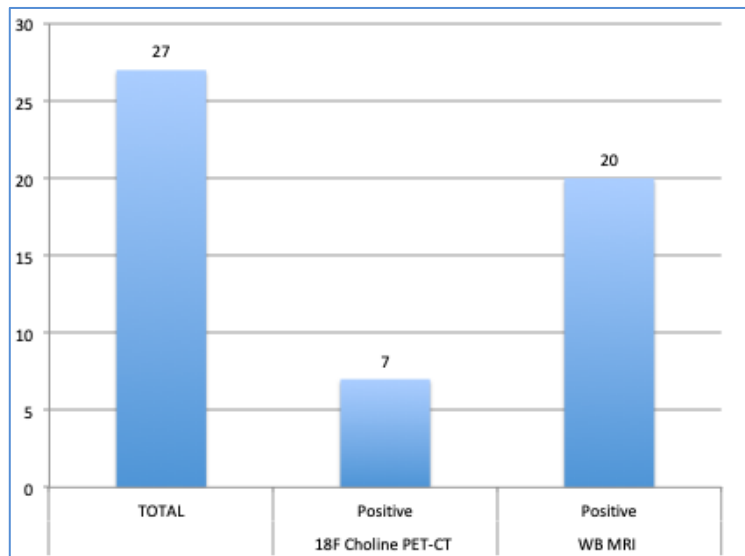
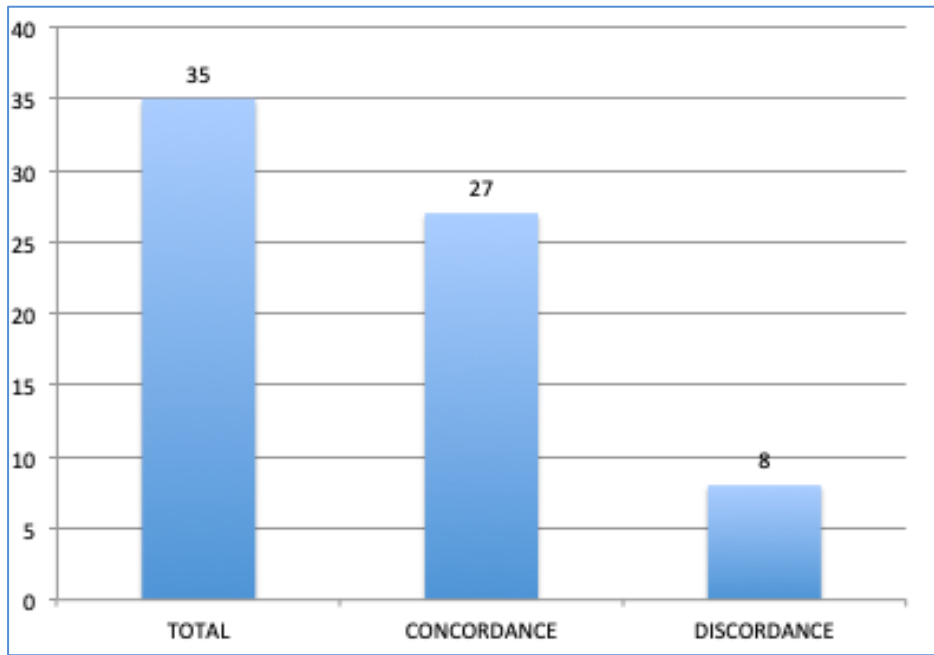
The baseline demographics have been listed in Table 1

Variable	
Age in years Median (range)	69.5 ± 6.9
PSA at time of scan , Median (IQR)	3.29 (2.4-5.3)
Median PSA at time of EBRT	14.7 ng/ml (Inter Quartile Range IQR 7.78 -36)
D'Amico Classification	
High-risk:	36 (72)
Intermediate risk:	8 (16)
Low risk:	4 (8)
PSA Nadir Median (IQR)	0.3 (0.1-0.6)

*Missing baseline data n=2

Table 1 – Baseline Demographics

The data related to concordance and discordance between Whole Body MRI, ¹⁸F Choline PET-CT and Bone Scan are shown in Tables 2-7 below.



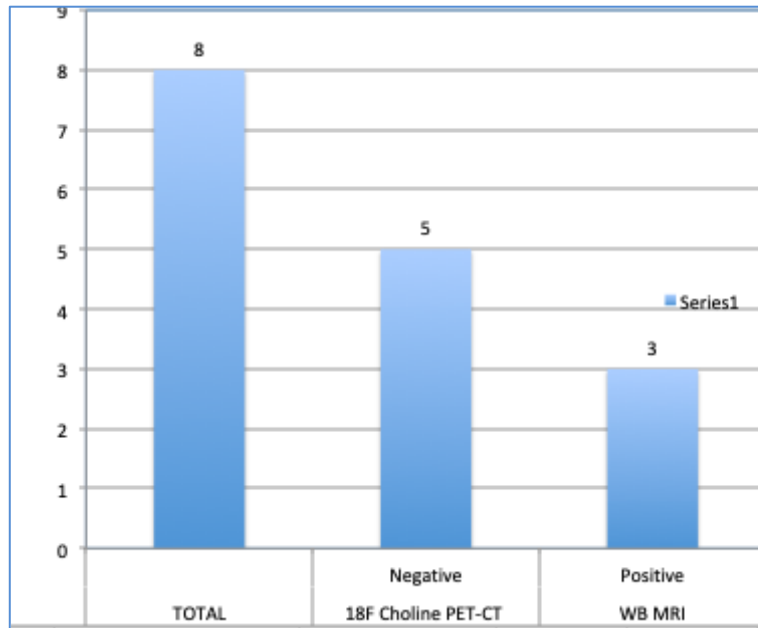


Table 2: Concordance and discordance in local tumour detection on WB-MRI and ¹⁸F Choline PET-CT.

Out of 35 patients, with local tumour there was agreement between WB-MRI and ¹⁸F Choline PET/CT in 20 cases (Kappa score 0.311; p=0.056). There were 3 cases in which ¹⁸F Choline PET/CT was negative and WB-MRI was positive for local tumour. There were 7 cases that ¹⁸F Choline PET/CT reported positive for local tumour when WB-MRI was negative.

		¹⁸F Choline PET-CT N Stage			Total
		N0	N1	N2	
Whole Body MRI Nodal Stage	0	1	0	0	1
	NX	1	0	0	1
	N0	12	1	0	13
	N1	0	2	1	3
	N2	0	0	1	1
Total		14	3	2	19

Table 3: Concordance nodal disease WB-MRI and ¹⁸F Choline PET-CT

Concordance between WB- MRI and ¹⁸F Choline PET-CT for NX-0 disease occurred in 14/19 cases Kappa score 0.548 (p=0.00032). There was one case reported as N1 disease on WB-MRI that was reported as N2 on ¹⁸F Choline PET-CT. WB-MRI and ¹⁸F Choline PET-CT were concordant in 4 cases for the same nodal site (external iliac node) kappa = 0.333 (p=0.121). However, in 4 other cases, sites reported by WB-MRI as positive for nodal disease, were not concordant with the same site on ¹⁸F Choline PET-CT.

		WB-MRI Nodal Site				Total
		External Iliac	Internal Iliac	Common Iliac	Para-aortic	
¹⁸F Choline PET/CT Nodal Site	External Iliac	4	0	0	1	5
	Internal Iliac	1	1	1	0	3
Total		5	1	1	1	8

Table 4: Sites of Nodal disease WB-MRI vs ¹⁸F Choline PET-CT

		¹⁸F Choline PET-CT Bone Sites Outcome		Total
		Negative	Positive	
WB-MRI Bone Sites Outcome	Negative	28	0	28
	Equivocal	5	0	5
	Positive	0	2	2
Total		33	2	35

Table 5: Concordance of bony disease WB-MRI and ¹⁸F Choline PET-CT.

Of 35 patients where bony metastatic disease outcome was reported, concordance between WB-MRI and ¹⁸F Choline PET-CT T was achieved in 30 cases. Of these 28 were negative on both WB-MRI and ¹⁸F Choline PET-CT and positive in 2 cases. These were also positive for same site (thoracic and lumbar spine disease). 5 patients were reported as having equivocal disease on WB-MRI that was negative on ¹⁸F Choline PET-CT (kappa score 0.411 p<0.0001)

		BS Bone Sites Outcome		Total
		Equivocal	Positive	
WB-MRI Bone Sites Outcome	Negative	1	0	1
	Positive	0	1	1
Total		1	1	2

Table 6: Concordance of bony disease WB-MRI and Tc^{99m} MDP Bone Scan.

Concordance was achieved in only one case for bone metastatic disease between WB-MRI and Bone scan (kappa score 0.333 p=0.157) at thoracic spine and rib.

		Bone Scan Bone Sites Outcome		Total
		Equivocal	Positive	
¹⁸F Choline PET-CT Bone Sites Outcome	Negative	2	0	2
	Positive	0	2	2
Total		2	2	4

Table 7: Concordance of bony disease ¹⁸F Choline PET-CT and Bone Scan.

WB-MRI vs ¹⁸ F Choline PET-CT for Local disease	0.311 (p=0.056)
WB-MRI vs ¹⁸ F Choline PET-CT for NX-0 disease	0.548 (p=0.00032)
WB-MRI vs ¹⁸ F Choline PET-CT for same nodal site (external iliac node)	0.333 (p=0.121)
WB-MRI vs ¹⁸ F Choline PET-CT for bony metastatic disease	0.411 (p<0.0001)
WB-MRI vs Bone scan for Bone metastatic disease	0.333 (p=0.157)
¹⁸ F Choline PET-CT vs Bone Scan for bony metastatic disease	0.333 (p=0.46)

Table 8: Kappa Score Concordance

Summary of findings for local, nodal and metastatic disease

Local disease

- a) Concordance between WB-MRI and Choline PET/CT for local disease occurred in 20/35 cases
Kappa score 0.311 (p=0.056).

Nodal disease

- b) Concordance between WB-MRI and Choline PET/CT for NX-0 disease occurred in 14/19 cases Kappa score 0.548 (p=0.00032).

- c) WB-MRI and Choline PET/CT were concordant in 4 cases for the same nodal site (external iliac node) kappa =0.333 (p=0.121). However, in 4 other cases these tests were not concordant for sites of nodal disease

Metastatic disease

- d) Concordance between WB-MRI and Choline PET/CT was achieved in 30/35 cases for bone metastases (Kappa=0.411 (p<0.0001)).

- e) Concordance was achieved in only one case for bone metastatic disease between WB-MRI and Bone scan (kappa score 0.333 p=0.157).

- f) Concordance between Choline PET/CT and bone scan was achieved in 2 cases for bony metastatic disease .However, there was discordance in two cases that were negative on Choline PET/CT and equivocal in Bone scan (Kappa = 0.333 (p=0.46)).

Overall Summary

Overall our study has shown that there is moderate agreement between WB- MRI and Choline PET/CT in the detection of NX-0 nodal disease and for bony metastatic disease. There was fair agreement for bony metastatic disease detected by WB-MRI and BS and also for Choline PET/CT and BS however significance was not achieved

COMPARISON WITH EXISTING STUDIES

In a study comparing 11C Choline PET/CT and MRI, 11C-choline PET/CT was superior in the detection of local recurrence and bone metastasis on a regional basis. Whole-body MRI including DWI showed similar diagnostic accuracy only for detecting lymph node metastases. It was concluded that compared with 11C-choline PET/CT, therefore, whole-body MRI including DWI cannot serve as alternative imaging modality for restaging prostate cancer (18)

In patients post primary treatment and being considered for salvage treatment, Conde-Moreno et al (19) performed a study in 35 patients. In this study however WB-MRI- DWI had a lower sensitivity, PPV, and NPV compared with Choline-PET/CT 44.93%, 86.11%, and 19.15%, vs. 97.10%, 93.06% and 77.78%, respectively. Specificity of WB-MRI-DWI was higher than Choline PET/CT 64.29% vs. 58.33%.

In order to evaluate local relapse in prostate cancer patients, a retrospective study of 21 patients with prostate cancer treated initially with surgery (n=12), radiotherapy (n=9) showed (11)C-choline PET/CT and multi-parametric MRI play a complementary role in the detection of local relapse in prostate cancer patients, with similar sensitivity for the detection of lymph involvement. Whole-body 11C-choline PET/CT technique is was also found to be useful for bone staging (20)

In men with treated with radical prostatectomy (n=82) or post EBRT (n=70), WB-MRI was evaluated for detection of metastases without hormonal treatment (21). WB-MRI had a sensitivity, specificity, PPV, NPV and Area Under Curve (AUC) of 99%, 98%, 98%, 96% and 0.971 respectively, for detection of bone metastases. For lymph node metastases, this was 98%, 99%, 97%, 98%, and 0.960 respectively. In this study ¹⁸FCholine-PET/CT was the comparative imaging technique and so detection differences between the two imaging investigations were not reported.

In a study of thirty patients (median prostate-specific antigen [PSA: 11.8 ng/mL]) with suspected recurrent prostate cancer following definitive treatment underwent ¹¹C-choline PET/CT and conventional imaging, including pelvic MRI, contrast-enhanced chest, abdomen, and pelvic CT, and bone scintigraphy. The authors aimed to compare the imaging modalities for prostate cancer restaging. ¹¹C-choline-PET/CT was more accurate in the detection of recurrent prostate cancer nodes and bony metastatic lesions compared to conventional imaging and had the advantage of restaging the disease in a single step (22).

WB-MRI- Diffusion weighted imaging (WB-MRI-DWI), BS and PSA as predictors for bone metastases in prostate cancer were evaluated (23) both in primary and post ADT/EBRT setting (n=38). WB-MRI-DWI appeared to detect more spinal lesions than BS (24 vs. 19). Overall, however more metastatic lesions were detected by BS than WB-MRI- DWI (53 vs. 49).

LeCouvret (24) compared DWI-WBMRI with BS/plain films and CT in 100 patients; 68 were felt to have metastases. The sensitivity of BS/plain films and WB-MRI for detecting bone metastases was 86 % and 98-100 %, respectively (p <0.04), and specificity was 98 % and 98- 100 %, respectively.

respectively. The sensitivity of CT and WB-MRI for detecting enlarged lymph nodes was similar, at 77-82 % for both; specificity was 95-96 % and 96- 98 %, respectively. The sensitivity of the combination of BS/plain films plus CT and WB-MRI for detecting bone metastases and/or enlarged lymph nodes was 84 % and 91-94 %, respectively ($p = 0.03-0.10$); specificities were 94-97 % and 91-96 %, respectively .

The diagnostic performance of ^{18}F Choline and MRI with diffusion weighted imaging (DWIMRI) was prospectively compared for local and regional lymph node (LN) staging before radical prostatectomy (RP) with extended pelvic lymphadenectomy (PLND) (25). In a patient-based analysis the sensitivity and positive predictive value were respectively 78% and 94% for ^{18}F -Choline and 33% and 84% for DWI MRI ($P = 0.015$). ^{18}F - despite excellent performance, it cannot replace MRI that remains better for tumoral localization and local evaluation, especially for seminal vesicle.

Venkitaraman R (16) compared the detection rate of metastatic disease by WB-MRI to BS in 39 patients diagnosed with local prostate cancer. Interestingly, the sensitivity for detection of skeletal metastases for both BS and WB-MRI was 70 % (95 % CI 0.42-0.98), the specificity 100 % and the positive predictive value 100 %. WB-MRI and BS differed in the areas of detection. For instance, seven patients had bone metastases on BS and seven had skeletal metastases by WB-MRI, with concordant findings in only four. BS detected more rib metastases, whilst MRI identified more metastatic lesions in the spine . This study showed that WBMRI and BS have similar specificity and sensitivity, but may have to be used as complementary investigations to detect skeletal metastases from prostate cancer, rather than as alternatives.

Methodological Limitations

- 1) There is lack of histological confirmation as bone biopsies are not common practice and lymph node dissection is performed in patients suitable for salvage therapy.
- 2) The PSA is low at the time of imaging. The median PSA at the time of imaging was 3.29 ng/ml.
- 3) There were only 2 cases of metastatic disease in the cohort included in this study.
- 4) Whilst Bone Scan reports as positive or equivocal when present, all other reports did not have definitive negative report thereby limiting analyses.

Clinical Implications

WB-MRI cannot be the only imaging modality for investigation of prostate cancer.

Future research

- a) The study opens future avenues for biomarkers which can be used for investigation of biochemical relapse of prostate cancer. Despite known low sensitivity and specificity of ¹⁸F Choline, the results of the current study are comparable and suggest that WB-MRI cannot be used alone for staging.
- b) Larger studies with longer follow up are required before WB-MRI can be considered to fully replace bone scan and Choline PET/CT.
- c) Future studies need to include cohort of cases with metastatic disease so that lesion by lesion analysis can be performed.

- d) Bone biopsy has always been a challenging issue and feasibility of performing this should be considered.
- e) Any index test whether it is a new radionuclide or WB-MRI technique has to avoid reporting bias and clinician should be blinded to the outcome of index test. Over longer follow up the results of the index and reference tests should be paired for change in morphology, number or size of the original lesion detected.
- f) Recently, the development of metabolic imaging methods has been aimed at improving diagnosis of biochemical recurrent prostate cancer (BRPCa), when an increase of prostate-specific antigen (PSA) serum values is detected following curative primary treatments as radical prostatectomy or radiation therapy (26) (27) . Radiolabelled PSMA PET/CT has proven to be clearly superior in detecting BRPCa lesions at low PSA levels (≤ 1 ng/ml) when compared to radiolabelled choline PET/CT. On the other hand, the superiority of radiolabelled PSMA PET/CT was less evident in patients with PSA > 1 ng/ml. More studies and in particular cost-effectiveness analyses comparing these imaging methods are warranted.

CONFLICT OF INTEREST:

None

Conclusion

WB-MRI has similar detection rates of recurrent disease compared to bone scan and Choline PET/CT. Further studies are required to determine if WB-MRI or PET-CT with a specific biomarker can replace current standard of care investigations. At present WB-MRI cannot be used alone as imaging modality for investigation of biochemical relapse of Prostate Cancer.

References

1. Bubendorf L, Schöpfer A, Wagner U, Sauter G, Moch H, Willi N, et al. Metastatic patterns of prostate cancer: an autopsy study of 1,589 patients. *Hum Pathol.* 2000 May;31(5):578–83.
2. Hellman S, Weichselbaum RR. Oligometastases. *J Clin Oncol.* 1995 Jan;13(1):8–10.
3. Niibe Y, Hayakawa K. Oligometastases and Oligo-recurrence: The New Era of Cancer Therapy. *Jpn J Clin Oncol.* 2010 Feb 1;40(2):107–11.
4. Evangelista L, Cimitan M, Zattoni F, Guttilla A, Zattoni F, Saladini G. Comparison between conventional imaging (abdominal–pelvic computed tomography and bone scan) and [18F]choline positron emission tomography/computed tomography imaging for the initial staging of patients with intermediate- to high-risk prostate cancer: A retrospective analysis. *Scandinavian Journal of Urology.* 2015 Sep 3;49(5):345–53.
5. Soyka JD, Muster MA, Schmid DT, Seifert B, Schick U, Miralbell R, et al. Clinical impact of 18F-choline PET/CT in patients with recurrent prostate cancer. *Eur J Nucl Med Mol Imaging.* 2012 Jun 1;39(6):936–43.
6. Conde-Moreno AJ, Herrando-Parreño G, Muelas-Soria R, Ferrer-Rebolleda J, Broseta-Torres R, Cozar-Santiago MP, et al. Whole-body diffusion-weighted magnetic resonance imaging (WB-DW-MRI) vs choline-positron emission tomography-computed tomography (choline-PET/CT) for selecting treatments in recurrent prostate cancer. *Clin Transl Oncol.* 2017 May 1;19(5):553–61.
7. Hricak H, Choyke PL, Eberhardt SC, Leibel SA, Scardino PT. Imaging prostate cancer: a multidisciplinary perspective. *Radiology.* 2007 Apr;243(1):28–53.
8. Tuncel M, Souvatzoglou M, Herrmann K, Stollfuss J, Schuster T, Weirich G, et al. [11C]Choline positron emission tomography/computed tomography for staging and restaging of patients with advanced prostate cancer. *Nuclear Medicine and Biology.* 2008 Aug 1;35(6):689–95.
9. Weber WA, Grosu AL, Czernin J. Technology Insight: advances in molecular imaging and an appraisal of PET/CT scanning. *Nat Clin Pract Oncol.* 2008 Mar;5(3):160–70.
10. Afshar-Oromieh A, Zechmann CM, Malcher A, Eder M, Eisenhut M, Linhart HG, et al. Comparison of PET imaging with a 68Ga-labelled PSMA ligand and 18F-choline-based PET/CT for the diagnosis of recurrent prostate cancer. *Eur J Nucl Med Mol Imaging.* 2014 Jan 1;41(1):11–20.
11. Lauenstein TC, Goehde SC, Herborn CU, Goyen M, Oberhoff C, Debatin JF, et al. Whole-body MR imaging: evaluation of patients for metastases. *Radiology.* 2004 Oct;233(1):139–48.

12. Nakanishi K, Kobayashi M, Nakaguchi K, Kyakuno M, Hashimoto N, Onishi H, et al. Whole-body MRI for detecting metastatic bone tumor: diagnostic value of diffusion-weighted images. *Magn Reson Med Sci*. 2007;6(3):147–55.
13. Castellucci P, Fuccio C, Nanni C, Santi I, Rizzello A, Lodi F, et al. Influence of trigger PSA and PSA kinetics on 11C-Choline PET/CT detection rate in patients with biochemical relapse after radical prostatectomy. *J Nucl Med*. 2009 Sep;50(9):1394–400.
14. Luboldt W, Küfer R, Blumstein N, Toussaint TL, Kluge A, Seemann MD, et al. Prostate carcinoma: diffusion-weighted imaging as potential alternative to conventional MR and 11C-choline PET/CT for detection of bone metastases. *Radiology*. 2008 Dec;249(3):1017–25.
15. Suva LJ, Washam C, Nicholas RW, Griffin RJ. Bone metastasis: mechanisms and therapeutic opportunities. *Nat Rev Endocrinol*. 2011 Apr;7(4):208–18.
16. Venkitaraman R, Cook GJR, Dearnaley DP, Parker CC, Khoo V, Eeles R, et al. Whole-body magnetic resonance imaging in the detection of skeletal metastases in patients with prostate cancer. *J Med Imaging Radiat Oncol*. 2009 Jun;53(3):241–7.
17. Hernandez DJ, Nielsen ME, Han M, Partin AW. Contemporary evaluation of the D'Amico risk classification of prostate cancer. *Urology*. 2007 Nov;70(5):931–5.
18. Wieder H, Beer AJ, Holzapfel K, Henninger M, Maurer T, Schwarzenboeck S, et al. 11C-choline PET/CT and whole-body MRI including diffusion-weighted imaging for patients with recurrent prostate cancer. *Oncotarget*. 2017 Sep 12;8(39):66516–27.
19. Conde-Moreno AJ, Herrando-Parreño G, Muelas-Soria R, Ferrer-Rebolleda J, Broseta-Torres R, Cozar-Santiago MP, et al. Whole-body diffusion-weighted magnetic resonance imaging (WB-DW-MRI) vs choline-positron emission tomography-computed tomography (choline-PET/CT) for selecting treatments in recurrent prostate cancer. *Clinical and Translational Oncology*. 2017;19(5):553–61.
20. Garcia JR, Romera N, Cozar M, Soler M, Moragas M, Escobar M. (11)C-choline PET/CT and multiparametric MRI in patients with biochemical relapse of prostate cancer. *Actas Urol Esp*. 2015 May;39(4):259–63.
21. Barchetti F, Stagnitti A, Megna V, Al Ansari N, Marini A, Musio D, et al. Unenhanced whole-body MRI versus PET-CT for the detection of prostate cancer metastases after primary treatment. *Eur Rev Med Pharmacol Sci*. 2016;20(18):3770–6.
22. Kawanaka Y, Kitajima KD, Yamamoto S, Nakanishi Y, Yamada Y, Hashimoto T, et al. Comparison of 11C-choline Positron Emission Tomography/Computed Tomography (PET/CT) and Conventional Imaging for Detection of Recurrent Prostate Cancer. *Cureus*. 2018 Jul 11;10(7):e2966.
23. An H, Tao N, Li J, Guan Y, Wang W, Wang Y, et al. Detection of prostate cancer metastasis by whole body magnetic resonance imaging combined with bone scintigraphy and PSA levels. *Cellular Physiology and Biochemistry*. 2016;40(5):1052–62.

24. Lecouvet FE, El Mouedden J, Collette L, Coche E, Danse E, Jamar F, et al. Can whole-body magnetic resonance imaging with diffusion-weighted imaging replace Tc 99m bone scanning and computed tomography for single-step detection of metastases in patients with high-risk prostate cancer? *European urology*. 2012;62(1):68–75.
25. Pinaquy J-B, De Clermont-Galleran H, Pasticier G, Rigou G, Alberti N, Hindie E, et al. Comparative effectiveness of [(18) F]-fluorocholine PET-CT and pelvic MRI with diffusion-weighted imaging for staging in patients with high-risk prostate cancer. *Prostate*. 2015 Feb 15;75(3):323–31.
26. Treglia G, Pereira Mestre R, Ferrari M, Bosetti DG, Pascale M, Oikonomou E, et al. Radiolabelled choline versus PSMA PET/CT in prostate cancer restaging: a meta-analysis. *Am J Nucl Med Mol Imaging*. 2019;9(2):127–39.
27. Testa C, Pultrone C, Manners DN, Schiavina R, Lodi R. Metabolic Imaging in Prostate Cancer: Where We Are. *Front Oncol*. 2016;6:225.

Chapter 9: Summary of Conclusions

This research has addressed role of radiolabelled choline in prostate cancer. The thesis was divided into eight chapters and each chapter addressed a hypothesis with summarised conclusions as follows:

Chapter 1, addresses the introduction to the thesis and provides epidemiology, etiology, metastatic spread, current diagnostics and clinical need of new biomarker for risk stratification of prostate cancer.

Chapter 2, provides a detailed analysis of the distribution pattern of the three most used choline tracers: ^{18}F -methylcholine, ^{11}C -choline, and ^{18}F -ethylcholine in metabolically and anatomically disease-free patients. The knowledge gained from this was used in evaluation of radiolabelled choline PET-CT scans for feasibility, validation, assessment of skeletal metastatic disease and and comparison of Whole Body MRI and ^{18}F Choline as part of clinical trial.

Chapter 3, once the physiological distribution of radiolabelled choline was completed we performed a feasibility study, assessing dynamic ^{18}F Ethyl Choline PET and kinetic modelling in the clinical setting of biochemical relapse of Prostate Cancer. This work concluded that ^{18}F Choline can act as a biomarker to assess angiogenesis in prostate cancer.

Chapter 4 and 5, as ^{18}F Choline was found to have the potential to detect prostate cancer, further work was done related to detection of clinically significant and insignificant prostate

cancer. The findings on ^{18}F -FECH PET/CT and ^{18}F -FECH PET/MR were correlated with gold standard Template guided prostate mapping biopsy (TPM). I made key observation that multiple previous treatments can give false positive results and ^{18}F Choline PET/MR is imaging investigation of choice post HIFU as better anatomical details are available which complement the information gained. I also found that false negative results with ^{18}F Choline PET/MR can be due to very small volume (≤ 2 mm) disease.

Chapter 6, I noted that, not only prostate cancer but a number of pathologies can cause increased uptake of radiolabelled choline in the prostate and peri-prostatic tissue. As radiolabelled choline accumulates in cells with increased cell membrane turn over, the differential diagnosis of abnormal tracer accumulation includes a range of benign and malignant disease processes.

Chapter 7, Knowledge gained from evaluation of physiological distribution of choline (chapter 2) and differential diagnosis (chapter 6) was further extended to study the skeleton. I outlined the spectrum of skeletal findings on dual-phase ^{18}F -fluoroethylcholine (FECH) PET/CT performed during the work-up of patients referred for suspected prostate cancer relapse. My key observations were that SUV_{max} in isolation cannot be used to characterize these lesions as benign or malignant. Minimal overlap of benign and malignant lesions also exists.

Chapter 8, Finally the clinical utility of ^{18}F Choline was assessed in the setting of prospective trial in collaboration with Uro-oncology, Nuclear Medicine and Radiology departments. This work concluded that at present WB-MRI cannot be used alone as imaging modality for investigation of biochemical relapse of Prostate Cancer.

Future Directions

PSMA (prostate surface membrane antigen) is a transmembrane protein present in prostate cancer. Following encouraging results with Choline PET/CT and PET/MR, it is expected that Ga68/F18 labelled PSMA PET/CT imaging will emerge as a diagnostic technique with better sensitivity and specificity. Relapse of prostate cancer would be detected at low PSA levels and there would be early detection of metastatic disease. It is anticipated that there would be a global drive to introduce molecular imaging using novel biomarkers (such as PSMA imaging) as part of the work up of biochemical relapse of prostate cancer.

Radiolabelled Choline has emerged as a molecular imaging technique for several types of cancers as it provides useful information that cannot be provided by other conventional imaging. During the course of my research related to Prostate Cancer, several studies have been published exploring the feasibility of using radiolabelled Choline. These have provided future road map for inclusion of this biomarker into the diagnostic pathway of several other oncological and non-oncological conditions.

MRI is mainly used as imaging investigations in neuroimaging, despite excellent structural detail it has poor specificity for detection of viable tumour in treated brain tissue when surgery, radiation, chemotherapy or combination of treatments has been used. There is need to have more accurate modality for diagnosis, treatment planning and follow up of complex cases. The use of molecular imaging tracers such as ^{18}F -FDG has been explored. Physiological distribution of ^{18}F FDG i.e. avid accumulation by normal cortex, the low tumour/background signal ratio makes it difficult to distinguish the tumour from

normal surrounding tissues. The recent availability of choline labeled with a long half-life radioisotope as ^{18}F increases the possibility of studying this tracer's potential role in the staging of brain tumours particularly brain gliomas (1).

Another application of radiolabelled choline based tracers is primary hyperparathyroidism. In a meta-analysis for detection of parathyroid adenoma, the pooled detection rate was noted to be 97% and 94% on per patient-based and per lesion-based analysis respectively (2). According to Oxford criteria the level of evidence was 3a despite considerable heterogeneity between studies. Interestingly despite heterogeneity between studies. Radiolabelled Choline PET/CT has shown favourable results in detection of hyperfunctioning parathyroid tissue and may replace conventional Technetium $^{99\text{m}}$ -Sestamibi scintigraphy in preoperative parathyroid surgery planning. Further high-quality studies are required to confirm the accuracy of this technique.

Utility of radiolabelled choline PET CT in detection of hepatocellular carcinoma and extrahepatic disease has been explored (3). This is particularly important as there are limitations related to significant uptake of ^{18}F FDG only in poorly differentiated hepatocellular carcinoma(4). Radiolabelled choline has been shown to be more accurate than ^{18}F FDG (5). ^{11}C Choline has shown strong avidity for well-differentiated as well as moderately differentiated tumours (3). It has been postulated that use of ^{11}C Choline PET/CT into standard diagnostic algorithm managed by multidisciplinary team (MDT) can lead to a change in initial diagnosis/staging and management in 24% of patients (6). It has been proposed that a novel diagnostic algorithm to be refined in referral centres for hepatocellular carcinoma management(7).

Overall, while the desire to explore more specific biomarkers for different disease processes is promoting novel research ideas, it is anticipated that radiolabelled choline will have potential impact in the diagnostic work up of patients for several other oncological and non-oncological conditions.

References

1. Giovannini E, Lazzeri P, Milano A, Chiara Gaeta M, Ciarmiello A. Clinical Applications of Choline PET/CT in Brain Tumors. *Current Pharmaceutical Design*. 2015 Jan 1;21(1):121–7.
2. Broos WAM, van der Zant FM, Knol RJJ, Wondergem M. Choline PET/CT in parathyroid imaging: a systematic review. *Nuclear Medicine Communications*. 2019 Feb 1;40(2):96–105.
3. Yoon KT, Kim JK, Kim DY, Ahn SH, Lee JD, Yun M, et al. Role of 18F-fluorodeoxyglucose positron emission tomography in detecting extrahepatic metastasis in pretreatment staging of hepatocellular carcinoma. *Oncology*. 2007;72 Suppl 1:104–10.
4. Yamamoto Y, Nishiyama Y, Kameyama R, Okano K, Kashiwagi H, Deguchi A, et al. Detection of hepatocellular carcinoma using 11C-choline PET: comparison with 18F-FDG PET. *J Nucl Med*. 2008 Aug;49(8):1245–8.
5. Wu H, Wang Q, Li B, Li H, Zhou W, Wang Q. F-18 FDG in conjunction with 11C-choline PET/CT in the diagnosis of hepatocellular carcinoma. *Clin Nucl Med*. 2011 Dec;36(12):1092–7.
6. Lopci E, Torzilli G, Poretti D, de Neto LJS, Donadon M, Rimassa L, et al. Diagnostic accuracy of ¹¹C-choline PET/CT in comparison with CT and/or MRI in patients with hepatocellular carcinoma. *Eur J Nucl Med Mol Imaging*. 2015 Aug;42(9):1399–407.
7. Lanza E, Donadon M, Felisaz P, Mimmo A, Chiti A, Torzilli G, et al. Refining the management of patients with hepatocellular carcinoma integrating 11C-choline PET/CT scan into the multidisciplinary team discussion. *Nuclear Medicine Communications*. 2017 Oct 1;38(10):826–36.

Appendices

Appendix 1-Publications

1-Multicenter study evaluating extra prostatic uptake of ¹¹C-Choline, ¹⁸F-Methylcholine, and ¹⁸F-Ethylcholine in male patients: physiological distribution, statistical differences, imaging pearls, and normal variants. Haroon A, Zaroni L, Celli M, Zakavi R, Beheshti M, Langsteger W, Fanti S, Emberton M, Bomanji J. Nucl Med Commun. 2015 Nov;36(11):1065-75. doi: 10.1097/MNM.0000000000000372. PMID: 26340086

2-¹⁸F-FECH PET/CT to assess clinically significant disease in Prostate Cancer: Correlation with maximum and total cancer core length obtained via MRI-Guided Template Mapping Biopsies. Haroon A, Ahmed HU, Cathcart P, Almuhaideb A, Kayani I, Dickson J, Kirkham A, Freeman A, Emberton M, Bomanji J. AJR Am J Roentgenol. 2016 Dec;207(6):1297-1306. doi: 10.2214/AJR.15.15679. Epub 2016 Sep 9. PMID: 27611962

3-Spectrum of metastatic and nonmetastatic skeletal findings with dual-phase ¹⁸F-FECH PET/CT in patients with biochemical relapse of prostate cancer. Haroon A, Syed R, Endozo R, Allie R, Freeman A, Emberton M, Bomanji J. Nucl Med Commun. 2017 May;38(5):407-414. doi: 10.1097/MNM.0000000000000665. PMID: 28379896 Clinical Trial.

4-Phenotypic appearances of prostate utilizing PET-MRI and PET-CT with ⁶⁸Ga PSMA, radiolabelled Choline and ⁶⁸Ga DOTATATE Haroon A, Afaq A, Nuthakki S, Freeman A, Biassoni L, Fanti S, Beheshti M, Jan H, Vinjamuri S, Emberton M, Bomanji J. Nucl Med Commun. 2018 Mar;39(3):196-204. doi: 10.1097/MNM.0000000000000797. PMID: 29384832

5-Localising occult prostate cancer metastasis with advanced imaging techniques (LOCATE trial): a prospective cohort, observational diagnostic accuracy trial investigating whole-body magnetic resonance imaging in radio-recurrent prostate cancer. Adeleke S, Latifoltojar A, Sidhu H, Galazi M, Shah TT, Clemente J, Davda R, Payne HA, Chouhan MD, Lioumi M, Chua S, Freeman A, Rodriguez-Justo M, Coolen A, Vadgama S, Morris S, Cook GJ, Bomanji J, Arya M, Chowdhury S, Wan S, Haroon A, Ng T, Ahmed HU, Punwani S. BMC Med Imaging. 2019 Nov 15;19(1):90. doi: 10.1186/s12880-019-0380-y. PMID: 31730466 **Free PMC article.** Clinical Trial.

6- The FORECAST study - Focal recurrent assessment and salvage treatment for radio recurrent prostate cancer. Kanthabalan A, Shah T, Arya M, Punwani S, Bomanji J, Haroon A,

Illing RO, Latifoltojar A, Freeman A, Jameson C, van der Meulen J, Charman S, Emberton M, Ahmed HU. *Contemp Clin Trials*. 2015 Sep; 44:175-186. doi: 10.1016/j.cct.2015.07.004. Epub 2015 Jul 13. PMID: 26184343.

7- Role of focal salvage ablative therapy in localised radiorecurrent prostate cancer. Kanthabalan A, Arya M, Punwani S, Freeman A, Haroon A, Bomanji J, Emberton M, Ahmed HU. *World J Urol*. 2013 Dec;31(6):1361-8. doi: 10.1007/s00345-013-1100-9. PMID: 24121817.

Abstracts

1-Dual phase ¹⁸F-FDG PET/CT imaging in evaluation of “radio-recurrent” prostate cancer. Athar Haroon, Ahmad Almuhaideb, John Dickson, Hashim Ahmed, Rizwan Syed, Alex Kirkham, Irfan Kayani, Mark Emberton and Jamshed Bomanji. *Journal of Nuclear Medicine* May 2011, 52 (supplement 1) 1901

2-¹⁸F Choline PET/CT for assessing disease recurrence: Correlation with TRUS, MR template-guided prostate mapping biopsies. Athar Haroon, Ahmad Almuhaideb, John Dickson, Mark Emberton, Irfan Kayani, Hashim Ahmed, Alex Freeman, Alex Kirkham, Jamshed Bomanji and Ashley Groves. *Journal of Nuclear Medicine* May 2012, 53 (supplement 1) 1415.

3-Sequential and simultaneous PET/MR, ¹⁸F FDG PET/CT, ¹⁸F Choline and Gallium Octreotate PET/CT appearances of the prostate and peri-prostatic region. Athar Haroon, Khalsa Al-Nabhani, Ming Young Wan, Rizwan Basit, Svetislav Gacinovic, Raymond Endozo, Shonit Punwani, Shane Blanchflower, Jamshed Bomanji and Ashley Groves. *Journal of Nuclear Medicine* May 2012, 53 (supplement 1) 1014.

4-Uptake of ¹¹C Choline, ¹⁸F Methyl Choline and ¹⁸F Ethyl Choline: Physiological distribution, statistical differences, and imaging pearls. A.Haroon, L Zanoni, M Celli, R Zakavi, M Beheshti, W Langsteger, S Fanti, J Bomanji. *BNMS Annual Meeting*, 21-24 April 2013.

5-Incremental value of ¹⁸F Choline PET/CT in detection and characterization of skeletal findings in suspected biochemical relapse: First UK Experience. A.Haroon, J.Afgan, R.Allie, R.Endozo, M.Emberton, J.Bomanji

6-Positron Textural Gradient (PTG) analysis of Prostate Gland in Patients Undergoing ¹⁸F Choline PET/CT: First UK Experience. Athar Haroon, Sally Kamil, Asim Afaq, Yassine Bouchareb, Andreia Santos, Ines Costa, Mark Emberton, Jamshed Bomanji. BNMS 32nd Annual Meeting, 31March-2nd April Brighton Conference Centre.

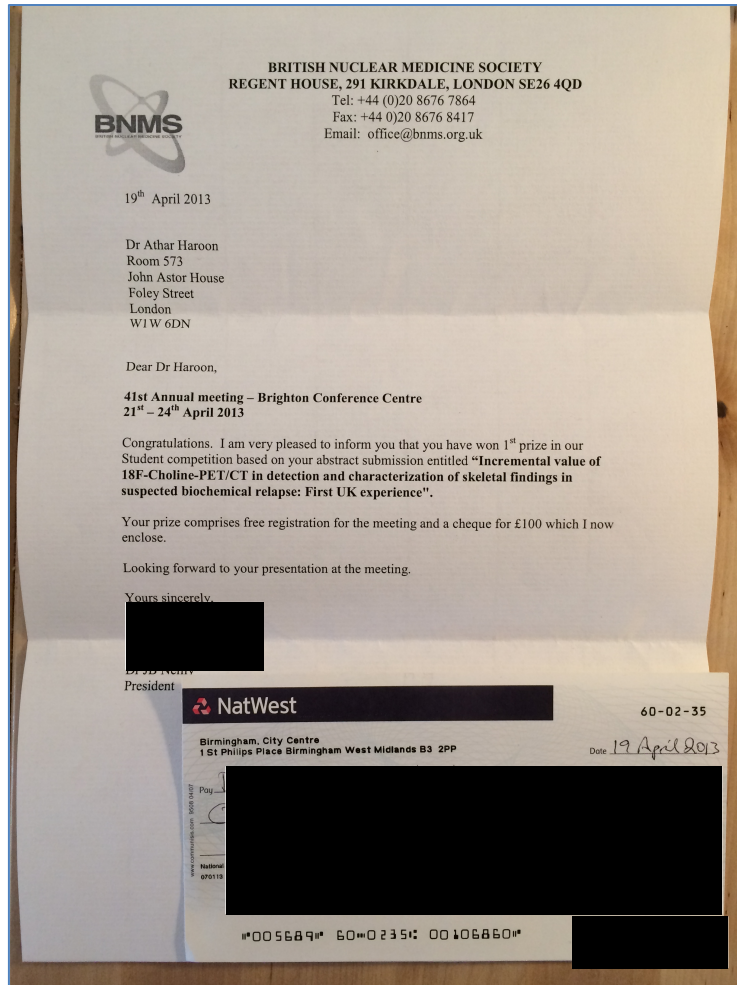
7-Dynamic PET/CT utilising ¹⁸F Fluoro-Ethyl-Choline(FECH) for Prostate Cancer: First UK experience with focus on imaging logistics. A.Haroon, A.Almuhaideb, J.Dickson, M.Emberton, N.Soomro, J.Bomanji

8-Dual Phase ¹⁸F Fluoro-Ethyl-Choline (FECH) PET/CT imaging in evaluation of Radiorecurrent Prostate Cancer. Athar Haroon, Ahmad Almuhaideb, John Dickson, Irfan Kayani, Naeem Soomro, Mark Emberton, Jamshed Bomanji

9-The FORECAST Trial MRI and targeted biopsies compared to Transperineal mapping biopsies for targeted ablation in recurrent prostate cancer after radiotherapy. Taimur Shah, Abi Kanthabalen, Marjorie Otieno, Menelaos Pavlou, Rumana Omar, Sola Adeleke, Francesco Giganti, Chris Brew-Graves, Norman R. Williams, Jack Grierson, Haroon Miah, Amr Emara, Athar Haroon, Arash Latifoltojar, Harbir Sidhu, Joey Clemente, Alex Freeman, Clement Orczyk, Ashok Nikapota, Tim Dudderidge, Richard G. Hindley, Jaspal Virdi, Mani Arya, Heather Payne, Anita Mitra, Jamshed Bomanji, Mathias Winkler, Gail Horan, Caroline Moore, Mark Emberton, Shonit Punwani, Hashim U Ahmed, FORECAST Trial Study Group. 2021 ASCO June 4-8TH 2021 annual meeting.

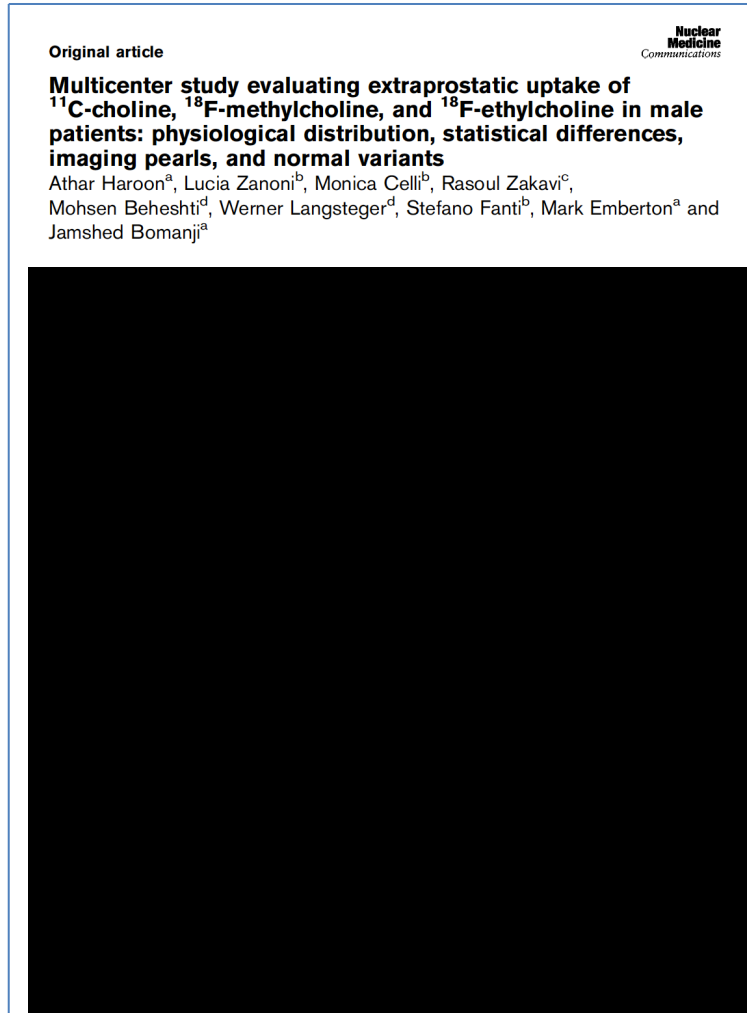
Appendix 2 -Academic output

A) Prizes/Awards: British Nuclear Medicine Society Annual Meeting-1ST Student Research Prize





B) Publications as First Author


- 1) Multicentre study evaluating extra prostatic uptake of ^{11}C -Choline, ^{18}F -Methyl Choline and ^{18}F Ethyl Choline in male patients: Physiological distribution, statistical differences, imaging pearls and normal variants.



Log in or Register Subscribe to journal Get new issue alerts

NMC 

Articles Search  Advanced Search

Articles & Issues Collections For Authors Journal Info History 

Wolters Kluwer


2) ^{18}F -FECH PET/CT to assess clinically significant disease in Prostate Cancer: Correlation with Maximum and Total Cancer Core Length Obtained via MRI-Guided Template Mapping Biopsies


Nuclear Medicine and Molecular Imaging • Original Research


^{18}F -FECH PET/CT to Assess Clinically Significant Disease in Prostate Cancer: Correlation With Maximum and Total Cancer Core Length Obtained via MRI-Guided Template Mapping Biopsies


Athar Haroon^{1,2}
Hashim U. Ahmed³
Paul Cathcart³
Ahmad Almuhaideb¹
Irfan Kayani¹
John Dickson¹
Alex Kirkham⁴
Alex Freeman⁵
Mark Emberton³
Jamshed Bomanji¹

3) Spectrum of metastatic and non-metastatic skeletal findings with dual-phase ^{18}F FECH PET-CT in patients with biochemical relapse of prostate cancer.

Log in or Register Subscribe to journal Get new issue alerts 

NMC 

Articles Search  Advanced Search

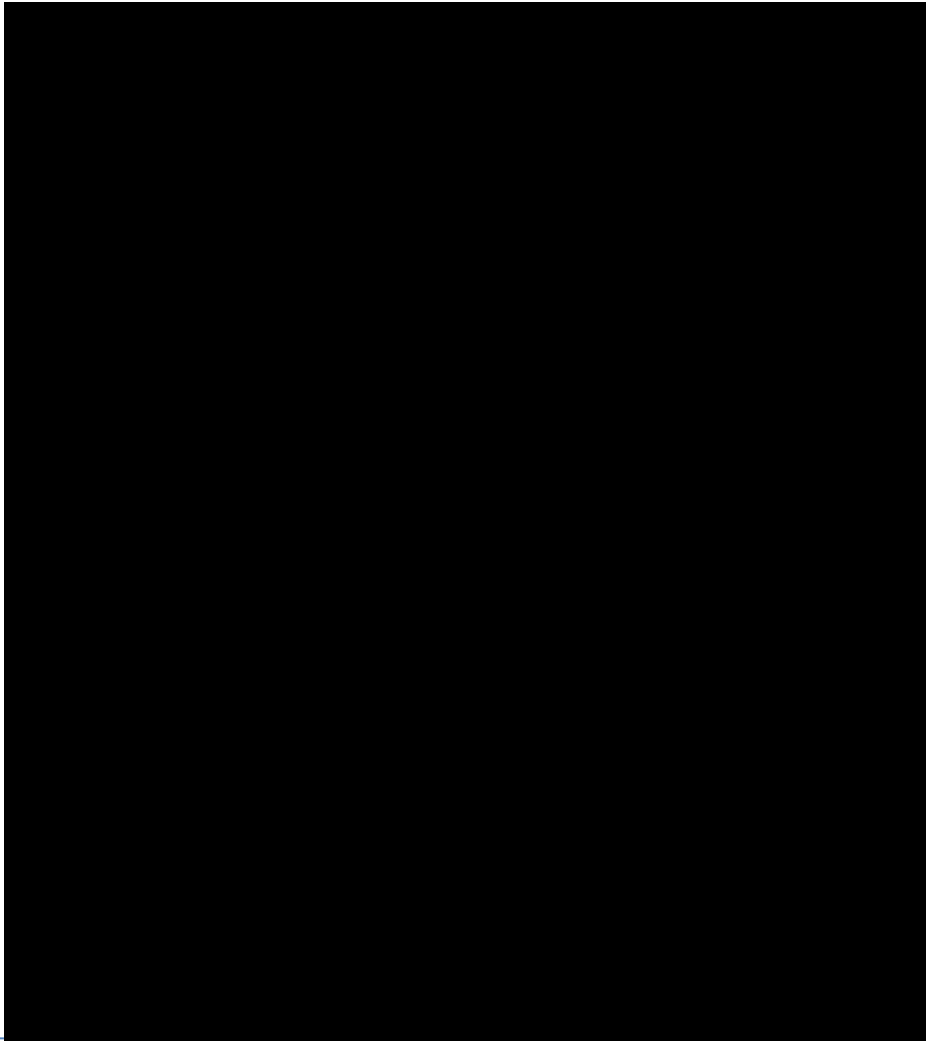
Articles & Issues Collections For Authors Journal Info History 

Original article


**Nuclear
Medicine**
Communications


Spectrum of metastatic and nonmetastatic skeletal findings with dual-phase ^{18}F -FECH PET/CT in patients with biochemical relapse of prostate cancer


Athar Haroon^a, Rizwan Syed^b, Raymond Endozo^b, Rayjanah Allie^b, Alex Freeman^c, Mark Emberton^d and Jamshed Bomanji^b




4) Phenotypic appearances of prostate utilizing PET-MRI and PET-CT with Ga68 PSMA, Radiolabelled Choline and Ga68 DOTATATE

Log in or Register Subscribe to journal Get new issue alerts  Wolters Kluwer

NMC 

Articles Search  Advanced Search

Articles & Issues Collections For Authors Journal Info History 

Review article **Nuclear
Medicine**
Communications

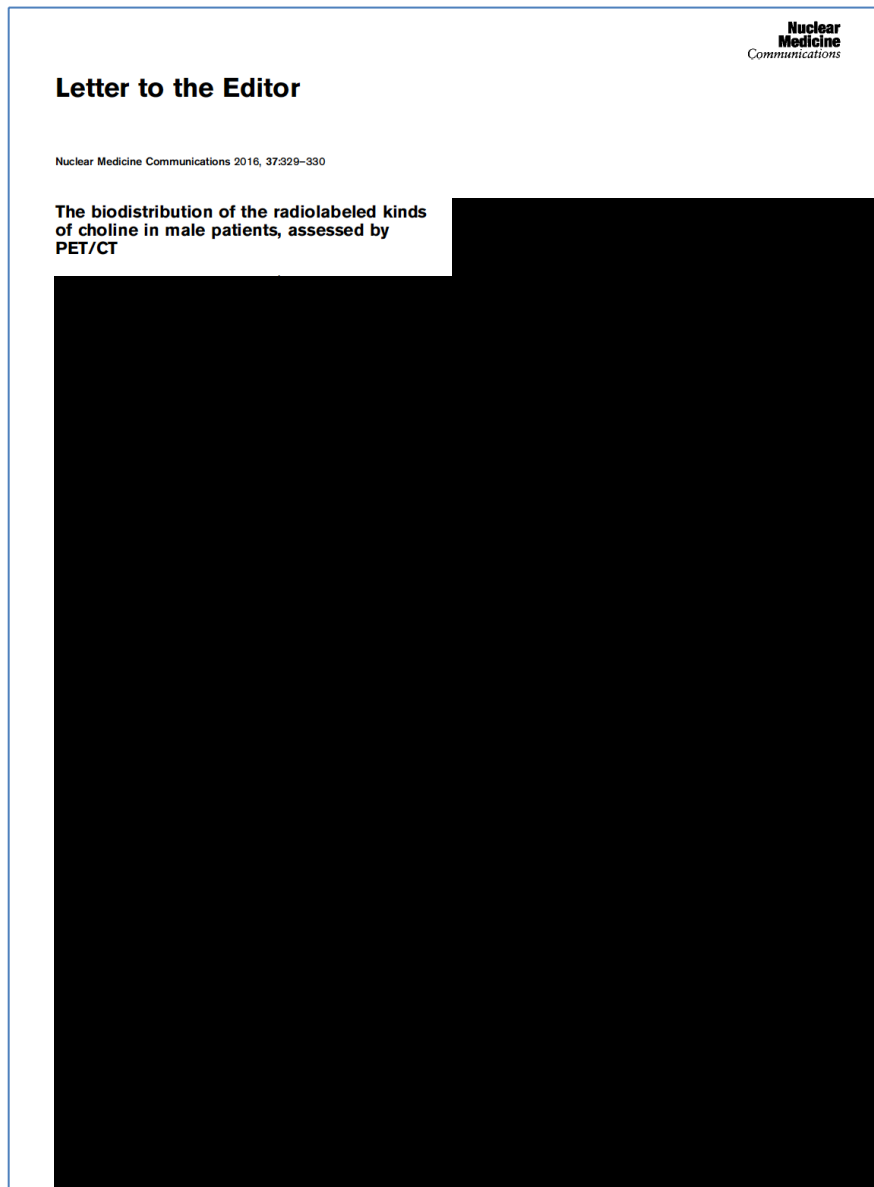
Phenotypic appearances of prostate utilizing PET-MRI and PET-CT with ⁶⁸Ga-PSMA, radiolabelled choline and ⁶⁸Ga-DOTATATE

Athar Haroon^{a,b}, Asim Afaq^b, Soujanya Nuthakki^g, Alex Freeman^c, Lorenzo Biassoni^e, Stefano Fanti^h, Mohsen Beheshtiⁱ, Hikmat Jan^a, Sobhan Vinjamuri^f, Mark Emberton^d and Jamshed Bomanji^b

T
m
d
a
m
P
r
e
v
e
d
d
p
m
c
r
l
d
g
u

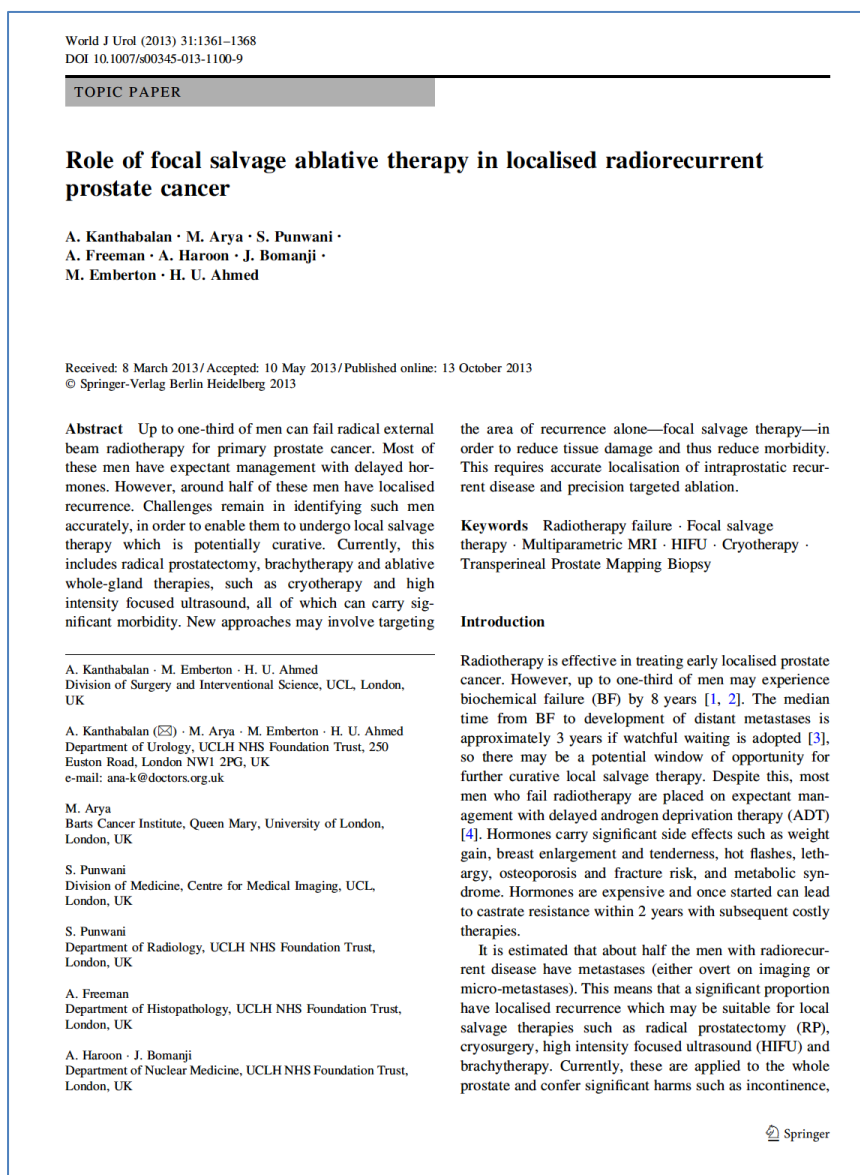
I
P
a
P
u
C
s
d
B
o
P
r
a
P
E
A
M
S
a
o

C) Letter to Editor



D) Publications as Co-Author

1) Role of Focal salvage ablative therapy in localised radio recurrent prostate cancer.




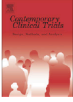
2) The FORECAST study-Focal recurrent assessment and salvage treatment for radiorecurrent prostate cancer.


Contemporary Clinical Trials 44 (2015) 175–186

Contents lists available at ScienceDirect

Contemporary Clinical Trials

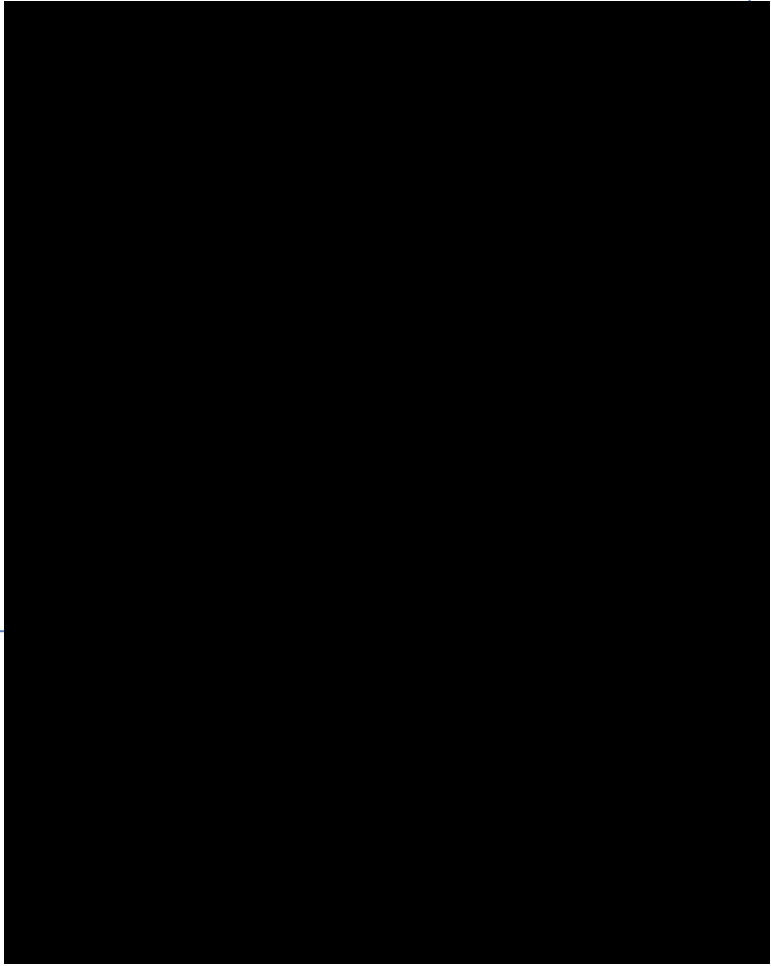
journal homepage: www.elsevier.com/locate/conclintrial

The FORECAST study – Focal recurrent assessment and salvage treatment for radiorecurrent prostate cancer 

A. Kanthabalan^{a,b,*}, T. Shah^a, M. Arya^b, S. Punwani^{c,e}, J. Bomanji^f, A. Haroon^g, R.O. Illing^g, A. Latifoltojar^{b,e}, A. Freeman^d, C. Jameson^d, J. van der Meulen^h, S. Charman^h, M. Emberton^{a,b}, H.U. Ahmed^{a,b}

^a Division of Surgery and Interventional Science, University College London, UK
^b Department of Urology, UCLH NHS Foundation Trust, UK
^c Department of Radiology, UCLH NHS Foundation Trust, UK
^d Department of Pathology, UCLH NHS Foundation Trust, UK
^e Centre for Medical Imaging, Division of Medicine, University College London, UK
^f Institute of Nuclear Medicine, UCLH NHS Foundation Trust, UK
^g Centre for Medical Imaging and Computing, University College London, UK
^h London School of Hygiene and Tropical Medicine, London, UK



E) Abstracts

 **Value Initiative**
SOCIETY OF NUCLEAR MEDICINE & MOLECULAR IMAGING

Donate | Join/Renew | Store | View Cart | Log In

Value Initiative | Physicians | Technologists | Scientists | Residents | Healthcare Provider | Patients

NEWS & PUBLICATIONS | MEMBERSHIP | EDUCATION | MEETINGS & EVENTS | ADVOCACY | EVIDENCE & QUALITY | RESEARCH | ABOUT SNMMI

 **JNM**
The Journal of Nuclear Medicine

Advanced Search

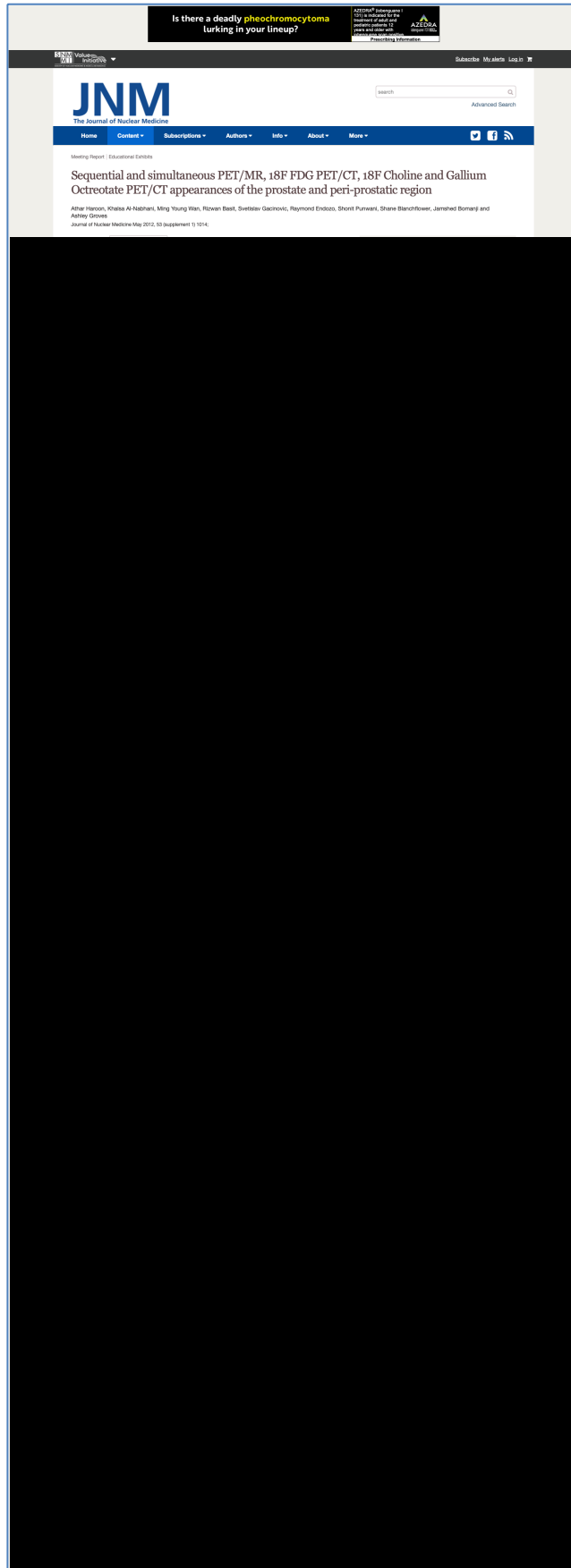
Home | Content | Subscriptions | Authors | Info | About | More

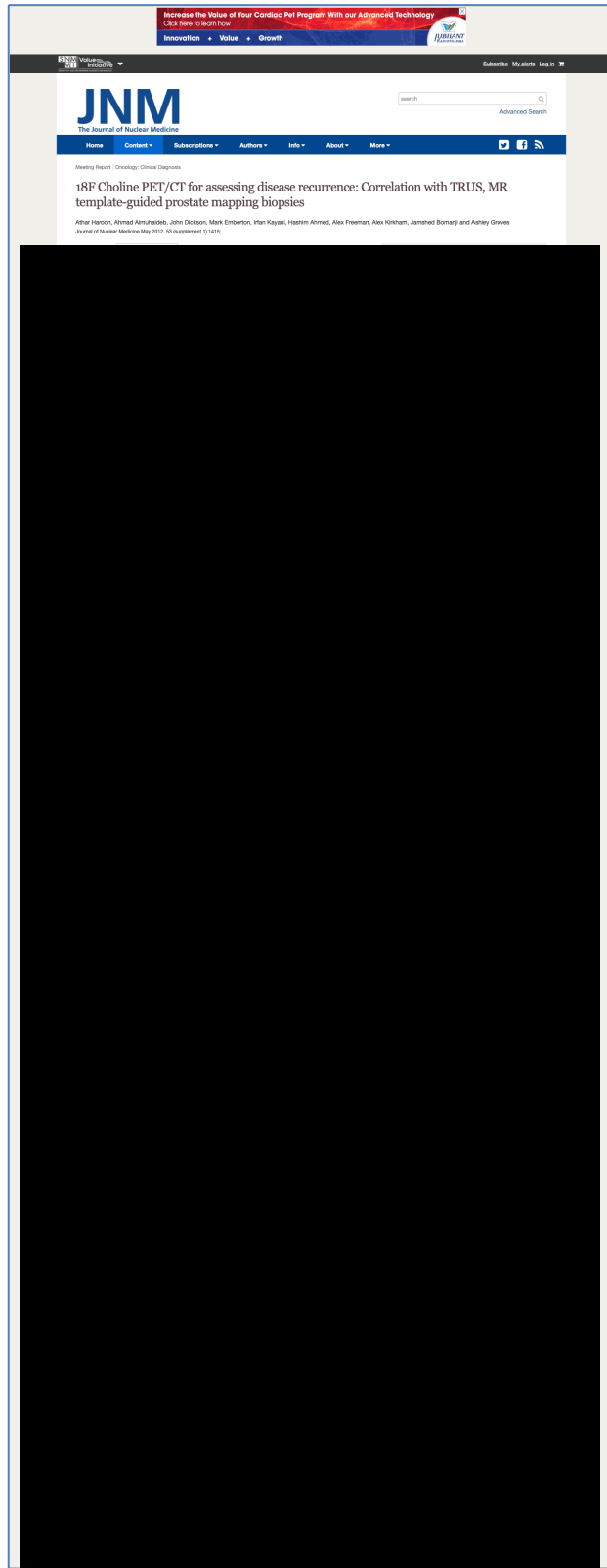
Meeting Report | Oncology: Clinical Diagnosis: Prostate/GU

Dual phase ^{18}F -FDG PET/CT imaging in evaluation of “radio-recurrent” prostate cancer

Athar Haroon, Ahmad Almuhaldeb, John Dickson, Hashim Ahmed, Rizwan Syed, Alex Kirkham, Irfan Kayani, Mark Emberton and Jamshed Bomanji
Journal of Nuclear Medicine May 2011, 52 (supplement 1) 1901;










BRITISH NUCLEAR MEDICINE SOCIETY
ANNUAL MEETING

21 - 24 APRIL 2013

Brighton Conference Centre

www.bnms.org.uk

A maximum of 15 CME/CPD credits
have been awarded to the meeting







16.30 41 Uptake of ^{11}C Choline, ^{18}F Methyl Choline and ^{18}F Ethyl Choline: Physiological distribution, statistical differences and imaging pearls.

A Haroon¹, L Zanoni², M Celli², R Zakavi³, M Beheshti⁴, W Langsteger⁴, S Fanti², J Bomanji¹
¹University College London Hospital NHS Trust, ²University Hospital Sant'Orsola Malpighi, Bologna, Italy, ³Mashad University of Medical Sciences Iran, ⁴St. Vincent 's Hospital, Austria



32ND Annual Meeting
BRITISH NUCLEAR MEDICINE SOCIETY
31st March - 2nd April 2004
BRIGHTON CONFERENCE CENTRE



www.bnms.org.uk

MAXIMUM 14 CPD/CME CREDITS

PROGRAMME

9 Incremental value of ¹⁸F-Choline-PET/CT in detection and characterization of skeletal findings in suspected biochemical relapse: First UK experience

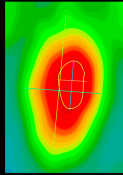
A. Haroon, J. Afgan, R. Allie, R. Endozo, M. Emberton and J. Bomanji

University College London Hospital NHS Trust, UK

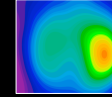
Objective: To evaluate role of ¹⁸F-fluoroethylcholine (FECH) PET/CT in detecting skeletal findings in patients with relapsed prostate cancer.

Methods: A total of 300, ¹⁸F Ethyl Choline PET/CT scans were prospective evaluated for skeletal findings in suspected prostate cancer relapse. Patient age ranged from 50–90 years (median 71 years) and PSA values ranged from 0.04–372 (Roche Modular method). Low dose CT component of PET in combination with conventional imaging (CT & MRI, X-rays) and

Positron Textural Gradient (PTG) analysis of Prostate Gland in Patients Undergoing ¹⁸F-Choline PET/CT: First UK Experience



Athar Haroon¹, Sally Kamil², Asim Afaq³, Yassine Bouchareb¹, Andreia Santos¹, Ines Costa¹, Mark Emberton³, Jamshed Bomanji³



¹Barts Health NHS Trust, London, United Kingdom,

²The University of Jordan, Faculty of Medicine, Amman, Jordan,

³University College London Hospital NHS Trust, London, United Kingdom

Background

- There were around 46,700 new cases of prostate cancer in the UK in 2014, that's 130 cases diagnosed every day.
- Prostate cancer is the second most common cancer in the UK (2014).
- Prostate cancer accounts for 13% of all new cases in the UK (2014).
- In males in the UK, prostate cancer is the most common cancer, with around 46,700 cases diagnosed in 2014.
- More than half (54%) of prostate cancer cases in the UK each year are diagnosed in males aged 70 and over (2012-2014).
- Incidence rates for prostate cancer in the UK are highest in males aged 90+ (2012-2014).
- Since the early 1990s, prostate cancer incidence rates in males have increased by more than two-fifths (44%) in the UK; this is linked with PSA testing¹.

Objective:

- Feasibility of translating metabolic information into PTG.
- Demonstrate zonal gradients spectrum with PTG
- Compare PTG with visual detection
- Evaluate unifocal and multifocal nature of disease with PTG

Material and methods:

This retrospective analysis consisted of 20 patients who had ¹⁸F-Choline PET-CT examination to investigate biochemical relapse of prostate cancer. 300-380 MBq of ¹⁸F-Choline intravenously, low dose CT and PET (whole body 60min and 90min pelvic images) were acquired. Choline expression was translated into positron texture gradient with inverse log 20 scale. The depth of PTG gradient was assessed in millimetres.

Results:

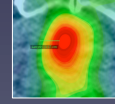
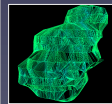
A total of 309 zonal gradients were evaluated in 29 PET/CT exams (age range 55-83 (av 66 yrs), PSA range 0.11-250. 11 patients had single exam and 9 patients had 2 exams. On visual assessment Choline avid disease was identified in 22/29 scans while with PTG analysis Choline expression was seen in 28/29 scans; unifocal in 7 and multifocal in 21. The range of depth of PTG was 4-23 mm. Difference in PTG depth was measured in 9 cases who had follow up PET. Complete response was seen in 2, <30% change in gradient depth (stable gradient) in two, >30% change in gradient depth (partial response) in five cases.

Conclusion:

This study shows that positron textural analysis gradient is feasible in prostate cancer and identifies 19 zonal gradients. PTG is superior than visual assessment in identification of Choline avid disease and can demonstrate unifocal and multifocal nature of disease. This technique has the potential to assess treatment response.

References:

- 1- Cancer Research UK; Prostate Cancer Statistics; Prostate Cancer Incidence; www.cancerresearchuk.org



3D volumetric reconstruction using segmentation, Inverse Log 20 and reconstruction filter using power crust with wireframe of ¹⁸F Choline avid prostate cancer.

“Dynamic PET/CT” utilising 18F-Flouro-Ethyl-choline (FECH) for Prostate Cancer: First UK experience with focus on imaging logistics

A. Haroon¹, A. Almuhaideb¹, J. Dickson¹, M. Emberton¹, N. Soomro², J. Bomanji¹; ¹University College Hospitals London, London, UNITED KINGDOM, ²Freeman Hospital, The Newcastle Upon Tyne Hospitals, Newcastle Upon Tyne, UNITED KINGDOM.

Objectives:In this study, we prospectively evaluated the role of “Dynamic 18F-FECH PET/CT” for the assessment of disease recurrence in patients with biopsy proven prostate cancer.**Methods:** We performed a feasibility study to evaluate the best possible protocol for imaging radio-recurrent prostate cancer using 18F-FECH PET/CT. We prospectively acquired dynamic PET/CT studies in 25 patients (for first 20 minutes), 60 minutes whole body scan and 90 minutes single section pelvic views. 370MBq 18F- FECH was injected intravenously. Tracer uptake in the prostate was measured and expressed as maximum standardized uptake value (SUV max). The 18F- FECH PET/CT study was classified as positive or negative based on the presence or absence of evident disease. The abnormal areas were further evaluated with either ultrasound guided core biopsy or MRI template guided biopsy.**Results:**The dynamic data set (20 minutes) was further subdivided into 3 sub-sections i-e 2-5 minutes, 5-10 minutes and 10-15 minutes. Anatomical delineation of the prostatic lobes was done using CT component of the study. Dynamic data was acquired on PET only images after manually drawing across the areas of abnormal tracer uptake. Time activity curves were plotted utilising Xeleris software (GE Healthcare). For the sub sections of dynamic study, the activity curves were also plotted over the abnormal location.The age range was 48-81 years. The prostate specific antigen (PSA) range was 0.12-45 (Unit: ug/L; normal range 0.00-4.00; Roche Modular method). We observed that in patients with disease, time activity curves consisted of initial rapid rise with increased activity which persisted in the 60 minutes and 90 minutes scans. The normal prostatic tissue showed initial rise with a quick washout. The lesions were better localised on the 60 minute images with a trend to form a focus or diffuse areas of increased tracer

uptake.**Conclusions:** The dynamic FECH PET/CT time activity curves for benign and malignant areas differ, the lesions are better localised on 60 minutes and 90 minutes images. We do not encourage the use of dynamic PET/CT as part of routine practice.

Dual phase 18F-Flouro-Ethyl-Choline (FECH) PET/CT imaging in evaluation of radiorecurrent Prostate cancer



Athar Haroon, Ahmad Almuhaideb, John Dickson, Irfan Kayani,
Naeem Soomro*, Mark Emberton, Jamshed Bomanji

Institute of Nuclear Medicine, University College London Hospitals NHS Trust
*Freeman Hospital, Newcastle Upon Tyne Hospitals NHS Foundation Trust, UK



OBJECTIVES:

In this study, we prospectively evaluated the role of dual phase 18F -PET/CT for the assessment of disease recurrence in patients with biopsy proven prostate cancer who had received different treatments for prostate cancer.

METHODS:

A total of 56 patients with radio-recurrent prostate cancer and biochemical and clinical suspicion of radio-recurrent disease underwent dual phase 18F- FECH PET/CT. 370MBq 18F- FECH was injected IV and whole body images were acquired at 60 minutes and limited (1 bed position) pelvic view at 90 min post-injection. Tracer uptake in the prostate was measured and expressed as maximum standardized uptake value (SUV max) on initial and delayed image data sets. The pattern of uptake on 18F- FECH PET/CT study was further classified as focal or diffuse in both lobes of the prostate.

RESULTS:

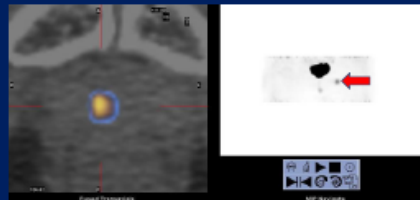
The age range was 52-88 years. The prostate specific antigen (PSA) range was 0.12-45 (Unit: ug/L; normal range 0.00-4.00; Roche Modular method). Out of 56 patients, the pattern of uptake in the right lobe on 60 minutes scan was diffuse in 17, focal in 21 and normal background uptake in 18 patients. On the left side, diffuse uptake was seen in 24, focal in 14 and normal background uptake in 18 patients. On 90 minutes images, the pattern of uptake in the right lobe was diffuse in 18, focal in 24 and 14 showed normal background uptake. On the left side diffuse uptake was seen in 25, focal in 15 and normal background uptake in 16 patients. The results of the 18F- FECH PET CT data were correlated with ultrasound guided core biopsies and state of the art MRI template guided biopsies. The cumulative specificity and sensitivity were 66% and 84% respectively.

CONCLUSIONS:

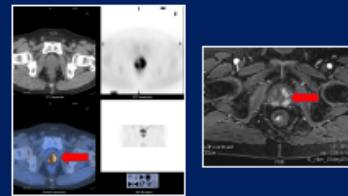
Both 60 and 90 min imaging with 18F-Flouro-ethyl-choline PET/CT scan facilitates lesion localisation in radio-recurrent prostate cancer and improves the diagnostic confidence of physicians for further therapeutic interventions



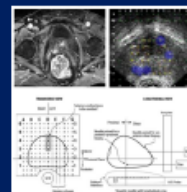
18F Choline PET CT -MIP image showing sites of normal biodistribution
Note: abnormal uptake in both lobes of the prostate (arrow)



18F Choline PET CT fused image showing focal uptake in the Prostate . There is tracer uptake in the left inguinal node (arrow) which was confirmed as metastases



18F Choline PET CT and Dynamic contrast enhanced MRI showing diffuse abnormal uptake and enhancement in the left lobe of the prostate with focal extension to the right lobe



MR TEMPLATE AND TRANS-RECTAL ULTRASOUND GUIDED BIOPSY EQUIPMENT




The FORECAST Trial

MRI and targeted biopsies compared to transperineal mapping biopsies for targeted ablation in recurrent prostate cancer after radiotherapy

Taimur T. Shah, Abi Kanthabalan, Marjorie Otieno, Menelaos Pavlou, Rumana Omar, Sola Adeleke, Francesco Giganti, Chris Brew-Graves, Norman R. Williams, Jack Grierson, Haroon Miah, Amr Emara, Athar Haroon, Arash Latifoltojar, Harbir Sidhu, Joey Clemente, Alex Freeman, Clement Orczyk, Ashok Nikapota, Tim Dudderidge, Richard G. Hindley, Jaspal Virdi, Mani Arya, Heather Payne, Anita Mitra, Jamshed Bomanji, Mathias Winkler, Gail Horan, Caroline Moore, Mark Emberton, Shonit Punwani, Hashim U. Ahmed, FORECAST Trial Study Group...

181 patients
Biochemical or clinical suspicion of recurrent cancer after previous radiotherapy



Prostate mpMRI
Choline PET-CT
Bone Scan

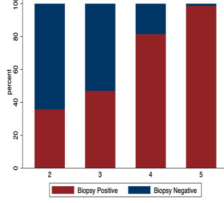
+

Transperineal Mapping Biopsy & Targeted Biopsy

Accuracy of MRI-targeted biopsy

Sensitivity 92% (95%CI 83-97%)
Specificity 75% (95%CI 45-92%)
PPV 94% (95%CI 86-98%)
NPV 65% (95%CI 38-86%)

Detection with Likert score on mpMRI



Performance of mpMRI-Targeted Biopsies

- 4/72 (6%) cancers were missed on systematic biopsies alone
- 6/72 (8%) were missed on MRI-targeted biopsies alone

N = 13 (7%)
Nodal Disease
N=38 (21%)
Metastases

N = 20
Nodes or Metastases Systemic Therapy AND Salvage Focal Ablation

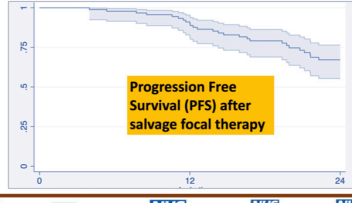
N = 128 (71%)
Localised Disease

Salvage Focal Ablation N= 93
Cryotherapy (Anterior)
HIFU (Posterior)

N = 73
Localised Disease
Salvage Focal Ablation

Salvage Focal Ablation (N=93)

- Urinary continence preserved in 78/93 (84%)
- 5/93 (5%) CTCAE grade 3+ adverse events
- No rectal injuries
- No cancer-related mortality over 2 years



ASCO 2021 ANNUAL MEETING

FORECAST evaluated the whole diagnostic & treatment pathway in recurrent cancer after previous prostate radiotherapy, linking diagnostics, staging and therapy

Prostate mpMRI and Targeted biopsies accurately detect and localise recurrent cancer after previous radiotherapy

Salvage Focal Ablation has low levels of adverse events, preserves continence in over 8 in 10 patients and confers good cancer control in patients with both localised and metastatic cancer

UCL Imperial College London

NHS Imperial College Healthcare

University College London Hospitals NHS Trust

The Queen Elizabeth Hospital King's Lynn

University Hospital Southampton

Hampshire Hospitals NHS Foundation Trust

The Princess Alexandra Hospital

Brighton and Sussex University Hospitals NHS Trust

Funded by Pelican Cancer Foundation, National Institute of Health and Research and the Medical Research Council [UK], ClinicalTrials.gov, NCT01883128; UK ethics committee approval, reference, 13/LO/1401

F) Book Chapters

PET-Clinics

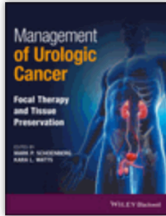
Fluorocholine PET/ Computed Tomography Physiologic Uptake, Benign Findings, and Pitfalls

Mohsen Beheshti, MD, FEBNM^{a,*}, Athar Haroon, MD^b,
Jamshed B. Bomanji, MD, MBBS, PhD, FRCR, FRCP^b,
Werner Langsteger, MD^a



PET Clin ■ (2014) ■-■
<http://dx.doi.org/10.1016/j.cpet.2014.03.001>
1556-8598/14/\$ – see front matter © 2014 Elsevier Inc. All rights reserved.

pet.th



Management of Urologic Cancer: Focal Therapy and Tissue Preservation

Editor(s):
Mark P. Schoenberg Kara L. Watts

First published: 9 June 2017

Print ISBN: 9781118864623 | Online ISBN: 9781118868126 | DOI: 10.1002/9781118868126

© 2017 John Wiley & Sons Ltd.

5

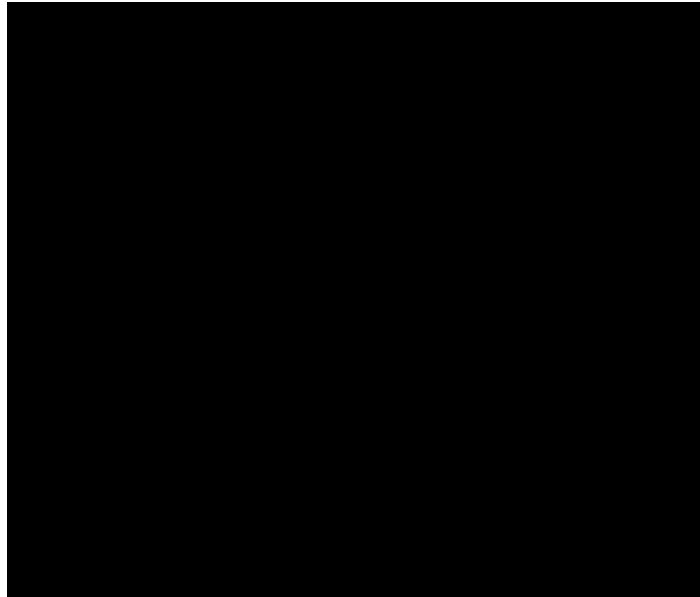
MRI and Metabolic Imaging

Louise Dickinson, MRCS, PhD,¹ Francesco Fraioli, MD, FRCR,²
Athar Haroon, MBBS, FRCR,³ and Clare Allen, MBBS, FRCR¹

¹Department of Radiology, University College Hospital, London, UK

²Institute of Nuclear Medicine, University College Hospital, London, UK

³Department of Radiology, St Bartholomew's Hospital, London, UK

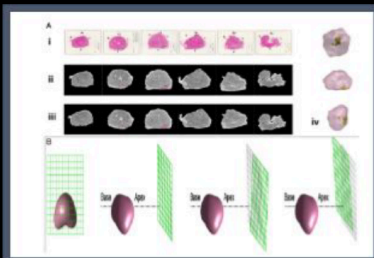


Management of Urologic Cancer: Focal Therapy and Tissue Preservation, First Edition.
Edited by Mark P. Schoenberg and Kara L. Watts.
© 2017 John Wiley & Sons Ltd. Published 2017 by John Wiley & Sons Ltd.

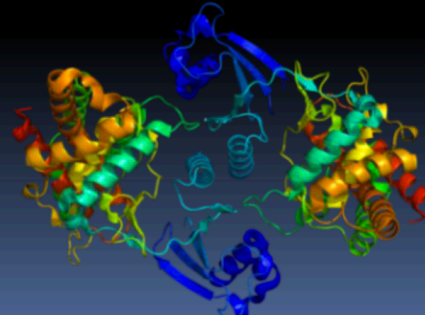
G) Lectures on Prostate Cancer (Local , regional, national, and international)

NCRI PET-CT Study Day

^{18}F -Choline imaging in Prostate Cancer



Athar Haroon FRCR
Institute of Nuclear Medicine
University College London Hospitals NHS Trust
London, UK



12.10 **PET/CT/MRI in Prostate Cancer**

Dr Athar Haroon, Institute of Nuclear Medicine, UCLH



Multi-parametric imaging of prostate cancer - can it facilitate a paradigm shift in management?

28 February 2014

Venue: The British Dental Association

5 CPD credits

The course covers the use of multi-parametric imaging methods for the local and metastatic staging of prostate cancer, how these contribute to the clinical localisation of disease and the merits of each method. It will demonstrate how multi-parametric imaging can be inserted into the cancer management pathway and how it may facilitate an improvement in patient care. There will be illustration of cases by expert radiologists. The clinical relevance to patient management will be provided by prostate urologist and oncologists. A scientific session will highlight the most recent advances in prostate imaging.

Programme

- 08:00 **Poster display and set up**
- 09:00 **Registration and refreshments**
- 09:30 **Introduction - what is multi-parametric imaging?**
Dr Shonit Punwani, Senior Lecturer and Honorary Consultant Radiologist, University College London Hospital
- 09:45 **Session: Managing patients with prostate cancer - what's our problem?**
- 09:45 **Multi-parametric prostate MRI - can it improve patient care?**
Mrs Caroline Moore, Senior Clinical Researcher, Division of Surgical and Interventional Sciences, UCL and Honorary Consultant Urologist, University College London Hospital
- 10:15 **What happens to patients with metastatic disease?**
Dr Heather Payne, Consultant Clinical Oncologist, University College London Hospital
- 10:45 **Refreshments and poster session**
- 11:30 **Session: Multi-parametric imaging - where are we at?**
- 11:30 **Multi-parametric prostate MRI basics**
Dr Alex Kirkham, Consultant Uro-radiologist, University College London Hospital
- 12:00 **Icing on the cake - histologically validated examples**
Dr Clare Allen, Consultant Uro-radiologist, University College London Hospital
- 12:30 **Problems with detecting metastatic disease - does nuclear medicine have the answer?**
Dr Athar Haroon, Consultant Nuclear Medicine Physician and Radiologist, St Bartholomew's Hospital/University College London
- 13:00 **Whole body MRI for metastatic prostate cancer**
Professor Anwarud Din, Consultant Radiologist and Professor of Cancer Imaging, Mount Allison University
- 13:30 **Lunch and poster session**
- 13:30 **Session: Scientific session - where are we going?**
- 14:30 **Scientific session - 9 x 10 minute presentations selected from abstract submissions (10 x 10 minute presentation with 3 minutes of questions)**
Moderators: Dr Alex Kirkham and Dr Shonit Punwani
- 16:10 **Investigator award and closing remarks**
Dr Shonit Punwani, Senior Lecturer and Honorary Consultant Radiologist, University College London Hospital
- 16:20 **Close of meeting**

REGISTRATION FEES:

Non-member £195 BIR Consultant member £125
BIR Non-consultant member £95
BIR Retired/Trainee/Student member £50

Join the BIR today to benefit from reduced delegate rates for our events, membership information can be found online at:
<http://www.bir.org.uk/join-us/>

For more information about membership and to register visit
www.bir.org.uk
Registered charity no: 215869

Kindly supported by:



GE imagination at work



Nuada Medical
SPECIALIST IMAGING
Precision imaging for nuanced care
www.nuadamedical.co.uk

PHILIPS
SIEMENS

Bayer HealthCare has provided sponsorship for the cost of the exhibition stand only at this meeting.



BIR
The British Institute of Radiology

5
FEBRUARY
2018

APPROVED BY THE
BIR

Platinum Sponsors

BAYER
Bayer have part funded this event

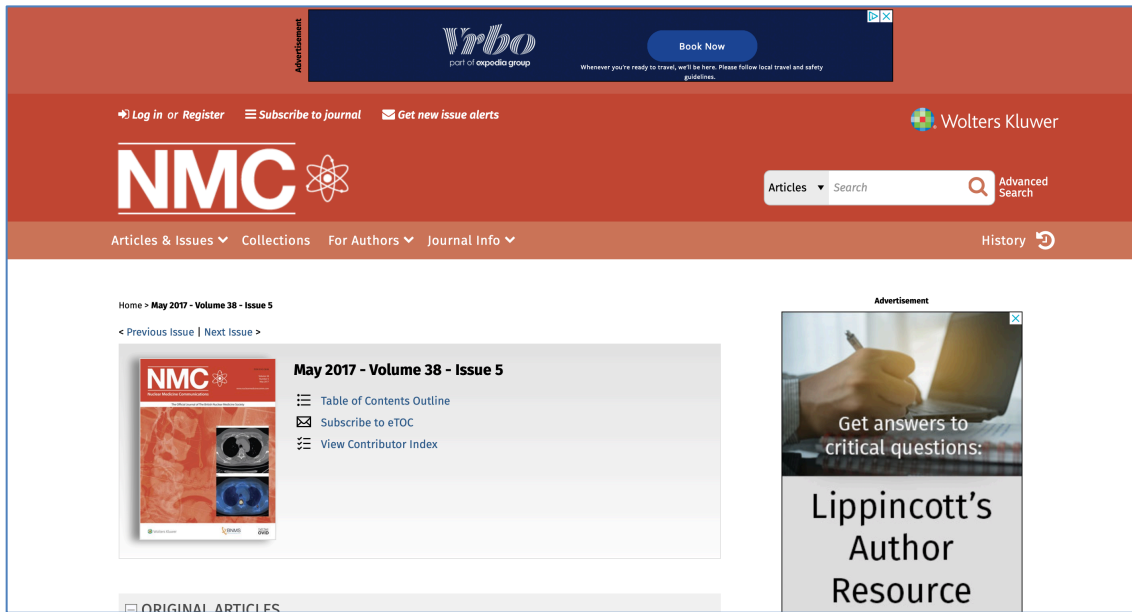
PHILIPS

SIEMENS Healthineers

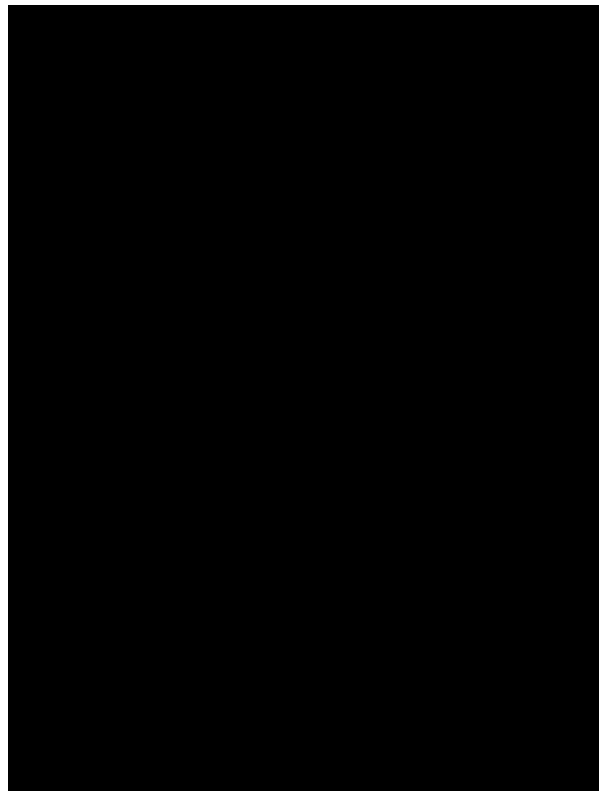
BIR THERANOSTICS SERIES: PROSTATE CANCER
Venue: The Royal Society of Medicine, London
CPD: 7 CREDITS

11:30	18F-NaF PET imaging In Prostate cancer Dr Mohsen Beheshti, Senior Physician, PET/CT Center, St Vincent's Hospital, Linz, Austria	14:30	Bone palliation therapy (alpha emitters) Dr John Buscombe, Consultant in Nuclear Medicine, Cambridge University Hospital
12:00	18F-choline PET imaging in Prostate cancer Professor Gary Cook, Professor of PET Imaging / Honorary Consultant, King's College London / Guy's & St Thomas' Hospitals	15:00	177Lu-PSMA therapy Dr. med. Andrei Todica, Senior Physician, Department of Nuclear Medicine, Ludwig-Maximilians University of Munich
12:30	68Ga-PSMA PET imaging in prostate cancer Prof. Dr. med. Ken Herrmann, Director of the Clinic for Nuclear Medicine, Essen University Hospital, Germany	Session 4- PET/MRI and Case based discussion Chairs: Dr Vineet Prakash and Dr John Buscombe	
13:00	Lunch	15:30	Refreshments
Session 3- Radionuclide therapy Chairs: Dr Shaunak Navalkisoor and Dr Athar Haroon		16:00	Case based interaction Dr Asim Afaq, Consultant Radiologist, University College London Hospital NHS Foundation Trust
14:00	Diagnostic performance and clinical utility of Fluciclovine (18F) in men with biochemically recurrent prostate cancer Prof Fergus Gleeson, Consultant Radiologist and Professor of Radiology, Oxford University Hospitals NHS Foundation Trust	16:30	Case based interaction Dr Athar Haroon, Consultant Radiologist and Nuclear Medicine, Bart's Health NHS Trust
		17:30	Closing Remarks

H) Title cover image



May 2017 Edition of Nuclear Medicine Communications published an image from my work at Institute of Nuclear Medicine University College London Hospital as title image.



APPENDIX 3 -Ethics approval letter



Health Research Authority

Revised on 24 March 2014

NRES Committee London - City & East

Bristol Research Ethics Committee Centre

Whitefriars Level 3, Block B, Lewins Mead

Bristol

BS1 2N

Telephone: 01173421386

Facsimile: 01173420445

31 October 2013

Mr Hashim Uddin Ahmed

MRC Clinician Scientist and Clinical Lecturer in Urology UCL

Division of Surgery and Interventional Science 67 Riding House Street, London

W1P 7NN

Dear Mr Ahmed

Study title: **An evaluation of a novel imaging based complex diagnostic and therapeutic pathway intervention for men who fail radiotherapy for prostate cancer.**

REC reference: **13/LO/1401**

IRAS project ID: **128104**

Thank you for your letter of 22 Oct 2013, responding to the Committee's request for further information on the above research and submitting revised documentation.

The further information was considered in correspondence by a sub-committee of the REC. A list of the sub-committee members is attached.

Confirmation of ethical opinion

On behalf of the Committee, I am pleased to confirm a favourable ethical opinion for the above research on the basis described in the application form, protocol and supporting documentation as revised, subject to the conditions specified below.

We plan to publish your research summary wording for the above study on the NRES website, together with your contact details, unless you expressly withhold permission to do so.

Publication will be no earlier than three months from the date of this favourable opinion letter. Should you wish to provide a substitute contact point, require further information, or wish to withhold permission to publish, please contact the Co-ordinator Mr Rajat Khullar, nrescommittee.london-cityandeast@nhs.net.

Ethical review of research sites

NHS sites

The favourable opinion applies to all NHS sites taking part in the study, subject to management permission being obtained from the NHS/HSC R&D office prior to the start of the study (see "Conditions of the favourable opinion" below).

Non-NHS sites

Conditions of the favourable opinion

The favourable opinion is subject to the following conditions being met prior to the start of the study.

Management permission or approval must be obtained from each host organisation prior to the start of the study at the site concerned.

Management permission ("R&D approval") should be sought from all NHS organisations involved in the study in accordance with NHS research governance arrangements.

Guidance on applying for NHS permission for research is available in the Integrated Research Application System or at <http://www.rdforum.nhs.uk>.

Where an NHS organisation's role in the study is limited to identifying and referring potential participants to research sites ("participant identification centre"), guidance should be sought from the R&D office on the information it requires to give permission for this activity.

For non-NHS sites, site management permission should be obtained in accordance with the procedures of the relevant host organisation.

Sponsors are not required to notify the Committee of approvals from host organisations

Registration of Clinical Trials

All clinical trials (defined as the first four categories on the IRAS filter page) must be registered on a publicly accessible database within 6 weeks of recruitment of the first participant (for medical device studies, within the timeline determined by the current registration and publication trees).

There is no requirement to separately notify the REC, but you should do so at the earliest opportunity e.g., when submitting an amendment. We will audit the registration details as part of the annual progress reporting process.

To ensure transparency in research, we strongly recommend that all research is registered but for non-clinical trials this is not currently mandatory.

If a sponsor wishes to contest the need for registration, they should contact Catherine Blewett (catherineblewett@nhs.net), the HRA does not, however, expect exceptions to be made.

Guidance on where to register is provided within IRAS.

It is the responsibility of the sponsor to ensure that all the conditions are complied with before the start of the study or its initiation at a particular site (as applicable).

Approved documents

The final list of documents reviewed and approved by the Committee is as follows:

<i>Document</i>	<i>Version</i>	<i>Date</i>
Covering Letter		21 September 2013
GP/Consultant Information Sheets	1	21 March 2013
Investigator CV		06 April 2013
Other: Letter from funder: National Institute Health and Pelican Cancer Foundation		15 August 2013
Other: Peer Review - Anon for Ahmed		01 April 2013
Participant Consent Form: Participant Consent Form	1.2	22 October 2013
Participant Information Sheet: Participant Information Sheet	1.4	04 October 2013
Protocol	1.3	22 October 2013
Questionnaire: FORECAST IIEF IPSS and EPIC		
REC application	1	20 August 2013
Response to Request for Further Information		

Statement of compliance

The Committee is constituted in accordance with the Governance Arrangements for Research Ethics Committees and complies fully with the Standard Operating Procedures for Research Ethics Committees in the UK.

After ethical review

Reporting requirements

The attached document "*After ethical review – guidance for researchers*" gives detailed guidance on reporting requirements for studies with a favourable opinion, including:

- Notifying substantial amendments
- Adding new sites and investigators
- Notification of serious breaches of the protocol
- Progress and safety reports
- Notifying the end of the study

The NRES website also provides guidance on these topics, which is updated in the light of changes in reporting requirements or procedures.

Feedback

You are invited to give your view of the service that you have received from the National Research Ethics Service and the application procedure. If you wish to make your views known, please use the feedback form available on the website.

Further information is available at National Research Ethics Service website > After Review

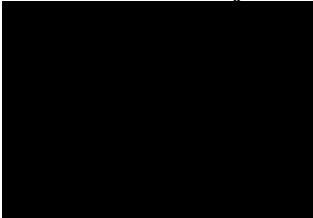
13/LO/1401

Please quote this number on all correspondence

We are pleased to welcome researchers and R & D staff at our NRES committee members' training days – see details at <http://www.hra.nhs.uk/hra-training/>

With the Committee's best wishes for the success of this project.

Yours sincerely



**pp Professor Arthur T.
TuckerChair**

Email: nrescommittee.london-cityandeast@nhs.net

*Enclosures: List of names and professions of members
who were present at the meeting and those who submitted
written comments*

*“After ethical review – guidance
for researchers”*

Copy to: Mr Stuart Braverman, Joint Research Office

**NRES Committee London - City & East Attendance at Sub-Committee of the
REC meeting in correspondence**

APPENDIX 4- Clinical Trial Performa

FORECAST PET-CT Reporting Performa

FORECAST
PET Imaging Report

Please send completed forms to

Dr Abi Kanthabalan

Division of Surgery and Interventional Science, University College London

250 Euston Road London, NW1 2PG





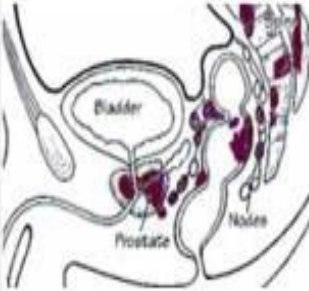
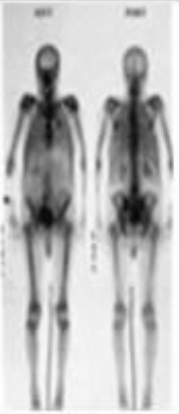
T: 0207 679 9092 F: 0203 447 9303

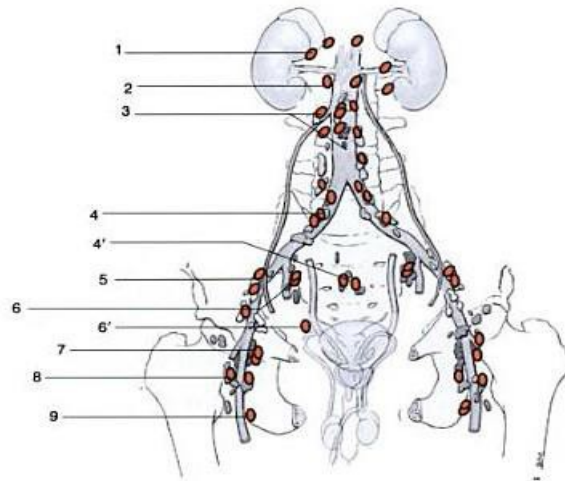
E: abi.kanthabalan@ucl.ac.uk

Additional instructions for completing forms

PET imaging guidance (To be completed by the Trial Nuclear Medicine Physician)

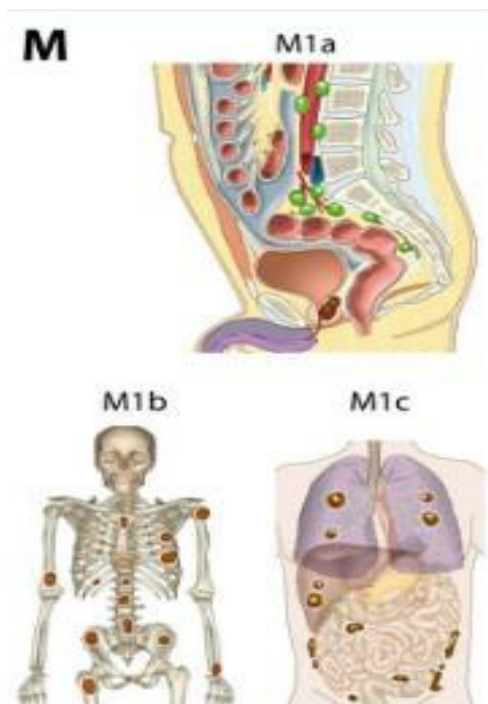
See table below for definitions of T, N and M staging

<p>T1</p>  <p>T1 Clinically inapparent; tumor not palpable or visible by imaging</p> <p>T1a Incidental finding during transurethral resection of prostate; < 5% of tissue resected</p> <p>T1b Incidental finding during transurethral resection of prostate; > 5% of tissue resected</p> <p>T1c Tumor identified by needle biopsy (e.g. because of elevated PSA)</p>	<p>T2</p>  <p>T2 Tumor confined within prostate (palpable or visible on TRUS)</p> <p>T2a Involves half of a lobe or less</p> <p>T2b Involves more than half of a lobe one lobe but not both lobes</p> <p>T2c Tumor involves both lobes</p>	<p>T3</p>  <p>T3 Tumor extends through prostatic capsule, bladder neck or seminal vesicle</p> <p>T3a Unilateral extracapsular extension</p> <p>T3b Bilateral extracapsular extension</p> <p>T3c Tumor invades seminal vesicle(s)</p>	<p>T4</p>  <p>T4 The tumor has spread or attached to tissues next to the prostate (other than the seminal vesicles)</p> <p>T4a The tumor has spread to the neck of the bladder, the external sphincter (muscles that help control urination), or the rectum</p> <p>T4b The tumor has spread to the floor and/or the wall of the pelvis.</p>
<p>N0-3</p> 	<p>M0-1</p> 	<p>N0 Cancer has not spread to any lymph nodes.</p> <p>N1 Cancer has spread to a single regional lymph node (inside the pelvis) and is not larger than 2 centimeters</p> <p>N2 Cancer has spread to one or more regional lymph nodes and is larger than 2 centimeters (¾ inch), but not larger than 5 centimeters</p> <p>N3: Cancer has spread to a lymph node and is larger than 5 centimeters</p> <p>M0: The cancer has not metastasized (spread) beyond the regional lymph nodes</p> <p>M1: The cancer has metastasized to distant lymph nodes (outside of the pelvis), bones, or other distant organs such as lungs, liver, or brain</p>	



Note: Regional pelvic lymph nodes

Illustrated above - regional defined as (4') presacral, (5) external iliac, (6') obturator, (6) internal iliac. Other sites are considered as metastatic nodes.



Note: M Staging

Illustrated above — Sub classification of metastatic disease stage. M1a – non-regional nodal involvement; M1b — metastatic bone disease and M1c — another organ involvement

SITE

PET IMAGING

Total time to report _____Minutes

PET imaging quality

Please circle:

Good

Adequate

Poor

LOCAL TUMOR

LOCAL TUMOUR						
LOCATION	APICAL RIGHT	APICAL LEFT	BASAL RIGHT	BASAL LEFT	NOT VISIBLE	
SUVmax						
T stage	T1	T2a T2b T2c	T3a T3b T3c	T4a T4b		Confidence(Circle) 1-Low 2-Adequate 3-Equivocal 4-Good 5-Excellent
N stage	NX	N0	N1	N2	N3	Confidence(Circle) 1-Low 2-Adequate 3-Equivocal 4-Good 5-Excellent

NODAL SITES

Confidence with main classification as negative, equivocal, or positive

NODAL SITES	NEGATIVE	EQUIVOCAL (?REACTIVE/? INFLAMMATORY)	POSITIVE	SIZE	SUVmax
REGIONAL NODES					
External iliac					
Internal Iliac					
Obturator					
Common Iliac					
Presacral					
Aortic					
METASTATIC NODES					
Inguinal					
Common iliac					
Para-aortic					
Other abdominal					
Nodes Above diaphragm to check					
Neck nodes					

M stage

(Soft tissues)

Confidence with main classification as negative, equivocal, or positive

	NEGATIVE	EQUIVOCAL (?REACTIVE/ ? INFLAMMAT ORY)	POSITIVE	L (LYTIC) S (Sclerotic)M (Mixed)	SUVmax
Brain					
Lung (L)					
Lung (R)					
Pleura (L)					
Pleura (R)					
Liver (left lobe)					
Liver (right lobe)					
Spleen					
Adrenal (L)					
Adrenal (R)					
Kidney (L)					
Kidney (R)					
Pancreas					
Mesentery/Peritoneum					
Bowel					
SOFT TISSUES Neck/Chest					
SOFT TISSUES Abdomen/Pelvis SOFT TISSUES Limbs					

OTHER					
-------	--	--	--	--	--

M Stage Continues

Skeletal sites in number 0 <5 >5

(Skeletal sites maximum 5 –mention the one with maximum metabolic activity)

NODAL SITES	NEGATIVE	EQUIVOCAL (?REACTIVE/? INFLAMMATORY)	POSITIVE	SIZE	SUV max
Skull					
Cervical Spine					
Thoracic Spine					
Lumbar Spine					
Pelvis					
Sternum					
Clavicle/Scapula (L)					
Clavicle/Scapula (R)					
Ribs (L)					
Ribs (R)					
Upper Limb (L)					
Upper Limb (R)					
Lower Limb (L)					
Lower Limb (R)					

I certify that I have reported this image without prior knowledge of the MRI

reportSigned

Print Name/Initials

Date

FORECAST-Bone Scan Performa

FORECAST
Bone Scan Report

Please send completed forms to

Dr Abi Kanthabalan

Division of Surgery and Interventional Science, University College London

250 Euston Road London, NW1 2PG

T: 0207 679 9092 F: 0203 447 9303

E: abi.kanthabalan@ucl.ac.uk

Additional instructions for completing forms

Bone Scan (To be completed by the Trial Nuclear Medicine Physician)

External Scan Name of external Site

UCLH Scan



SITE

Bone Scan

Total time to report _____ Minutes

Bone Scan quality

Please circle:

Good

Adequate

Poor

Skeletal sites in number 0 <5 >5

(Skeletal sites maximum 5 –mention the one with maximum metabolic activity)

	NEGATIVE	EQUIVOCAL (?REACTIVE/? INFLAMMATORY)	POSITIVE	SIZE	SUV max
Skull					
Cervical Spine					
Thoracic Spine					
Lumbar Spine					
Pelvis					
Sternum					
Clavicle/Scapula (L)					
Clavicle/Scapula (R)					
Ribs (L)					
Ribs (R)					
Upper Limb (L)					
Upper Limb (R)					
Lower Limb (L)					
Lower Limb (R)					

I certify that I have reported this image without prior knowledge
of the MRI report Signed

Print Name/Initials

Date

APPENDIX 5-Radiopharmacy-Synthesis of ^{18}F Choline

1- Irradiation of the target

High purity H_2^{18}O is purchased and is irradiated with a high energy proton beam (16 MeV) to produce $[\text{}^{18}\text{F}]^-$ fluoride anions in an aqueous medium. The irradiation time and the beam current are set to achieve the required final activity of $[\text{}^{18}\text{F}]\text{FEC}$ at the end of the synthesis (Typically $50\mu\text{A}$ for 60 minutes). Longer or stronger irradiation simply increases the amount of ^{18}F (activity) produced but other products cannot be formed. On completion of the irradiation, the solution is transferred to the synthesis unit. The delivery is performed using Helium gas to flush the target. The synthesis unit, which is in a class C lead shielded Hot Cell, is prepared prior to the delivery of the radioisotope.

2-Separation of the $[\text{}^{18}\text{F}]$ -fluoride from the $[\text{}^{18}\text{O}]$ -water and drying of the fluoride

The irradiated water containing the ^{18}F fluoride produced is passed over an anion exchange resin (Sep-Pack Accell Plus QMA), by way of a vacuum. The anion species (^{18}F fluoride) are trapped on this resin and the $[\text{}^{18}\text{O}]$ enriched water is collected in a vial for reprocessing. ^{18}F -fluoride is eluted by a mixture of Kryptofix, K_2CO_3 (5% of 1M)

and Acetonitrile from the anion-exchange cartridge into the reactor vial. The mixture in the reactor is evaporated to dryness under vacuum and stepwise heating from 60 to 80°C. A volume of 1.0 mL acetonitrile is added to the dry residue which is then heated (90-100°C) under helium flow to remove any residual moisture in the chemical reactor.

3-Addition of Ethylene Glycol Ditosylate (EGDT)

Ethylene Glycol DiTosylate in Acetonitrile is added to the dry residue. The first reaction step is to produce the intermediate product, ^{18}F -fluorethyl tosylate, and it takes place for 4 minutes at 85°C. After evaporation of Acetonitrile, DiMethyl Amino Ethanol is added, and the second reaction step is carried out at 100°C for 5 minutes to form ^{18}F -FEC.

4. Purification

The reactor is then cooled, and the product is diluted in ethanol and passed through a set of SPE cartridges consisting of a tC18 cartridge and 2 cation-exchange (CM) cartridges. The cartridges are washed with ethanol and water to remove ^{18}F -fluoride, Kryptofix and other possible impurities. Finally, the ^{18}F -FEC is eluted by 12ml 0.9% Sodium Chloride solution into the product vial. The synthesis is performed in

a closed system under automatic control. The final product is eluted in sterile isotonic saline. The correct operation of this process depends on both procedural controls (e.g., to ensure reagents are added to the correct vessels at set up) and the control system to execute the steps in the appropriate sequence at the appropriate time.

5. **Dispensing of [¹⁸F]FEC:**

The ¹⁸F-FEC is passed to the dispensing hot cell, by flushing the product vial with Helium gas, where the radioactivity of the [¹⁸F]FEC bulk solution is measured in an ionisation chamber. The ¹⁸F-FEC is diluted with 0.9% Sodium Chloride solution to achieve the required radioactive concentration. The product is dispensed into vials either to a required volume (QC vials) or to a required activity. The dispensing, which is performed in open vials by an automated dispensing system, is based on calculated activity and measured by weight on a balance. The dispenser can dispense 1-34 vials, where a selectable number are used for sampling and testing. After the filling procedures the vials are crimped and delivered to the sterilizer

6. Sterilisation of [¹⁸F]FEC:

The steriliser is integrated with the dispenser as one unit. The movement of vials into and out of the steriliser is carried out by the same automated system. Sterilisation is performed by means of steam with pressure. Following completion of the sterilisation step (heating to achieve a F_0 value of greater than 60 minutes in all vials), the vials are discharged out from the system into lead containers.

APPENDIX 6 -Standard Operating Procedures

18F Choline PET CT

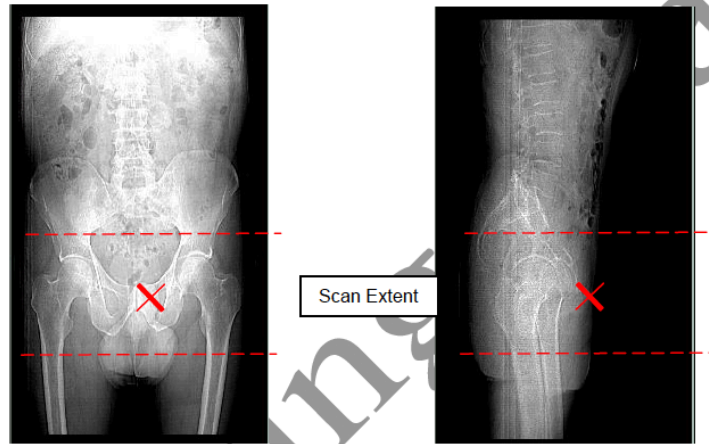
OVERVIEW	
<p>This examination is a part of a feasibility study to assess the usefulness of Fluoro-ethyl choline PET/CT for prostate cancer, together with lymph node involvement and metastatic spread of this cancer. Choline positron emission tomography (PET)/computed tomography (CT) is a currently used diagnostic tool in restaging prostate cancer (PCa) patients with increasing prostate-specific antigen (PSA) after either radical prostatectomy (RP) or external-beam radiation therapy (EBRT).</p> <p>Choline uptake is increased in cancer in relation to tumor-related increases in cellular membrane synthesis and upregulation of choline kinase. The primary tumour and local recurrence show avidity for F-18-choline. True positive uptake in lymph nodes is seen on the whole body or delayed views. False -ve nodes are also observed but usually they are less than 5mm in size. Approximately 24% of bone lesions show FCH uptake and have no morphologic changes on CT and this is due to bone marrow infiltration.</p> <p>It is important to remember that choline uptake in primary and lymph node metastases declines during hormone therapy.</p>	
REQUEST	
Valid reasons for examination:	
Suspected Prostate Cancer and metastases	
Valid referrers:	
See SOP V_2	
Persons who may justify / authorise:	
See SOP P_1	
Booking:	
<ul style="list-style-type: none"> This investigation involves a 20 minute dynamic scan, a whole-body scan at 60 minutes after the injection followed by a further 15 minute (single section) static scan at 90 minutes post injection. 	
PATIENT PREPARATION	
<ul style="list-style-type: none"> As for INM SOP PET_01 	
RADIOPHARMACEUTICAL AND ADMINISTRATION	
Radiopharmaceutical:	18F-Fluoroethylcholine (FECh)
ARSAC Serial No:	tbc
DRL: (Maximum usual activity)	370MBq
ED:	12.95 mSv (DeGrado 2002)
Minimum dose for paediatrics:	N/A
Advice re breastfeeding:	tbc
Persons who may administer:	Departmental List
Route of administration: (IV etc)	IV
Advice after administration:	tbc
INJECTION	
Patient Preparation	
As SoP PET_1. Ask patient to change into a gown, and check for metal objects.	
Administration	

This investigation is a dynamic study which will involve the injection of FECh with the patient on the imaging couch. All other administration details are the same as that given in SoP PET_1 (CHECK)

ACQUISITION TECHNIQUE

Scan Extent

Position centre of field of view over the prostate which is often found posterior to the symphysis pubis.



Scanning Parameters

Dynamic

Landmark	Symphysis Pubis	
CT Acquisition Protocol	8.10 18F FECh DYN PROSTATE PETCT	
CT Acquisition Parameters	Scout 120 kVp, 10 mA CT 140 kVp, 80 mA, 0.8s, Pitch 1.75 (1.375 DVCT) CT Slices 5mm (70cm FoV PETAC), 2.5mm (50cm FoV Std), 2.5mm (50cm FoV Lung)	
PET Acquisition Protocol	FECh_PROSTATE_DYN_3D	
PET Acquisition Parameters	3D, 10 x 1min & 5 x 2min frames (List), Randoms from Singles	
PET Recon Protocols	AC_3D	NAC_2D
PET Recon Parameters	Iterative, 21 (20) Subs, 2 lters Z-axis filter: Heavy Post-Filter: 6 mm Slice Thickness 3.27mm Recon. Diameter 70cm	Iterative, 21 Subs, 2 Iterations Z-axis filter: Heavy Post-Filter: 5.4 mm Slice Thickness 3.27mm Recon. Diameter 70cm

Wholebody

Landmark	Sternal Notch (Default)	
CT Acquisition Protocol	8.11 18F FECH 3D WB PETCT	
CT Acquisition Parameters	Scout 120 kVp, 10 mA CT 140 kVp, 80 mA, 0.8s, Pitch 1.75 (1.375 DVCT) CT Slices 5mm (70cm FoV PETAC), 2.5mm (50cm FoV Std), 2.5mm (50cm FoV Lung)	
PET Acquisition Protocol	FECH_PROSTATE_3D_WB	
PET Acquisition Parameters	3D, 5 Minutes / Bed, 9 slice overlap, Randoms from Singles	
PET Recon Protocols	AC_3D	NAC_3D
PET Recon Parameters	Iterative, 21 (20) Subs, 2 lters Z-axis filter: Heavy Post-Filter: 6 mm Slice Thickness 3.27mm Recon. Diameter 70cm	Iterative, 21 Subs, 2 Iterations Z-axis filter: Heavy Post-Filter: 5.4 mm Slice Thickness 3.27mm Recon. Diameter 70cm

Single Section

Landmark	Symphysis Pubis	
CT Acquisition Protocol	8.12 18F FECH 3D STAT PROSTATE PETCT	
CT Acquisition Parameters	Scout 120 kVp, 10 mA CT 140 kVp, 80 mA, 0.8s, Pitch 1.75 (1.375 DVCT) CT Slices 5mm (70cm FoV PETAC), 2.5mm (50cm FoV Std), 2.5mm (50cm FoV Lung)	
PET Acquisition Protocol	FECH_PROSTATE_3D_STAT	
PET Acquisition Parameters	3D, 15 Minutes / Bed, Randoms from Singles	
PET Recon Protocols	AC_3D	NAC_2D
PET Recon Parameters	Iterative, 21 (20) Subs, 2 lters Z-axis filter: Heavy Post-Filter: 6 mm Slice Thickness 3.27mm Recon. Diameter 70cm	Iterative, 21 Subs, 2 Iterations Z-axis filter: Heavy Post-Filter: 5.4 mm Slice Thickness 3.27mm Recon. Diameter 70cm

Imaging

1. Ask patient to empty their bladder.
2. With the patient on the couch, perform the scout and the CT scan with their arms crossed across their chest. The prostate (shown below) should be positioned in the centre of the field of view.
3. Inject the FECh into the patient in the normal manner, and ask a colleague to start a dynamic scan at the time of injection. **Make sure the patient does not move.**
4. For late scanning at 60 minutes post injection, the venflon can be removed, although the patient should void their bladder and position their arms in the same position as the dynamic study.
5. Use 8.10 18F FECH DYN PROSTATE PETCT for immediate dynamic imaging
6. Use 8.11 18F FECH 3D WB PETCT for wholebody imaging
7. Use 8.12 18F FECH 3D STAT PROSTATE PETCT for late imaging at 90 minutes p.i.

RIS

1. At the end of the procedure the person who performed the image acquisition should

‘Examine’ the patient on RIS. This is necessary to define the IRMER operator for the procedure. The injector of FDG will already have ‘Examined’ the injection part of the study.

NB:

- Bladder should be emptied between wholebody and prostate imaging to acquire optimal prostate images.
- Arms can be placed down, crossed over upper chest for prostate imaging.

ADVICE TO PATIENT ON DISCHARGE

DATA ANALYSIS

Follow the standard whole body FDG protocol INM SOP PET_01

DATA DISPLAY

Follow the standard whole body FDG protocol INM SOP PET_01

REPORTING

Persons who may report:

INM Practitioners

Reporting procedure:

- Standardised criterion will be used for reporting PET CT (see protocol)
- PET CT to be reported by local hospital imaging team

DATA ARCHIVE

- Follow the standard whole body FDG protocol INM SOP PET_01

ADDITIONAL COMMENTS

REVISION HISTORY

Rev No	Date	Author	Changes	Reviewed by
0.1	Mar10	JCD	Proposed Protocol. Draft version, as used for pt#1	
1.0	05 Oct 2010	JB	Reviewed, revised and authorised Overview and referral criteria added	JB

18F Choline PET-MR SOP

<p>Overview</p> <p>The PET MR exam is a combined imaging study where both MR and PET images are acquired over the same area of the patient. This examination is used to assess primary prostate cancer, together with lymph node involvement and metastatic spread of this cancer. Choline positron emission tomography (PET) is a currently used diagnostic tool in restaging prostate cancer (PCa) patients with increasing prostate-specific antigen (PSA) after either radical prostatectomy (RP) or external-beam radiation therapy (EBRT). Choline uptake is increased in cancer in relation to tumour-related increases in cellular membrane synthesis and upregulation of choline kinase. The primary tumour and local recurrence show avidity for F-18-choline. True positive uptake in lymph nodes is seen on the whole body or delayed views. False -ve nodes are also observed but usually they are less than 5mm in size. It is important to remember that choline uptake in primary and lymph node metastases declines during hormone therapy. The PET images provide a functional image of the radiopharmaceutical distribution in the patient, while the MR images provide an image of the anatomy which is used for localizing the radiopharmaceutical uptake and for attenuation correction of the PET images</p>
<p>Request</p>
<p>Valid reasons for examination:</p> <ul style="list-style-type: none"> • Prostate Ca • Rising PSA • Metastatic disease
<p>Valid referrers:</p> <p>See SOP V_2</p>
<p>Persons who may justify / authorise:</p> <p>See SOP P_1</p> <p>RIS JUSTIFICATION CODE: INVPM 106</p>

Booking:	
<ul style="list-style-type: none"> • The patient should be provisionally screened with the MR safety questionnaire prior to booking to identify any contraindication. • Patient is asked to arrive 90 minutes before the due time for scanning. This is to allow time for them to relax, be clerked and cannulated as required. • Be aware the dose comes from off site and is sometimes subject to delays. • The patient or ward is sent an appointment letter. This letter contains a brief description of the test. • If the patient is a private patient refer to SOP for private patients/ FDG. Patient's bill should be settled prior to scan starting. 	
Patient Preparation	
<ul style="list-style-type: none"> • The patient is able to eat and drink as normal for this test • There are no restrictions on diet or medication • The weight limit for the PET-MR scanner is 200kg. If it is known in advance that the patient approaches this weight, ask them to come to the department prior to giving them an appointment to see if they will fit the scanner's aperture. • 	
Radiopharmaceutical and Administration	
Radiopharmaceutical:	F18 Choline
ARSAC Serial No:	9a44iii
DRL: (Maximum usual activity)	370MBq
ED:	12.95 mSv
Minimum dose for paediatrics:	Not Applicable
Advice re breastfeeding:	Not applicable
Persons who may administer:	Departmental List
Route of administration: (IV etc)	IV
Advice after administration:	Patient is advised to sit and relax after injection and void bladder before scanning – uptake time 60mins.
Injection	

Patient Preparation

1. Check the patient's name and DoB as per INM_EP09
2. Ask patient to fill in MR safety questionnaire and front side of the clerking sheet. Double check these verbally with the patient. Ask the patient to remove all metal objects from on or around their body. This includes wallet, keys, mobile phone etc.
3. Check that the patient is not pregnant or breastfeeding. INM_EP03
4. If the patient needs to be accompanied by a nurse or parent, ensure they complete a safety form and if female is not pregnant.
5. Take the height and the weight of the patient and add to the clerking sheet.
6. Ask the patient to change into a gown ready for the scan
7. Ask patient to sit in the cannulation chair, make sure that they are comfortable. Explain the procedure to them. Tell them that after being cannulated they will be left to rest for 45 minutes
8. Cannulate the patient, using a venflon. Attach a 3-way tap and check Patients' glucose level. using the Glucometer. If glucose levels are above 8 mmol/l call the duty doctor. If very high, a decision to give insulin may be made. If very low, the patient will need extra observation. Finally check that the line is patent with a saline flush.

Administration

9. Ensure that the radionuclide calibrator setting is on F18. Draw up 370mBq +/- 10% of F18 ECH using a 5ml syringe in the lead syringe holder. Note the time the dose is dispensed, from the clock in the lab on the clerking sheet. This clock should be set with the PET/MR computer system and checked regularly to make sure that they are in sync.
10. Note the activity in MBq and the volume on the clerking sheet and unpacking sheet.
11. Give the patient the injection; note the time (from the same clock in the dispensing bay). Assay the syringe and needle again after the injection, note the activity and time on the clerking sheet.
12. The injector should sign the clerking sheet and will 'Examine' the injection part of the procedure on RIS straight away.
13. Offer the patient a blanket if they are cold and a bottle of water if they would like one.
14. The default uptake time (interval between F18-Choline administration and start of PET acquisition) is 60 minutes.

Acquisition Technique

Scanning Parameters

Landmark	Forehead	
MR Acquisition Protocol	INVPM106	
MR Sequences	Survey T1 Dixon Coronal MRAC – 5 beds T2 HASTE Axial T1 Dixon Axial MRAC Pelvis – 1 bed	Diffusion Pelvis Region Specific Sequences as appropriate
PET Acquisition Parameters	3D, 3Minutes / Bed, Randoms from Singles	
PET Recon Parameters	Iterative Iterative 3 Iterations 21 subsets 172 matrix, Smooth: Gaussian FWHM 5 mm	

Prior to Scan

15. Ask the patient to go to the toilet prior to positioning on the bed.
16. Ensure belongings are locked away
17. Escort the patient to the scan room and place the locker key on the wall mounted hooks

Positioning

18. Explain the procedure to the patient so that they are aware that they must lie still so that the MR and PET maybe aligned.
19. Position the patient on the bed with their head in the head and neck coil.
20. Put the knee pad under the patient's knees for comfort.
21. Make sure the patient is warm and comfortable.
22. Give the patient ear plugs and explain the purpose of the emergency buzzer.
Make patient aware of the voice intercom between them and the control room

23. Ensure their shoulders are touching the edge of the coil. Place an appropriate number of body coils across the patient, covering from chest to below pelvis. Ensure they are plugged in.
24. Position anterior element of head & neck coil over the patient, ensuring that it is plugged in.
25. Ask patient to close their eyes whilst the laser light is on.
26. Use the laser to position on the forehead.
27. Using the table move buttons move patient to the iso-centre of the magnet.
28. Remind the patient to lie still.
29. Once the patient is within the magnet leave the scan room and close the door

Acquisition Preparation

30. In the control room, click on *patient*, and then click on *Browser*.
31. Select the appropriate patient from the scheduler
32. **If the patient is not on the scheduler list, then enter manually by pressing *Patient then Register*.**
33. Enter all the patient demographics including height and weight.
34. Click on *Exam*.
35. Select the Clinical Choline folder and select the INVPM106 protocol within this, depending on patient's clinical indications.
36. Prior to Starting the PET acquisition enter the administered activity and time of injection.

Acquiring the Image

37. Check all staff are clear of the scanning room before the scan starts.
38. Scan as per exam card. The protocol will automatically move bed positions and will run each sequence in turn.
39. The following sequences should be acquired with breathhold on end expiration: T1 VIBE, MRAC, T1 Dixon.

Data Checking

1. The μ map and reconstructed PET AC data should be checked prior to taking the patient off the scanner. If any μ map errors are noted, please repeat the MRAC for the specific bed position. In case of errors over the lungs it can be helpful to shift the bed position and repeat a single bed MRAC and PET acquisition over the new lung position.
2. If the bladder activity is significant and affects the visualisation of prostate and lymph nodes on PET, please ask the patient to empty their bladder again and perform a 1 bed scan over the pelvis. In case of persisting scatter artifact around

the bladder, please perform a PET AC retrospective reconstruction with the scatter correction option disabled.

RIS

3. At the end of the procedure the person who performed the image acquisition should 'Examine' the patient on RIS. This is necessary to define the IRMER operator for the procedure. The injector of F18-Choline will already have 'Examined' the injection part of the study.

Advice to Patient on Discharge

- Take the venflon out of the patient's arm, cover the site with gauze.
- Advise the patients that the result will be reported in on the next 24 hrs/working day and sent to their referring practitioner.
- Advise to drink extra fluids for the day
- Advise to avoid pregnant women and small children for 4 to 6 hours

Data Analysis

- Routinely no analysis or quantification is required for this protocol.

Data Display

1. Create a 3D AC on the Mac
2. Create a fused image with the T2 composed and AC on the Mac
(Please see the Mac SOP for how to do this or ask a radiographer)

Reporting

Persons who may report:

INM Practitioners

Reporting procedure:

Abnormal findings, normal variants, and relevant question asked in the original request form will be addressed.

Data Archive see SOP Data management

- Raw Data IF REQUESTED to CCPETMRSV01
- All other data to CERBERUS
- AC, NAC, T2 Composed and T1 Composed to Mac
- Recons from the Mac sent to Cerberus and PACS

Additional Comments

